A DIGITAL FILTER/ESTIMATOR FOR THE CONTROL OF LARGE SHIPS IN CONFINED WATERS

Lieutenant Commander Michael John Dove M.Sc. C.Eng. R.N.

This thesis is submitted to the Council for National Academic Awards in partial fulfilment of the requirements for the degree of Doctor of Philosophy.

SPONSORING ESTABLISHMENT:-

PLYMOUTH POLYTECHNIC,

DRAKE CIRCUS,

PLYMOUTH

COLLABORATING ESTABLISHMENTS:-

NATIONAL MARITIME INSTITUTE, LONDON

SPERRY GYROSCOPE CO., DORSET

SEPTEMBER 1984

A DIGITAL FILTER/ESTIMATOR FOR THE CONTROL OF LARGE SHIPS IN CONFINED WATERS

M. J. DOVE

ABSTRACT

Aeronautical and marine casualty statistics indicate that the human being, when under stress or at times of peak load, can be a poor co-ordinator of the information available to him, particularly when that information is from a number of different sources, as is often the case in modern ships. Integration and co-ordination of information and its useful application in a closed loop feedback system can reduce the probability of accident as has already been demonstated in the case of automatic landing systems for aircraft.

This thesis describes the development of a digital filter/estimator for use in conjunction with an optimal controller in the automatic guidance of large ships in the approaches to a port.

A non-linear mathematical model of a ship is developed and validated by comparison with data from an actual ship. The model is then used in digital computer simulations of the passage of a twin screw car ferry into the Port of Plymouth. The simulations show that the control and guidance system is capable of safely navigating the vessel along the predetermined track through noisy measurements of position, course and speed.

A reduced non-linear digital simulation model is then used in the design of a minimum variance filter suitable for installation in a physical model of the car ferry. Tests with this physical model confirm the earlier full scale digital computer simulations, showing that a minimum variance filter is capable of giving very good estimates of the measured states, even though the measurement subsystems are unable to give accurate information because of noise. In the event of a malfunction of one or more of these measurement systems it is shown that the filter continues to give good estimates of all the states.

Mike Dove's Thesis

(*) A 54 Subroutine OPTFIL contains errors – argument?
A 35 Subroutine MATINV line numbers
General errors in program listings:
A18, 22, 25, 29, 44, 54, 57, 58, 61, 77 in appendix 6 etc.

Title page: collaborating establishments to be shown
Abstract: needs a title and author, non-linear needs a hyphen
Contents: non-linear again
1 head-on hyphen
7 VLCC's delete '
12 sub-systems hyphen
17, 18 quasi-linear hyphens, non-linear also
* 18 heave, pitch and roll motions small.
* 19 deep water – isn't there some conflict here? (page 20?)
21 equation 2.2 – missing operator (+)?
23 as 17
29, 30 quasi-linear, hyphen
and in probably all subsequent occasions.
36 electro-magnetic hyphen
general omission of hyphens in appropriate places
42 astmospheric
45 incorrect use of ' noted in plurals – and on other pages
48 Power of Kalman filter lies in recursion but recursive subroutines were not used – would they be beneficial?
(*) 51 The Optimal Filter – link to A54 – errors?
there must be a page missing since labels 9997 and 9998 are not shown
55 ; and.
URCHIN not defined on page 33 as a model "ship".
125 Problems associated with translating Fortran to Basic – simplifications?
130 Limitations imposed by computer resulted in simplification of filter and controller — effect of these modifications? Any problems as a result? Is it worth improving the hardware as a consequence? Future development using better computers? – answered on 158
140 et seq. Colour codings for diagrams?

Title page: full name } to be added
collaborating establishment

M

P157 test should read text
138 AA(4, 41 = should read AA(4, 4)

M. ~~Holt~~ Coult

Penryn

14, Trevethan Rd

76356 (PM)

Merit Table Cards

CORRECTIONS

PAGE	
28	Correct Equations (3.13) and A, B, C below.
47	l. 3 disturbances.
46-47	Make sure this section is understood
50	l. 13 equations.


QUIBERON
Brittany Ferries

DECLARATION

No part of this thesis has been submitted for any award or degree at any other institute.

While registered as a candidate for the degree of Doctor of Philosophy the author has not been a registered candidate for another award of the C.N.A.A. or of a University.

A photocopy of a paper published in connection with this research is bound at the end of the thesis.

ACKNOWLEDGEMENTS

My thanks are due to the following people for their help in the preparation of this thesis:-

Dr. C. T. Stockel of Plymouth Polytechnic for acting as Director of Studies.

Mr. T. H. Bouncer of Plymouth Polytechnic for acting as Supervisor.

Dr. D. J. MacKinnon of the Rutherford-Appleton Research Laboratories for acting as Supervisor and for giving me the inspiration to undertake this research.

Mr. P. W. Fortescue of Southampton University for his help during the initial stages.

Captain I. Gregory of Plymouth Polytechnic for his support, and for making available the facilities of the Department of Marine Technology at Plymouth Polytechnic.

Professor D. E. Fussey for making available the facilities of the Department of Mechanical Engineering at Plymouth Polytechnic.

Mr. M. J. Stringer for his help in the development of software and hardware for the physical model, and all those technicians of the

Learning Resources Centre and Departments of Mechanical Engineering and Marine Technology at Plymouth Polytechnic who helped with this project.

My wife, Rita, for her preparation of the final manuscript and whose unfailing support and encouragement made this thesis possible.

My sons, Keith and Simon, for proof reading my manuscript and for help in its final preparation.

A DIGITAL FILTER/ESTIMATOR FOR THE CONTROL OF LARGE SHIPS IN CONFINED WATERS

M. J. DOVE

ABSTRACT

Aeronautical and marine casualty statistics indicate that the human being, when under stress or at times of peak load, can be a poor co-ordinator of the information available to him, particularly when that information is from a number of different sources, as is often the case in modern ships. Integration and co-ordination of information and its useful application in a closed loop feedback system can reduce the probability of accident as has already been demonstated in the case of automatic landing systems for aircraft.

This thesis describes the development of a digital filter/estimator for use in conjunction with an optimal controller in the automatic guidance of large ships in the approaches to a port.

A non-linear mathematical model of a ship is developed and validated by comparison with data from an actual ship. The model is then used in digital computer simulations of the passage of a twin screw car ferry into the Port of Plymouth. The simulations show that the control and guidance system is capable of safely navigating the vessel along the predetermined track through noisy measurements of position, course and speed.

A reduced non-linear digital simulation model is then used in the design of a minimum variance filter suitable for installation in a physical model of the car ferry. Tests with this physical model confirm the earlier full scale digital computer simulations, showing that a minimum variance filter is capable of giving very good estimates of the measured states, even though the measurement subsystems are unable to give accurate information because of noise. In the event of a malfunction of one or more of these measurement systems it is shown that the filter continues to give good estimates of all the states.

CONTENTS

CHAPTER 1.

EXISTING PILOTAGE METHODS.

1.1 Introduction.

There can be little doubt that the overall standards of safety at sea are high, particularly with the traditional maritime nations. Cockcroft(1981) states that of a total of 22,600 ships, over 1000 gross registered tons, trading in 1979, 9400 were from the traditional maritime nations. He goes on to say that during the period 1977-79 these countries lost 16 ships out of a total of 189 worldwide losses. Thus the traditional maritime nations ran 41.59 per cent of the ships and incurred only 8.4 per sent of the losses. This does suggest that high standards are not universal and there may be considerable resentment among operators of high standard ships when casualties to sub-standard vessels result in the implementation of measures, such as marine traffic management systems, which give rise to increased operating costs.

However this does not alter the fact that the total number of incidents is small compared with the number of vessels in service. Cockcroft (1978) states that during the period 1972-76 for ships over 10,000 grt, the ratio of collisions to total numbers is 0.64%, whilst Fujii (1982) gives the probability of head-on collision in the Dover Strait as 0.008%. This figure is increased to 0.3% in the Uraga Strait of Japan.

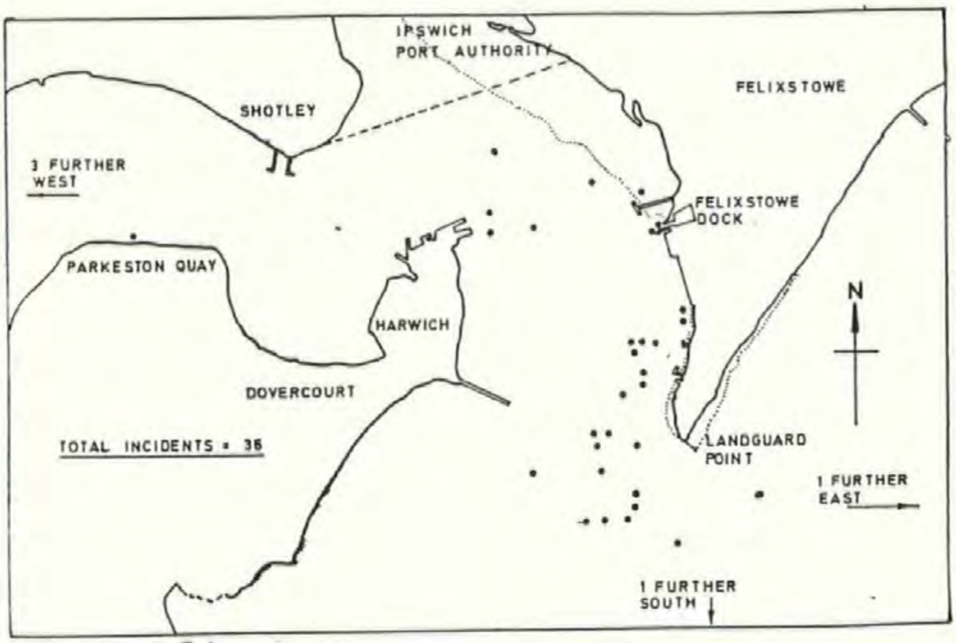

Fig.1.1 Incidents in the Port of Harwich in 1976.

In the approaches to a port, however, a different picture starts to emerge. In an analysis of marine accidents in ports and harbours the National Ports Council (1976) concludes that two thirds of ship collisions occur in port and harbour areas. Figure 1.1 shows the location of incidents in the port of Harwich in 1976 whilst figures 1.2 and 1.3 give the locations of reported groundings and collisions in the Humber for the period 1969-79. Coldwell (1981) shows that there are 100 traffic movements per day in the Humber Seaway, resulting in either a collision, or a collision with a floating mark, or a grounding, at least once a week. Fujii and Shiobara (1971) have analysed a number of collisions. In the case of 654 collisions to all sizes of vessel they report that 30.4% take place in Straits, 44.6% in harbours, and 25% in the open sea.

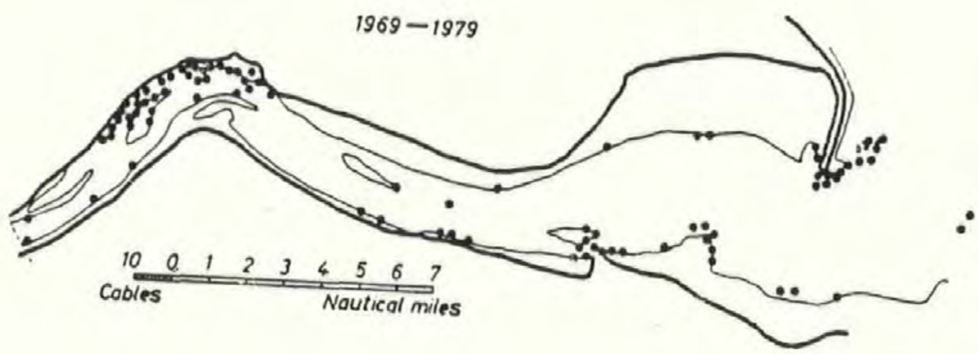

Fig.1.2 Groundings in the Humber Seaway (1969-1979)

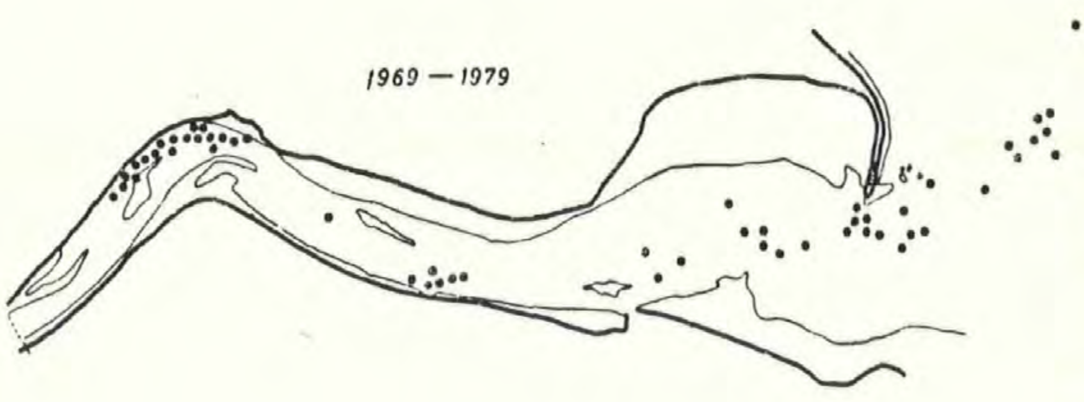

Fig.1.3 Collisions in the Humber Seaway (1969-1979)

Visibility is a major factor in the working of a port and whilst the number of accidents may not increase in poor visibility this may be due to a decrease in the number of vessel movements, leading to loss of earnings for both the port and the ship operator. The cost of an accident will also increase as the ship's size increases. Not only will the cost due to loss of earning capacity be greater, but the cost of repair or replacement will increase. Environmental aspects must also be considered. These may include the spillage of large quantities of crude oil at, or near, the approaches to a port, or an explosion on board a ship berthed near the centre of a densely populated area. The social costs of an accident might even exceed the cost of repair or replacement. Stratton and Silver (1970) report that the settlement of three million pounds in the Torrey Canyon case was less than the total expense incurred in pollution clearance along the Cornish coastline.

Safety, cost and the environment, are the main factors which have led to a greater degree of control over the movement of ships in confined waters. The reasons for increased control are well documented in, for example, the Proceedings of the International Symposium on Vessel Traffic Services (1981) and may be summarised as :-

1. The requirement to use port facilities as economically as possible;
2. The limitations brought about by the increased size and draft of ships when compared with channel widths and depths;
3. The limitations of weather including fog and poor visibility.

Marine Traffic Control Systems (M.T.C) are being developed and used in many of the World's ports. The development of a shipborne automatic control system to be used in the pilotage phase of a voyage would complement M.T.C. and improve its efficiency by allowing ships to be berthed automatically in all weather conditions. Safety factors would be improved and hence the costs of damage, and probably insurance, would be reduced, whilst helping to dispel public unease over the social and pollution problems resulting from a collision or grounding in the approaches to a port. This thesis is concerned with the design of such a system. In particular it concentrates on the problem of obtaining the best possible values of the measured states to be used as inputs to an optimal controller.

1.2 Traditional Methods of Pilotage

In the process of bringing a vessel safely to her berth great emphasis is placed upon the skills of the Master and pilot; these skills are the traditional ones of seamanship and ship handling. The ship is conned along the buoyed channel and, provided the speed is kept below an acceptable limit (normally defined by the harbour authority), provided she is kept within the buoyed channel, and provided the necessary action is taken to avoid collision, safe pilotage and berthing will take place. The experienced navigator does not often need to perform the practice of "putting her on the chart" within the confines of the port, as knowledge of his position relative to buoys and landmarks will normally be sufficient. During the pilotage the experienced man relies heavily on transits. He watches the jackstaff in the bows and estimates the rate of swing of the vessel against the sky-line. He knows that when a particular pylon and chimney stack, say, are in line it is time to start applying helm to go round the next bend, and so on. He is aware of the characteristics of the vessel and knows how to allow for the direct influences of wind, sea and tide.

The safe berthing of a VLCC involves not only the last few hundred metres of approach. In order to give sufficient time to secure all tugs and leave a safety margin before moderate braking must commence it is important that the berthing pilot should take over the ship at considerably more than a mile from the berth, and at a speed of about four knots. The figures quoted here are for berthing a super tanker at the Esso Oil Terminal, Fawley, Southampton, but they are typical of the requirements of any port where an estuarial phase exists. Ideally the pilot will then attempt to stop the ship abeam of the jetty and move her bodily alongside, keeping her parallel to the jetty throughout. In practice, however, corrections have to be made for quite substantial swings and overshoots, and to obtain maximum directional control with the rudder docking is normally commenced against the flow of the tide, so that on a flood tide the ship will have to be turned before berthing.

The increasing size of tankers and bulk carriers has made the judgement of speeds and distances for the final berthing phase progressively more difficult. It is well known that the momentum possessed by even a very slowly moving VLCC is very large. To reduce this momentum it is necessary to decrease the sideways velocities. However, the human eye cannot perceive very slow motions. Van Manen and Hooft (1970) suggest that the smallest yaw velocity the eye can detect is about 1 minute of arc/second; an analysis of ship manoeuvrability experiments on full-scale vessels shows that they move so slowly during berthing that a fair amount of the accompanying alterations in acceleration and velocity are not perceptible to the man on the bridge. Thus, some information is not available to the pilot due to his own physiological limitations.

To meet the need for much more accurate information on sideways velocities a version of Doppler radar, known as SAMI (Speed of Approach Measurement Indicator), has been developed by the Royal Radar Establishment. With the aid of this sensor, which is capable of measuring rates down to 0.015 m/s or 0.03 knots, a consistent reduction in the velocity of impact has been achieved. At Fawley for example, the jetty fenders had been designed to absorb impacts of up to 0.1 m/s with the ship parallel to the jetty. Pilots now aim to arrive at speeds of less than 0.06 m/s, and in most cases speeds less than 0.03 m/s are achieved.

Although Doppler speed measurements are available from the jetty the pilot still requires an overall picture. In practice he must rely upon the ship's officers and crew for information from revolution indicator, compass, log, radar, telegraph and rudder indicator, but there is still a strain upon him and the possibility exists that too many things will claim his attention at one time. That there have been so few accidents involving VLCC's is a tribute to the ability of the pilots involved, rather than the control system employed.

1.3 The Case for Automatic Pilotage

The existing methods have evolved over a great length of time, and in the main the complicated process of pilotage and berthing is carried out without the aid of a great deal of sophisticated equipment. There is no denying, however, that impressive improvements in berthing have been brought about by the use of Doppler radar. This serves to highlight the weaknesses of the traditional methods when applied to large ships and when one considers that a major factor in ship and aircraft casualties is human error (The Panel on Human Error in Merchant Marine Safety (1976) showed that 85% of all marine collisions were due to human error) it becomes apparent that shipping must be controlled in the berthing and estuaral phases of a voyage. In the majority of cases this control is being exercised through the auspices of a port navigation service, which exists primarily to pass information to the ship. In the past this information has largely been advice, such as the number of vessels moving in the channel, the tugs available, or the berth allocated. More recently navigational data has been supplied, for example, from a shore-based radar system, and increasingly there is a movement towards a greater degree of control from ashore. Marine traffic control systems are showing that, although much of the equipment is still of a provisional character, the shore-based direction of large ships is not only feasible but straightforward, and the port navigation services have the capacity to fulfil tasks of this nature.

In the context of automatic pilotage a control system is defined as a device which controls the flow of energy or information within the system in such a manner as to achieve optimal performance. The system may be completely automatic as in the automatic steering devices found in most modern ships or it may include the human operator as part of the system, as in manual steering systems. There may also be a mixture of the two and in this context Koyama (1972) has predicted improvements to the course keeping and handling qualities of an unstable ship by adding subsidiary automatic control to manual steering.

A common argument against any form of automatic navigation is that it will further reduce the individual's right to freedom of the seas. In commercial terms this may be seen as a conflict between the traditional role of the mariner and the organisation he serves. Further, it is suggested that the traditional methods allow the navigator maximum flexibity. For example, if a tug's wire parts he can resort to a contingency plan involving, say, main engines and an anchor. What is perhaps ignored in these arguments is that the ship is part of a very complex transportation system, with the needs of organization, of necessity, restricting the role of the mariner.

Further, while no automatic control system could claim to be as adaptable as the human controller, provided the degree of reliability is approaching 100% a much more precise and consistent process would be achieved by automatic means. In the case of system failure there would always be the need for the navigator to "manually override"; thus the introduction of automatic control would make the existing flexible system the last rather than the first resort, so that the safety factor would be improved.

A note of caution needs to be introduced at this point however. Non-automatic piloting calls for considerable experience. With the advent of shipbourne automatic systems, where does the human gain his experience? As a relatively inexperienced navigator will he be satisfactory as a fall back in the event of system failure? The answer to the second of these questions is probably no, although reports from the 1982 Falklands Campaign suggest that the British seafarer has lost none of his traditional skills, in spite of the automatic control systems and electronic aids at his disposal. The answer to the first of these questions seems to be bound up with developments in ship manoeuvring simulators. The growing interest in training mariners under the circumstances which may confront them on board ship, may further be strengthened by the training of pilots for an automatic era, and would certainly have an offshoot in improved training programmes in which ships' officers, pilots, and the shore-based port navigation service staff could be involved, thus leading to improved confidence in and reliability on the port navigation service.

Reference has already been made to the traditional skills of ship handling and seamanship and to the interpretation placed by the experienced navigator on transits, buoys, landmarks, tides and winds. The control engineer would look upon the pilotage from a different angle. He would visualise the ship as a multi-loop feedback system, considering errors in position and velocity. To minimize these errors he would seek to measure rate of change of position (linear velocity), course error and rate of change of heading (angular velocity), together with along-track and off-track position errors, using these parameters to keep the ship on a desired track. But in effect the ship's officer is doing the same thing. In looking for position errors he has only to glance at buoys or other navigational marks to know whether the ship is on track. When position errors are detected the helmsman is ordered to alter course to correct this error. For his part the helmsman, once given a course to steer, detects errors in this course and corrects accordingly.

There are, of course, many problems to be considered when developing a completely new system. The cost of design and development will be high, and production costs, initially at least, will reflect these high development costs. The incremental benefits to be derived from such a system are, it would argued, very small, since standards are already high, and may not justify the expense. However it must be pointed out that the fitting of advanced electronic navigation systems has led to substantial savings in time and fuel costs. The fitting of an automatic pilotage system would then help to minimise delays in the approaches to a port; probably reduce insurance costs, and the cost of the system would be a small fraction of the cost of the ship together with the value of her cargo.

Safety and reliability may be taken together and here one can draw upon the experience and developments in the aero-space industry. Reliability today is extremely high; taking a navigation satellite as an example it is designed to have a life of at least ten years. In automatic landing systems fail safe devices are fitted so that the probability of error is considered a factor of ten better than the probability of the aircrew making an error.

The overall performance of the system might be limited by the inputs from the sensors, as many navigation aids have limitations when used in confined waters. For example a marine radar may only have a bearing error of one degree, while Decca Hi-fix may experience distortion of the grid near metal objects and doppler radar is slightly affected by reduced visibility. Off-shore these are all acceptable errors, but in the final stages of pilotage the sensor errors may lead to unacceptable system errors, unless some method of minimising random errors is incorporated.

No system can be completely reliable, although modern integrated systems using Kalman Filter techniques are able to accept partial failure, especially in the measurement sub-systems. Thus a fall-back or stand-by system would have to be incorported. This might consist of a second or alternative system, but is more likely to be a manual override. This brings one to the human aspects. Lack of experience will be increased by the use of a reliable automatic system, but there is also the job satisfaction of the navigator to be considered. It is certainly true to say that he would not get the same sense of achievement from supervising an automatic system as he would from using the existing methods.

None of these problems is insurmountable, but they do suggest that the transition to an automatic system would take place over a period of several years. Both Holder (1975) and Zuidweg (1970) suggest that automation at sea is on the increase. Among the interrelated factors which contribute to the continued development in this area they list the difficulties in retaining qualified personnel in sufficient numbers, the growing need for optimal operation of ships, increasing traffic density and ship size, and advances in technology. This author(1974) has suggested that marine traffic control systems (MTC) could be further improved by the development of automatic systems for the pilotage of large ships. Any increase in control in congested waters will not be developed rapidly, easily or inexpensively, but there would appear to be no other long term alternative. The Conference on Mathematical Aspects of Marine Traffic (1979) highlighted some of the problems and suggested some methods to overcome them. These include Traffic Routing Schemes, Vessel Traffic Services and the use of improved navigation systems, both ashore and afloat.

1.4 The Present Work

The aim of this project was to design an optimal filter/estimator as part of an automatic track and heading control system, to be used in large ships in the approaches to a port. In this context the port approaches were defined as the area between the pilotage station and the vessel's berth. It did not include the process of berthing the vessel. The work was part of a larger research project carried out by a small team at Plymouth Polytechnic. The research was directed towards possible control and guidance systems which might be used rather than the human and environmental problems which would have to be solved before a ship could be automatically berthed in a manner similar to the automatic landing of an aircraft.

The work of Kalman and Koepcke (1958), Joseph and Tou (1961), and

Gunckel and Franklin (1963) reduced a given optimal control problem to two separate optimisation problems, and became known as the Separation Principle. Its most striking feature is that the feedback control gain matrix is independent of all statistical parameters in the problem, whereas the optimal filter is independent of the matrices in the performance measure. This provided a natural breakdown of work as indicated in Figure 1.4. At the start of the project the two researchers, R.S.Burns and the author of this thesis, developed suitable mathematical models for use in the computer simulations. R.S.Burns (1984) then concentrated on the design of an optimal controller whilst the author's work was directed towards the best estimate of the state vector using minimum variance techniques.

Chapters 2/3 describe the linear, quasi-linear, and non-linear mathematical models developed for use in the digital computer simulations using the Polytechnic Prime 850 digital computer. During the period of the research a Prime 9950 was added. After a brief survey of navigational sensors Chapter 4 describes the use of variance as an indication of random errors. This leads to the requirement for minimum variance filters. The design procedure for the minimum variance filter is described in Chapters 4 and 8.

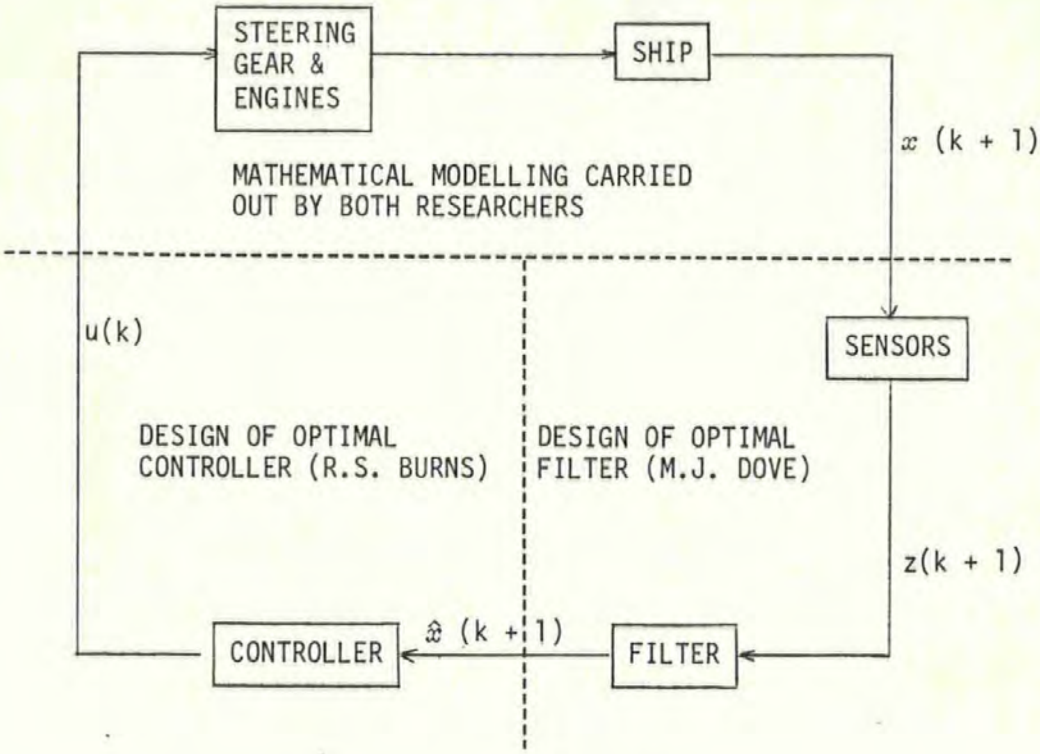

Fig.1.4 Division of Work

A description of the work carried out using the various full scale computer model simulations is given in Chapters 5 and 6. Work started with a linear model of a Mariner hull and was developed through quasi-linear to non-linear full scale computer models using the Mariner hull and a twin screw car ferry. A full analysis of results is given, showing the need for a non-linear computer model in this type of simulation work.

The complex "eight state" full scale computer model of the car ferry was then simplified to a "four state" model and tested in computer simulations. The filter software was then developed for use in a "physical" model of the car ferry. This "physical" model was fitted with an optimal controller and estimator and tests were carried out on a reservoir. Details and results are given in Chapters 8 and 9.

Results from the digital computer simulations and "physical" model tests are discussed in Chapters 7 and 9. These show that both the computer and actual models correctly simulate the passage of a large ship in the approaches to a port and that the combination of an optimal filter and controller, together with correctly chosen sensors can be used to automatically control the vessel so that it follows the correct track in to, or out of harbour.

CHAPTER 2
THE LINEAR MATHEMATICAL MODEL

2.1 Introduction

From the early 1960's feedback control theory was given a strong impetus by optimization theory, as developed by Kalman and Bucy (1961). The approach relied heavily upon the matrix formulation of "state variables" and advanced presentation of control and estimation theory requires an understanding of this viewpoint.

Most formulations of the control and estimation problem implicitly contain multiple inputs and outputs and are referred to as multi-variable systems. Consideration was given here to the problem of obtaining such a mathematical model, or models, of the ship's motion through the responses of this system to external stimuli. The mathematical models used were thus required to be in state space form if optimal control and estimation techniques were to be employed and if on-line computer control was to be implemented.

The constant forward speed linear model was based upon the work of Zuidweg (1970). This chapter describes its development. However, in restricted waters it is necessary to allow for variation in forward speed and large alterations of course. Chapter 3 goes on to describe how a quasi-linear model, based upon non-dimensional hydrodynamic coefficients and incorporating the surge equation, was developed. From this quasi-linear model emerged the full non-linear model. The work included formulation of the continuous state equations (time invariant for the linear model and time variant for the quasi- and non-linear models) together with the techniques used to obtain the solutions in discrete time. The time variant nature of the quasi-linear and non-linear models required computation of the discrete state transition matrix at each sampling instant. Open loop simulations were carried out for all three models. The results obtained were compared with actual ship data based upon a Mariner class hull.

2.2 Co-ordinate Systems and Sign Conventions

Within the confines of a port the heave, pitch and roll motions were considered sufficiently small for their influence on sway, surge and yaw to be negligible. It was then assumed that the ship's centre of gravity was constrained to a horizontal plane, to be referred to as the plane of motion and that the longitudinal and lateral axes remained in this plane at all times.

Two right-handed co-ordinate systems were used, the first with respect to the ship (x_s, y_s) the second with respect to the sea bed (x_o, y_o). These are shown in Figure 2.1, and the positive directions are as indicated. The origin of the ship co-ordinate system was assumed to be at the ship's centre of gravity. The axes of the earth co-ordinate system are as illustrated in Figure 2.1 to conform with standard navigational practice, i.e. the x_o axis corresponds to the direction of True North. The positive directions are as given in Figure 2.1

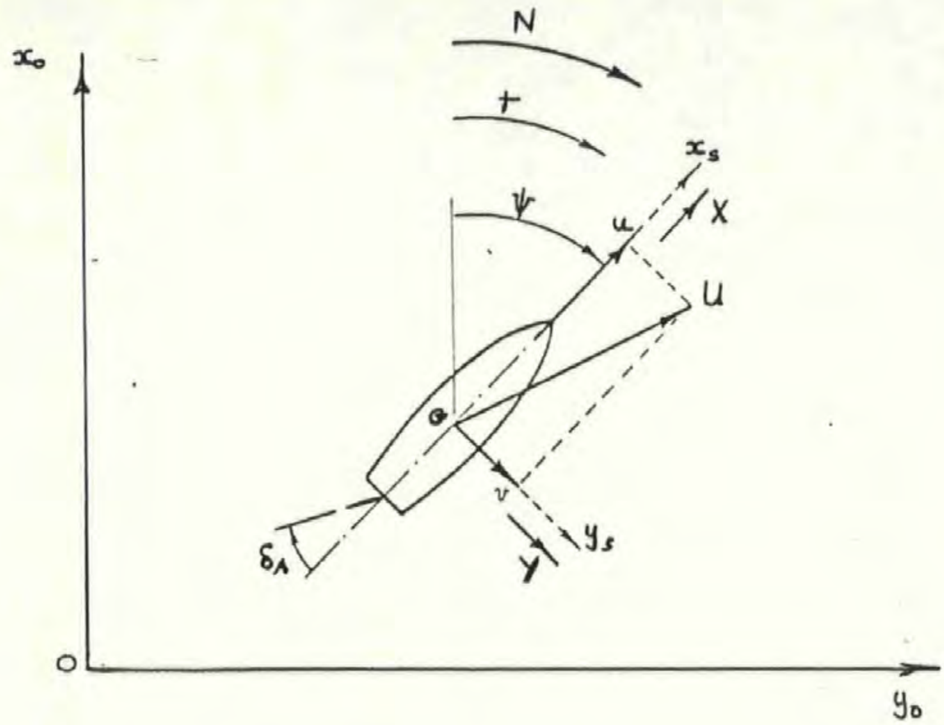

Fig.2.1 Co-ordinate Systems

2.3 Development of the Linear Model

It is convenient to describe the motion in terms of a moving system of axes coincident with the mass centre of the hull as illustrated in Figure 2.1. This gives rise to an Eulerian set of equations of motion which may written in the form:-

$$
\begin{aligned}
m\dot{u} - mvr &= X \\
m\dot{v} + mur &= Y \qquad (2.1) \\
I_z\dot{r} &= N
\end{aligned}
$$

For deep water conditions it is then assumed that the forward speed of the vessel is constant and the X equation can be discarded. Thus only the lateral and angular movements are considered in the development of the linear model. The linear equations are retained by assuming that the transverse and angular velocities and accelerations of the ship are with respect to the water, plus the effects of rudder. <This author (1977)>.

In modelling disturbance inputs such as wind, waves, current and depth of water it was assumed that in the approaches to a port:-

(i) Wave excitation can be ignored;

(ii) Accelerations of current and wind are small enough to be neglected;

(iii) The depth of water is such that the mathematical model is not affected.

Techniques employed in obtaining expressions for hydrodynamic forces are well covered in the literature, for example Lewison (1973). The identities of Y and N can be found by linearising them as first order approximations using Taylor's series expansion. The second and third parts of equation (2.1) may then be re-written as:-

$$m\dot{v} + mur = Y_{\dot{v}}\dot{v} + Y_v v + Y_{\dot{r}}\dot{r} + Y_r r + Y_\delta \delta_R + Y_v v_c + Y_{va} v_c$$

$$I_z\dot{r} = N_{\dot{v}}\dot{v} + N_v v + N_{\dot{r}}\dot{r} + N_r r + N_\delta \delta_R + N_v v_c + N_{va} v_c$$

Rearranging the above equations and expressing them in matrix form gives:-

$$\begin{bmatrix} \dot{v} \\ \dot{r} \end{bmatrix} = \begin{bmatrix} F_{22} & F_{23} \\ F_{32} & F_{33} \end{bmatrix} \begin{bmatrix} v \\ r \end{bmatrix} + \begin{bmatrix} F_{21} \\ F_{31} \end{bmatrix} \delta_A + \begin{bmatrix} G_{22} & G_{23} \\ G_{32} & G_{33} \end{bmatrix} \begin{bmatrix} v_c \\ v_a \end{bmatrix} \tag{2.2}$$

Where,

$$\begin{bmatrix} F_{22} & F_{23} \\ F_{32} & F_{33} \end{bmatrix} = \begin{bmatrix} m-Y_v & -Y_r \\ -N_v & I_z-N_r \end{bmatrix}^{-1} \begin{bmatrix} Y_v & Y_r-mu \\ N_v & N_r \end{bmatrix}$$

and,

$$\begin{bmatrix} F_{21} \\ F_{31} \end{bmatrix} = \begin{bmatrix} m-Y_v & -Y_r \\ -N_v & I_z-N_r \end{bmatrix}^{-1} \begin{bmatrix} Y \\ N \end{bmatrix}$$

$$\begin{bmatrix} G_{22} & G_{23} \\ G_{32} & G_{33} \end{bmatrix} = \begin{bmatrix} m-Y_v & -Y_v \\ -N_v & I_z-N_r \end{bmatrix}^{-1} \begin{bmatrix} Y_v & Y_a \\ N_v & N_a \end{bmatrix}$$

2.4 The Steering Gear and Main Engine Models

The steering gear and main engine were both modelled by first order differential equations. For the steering gear, if δ_D is the demanded rudder angle and δ_A the actual rudder angle, then:-

$$\delta_A = (\delta_D - \delta_A)/T_R \tag{2.3}$$

where T_R is the closed-loop time constant of the steering gear.

Similarly, for the main engine, if n_D is the demanded engine speed and n_A the actual speed, then,

$$n_A = (n_D - n_A)/T_N \tag{2.4}$$

where T_N is the closed loop time constant of the main engines.

2.5 Ship and Earth Axes

The forward and lateral components of velocity relative to the ship's reference system are u and v. They may be related to the y axis of the earth's reference system by:-

$$y_o = u \sin\psi + v \cos\psi \tag{2.5}$$

If ψ is small then (2.5) becomes:-

$$y_o = u\psi + v \tag{2.6}$$

2.6 State Space Formulation of the Linear Model

Equations (2.2), (2.3) and (2.6) are now combined and expressed in state space form as:-

$$\begin{bmatrix} \dot{\delta}_A \\ \dot{v} \\ \dot{r} \\ \dot{\psi} \\ \dot{y}_o \end{bmatrix} = \begin{bmatrix} -1/T_R & 0 & 0 & 0 & 0 \\ F_{21} & F_{22} & F_{23} & 0 & 0 \\ F_{31} & F_{32} & F_{33} & 0 & 0 \\ 0 & 0 & 1 & 0 & 0 \\ 0 & 1 & 0 & u & 0 \end{bmatrix} \begin{bmatrix} \delta_A \\ v \\ r \\ \psi \\ y_o \end{bmatrix} + \begin{bmatrix} 1/T_R \\ 0 \\ 0 \\ 0 \\ 0 \end{bmatrix} \delta_D + \begin{bmatrix} 0 & 0 \\ G_{22} & G_{32} \\ G_{32} & G_{33} \\ 0 & 0 \\ 0 & 0 \end{bmatrix} \begin{bmatrix} \bar{V}_c \\ V_a \end{bmatrix} \tag{2.7}$$

Equation (2.7) is the form of the state variable equation for the time varying linear system.

$$\underline{\dot{x}}(t) = \underline{F}\underline{x}(t) + \underline{G}_c\underline{u}(t) + \underline{G}_D\underline{w}(t) \tag{2.8}$$

The linear equation (2.7) was not used in the computer simulations, but is the base from which the quasi- and non-linear models were developed. As such it is included here for completeness.

CHAPTER 3

NON-LINEAR MATHEMATICAL MODELS

3.1 The Quasi-Linear Model

The linear equations of motion (2.2) only include the first terms of the Taylor expansion. They do not therefore make allowance for alterations of course or speed and are of limited use when considering the movement of a ship in the approaches to a port where large heading and speed changes must take place if the vessel is to successfully navigate the buoyed channel. However the linear model has been extensively used by researchers such as Zuidweg (1970) and Bech (1972). It was therefore decided to continue along these lines by assuming that the vessel would follow a straight track during each sample time. If sample times were kept small it was reasoned that the linear equations could then be extended to incorporate the surge equation and thus make allowance for variations in forward speed. Because the forward speed appears in the state transition matrix however, this is no longer constant and has to be recalculated after each sample time.

To allow for forward speed and to incorporate engine revolutions the state, control and disturbance vectors are now defined as:-

$$
\begin{array}{lll}
X_1 = \delta_A & u_1 = \delta_D & w_1 = u_c \\
X_2 = n_A & u_2 = n_D & w_2 = v_c \\
X_3 = x & & w_3 = u_a \\
X_4 = u = \dot{x} & & w_4 = v_a \\
X_5 = y & & \\
X_6 = v = \dot{y} & & \\
X_7 = \psi & & \\
X_8 = r = \dot{\psi} & &
\end{array}
$$

The equations for surge, sway and yaw can then be written:-

$$m\dot{u} - mrv = X_{\dot{u}}\dot{u} + X_u(u+u_c) + X_n n_A + X_{ua} u_a \tag{3.1}$$

$$m\dot{v} + mru = Y_{\dot{v}}\dot{v} + Y_v(v+v_c) + Y_{\dot{r}}\dot{r} + Y_r r + Y_\delta \delta_A + Y_n n_A + Y_{va} v_a \tag{3.2}$$

$$I_z\dot{r} = N_{\dot{v}}\dot{v} + N_v(v+v_c) + N_{\dot{r}}\dot{r} + N_r r + N_\delta \delta_A + N_n n_A + N_{va} v_a \tag{3.3}$$

From (3.1)

$$\dot{u} = X_2 n_A + X_4 u + X_6 v + X_{w1} u_c + X_{w3} u \tag{3.4}$$

The notation followed here is to give a suffix according to the position in the state vector, i.e. X_1 relates to δ_A the first state vector and is here given suffix 1, X_8 relates to r, the eighth state vector, and so on.

Where a double suffix appears the coefficient relates to the derivative of the appropriate state. For example suffix 88 relates to the derivative of the eighth state. Coefficients relating to the disturbance vector are given the suffix such as w1, w2 according to their position in the disturbance matrix.

From (3.2)

$$\dot{v} = Y_1 \delta_A + Y_2 n_A + Y_4 u + Y_6 v + Y_8 r + Y_{88} r + Y_{w2} v + Y_{w4} v_a \qquad (3.5)$$

From (3.4)

$$\dot{r} = N_1 \delta_A + N_2 n_A + N_6 v + N_{66} v + N_8 r + N_{w2} v_c + N_{w4} v_a \qquad (3.6)$$

The dimensionalised hydrodynamic coefficients are obtained by multiplying the non-dimensionalised coefficients by the appropriate combinations of forward speed, length and water density. The appropriate dimensionalising factor for each coefficient is given in Appendix 4. The terms such as X, Y, and N were obtained in the process of re-arrangement. They are defined in Appendix 2.

It is now necessary to eliminate u, v and r from the right-hand side of each of the equations (3.4), (3.5) and (3.6), then after suitable re-arrangement and combination with equations (2.3) and (2.4) the equation set is given by equation set (3.7). The terms K, L, M were obtained in the process of re-arrangement and elimination. They are defined in Appendix 2 and all the computer subroutines used in the rearrangement process are listed in Appendix 7.

$$
\begin{bmatrix} \dot{\delta}_A \\ \dot{n}_A \\ \dot{x} \\ \dot{u} \\ \dot{y} \\ \dot{v} \\ \dot{\psi} \\ \dot{r} \end{bmatrix} = \begin{bmatrix} -1/T_R & 0 & 0 & 0 & 0 & 0 & 0 & 0 \\ 0 & -1/T_N & 0 & 0 & 0 & 0 & 0 & 0 \\ 0 & 0 & 0 & 1 & 0 & 0 & 0 & 0 \\ 0 & K_2 & 0 & K_4 & 0 & K_6 & 0 & 0 \\ 0 & 0 & 0 & 0 & 0 & 1 & 0 & 0 \\ L_1 & L_2 & 0 & L_4 & 0 & L_6 & 0 & L_8 \\ 0 & 0 & 0 & 0 & 0 & 0 & 0 & 1 \\ M_1 & M_2 & 0 & M_4 & 0 & M_6 & 0 & M_8 \end{bmatrix} \begin{bmatrix} \delta_A \\ n_A \\ x \\ u \\ y \\ v \\ \psi \\ r \end{bmatrix} +
$$

$$
\begin{bmatrix} 1/T_R & 0 \\ 0 & 1/T_N \\ 0 & 0 \\ 0 & 0 \\ 0 & 0 \\ 0 & 0 \\ 0 & 0 \\ 0 & 0 \end{bmatrix} \begin{bmatrix} \delta_D \\ n_D \end{bmatrix} + \begin{bmatrix} 0 & 0 & 0 & 0 \\ 0 & 0 & 0 & 0 \\ 0 & 0 & 0 & 0 \\ K_{w1} & 0 & K_{w3} & 0 \\ 0 & 0 & 0 & 0 \\ 0 & L_{w2} & 0 & L_{w4} \\ 0 & 0 & 0 & 0 \\ 0 & M_{w2} & 0 & M_{w4} \end{bmatrix} \begin{bmatrix} u_c \\ V_c \\ u_a \\ V_a \end{bmatrix} \tag{3.7}
$$

The values of x_o, y_o, u_o and v_o on the earth's reference axis system may be found at the (k+1)th instant by the relationships:-

$$
x_o(k+1) = x_o(k) + [x(k+1) - x(k)] \cos[\psi(k+1)] - [y(k+1) - y(k)] \sin[\psi(k+1)] \tag{3.8}
$$

$$
y_o(k+1) = y_o(k) + [y(k+1) - y(k)] \cos[\psi(k+1)] + [x(k+1) - x(k)] \sin[\psi(k+1)] \tag{3.9}
$$

$$
u_o(k+1) = u(k+1) \cos[\psi(k+1)] - v(k+1) \sin[\psi(k+1)] \tag{3.10}
$$

$$
v_o(k+1) = v(k+1) \cos[\psi(k+1)] + u(k+1) \sin[\psi(k+1)] \tag{3.11}
$$

3.2 Computation of Discrete Transition Matrices

Equation (3.7) is a set of first order differential equations and is represented in matrix form as:-

$$\underline{\dot{x}(t)} = \underline{F}\underline{x(t)} + \underline{G_c}\underline{u(t)} + \underline{G_D}\underline{w(t)} \tag{3.12}$$

For work using a digital computer this equation set must be converted to its discrete form, namely a set of difference equations given by:-

$$\underline{x(k+1)} = \underline{e^{FT}}\underline{X(k)} + \int_0^T \underline{e^{F(T-\tau)}}\underline{G_c}\,\underline{u(\tau)}\,d\tau + \int_0^T \underline{e^{F(T-\tau)}}\underline{G_D}\,\underline{w(\tau)}\,d\tau \tag{3.13}$$

or

$$\underline{x(k+1)} = \underline{A}\underline{x(k)} + \underline{B}\underline{u(k)} + \underline{C}\underline{w(k)} \tag{3.14}$$

where $\underline{A} = \underline{e^{FT}}$

and $\underline{B} = \int_0^T \underline{e^{F(T-\tau)}}\underline{G_c}\,d\tau = (\underline{e^{FT}}-\underline{I})\underline{F^{-1}}\underline{G_c}$

$\underline{C} = \int_0^T \underline{e^{F(T-\tau)}}\underline{G_D}\,d\tau = (\underline{e^{FT}}-\underline{I})\underline{F^{-1}}\underline{G_D}$

For general applications the exponential matrix may be evaluated by a digital computer program based on the following arrangement of the $\underline{A}$, $\underline{B}$ and $\underline{C}$ matrices.

$$\begin{aligned}\underline{A} &= \underline{I} + \underline{F}T + (\underline{F}T)^2/2 + \ldots\ldots + (\underline{F}T)^{L'-1}/(L'-1) + (\underline{F}T)^{L'}/L' \\ &= (\underline{I} + \underline{F}T\Big[\underline{I} + \underline{F}T/2(\underline{I} + \underline{F}T/3(I + \ldots. + \\ &\quad \{\underline{F}T/(L'-2)\}\{\underline{I} + [\underline{F}T/(L'-1)](I + \underline{F}T/L')\}))\Big])\end{aligned} \tag{3.15}$$

$$\begin{aligned}\underline{B} &= T(\underline{I} + \underline{F}T/2\Big[I + \underline{F}T/3(\underline{I} + \ldots\ldots + \\ &\quad \{\underline{F}T/(L'-2)\}\{I + [\underline{F}T/(L'-1)](\underline{I} + \underline{F}T/L')\})\Big])\ \underline{G_c}\end{aligned} \tag{3.16}$$

The solution for $\underline{C}$ is similar to that of $\underline{B}$, with $\underline{G_D}$ in place of $\underline{G_c}$. Starting with the innermost factor the number of terms, L', of the series approximation must be decided beforehand. As equations (3.15) and (3.16) are very similar, the computer evaluation of both series can be combined in a single routine.

In calculating the values of the $\underline{A}$, $\underline{B}$ and $\underline{C}$ matrices the non-dimensionalised hydrodynamic coefficients are first of all converted to their dimensionalised equivalents. These are then used to calculate $\underline{F}$, $\underline{G_c}$ and $\underline{G_D}$ in the state space equations. Equations (3.15) and (3.16) are then used to obtain the $\underline{A}$, $\underline{B}$ and $\underline{C}$ matrices which form the basis of the mathematical model of the ship. The computer routine for converting from continuous to discrete time is attributed to Cadzow and Marten (1970).

3.3 The Non-Linear Model

For the purposes of this research project it was hoped that the quasi-linear model would be sufficient. Indeed the result of the open loop test runs given in chapter 5 show some compatability with actual ship data. Closer examination however shows that, particularly in a tight turn, the quasi-linear model results did not always compare favourably with the data available from similar tests carried out with an actual ship. The ship chosen for the early simulation work was of the Mariner Class since much work has been done on this hull form and it was possible to compare computer simulation results with full scale data which was readily available from a very comprehensive study by Morse and Price (1961).

Abkowitz (1964) suggests that the Taylor expansion of hydrodynamic forces and moments should be expanded to include terms up to the third order whereas Strom-Tejsen (1965) has made a detailed study of the important non-linear terms and recommended including rv^2, v^3, δv^2 and δ^3 terms, the first term being the most important. Lewison (1973) and Gill (1976) (1977), both included non-linear terms in the equations, although Thom (1980) pointed out that the type and number of the higher order terms are still under discussion.

Taking into account the results of open loop tests on the quasi-linear model together with the above references it was decided to include non-linear terms in the equations. By including terms in v^2, r^2, $\delta_A{}^2$ and $n_A{}^2$ in the X equation, and terms in v^3, rv^2, $\delta_A{}^3$ and $\delta_A v^2$ in the Y and N equations it was found that digital computer simulations using the hydrodynamic coefficients for a Mariner hull compared well with the data given by Morse and Price (1961). Results of the Open Loop Tests on the non-linear model and comparisons with the Morse and Price data are given in Chapter 5.

It was still assumed however that course and speed were constant during each sample time, the state transition, control and disturbance matrices being recalculated during this period, and then used in the next set of calculations. Whilst these calculations presented no difficulty in the digital computer simulations using the Prime main frame computer, they did pose problems when designing a suitable filter for installation in the physical model. These non-linear equations then formed the basis for most of the computer simulation work carried out. The equations were used to model the ship and also in the computer simulation of the ship in the optimal filter. The equations of motion then become:-

$$m\dot{u} - mrv = X_{\dot{u}}\dot{u} + X_u(u+u_c) + X_{uu}u^2 + X_{uuu}u^3 + \overline{X}_{vv}v^2 + \overline{X}_{rr}r^2 + \overline{X}_{\delta\delta}\delta_A^2$$
$$+ \overline{X}_{un}un_A + \overline{X}_{nn}n_A^2 + X_{u\alpha}u_\alpha \tag{3.17}$$

$$m\dot{v} + mru = Y_{\dot{v}}\dot{v} + Y_v(v+v_c) + Y_{\dot{r}}\dot{r} + Y_r r + Y_\delta\delta + Y_n n_A + \overline{Y}_{vvv}v^3$$
$$+ \overline{Y}_{rvv}rv^2 + \overline{Y}_{\delta\delta\delta}\delta_A^3 + \overline{Y}_{\delta vv}\delta_A v^2 + Y_{v\alpha}v_\alpha \tag{3.18}$$

$$I_z\dot{r} = N_{\dot{v}}\dot{v} + N_v(v+v_c) + N_{\dot{r}}\dot{r} + N_r r + N_\delta\delta_A + N_n n_A + \overline{N}_{vvv}v^3$$
$$+ \overline{N}_{rvv}rv^2 + \overline{N}_{\delta\delta\delta}\delta_A^3 + \overline{N}_{\delta vv}\delta v^2 + N_{v\alpha}v_\alpha \tag{3.19}$$

where $\overline{X}_{uu} = (1/2)X_{uu}$, $\overline{X}_{uuu} = (1/6)X_{uuu}$ and similarly for other terms in X,Y, and N.

Using the same process as that used in the development of the quasi-linear model the state equations become:-

$$\dot{\delta}_A = (-1/T_R)\delta_A + (1/T_R)\delta_D \tag{3.20}$$

$$\dot{n}_A = (-1/T_N)n_A + (1/T_N)n_D \tag{3.21}$$

$$\dot{x} = u \tag{3.22}$$

$$\dot{u} = X_1\delta_A + X_2n_A + X_4u + X_6v + X_8r + X_{w1}u_c + X_{w3}u_\alpha \tag{3.23}$$

$$\dot{y} = v \tag{3.24}$$

$$\dot{v} = B_1\delta_A + B_2n_A + B_4u + B_6v + B_8r + B_{w2}v_c + B_{w4}v_\alpha \tag{3.25}$$

$$\dot{\psi} = r \tag{3.26}$$

$$\dot{r} = C_1\delta_A + C_2n_A + C_4u + C_6v + C_8r + C_{w2}v_c + C_{w4}v_\alpha \tag{3.27}$$

The X, B, and C coefficients are summarised in Appendix 3. As with quasi-linear terms of equation set (3.7) they are derived from the hydrodynamic coefficients of the vessel. Equations (3.20) to (3.27) can then be expressed in matrix form as:-

$$\begin{bmatrix} \dot{\delta}_A \\ \dot{n}_A \\ \dot{x} \\ \dot{u} \\ \dot{y} \\ \dot{v} \\ \dot{\psi} \\ \dot{r} \end{bmatrix} = \begin{bmatrix} -1/T_a & 0 & 0 & 0 & 0 & 0 & 0 & 0 \\ 0 & -1/T_N & 0 & 0 & 0 & 0 & 0 & 0 \\ 0 & 0 & 0 & 1 & 0 & 0 & 0 & 0 \\ X_1 & X_2 & 0 & X_4 & 0 & X_6 & 0 & X_8 \\ 0 & 0 & 0 & 0 & 0 & 1 & 0 & 0 \\ B_1 & B_2 & 0 & B_4 & 0 & B_6 & 0 & B_8 \\ 0 & 0 & 0 & 0 & 0 & 0 & 0 & 1 \\ C_1 & C_2 & 0 & C_4 & 0 & C_6 & 0 & C \end{bmatrix} \begin{bmatrix} \delta_A \\ n_A \\ x \\ u \\ y \\ v \\ \psi \\ r \end{bmatrix} +$$

$$\begin{bmatrix} 1/T_a & 0 \\ 0 & 1/T_N \\ 0 & 0 \\ 0 & 0 \\ 0 & 0 \\ 0 & 0 \\ 0 & 0 \end{bmatrix} \begin{bmatrix} \delta_D \\ n_d \end{bmatrix} + \begin{bmatrix} 0 & 0 & 0 & 0 \\ 0 & 0 & 0 & 0 \\ X_{w1} & 0 & X_{w3} & 0 \\ 0 & 0 & 0 & 0 \\ 0 & B_{w2} & 0 & B_{w4} \\ 0 & 0 & 0 & 0 \\ 0 & C_{w2} & 0 & C_{w4} \end{bmatrix} \begin{bmatrix} u_c \\ v_c \\ u_a \\ v_a \end{bmatrix} \qquad (3.28)$$

Equation set (3.28) represents the form used in computer simulations using data to represent a Mariner hull and later a twin screw car ferry. The hydrodynamic coefficients for the car ferry were obtained by carrying out a series of tests on a four metre model loaned from the National Maritime Institute in Feltham, London. Five models were used in the research programme. These were the quasi-linear and non-linear computer models based upon data from a full scale Mariner hull, a full scale non-linear model of the car ferry, a reduced non-linear computer model of the physical car ferry model, and the physical car ferry model itself. For ease of reference these have been given the names of some of the ships in which the author served. They are:-

TRELEVEN:	Quasi-linear full scale computer model of Mariner class hull
VIGILANT:	Non-linear full scale computer model of Mariner class hull
TREMAYNE:	Non-linear full scale computer model of twin screw car ferry
HEATHMORE:	Non-linear reduced computer model of car ferry model
CENTAUR:	Physical model of twin screw car ferry.

In the Open Loop Tests of Chapter 5 the data is compared with data from the USS COMPASS ISLAND, a Mariner Class ship which was in service with the United States Navy.

3.4 The Reduced Non-Linear Model

In the design of a suitable filter and controller for the physical model (CENTAUR) it became necessary to simplify the eight state mathematical model. This was mainly due to the memory limitations in the micro-computer to be used. A further restriction was the need to recalulate the state transition, disturbance and control matrices during each sample time. First thoughts were to consider those states to be measured in the Centaur model, namely heading, yaw rate, forward and lateral accelerations. However this posed problems in obtaining a suitable set of equations to be used on the computer model in the filter. Eventually it was decided to use forward and lateral velocities in place of the accelerations. In practice velocities would be obtained by integration. Due to the very small time constants involved the rudder and main engine models were ignored so that δ_A and n_A made up the control vector.

This led to the following reduced model:-

$$\begin{bmatrix} \dot{u} \\ \dot{v} \\ \dot{\psi} \\ \dot{r} \end{bmatrix} = \begin{bmatrix} X_4 & X_6 & 0 & X_8 \\ B_4 & B_6 & 0 & B_8 \\ 0 & 0 & 0 & 1 \\ C_4 & C_6 & 0 & C_8 \end{bmatrix} \begin{bmatrix} u \\ v \\ \psi \\ r \end{bmatrix} + \begin{bmatrix} X_1 & X_2 \\ B_1 & B_2 \\ 0 & 0 \\ C_1 & C_2 \end{bmatrix} \begin{bmatrix} \delta_A \\ n_A \end{bmatrix} + \begin{bmatrix} X_{w1} & X_{w3} & 0 & 0 \\ 0 & 0 & 0 & 0 \\ 0 & 0 & 0 & 0 \\ 0 & 0 & C_{w2} & C_{w4} \end{bmatrix} \begin{bmatrix} u_c \\ u_a \\ v_c \\ v_a \end{bmatrix} \tag{3.29}$$

In the use of Kalman Filter techniques a mathematical model of the system is required in the filter. The model given in equation set (3.29) (HEATHMORE), was also the basis of the computer model used in the Kalman Filter in the physical model (CENTAUR). The X, B, and C coefficients are the same as those used in equation set (3.28).

3.5 Discrete Form of the Equations.

Using equations (3.15) and (3.16) the continuous time set of first order differential equations (3.20) to (3.27) are transformed in to discrete time difference equations. These equations are set out for ease of reference as :-

$$\delta_A(k+1) = A_{11}\,\delta_A(k) + B_{11}\,\delta_D(k) \tag{3.30}$$

$$n_A(k+1) = A_{22} n_A(k) + B_{22} n_D(k) \tag{3.31}$$

$$x(k+1) = A_{32} n_A(k) + A_{33} x(k) + A_{34} u(k) + B_{32} n_D(k) + C_{31} u_c(k) + C_{33} u_a(k) \tag{3.32}$$

$$u(k+1) = A_{42} n_A(k) + A_{44} u(k) + B_{42} n_D(k) + C_{41} U_c(k) + C_{43} U_a(k) \tag{3.33}$$

$$y(k+1) = A_{51} \delta_A(k) + A_{55} y(k) + A_{56} v(k) + A_{58} r(k) + B_{51} \delta_D(k) + C_{52} v_c(k) + C_{54} v_a(k) \tag{3.34}$$

$$v(k+1) = A_{61} \delta_A(k) + A_{66} v(k) + A_{68} r(k) + B_{61} \delta_D(k) + C_{62} v_c(k) + C_{64} v_a(k) \tag{3.35}$$

$$\psi(k+1) = A_{71} \delta_A(k) + A_{76} v(k) + A_{77} \psi(k) + A_{78} r(k) + B_{71} \delta_D(k) + C_{72} v_c(k) + C_{74} v_a(k) \tag{3.36}$$

$$r(k+1) = A_{81} \delta_A(k) + A_{86} v(k) + A_{88} r(k) + B_{81} \delta_D(k) + C_{82} v_c(k) + C_{84} v_a(k) \tag{3.37}$$

Equations (3.30) to (3.37) now make up the matrix equation (3.14). All eight equations are used in the full scale computer simulations discussed in Chapters 5, 6 and 7. Only equations (3.32), (3.35), (3.36) and (3.37), in slightly amended form were used in the reduced non-linear model of equation sets (3.29) and (8.1).

CHAPTER 4

INTEGRATED NAVIGATION SYSTEMS

4.1 Brief Survey of Marine Electronic Navigation Systems.

The development of modern electronic navigation systems dates from the period 1939-45. It was to meet the exacting demands of World War II, writes Fennessy (1979), that a dramatic phase of development took place. This development was to form the basis of many of the systems in use today. Jones (1975), in a Duke of Edinburgh Lecture to the Institute of Navigation, outlined a number of systems which were developed in America, Germany and the United Kingdom, some of which were the forerunners of today's navigation aids. The direct measurement of range using electro-magnetic waves depends upon accurate measurement of the time taken for the radio signal to travel from transmitter to receiver. Prior to the development of frequency standards and atomic oscillators such measurement for a ship-shore system was impractical and hence the early systems tended to measure the difference in the time of arrival of two radio signals and thus position fixes were related to hyperbolic position lines. The Loran system was an early example of a hyperbolic position fixing system. Loran A was developed in the U.S.A. and was in use during World War II. In the United Kingdom Naval scientists developed what was to be known as the Decca Navigator; this was used by ships in D-Day landings of 6 June 1944. The Decca Navigator transmits continuous waves with the on-board receiver measuring the phase difference between the two radio signals. Both were in commercial use shortly after the end of hostilities. Since 1945 the use of navigation aids has steadily increased; whilst in the period since 1970, with the appearance of mini-computers and microprocessors, the growth has been more spectacular. This has been paralleled by decreasing costs due mainly to strides in semi-conductor technology.

A number of individual systems are now available to the commercial operator, and each has its advantages and disadvantages. The Omega system, for example, provides world — wide coverage, but is insufficiently accurate for inshore navigation. The Decca Navigator is sufficiently accurate for coastal navigation, but accuracy falls off with increasing range, due mainly to skywave interference. Furthermore each chain covers a relatively small area; hence a large number of Decca chains would be necessary to cover all the world's coastal areas, whereas the Transit Satellite System is sufficiently accurate for survey work, but the time between satellite passes makes it unsuitable for coastal navigation.

A typical fit in a British Merchant Ship would comprise a gyro compass with autopilot and repeater compasses, electromagnetic, pressure and/or Doppler log, Decca Navigator, Loran C together with Omega and/or the Transit Satellite Navigation System. This would give the navigator reasonable world-wide coverage and sufficient accuracy. Radar and a direction finder would also be fitted (these are legal requirements in British ships over 1600 gross registered tons). It is likely that an Automatic Radar Plotting Aid would also be included.

The Decca Navigator is a hyperbolic position fixing system providing accurate fixes for coastal navigation. The system is organised into chains, each comprising a master and usually three slave transmitters, providing a coverage of up to at least 240 nautical miles from the master transmitter. There are now some 50 operational chains throughout the world. Decca transmissions are between 70 and 130kHz. The system is still regarded by many as the most accurate, widely fitted system for inshore use but it has limited world-wide coverage and accuracy does fall off with range.

Loran C operates at 100kHz. It is a pulsed hyberbolic system managed and operated by the U.S. Coast Guard, with ground wave coverage over large parts of the northern hemisphere. It is the primary civil navigation system for the U.S. coastal confluence zone. The system is organised into chains and one station, the master, transmits first in a sequence. Each slave station (there are up to four in a chain) is synchronised with the master and transmits at a precise interval after the master. This coding delay, which is different for each slave in the chain, ensures that the signals from transmitters arrive everywhere in the coverage area, in a known sequence.

Omega is a very low frequency hyperbolic system which now provides continuous global coverage for ships and aircraft. Coverage is not only global but is also redundant with more than the minimum required signals available at any location. Receivers range from simple phase comparison units to fully automatic receivers which read out latitude and longitude.

The Navy Navigation Satellite System, or Transit, was developed initially for the U.S. Navy. It became available to non-military users in 1967. Each satellite transmits at 150 and 400MHz and the shipboard receiver measures Doppler shift to determine the relative velocity between satellite and receiver. Use is made of hyperbolic navigation and transferred position line principles to determine the ship's position so that only a single satellite is required for a fix. A single frequency receiver is adequate for most marine navigational purposes, but for highly accurate position fixing a dual frequency receiver is required. Such uses include hydrographic survey, land survey and the accurate positioning of off-shore platforms. For marine coastal navigation the limitation of Transit is the time interval between satellite passes, which can be several hours in some parts of the world.

The advent of Navstar or Global Positioning System (G.P.S.) may well make all other position fixing systems redundant as this satellite based system promises to give world wide cover with a high degree of accuracy. The state of development is described by Cook (1983) who suggests positional errors of less than 20 metres will be achieved. Henderson and Strada (1980) give details of a small scale sea trial in which a mean distance between the GPS solution and the navigator's plot of 25.3 metres was claimed for passages in and out of San Diego Naval Base in the United States. However, serious questions have been raised in the U.S.A. concerning GPS implementation and O'Sullivan (1982) states that it will be well into the 1990's before commercial users are allowed access.

There is then no single system in operation which will meet the requirements for a world-wide coverage with the required accuracy. Sage and Luse (1983) give the deficiencies for three systems, namely Transit, Omega and Loran. In the Transit satellite system for example the interval between fixes varies from 0.5 to 12 hours according to geographical position. Omega has a fix accuracy of only 2 to 4 nautical miles(rms). Thus while both of these systems give worldwide coverage they are both unsuitable for coastal navigation or pilotage. Other systems such as Loran C and the Decca Navigator give good accuracy at the centre of the chain, but the accuracy degrades with distance and time of day. These points serve to illustrate how the shipowner has often been left with a difficult choice when choosing suitable navigation aids. To further complicate the problem the choice has often been governed by political and financial considerations, rather than on sound technological judgements.

Single system deficiencies have led to the development of integrated systems of which there are now several on the market. For example Sage and Luse (1983) describe the use of a Kalman Filter to combine Omega and Transit, or Omega and Loran C in an improvement of fix accuracy, while Racal have recently announced a combined Decca Navigator, Loran C, Omega and Transit receiver. Most of these systems use filtering techniques to reduce measurement and disturbance errors. Before proceeding further it is necessary therefore to define the errors to be encountered in navigation fixes.

4.2 Systematic Errors

The measured values of position and velocity will be contaminated with noise, which may have been generated in the transmitter, receiver or in the propagating medium. The total error, made up of systematic and random components is then defined as the difference between the measured and true values.

Systematic errors are constrained by some physical law and may be expressed as a mathematical function of appropriate variables. The simplest systematic errors are constant functions such as improper lane entry in the Decca Navigator, or an uncorrected error in the gyro compass. More complex systematic errors, such as the propagation errors in the Omega system, are functions of time, atmospheric conditions and the relative positions of tramsmitter and receiver.

The correction of systematic errors is governed by knowledge of the physical law affecting the system. They may be removed by either applying a correction to the erroneous display, as in the gyro compass error, or calibrating the display, as would be the case in hydrographic survey work. For the vast majority of navigational purposes the systematic errors may be approximated and generalised for a large area or for a long time period. An example of this is the fixed error correction charts produced for the Decca Navigator. For accurate navigational fixing and hydrographic survey work the systematic errors must be applied more rigorously and re-calibration of instruments must be undertaken at frequent intervals.

4.3 Random Errors

Random errors arise from such causes as minute-to-minute changes in atmospheric conditions, short term phase changes in the equipment and errors in readings. They do not obey any physical law and can only be defined by the laws of probability. For navigational systems it is assumed that the distribution of random errors about the true value is Gaussian. The Decca Navigator Co. Ltd. (1976) state, for example, that an analysis of observations at monitor stations has shown that the random errors are disposed about the mean value in a very similar manner to the Gaussian distribution. The same reference goes on to state that 95% of observations are within twice the standard deviation, whilst the Decca distribution contains 75% of observations within the standard deviation. This means that fewer large errors appear in the tails of the Decca distribution than in the Gaussian, although for statistical working a normal distribution is assumed.

Position fixing systems, by definition, require the crossing of at least two position lines. A statistical treatment is then used which indicates the area around a fix in which the navigator can state that he is in with some predetermined level of certainty. Standard deviations are then used to produce an error ellipse, a diamond of error or a circle of probable error. The error ellipse is the most accurate, but the root mean square error criterion is now widely used for individual system errors.

$$d_{rms} = \sqrt{a^2 + b^2}$$

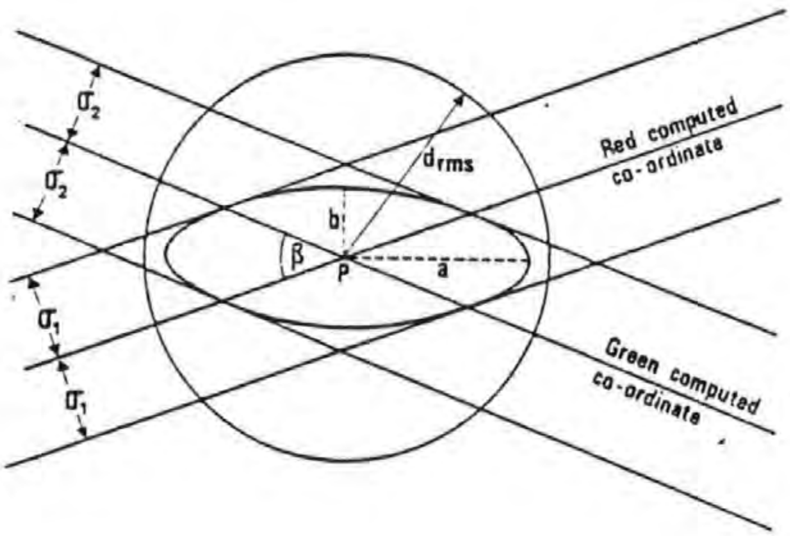

Figure 4.1 Relationship Between Error Ellipse and RMS Error

Figure 4.1 (The Decca Navigator (1976)), shows the computed position lines passing through the observation point P. The parallelogram formed by the displaced position lines would contain 68.26% x 68.26% = 46.6% of a large number of fixes taken at P. The circle drawn about P of radius equal to the r.m.s. error would contain approximately 68% of the plots, the exact percentage being dependent on the ratio of the major to the minor axis of the ellipse enclosed by the parallelogram. For the purposes of this research programme the root mean square error and the circle of error are used in connection with position fixing systems. Figure 4.2 shows the variations in one lane of a Decca Navigator for a night sample period.

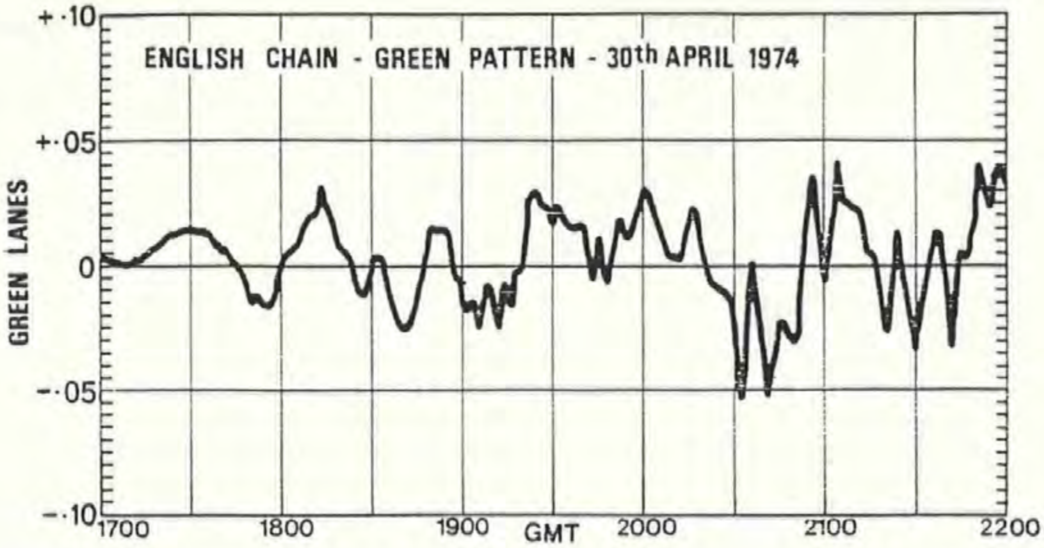

Figure 4.2 Variation of Decca Readings

4.4 Integration of Navigational Data

It has already been suggested that single system deficiencies have led to the development of integrated systems for world-wide use. In shore, particularly in the approaches to a port, and in the development of off-shore energy resources, there is a much greater need for accurate navigational data, giving a further impetus to the development of integrated systems. If it is assumed that the systematic errors can be allowed for then the requirement in an integrated system is to minimise in some way the random errors. A Gaussian distribution gives the best general fit for the spread of random errors and this implies a definition of these errors in terms of standard deviations or root mean square errors. As variance is the square of standard deviation the problem can be stated in terms of minimising the variance, which has led to the use of minimum variance or Kalman-Bucy filters. These have been developed extensively for aerospace, and latterly marine, navigation since the publication of the original work by Kalman and Bucy (1961).

During the 1950 s control engineering had developed to the point that state space techniques implemented in the statistical environment of "maximum likelihood" had yielded complementary mix type filters with variable gains. A detailed analysis showed that the performance of the complementary mix filters was tending asymptotically to a level of performance that was estimated to be an order of magnitude below that required in the Control and Guidance subsystem for the Apollo programme.

From the information theory viewpoint it became obvious that to achieve improvements of an order of magnitude it was necessary to supply the control process with significantly more information; to allow the control process to operate on information gathered during real-time operation rather than to operate only on assumptions made by the design engineer prior to the process; to remove limitations on the information processing power of the control process by allowing almost unlimited real-time computing power; and to maintain the maximum likelihood nature of the control process.

The Kalman Filter algorithm and engineering practices that are inseparable from the filter meet all the above requirements and was successfuly implemented on the Apollo project. The theory took tangible form in 1960 and a Kalman Filter was in operational use in 1963. Further developments saw its use in long range missiles, later still in military aircraft, and then in medium and short range missiles. The techniques have now been developed for commercial systems and are finding increasing use in marine vehicles, both for general navigation in Integrated Navigation Systems and in specialist vessels for such uses as hydrographic survey. Grimble et al (1980 b and c) describe the use of Kalman filtering techniques in dynamic ship-positioning systems used in the off-shore oil industry.

4.5 The Kalman Filter.

The precise form of the information supplied to the Kalman Filter is:-

i) A knowledge of the system error sources. Whereas complementary filters attempt to minimise the effect of error sources, termed state-variables, the model reference filter attempts to identify the coefficients of terms in an error model and calculate, hence nullify, their effect.

ii) A knowledge of the dynamical relationship between error sources. The concept which made the Kalman Filter implementable where more general methods had failed was the decision to enforce linearity on the error dynamics. In other words the dynamical relationship between error sources is assumed to be expressible in terms of a set of first-order linear differential equations.

iii) A knowledge of the form and the magnitude of random uncertainties within the system being controlled. The two categories of uncertainties are random disturbances which modify the state of the system, sometimes termed "system noise" or "plant noise", and random noise which corrupts observation of the state of the system and is usually termed "measurement noise". The information about the magnitude and form of system and measurement noise is presented continuously to the filter in the form of arrays whose diagonal terms contain a measure of the expected magnitude of the random effects (variances) and whose off-diagonal terms contain a measure of the expected dependence or correlation of the error sources on one-another (covariance). These arrays are termed covariance matrices.

Thus a great deal of information is being supplied to the control process and it is not surprising that a process which is capable of capitalising on this information produces significantly better results than those previously available. Kalman was able to capitalise on the information with a process that is both maximum likelihood and implementable in real-time using reasonable computing power.

4.6 The Nature of the Kalman Filter

Scovell et al (1980) describe the filter as a model reference, linear, simultaneous minimum variance, infinite memory, recursive, digital estimation technique. They explain these terms as:-

i) Model reference. The filter is characterised by containing a dynamical model of system errors.

ii) Linear. This model is expressible as a set of first-order linear differential equations.

iii) Simultaneous minimum variance. Kalman originally termed the procedure that he developed "maximum likelihood" and constrained the random effects to be normally distributed, sometimes termed Gaussian. He then invoked a theorem which states that the minimum variance procedure operating on Gaussian random effects is maximum likelihood and went on to develop a minimum variance procedure.

The term "Simultaneous" is included to indicate that Kalman phrased the optimisation procedure in such a way that each of the error terms (state variables) receives equal weighting, and that when information arrives which helps the filter deduce an improved estimate of the state of the system, the deduction is applied with equal vigour to each of the state variables.

iv) Infinite Memory. The Kalman Filter has the ability to remember its past mistakes, and when new information arrives the re-assessment of the values of the state-variables is made not only in the light of the new measurements, but also in the light of every previous measurement. The Kalman Filter is therefore termed "infinite memory".

v) Recursive. The power of the Kalman Filter lies very largely in the property that all the information required to make an optimal estimate at any instant is contained in a single set of variables which is updated recursively.

vi) Digital. The nature of the equations that require to be processed are such that a digital computer is essential.

From the above it is seen that the Kalman Filter takes the form of a single set of equations implemented in a digital computer and used in a recursive fashion.

4.7 The Kalman Filter Equations

The theory of the Kalman-Bucy filter is now well established, for example Medditch (1969) and Mattin (1982), and only the equations used in this research program are stated here. The system simulation and the Kalman filter have been modelled using their discrete forms. The system model is defined by the equations:-

$$\underline{x}(k+1) = \underline{A}(k+1,k)x(k)\ \underline{B}\ (k+1,k)\underline{u}(k) + \underline{C}(k+1,k)\underline{w}(k) \tag{4.1}$$

$$\underline{z}(k+1) = \underline{H}(k+1)\underline{x}(k+1) + \underline{v}(k+1) \tag{4.2}$$

Where $\underline{x}$ is the state vector; $\underline{u}$ is the control vector; $\underline{w}$ is the disturbance vector; $\underline{z}$ is the measurement vector; $\underline{v}$ is the measurement noise and $k=0,1,...,$ is the discrete time index. In addition $\underline{A}(k+1,k)$ is the state transition matrix; $\underline{B}(k+1,k)$ is the control transition matrix; $\underline{C}(k+1,k)$ is the disturbance transition matrix and $\underline{H}(k+1)$ is the measurement matrix. The term $(k+1,k)$ means calculated at time k and used in the interval k to k+1. The terms $\underline{w}(k)$ and $\underline{v}(k)$ are Gaussian noise sequences with the following first and second moments:-

$$E\left[\underline{w}(k)\right] = 0 \qquad E\left[\underline{w}(k)\underline{w}^T(m)\right] = \underline{N}\delta_{km}$$
$$E\left[\underline{v}(k)\right] = 0 \qquad E\left[\underline{v}(k)\underline{v}^T(m)\right] = \underline{M}\delta_{km}$$

and where δ_{km} is the Dirac function. The two processes are considered independent of each other and hence

$E\left[v(m)\,\omega^T(k)\right] = 0$. The state estimate $\hat{x}(k+1/k+1)$ is obtained by calculating the predicted state $\hat{x}(k+1/k)$ from

$$\underline{\hat{x}}(k+1/k) = \underline{A}(k+1,k)\underline{\hat{x}}(k/k) + \underline{B}(k+1,k)\underline{u}(k) \tag{4.3}$$

and then calculating the estimated state at the instant (k+1) using

$$\underline{\hat{x}}(k+1/k+1) = \underline{\hat{x}}(k+1/k) + \underline{K}(k+1)\left[\underline{z}(k+1)-\underline{H}(k+1)\underline{\hat{x}}(k+1/k)\right] \tag{4.4}$$

It should be noted here that the mathematical model used in the filter does not include the disturbances, or the disturbance transition matrix. However $\underline{C}(k+1,k)$ together with the disturbance noise covariance matrix $\underline{N}$ both appear in the filter gain equations below.

The Kalman gain matrix $\underline{K}(k+1)$ is obtained first by calculating the predicted error covariance matrix given by

$$\underline{P}(k+1,k) = \underline{A}(k+1,k)\underline{P}(k/k)\underline{A}^T(k+1,k) + \underline{C}(k+1,k)\underline{N}(k)\underline{C}^T(k+1,k) \tag{4.5}$$

for some initial error covariance $\underline{P}(k/k)$, and then calculating the Kalman filter gain from

$$\underline{K}(k+1) = \underline{P}(k+1/k)\underline{H}^T(k+1)\left[\underline{H}(k+1)\underline{P}(k+1/k)\underline{H}^T(k+1) + \underline{M}(k+1)\right]^{-1} \tag{4.6}$$

Finally the error covariance matrix is obtained using

$$\underline{P}(k+1/k+1) = \left[\underline{I}-\underline{K}(k+1)\underline{H}(k+1)\right]\underline{P}(k+1/k) \tag{4.7}$$

The above equations are used iteratively to obtain the state estimate at any future sampling time, given the initial state and error covariance, together with the measurement and disturbance noise covariances $\underline{M}$ and $\underline{N}$, the state, disturbance and control matrices, and the measurement matrix. Figure 4.3 gives an overall block diagram of the optimal filter. Details of the computational aspects are given in Appendix 7.

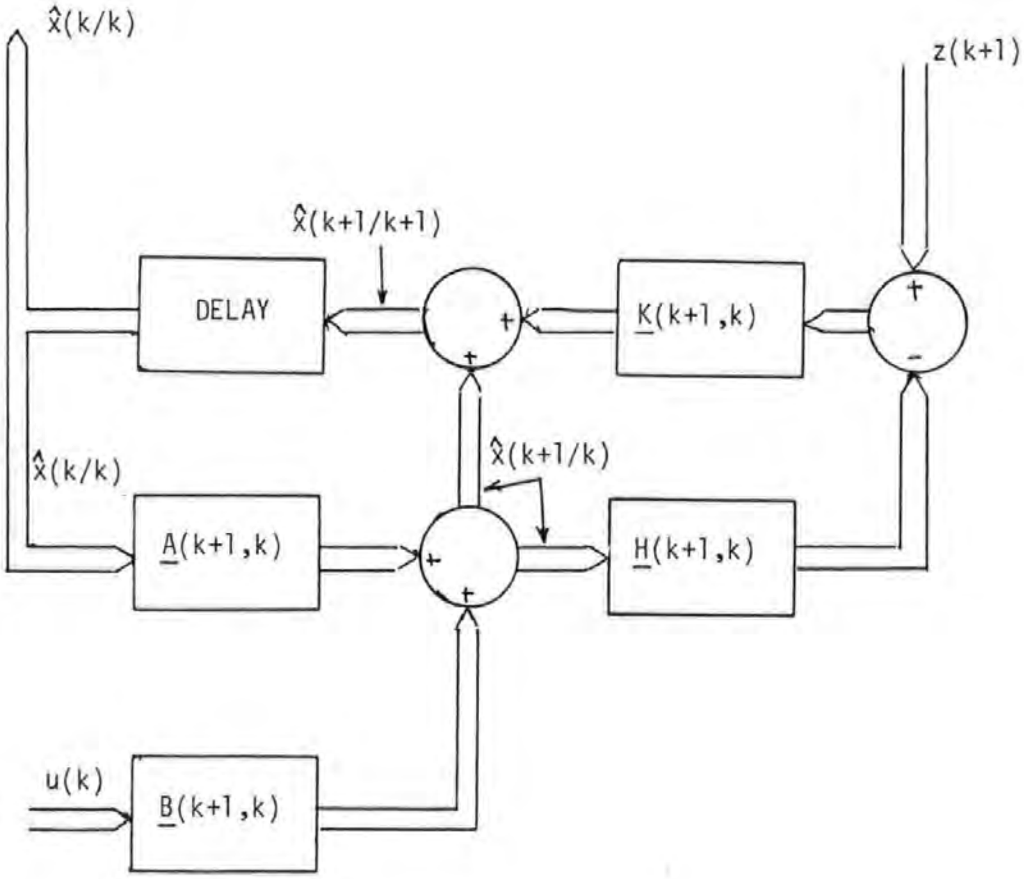

Figure 4.3 The Optimal Filter

4.8 Kalman Filter for a Non-Linear Ship Model

As the ship is a non-linear system the mathematical model used in the filter must be non-linear. It was assumed throughout that the course and speed of the vessel were constant during each sample time, with the new values being calculated during each sample period. These values were then assumed constant for the next sample period. This assumption allowed the linear Kalman filter theory to be applied, but it did mean that the transition matrices and filter gains had to be recalculated during each sample interval. This posed no problems during the computer simulations using the Prime main frame computer, but it did present difficulties during the later stages of the work when designing the software for the Texas Instruments microprocessor used in the actual model (CENTAUR) in tests on a reservoir. These problems will be dealt with in the chapter concerned with the physical model tests.

In addition to minimising variance, the Kalman filter concept implies that the disturbance noise is white with zero means. Wind and tide are taken to be made up of a fixed quantity with a random error superimposed. The random error then has a zero mean over the period of each passage in to and out of harbour. It will be shown that the addition and removal of the fixed values, referred to as mean values in the text, has little or no effect upon the filter capabilities. In the computer simulations typical values for Plymouth Sound were assumed.

The covariance matrix for the measurement noise was obtained from the standard deviations of the sensors used in the various tests. For the computer simulations it was assumed that a rudder angle indicator and revolution counter were available, together with a hyperbolic position fixing system, a doppler log to measure forward and lateral speeds, with a gyro compass and rate gyro to give heading and angular velocity. The measurement noise was assumed to have zero mean. Random number generator subroutines were used to obtain the measurement and disturbance random noise values used in the simulation.

There are two critical factors in the design of the optimal filter, firstly the modelling of the filter itself, i.e. how good is the model of the ship used in the filter, and secondly the values calculated for the matrix $\underline{K}(k+1)$. The mathematical model used in the filter software was derived from the ship's hydro-dynamic coefficients, which were obtained from published ship data, or, in the case of the physical model, by undertaking tank tests at the National Maritime Institute. Subroutines were then used to calculate the transition matrices from the data. These are described in Appendix 7.

CHAPTER 5

OPEN LOOP TESTS

5.1 Introduction

This Chapter describes work undertaken to test the validity of the mathematical model used in the digital computer simulations. This was achieved by carrying out simulations of the full scale trials for a known vessel and comparing the results with data available from actual full scale trials. The ship chosen for this early simulation work was of the Mariner Class since much work has been done on this hull form and it was possible to compare computer simulation results with full scale data which was readily available. Non-dimensional hydrodynamic coefficients for the Mariner ship used in the study are given in Appendix 4, whilst general data is given in Appendix 5. The values are based upon results from captive model tests by Strom-Tejsen (1965), Suarez (1963) and Brown and Alverstad (1974). The full scale manoeuvring data for the Mariner was obtained from a very comprehensive study by Morse and Price (1961).

The objective of the Morse and Price programme was to accumulate and analyse full scale data on the manoeuvring motions of the USS COMPASS ISLAND, a converted Merchant Ship of the Mariner Class. The task of the Compass Island was the evaluation of navigation equipment in the United States development of the Polaris submarines.

Three types of manoeuvre were carried out in the computer simulation and in each case the results were compared with those available from the full scale tests on the USS COMPASS ISLAND. The types of manoeuvre were:-

(i) Turning Circles;

(ii) Kempf Zig-Zag Manoeuvres;

(iii) Dieudonne Spiral Manoeuvres.

5.2 Turning Circles.

Turning circles are used to determine the effectiveness of the rudder to produce steady-state turning characteristics. The method of performing each manoeuvre was as follows:-

(i) Steady on approach speed and heading directly into the wind

(ii) Lay rudder over at maximum rate to specified value with no overshoot

(iii) Continue in turn for up to 540 degrees from the initial heading, at which time the run is terminated.

A number of computer simulations were carried out using a forward speed of 7.717m/s (15 knots). In each case the ship was turned to port and to starboard with the position co-ordinates recorded. For each set of conditions data was recorded for the linear full-scale computer model (URCHIN), the quasi— linear full-scale computer model (TRELEVEN), and the non-linear full-scale computer model (VIGILANT). As each of these simulations used the hydrodynamic coefficients of COMPASS ISLAND the four sets of data, including COMPASS ISLAND, were then plotted with common axes for comparison with the Morse and Price (1961) data for the USS COMPASS ISLAND. These results are shown in Figures 5.1 and 5.2.

5.3 Kempf Zig-Zag Manoeuvres

This manoeuvre provides a qualitative measure of the effectiveness of the rudder to initiate and check changes of heading. Hence the degree of overshoot of the heading angle curve (i.e. the ratio of amplitude of heading curve to amplitude of demanded rudder angle) and the phase between the two peak values are indicative of the dynamical stability and manoeuvrability of the ship.

The simulation runs were carried out at initial approach speeds of 7.717m/s (15 knots) and 5.1446m/s (10 knots) and rudder angles of 20 degrees. At the start of each simulation the demanded rudder angle was set to +20 degrees (Port) and the heading was checked every 5 seconds, with the computer program modified so that the demanded rudder changed to -20 degrees (Starboard) as soon as the heading angle amplitude exceeded the rudder angle amplitude. The process was then repeated several times to give the zig-zag manoeuvres illustrated in Figures 5.3, and 5.4.

5.4 Dieudonne Spiral Test

This manoeuvre is used to provide a qualitative measure of course stability for surface ships. The ship executes a large rudder deflection to one side, say 25 degrees to starboard. The rudder is then held in this position until a constant angular velocity is recorded. The rudder angle is then reduced to say 20 degrees starboard and held until a steady angular velocity is recorded. The process is repeated throughout the range of rudder angle from 25 degrees starboard to 25 degrees port and then from 25 degrees port back to 25 degrees starboard. The resulting plot of demanded rudder angle against constant yaw rates constitute the Dieudonne Spiral Test.

The simulation was performed at approach speeds of 7.717m/s (15 knots) and 2.5723m/s (5knots). The results for the linear and quasi—linear model are shown in Figures 5.5 and 5.6.

5.5 Discussion of Results - Linear and Quasi-Linear Models.

Figures 5.1, 5.2, 5.4, 5.5 and 5.6 show a comparison between linear, quasi-linear and actual vessels for turning circles, zig-zag manoeuvre and Dieudonne Spiral tests. In the turning circle tests it is seen that the linear model turns much tighter than the actual ship. For the spiral test it is immediately apparent that at rudder angles beyond 4 or 5 degrees the linear model becomes extremely inaccurate in a steady turn situation. In the real ship the rate of turn tends asymtotically towards a maximum value of about 0.9 degrees/second and this value cannot be extended, whatever rudder angle is applied. The linear model can however, in theory, have a higher and higher rate of turn, the more the rudder angle is increased. The real ship is also seen to have a small rate of turn when the rudder is amidships. This is a normal effect in single screw vessels due to the paddle wheel effect of the propeller. This feature is only simulated with the quasi- and non-linear models.

This shows then why only small rudder angles may be used for a linear model if reasonable accuracy is to be maintained. When subjected to a 20°/20° zig-zag manoeuvre, it is quite surprising to note that there is better agreement between the simulation and the real result than would be expected. Figure 5.4 shows the results from the zig-zag manoeuvre, as compared with the real ship. The yaw rate of the model reaches a higher value of some 1.5 degrees per second which is above the maximum value for the real ship, and because of this higher rate the overshoot is much greater, being about 8 degrees more than the real ship. For the first turn, however, the overshoot is only about 5 degrees more for the simulation than for the real ship, since the simulation is starting from zero and does not have so much time for the yaw rate to increase. It is interesting to note that the frequencies of the two results are almost exactly the same. The real ship is seen to overshoot more to port than to starboard, again due to propeller side thrust. When comparing the results obtained from the quasi-linear model with those from the actual ship, it will be seen that during turning circle manoeuvres the simulated Mariner hull turned in a tighter circle, producing a greater speed reduction and increased yaw-rate. This was not unexpected since similar results for a linear model have been obtained by Eda (1965). However when turning to port the quasi-linear model turns tighter than the linear model.

To make the yaw-rate closer to that of the real ship, additional terms must be included in the yaw equation. Abkowitz (1964) suggests that the Taylor expansion of hydrodynamic forces and moments should be expanded to include terms up to the 3rd order. Strom-Tejsen (1965) has made a detailed study of the important non-linear terms and recommends including rv^2, v^3, δv^2 and δ^3 terms, the first term being the most important.

On comparison with the real ship the propeller side thrust and moment terms Y_n and N_n were high and could afford to be reduced. These had the effect of making the ship turn tighter in a port-hand turn and less tight in a starboard-hand one. The results from the Kempf Zig-Zag manoeuvre shown in Figure 5.4 are better than expected. The periodic time for model and ship are almost identical. The effect of the propeller side thrust is to produce different positive and negative overshoot angles.

As with the turning circle manoeuvres discussed earlier, the spiral tests show the steady yaw-rate of the model is approximately double that of the actual ship, but a distinct improvement on the linear model. The intersection of the curves with the x-axis gives the rudder angle necessary for the vessel to travel in a straight line. For COMPASS ISLAND, between 0 and 1.5 degrees of starboard rudder were necessary, but for the model the value was 3 degrees, due to Y_n and N_n being too high. The hysterisis loop phenomenon, although clearly evident in the actual ship results, did not show itself in the simulation. Taking all tests together however it is seen that even with the quasi-linear model the results fall short of those for the real ship.

In a simulated 20 degree port rudder turn the steady state forward velocity was 3.357 m/s, or a 57% reduction of speed. During a similar manoeuvre, the USS COMPASS ISLAND settled down to a forward velocity of

5.15 m/s, or a 34% speed reduction. Due to the tightness of the turn the lateral velocity v and hence the drift angle, is greater than that of real ship. This increased angle of attack is the reason for the artificially low forward velocity. Strom-Tejsen (1965) recommends the use of u^2 and u^3 to be of major importance in the x-equation, together with v^3, r^2 and δ^2 terms which he suggests are of lesser importance.

5.6 Discussion of Results Non-Linear Model.

Figures 5.1 and 5.2 illustrate that even the quasi-linear model has its limitations. Reference has already been made to the full non-linear model. Figures 5.1, 5.2, 5.3, 5.7, 5.8 and 5.9 show the results of turning circle and zig-zag tests carried out on the full non-linear computer model using the hydrodynamic coefficients for the Mariner hull. Data from these open loop tests is now compared with data available from the USS COMPASS ISLAND tests.

Figure 5.1 shows turning circles for an approach speed of 7.717m/s (15 knots) with 20 degrees of rudder applied at the 'Execute Point'. For the turn to starboard both the real ship and the computer model turned in a circle of diameter close to 1000 metres. There is a great deal of similarity, and a considerable improvement over the quasi-linear turning circle, for the same approach speed and rudder angle. The non-linear full scale computer model (VIGILANT) settled down to a constant lateral speed of 0.9m/s compared with 0.85m/s for COMPASS ISLAND, Figure 5.8, whereas the yaw-rate peaks at 0.84 degrees/second after 0.6 minutes for VIGILANT compared with 0.82 degrees/second after 0.7 minutes for COMPASS ISLAND. (Figure 5.9). Figures 5.1 and 5.7 show that the times to complete a turn of 360 degrees and the steady-state forward speeds are comparable. Applying 20 degrees of port rudder at the same initial approach speed of 7.717m/s (15 knots) again shows marked similarity between the computer model and the actual ship. In particular it must be noted that the final forward speed is much closer to the actual value for the non-linear than the quasi-linear model, thus justifying the inclusion of the non-linear terms.

For the 10 degree rudder angles COMPASS ISLAND turned tighter than the VIGILANT to starboard, but VIGILANT turned tighter to port, perhaps indicating that the force and moment terms used for the single screw propeller were not quite as effective at the reduced rudder angle. However, lateral speed, yaw-rate and forward speed transients snd steady-state values were again comparable.

Turning now to the Kempf Zig-Zag results (Figure 5.3), at an initial approach speed of 15 knots VIGILANT peaks at 30 degrees to port and 25 degrees to starboard, with COMPASS ISLAND peaking at 32 degrees to starboard and 28 degrees to port with a periodic time of 3 minutes for TREMAYNE and 3.35 minutes for COMPASS ISLAND. At a 10 knot initial approach speed VIGILANT peaked at 28 degrees to port and 25 degrees to starboard with a periodic time of 4.16 minutes, whereas COMPASS ISLAND peaked at 27 degrees to port and 25 degrees to starboard with a periodic time of 4.5 minutes.

5.7 Conclusions

It has already been stated that the linear model was inadequate for the work undertaken, and that the quasi—linear model showed certain limitations. For the non-linear model (VIGILANT) there were still some discrepancies, particularly at the lower speeds and rudder angles. Looking at the results overall however there was sufficient similiarity to justify using this model in the computer simulations using the main frame computer. It must be born in mind that this thesis is concerned with the use of filter techniques to minimise noise. As such, one of the criteria is to produce a good replica of the system in the filter. It must also be pointed out that no allowance was made for shallow water effects in any mathematical model.

Finally the errors in the measurements made in the USS COMPASS ISLAND have to be considered. Position was plotted using a Dead Reckoning Tracer and forward speed measurements were obtained from the electro-magnetic log. Although an inertial system was used there would have to be some instrumentation error. Other factors which have to be considered are the wind and tide, which although minimal would have some effect. Each of these would contribute to larger differences between actual and computer model readings at slower speeds and smaller rudder angles. This is borne out by the experimental results.

Taking all these points into consideration and looking at the Open loop Tests as a whole there is sufficient similarity to justify use of the non – linear model in the main frame computer simulations which formed a major part of the thesis. Once a reasonable mathematical model of the ship was established this was used both to simulate the ship and as the mathematical model of the ship in the Kalman Filter. As long as the two models were reasonably correct they would satisfy the requirements of the research programme.

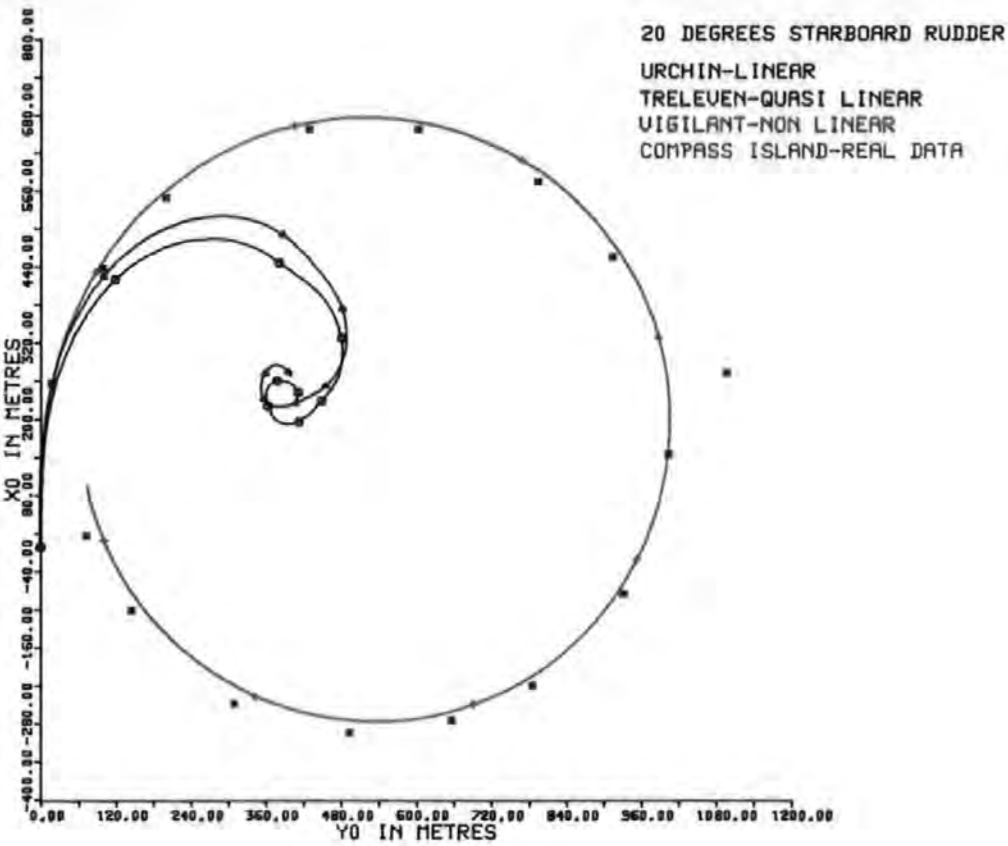

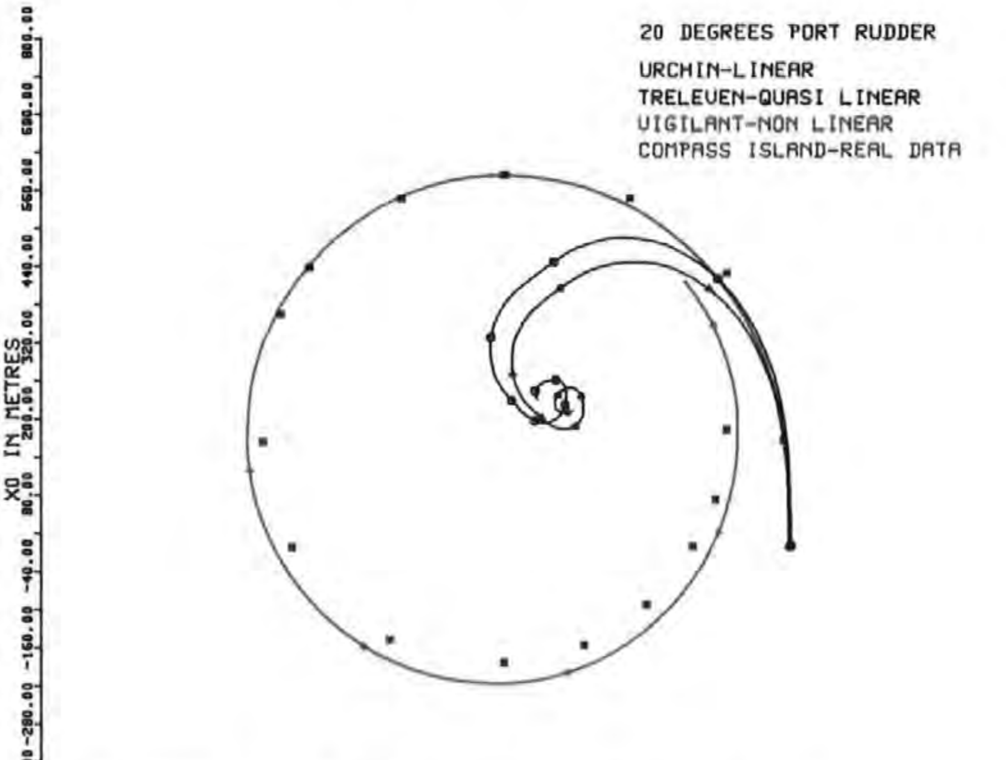

FIG 5.1 TURNING CIRCLES AT 15 KNOTS APPROACH SPEED

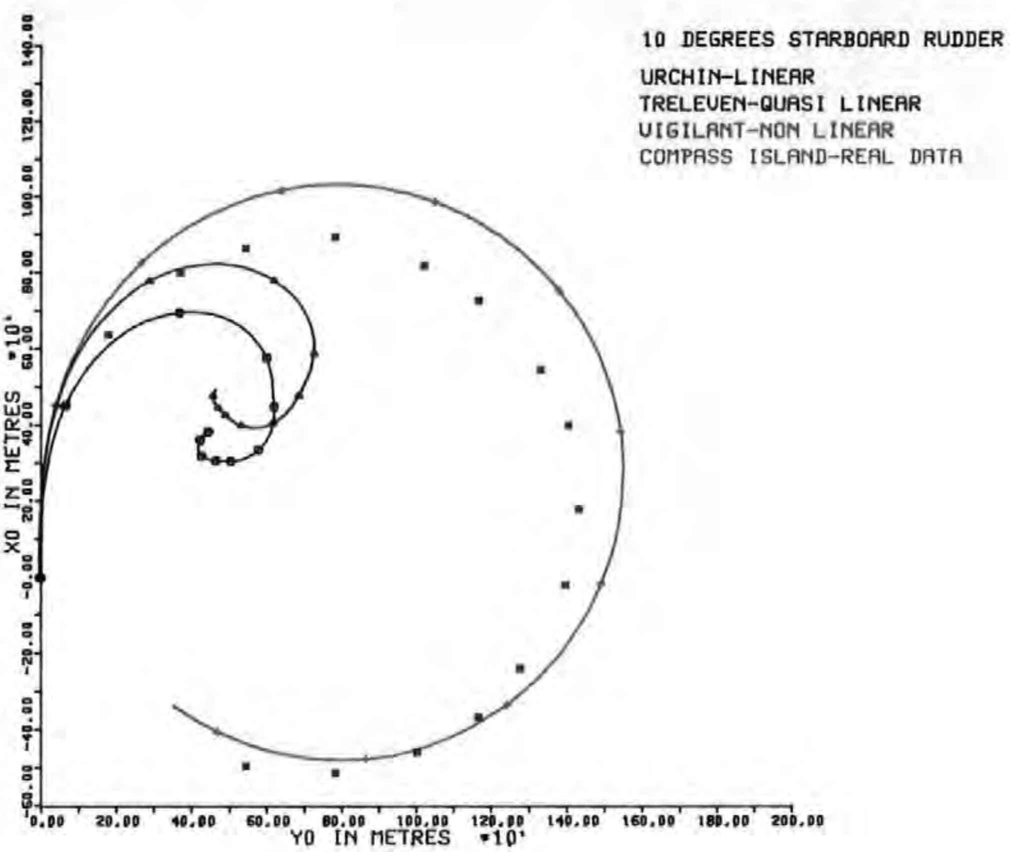

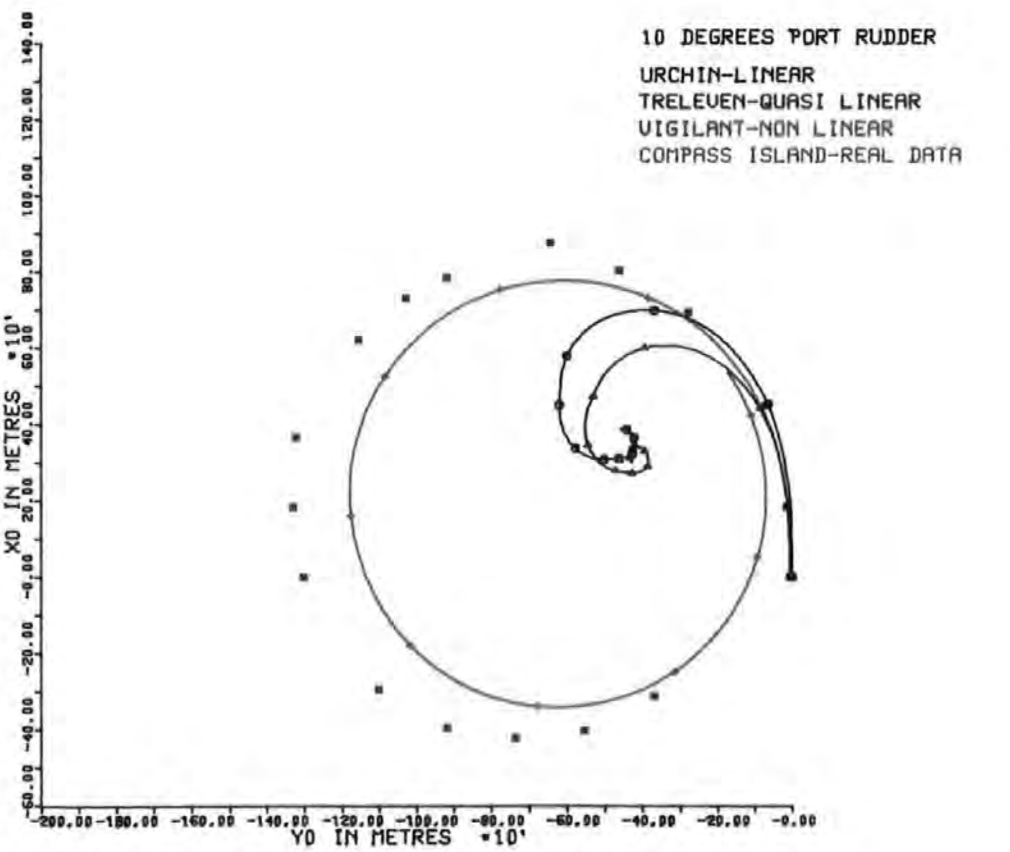

FIG 5.2 TURNING CIRCLES AT 15 KNOTS APPROACH SPEED

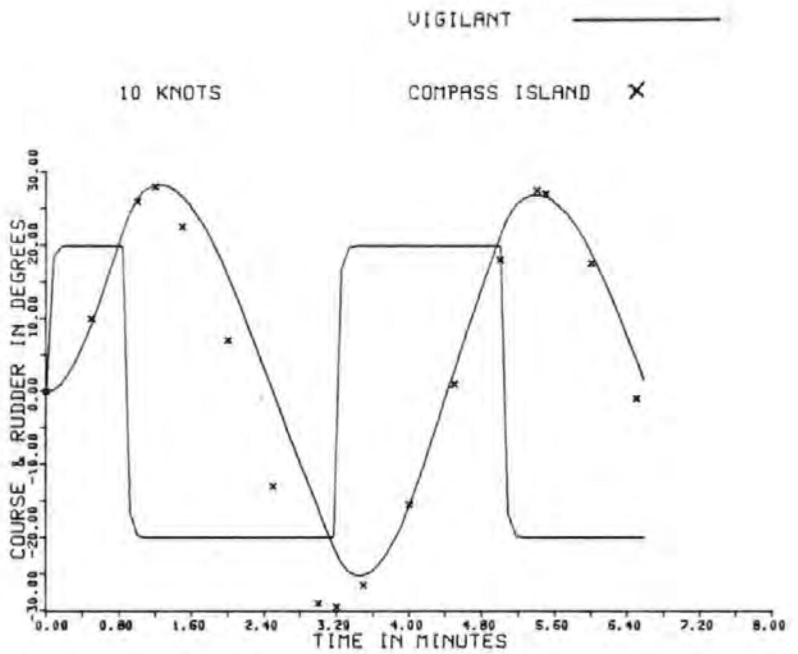

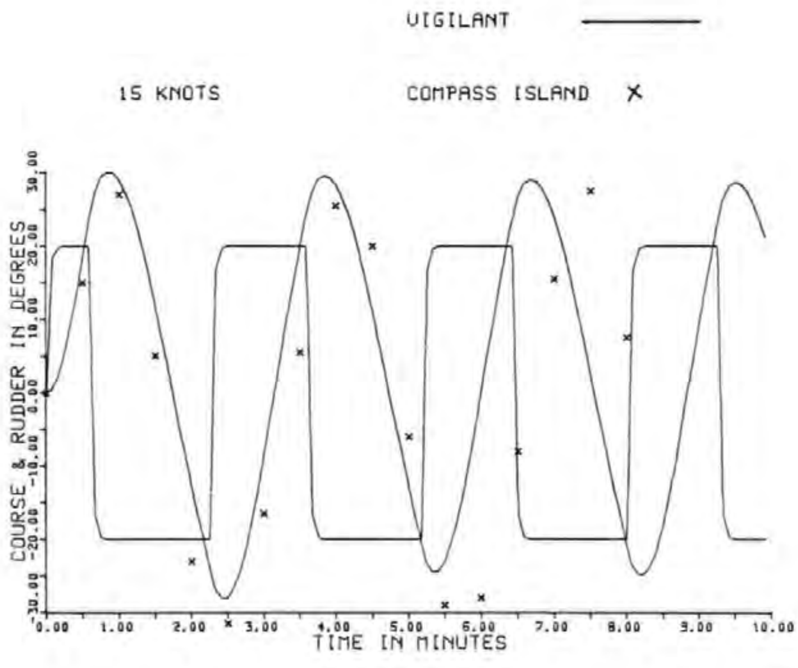

FIG 5.3 ZIG ZAG MANOEUVRES

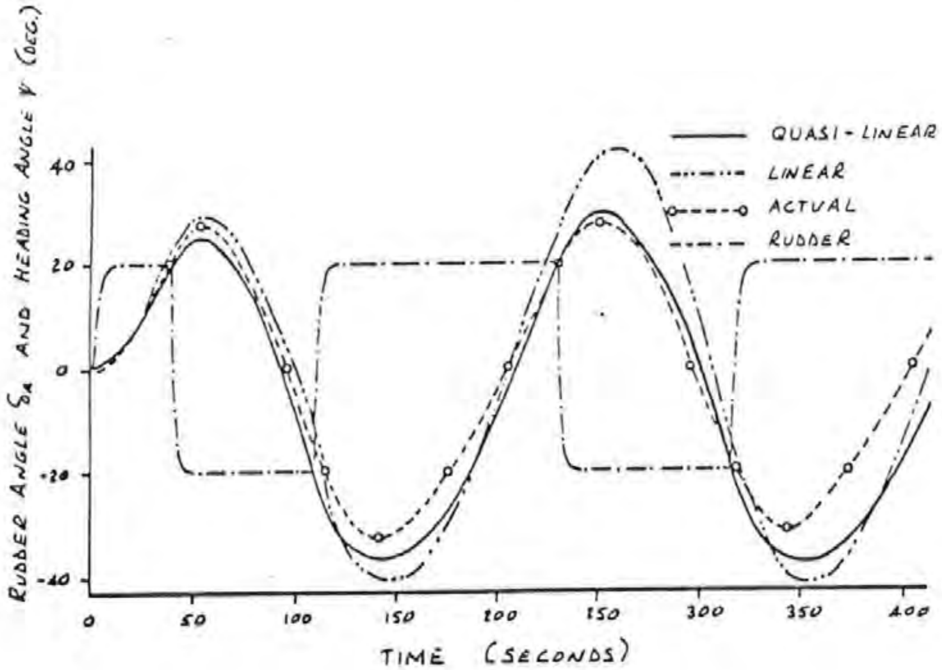

Figure 5.4 Zig Zag Manoeuvre at 15 Knots

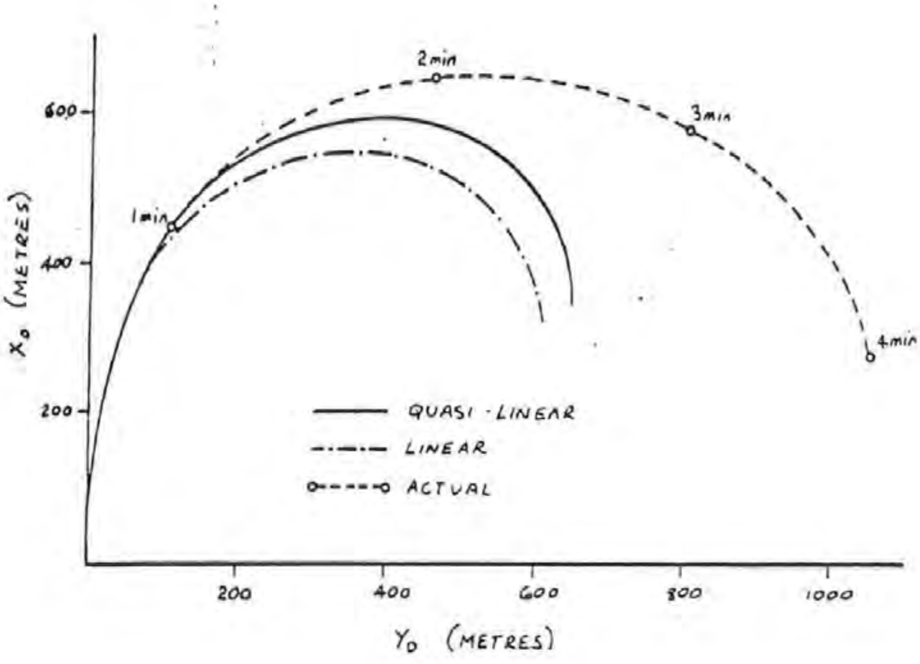

Figure 5.4a Turning Circles at 15 knots

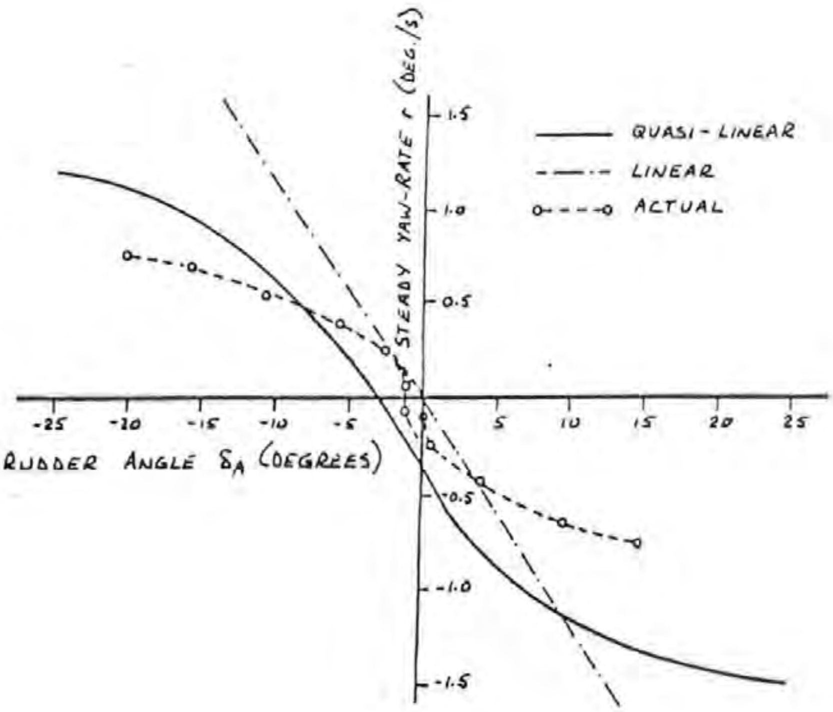

Figure 5.5 Dieudonne Spiral at 15 Knots

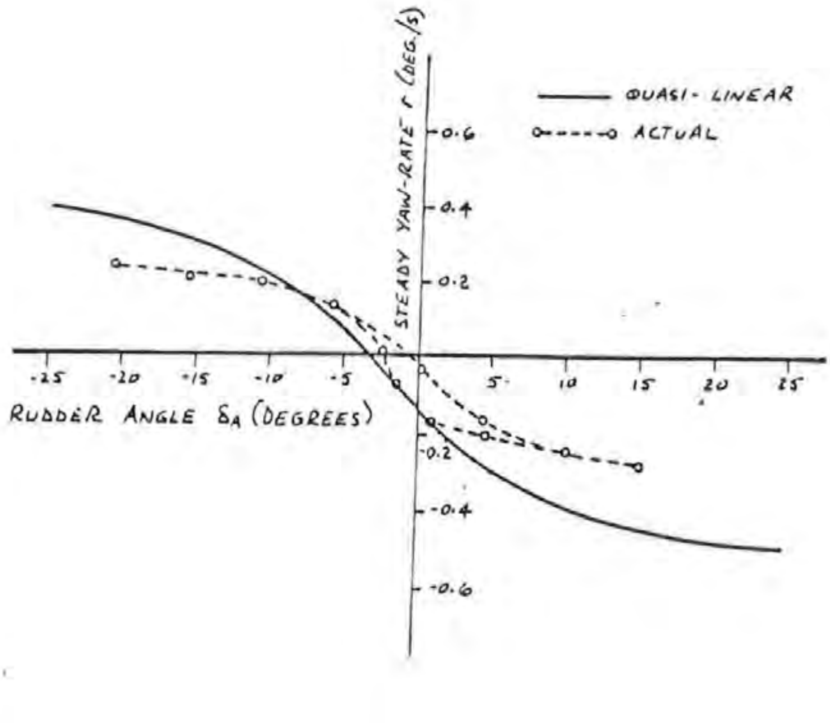

Figure 5.6 Dieudonne Spiral at 5 Knots

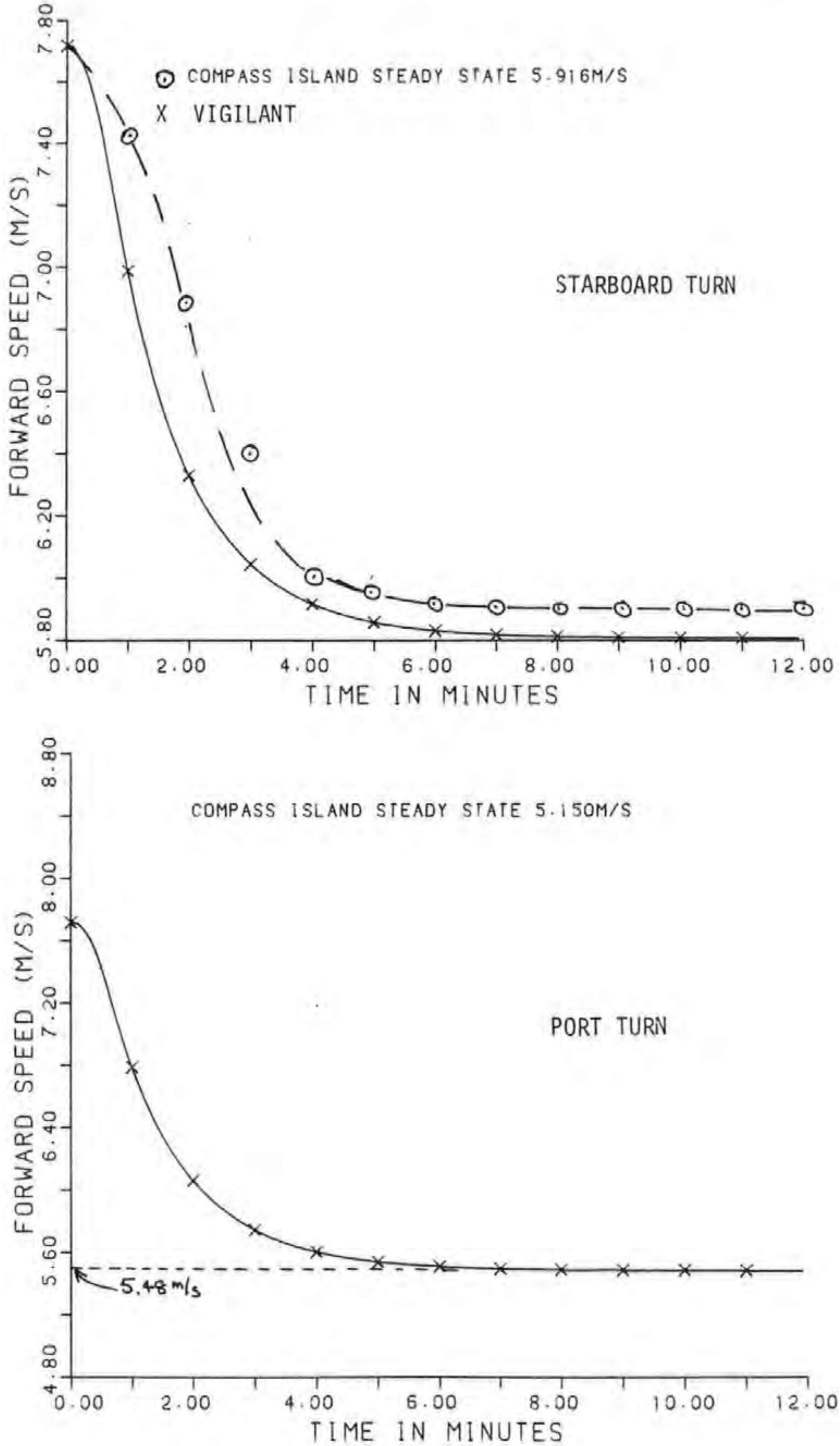

Figure 5.7 Forward Speeds for 20 Degrees Rudder at 15 Knots

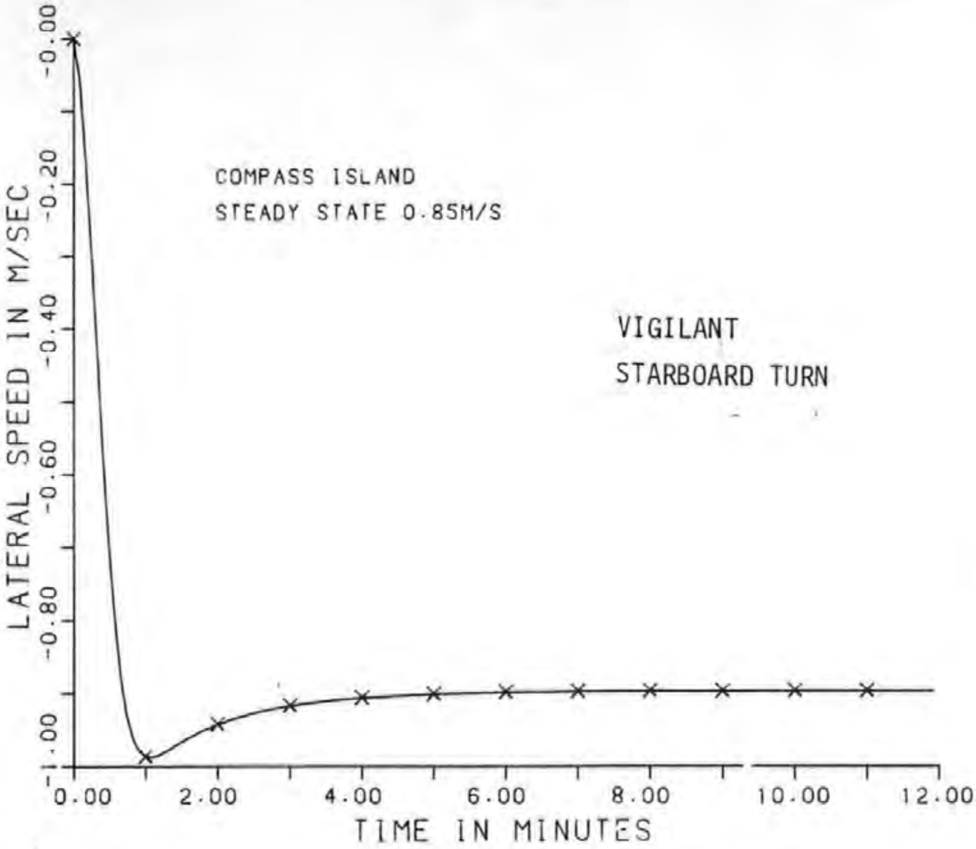

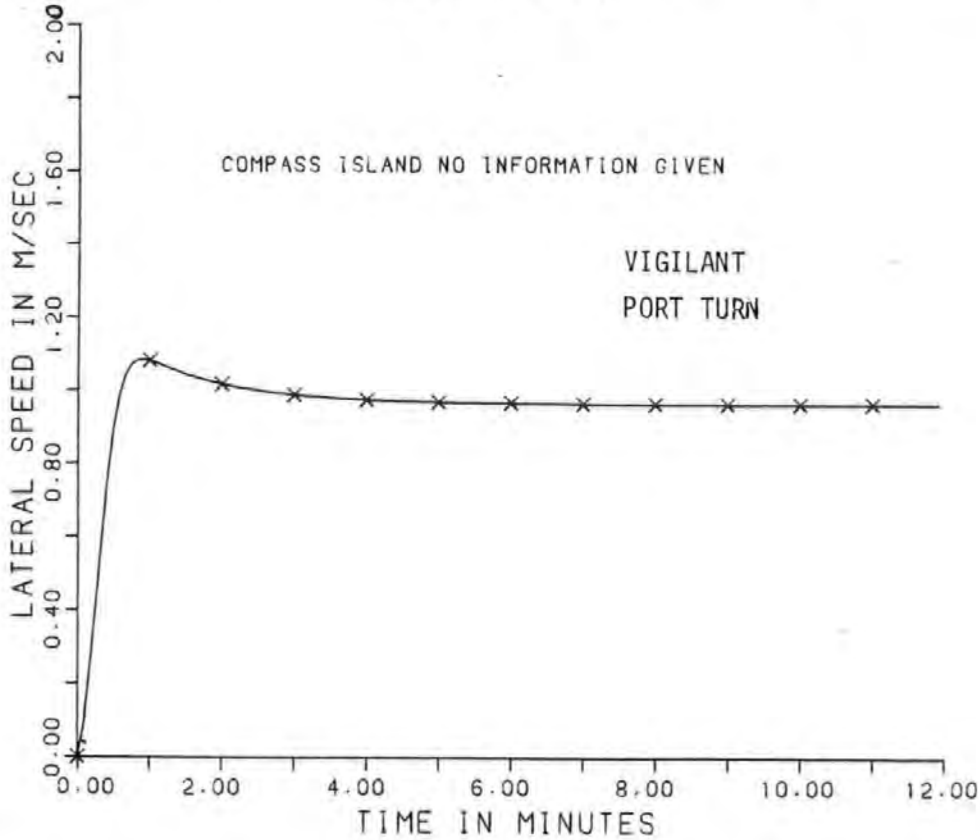

Figure 5.8 Lateral Speeds for 20 Degrees Rudder at 15 Knots

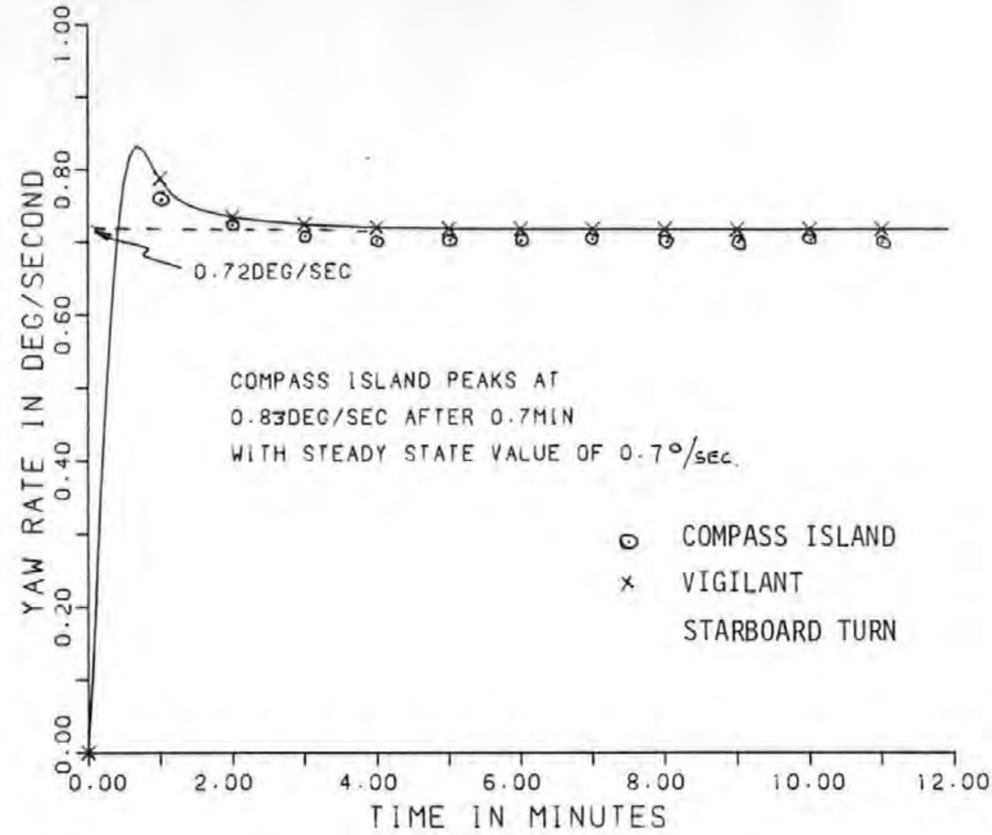

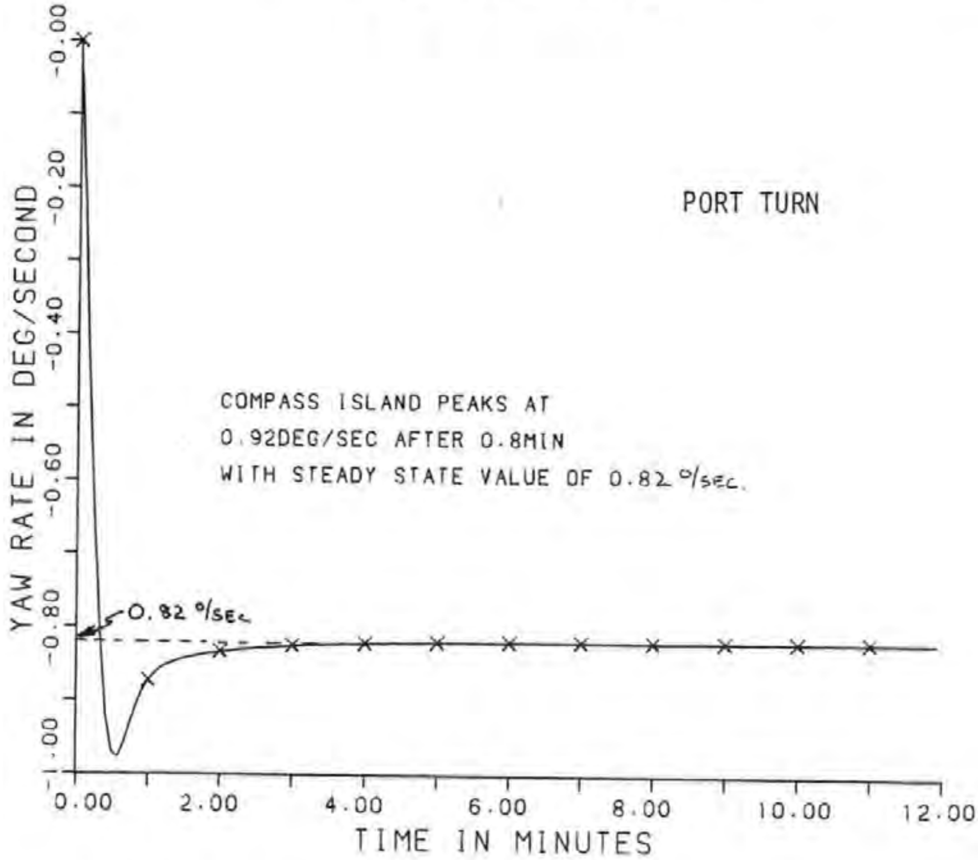

Figure 5.9 Yaw Rate for 20 Degrees Rudder at 15 Knots

CHAPTER 6
DIGITAL COMPUTER SIMULATIONS

6.1 Introduction

The experimental work described in this chapter involved digital computer simulations using the mathematical models described in Chapters 2 and 3. As a result of the open loop tests described in Chapter 5, it was then decided to use only the full non-linear models. With the acquisition of a physical scale model of a twin screw car ferry it was decided to concentrate the digital computer simulations on a full scale version of the car ferry model so that comparisons could be made. The bulk of the work was therefore carried out using this computer model (TREMAYNE in accordance with the nomenclature defined in Chapter 3). However, the series of tests began with the Mariner hull used in the open loop tests. Using this hull form a natural bridge from open to closed loop tests was established. Again using the nomenclature of Chapter 3 the non-linear mathematical model of a Mariner hull was named VIGILANT.

Initially the controller fitted was a simple proportional plus derivative heading controller. Later simulations involved the optimal track and heading controller developed by Burns (1984). This is described in Appendix 9.

The Optimal Filter, which uses the equations described in Chapter 4, takes as inputs the measured values of the state vector, $z(k+1)$, together with the previous values of the control vector, $\underline{u}(k)$. It produces a best estimate of the state vector $\underline{\hat{x}}(k+1/k+1)$ which then becomes the input to the controller, which in turn provides the demanded values of rudder angle and engine revolutions to guide the vessel automatically along a pre-defined track stored in the computer memory. The position of the vessel, together with her heading and speed are thus controlled simultaneously and automatically. Essentially there are three modes of operation to be considered. Knowledge of the statistical nature of the measurement errors together with data relating to wind and tide are used in the Kalman Filter to provide best estimates of the state vector. This is the navigation mode where the system is being used to provide the operator with more accurate position and velocity data than he would expect from using the individual measurement systems on their own. This information can be displayed upon a graphics terminal on the bridge, or at any remote position or it may be fed directly to the digital controller, which compares the estimated values with data stored in the computer memory and computes the necessary control in terms of rudder action and/or engine activity to minimise the errors. This is the fully automatic track keeping mode which is employed in this thesis.

A further mode of operation would involve an automatic hazard avoidance system so that the computer automatically assesses the risk of collision with other vessels and passes the appropriate instructions to the controller so that the correct avoiding action can be taken. This final mode of operation is not included in the present study but is the subject of other research projects in Plymouth Polytechnic, Davis (1981), Davis, Dove and Stockel (1982), Colley, Curtis and Stockel

(1984).

A simplified algorithm of the complete digital computer simulation is given in Figure 6.1, with an overall block diagram for control and guidance in Figure 6.2. Detailed flowcharts are given in Appendix 6, together with detailed explanations of the digital computer simulations.

6.2 The VIGILANT Model with Proportional plus Derivative Controller.

In the digital computer simulations it was necessary to simulate not only the mathematical model of the ship, but also the function of the on - board computer. In essence this on board computer would be dedicated to performing the functions of a digital controller and an optimal filter. Essentially these latter functions were carried out by using subroutines PDCON, or OPTCON for the controller and OPTFIL for the filters, with the Kalman Filter gain calculations using subroutine KBFLTR. The process of obtaining the transition matrices used in the equations representing the ship, was carried out using subroutine NAB. Details of each of these subroutines is given in Appendices 7 and 9. As the mathematical model of the ship is an essential part of the filter these values are also required in the filter. At this stage it is assumed that the values calculated for use in the mathematical model can also be used in the filter.

In these initial runs, using only a proportional plus derivative simple heading controller, the intention was to bridge the gap from open to closed loop tests, whilst setting the digital simulations to work.

The information concerning the magnitude and form of the disturbance and measurement noise is presented to the filter in the form of matrices whose leading diagonal terms contain a measure of the expected magnitude of the random effects, i.e. the variances, and whose off-diagonal terms contain a measure of the expected dependance or correlation of the error sources on one another. These are the covariance matrices $\underline{M}$ and $\underline{N}$.

Initially it was assumed that each of the eight states in the measurement vector was measured by an independent measurement system. This was realistic in terms of rudder angle and engine revolutions. However there would be correlation between the x and y co-ordinates of position as in practice position would probably be measured using a hyperbolic position fixing system. As the hyperbolic co-ordinates would then have to be converted to cartesian co-ordinates an error in the x co-ordinate would affect the measured value of the y co-ordinate. Similarly yaw rate would be measured in a marine auto pilot by using error rate damping rather than using a rate gyro to obtain velocity feedback. However for the purposes of the runs in these and other tests it was assumed that each component of the state vector was measured independently, with forward and lateral velocities being measured separately by independent Doppler sonar logs. A rate gyro was used to measure yaw rate, a gyro compass to give heading, with rudder indicators and engine revolution counter being mounted on the bridge and separate systems to measure the x and y co-ordinates of position. Thus the measurement noise co-variance matrix $\underline{M}$ consists of the measurement system variances in its leading diagonal and zeros in all the off diagonal positions.

Figure 6.3 shows a run where the standard deviations are taken as typical of ship fitted systems, namely rudder angle and engine revolutions 0.002 rad or rad/s, position 25.0 metres, speed 0.025 m/s, heading 0.017 rad and yaw rate 0.017 rad/s. These are referred to as standard conditions and are listed in Table 6.1. True, measured and filtered results are plotted on the same axes. For the ship track plot it is seen that the filtered track coincides with the true track, cutting through the measured track, which was produced by using a random number generator to calculate values about the given standard deviation. Similarly the forward and lateral speeds, each plotted against time, show the true and filtered values very close and cutting through the measured values. Rudder angle, course angle and yaw rate plots show similar results. Figure 6.3 only serves to indicate that the filter is effective, given, for the moment, the limitations indicated in the text.

For the remaining runs in this series only the ship track is plotted. In Figure 6.4 the mean values of tide and wind are removed. First comparisons of Figure 6.3 and 6.4 suggest that there is no difference in the two track plots, but on closer examination it is seen that the tracks do not exactly coincide, suggesting that the removal of the mean values changes only the track followed over the ground. This was to be expected as the controller is only required to correct heading errors. But in each case the filtered and true tracks are co-incident, confirming that the filter will minimise noise although, in this case, the presence of mean values of disturbances does not affect the functioning of the filter. In Figure 6.5 the disturbance and measurement noise values have each been increased by a factor of 5 to show the effect of filtering very noisy signals. Once again the true and filtered tracks coincide, and although the measurement plot is rather unrealistic it does indicate that the filter is effective in extreme conditions. In Figure 6.6 the measurement noise is reduced to one fifth of the figures given previously, but the disturbance noise remains high, although the mean values of the disturbance all remain at zero. In Figure 6.7 both the measurement and disturbance noise matrices are low (0.2 of the values quoted for Figure 6.3). Comparing Figures 6.6 and 6.7 it is seen that the fluctuations of the measured track are reduced in both cases, whilst the removal of large disturbance fluctuations does not affect the filtering, although it does of course alter the track followed by the craft. Comparing Figure 6.4 with Figure 6.7 however it is seen that the filtered tracks are very similar, showing that the track over the ground is controlled by, amongst other things, the disturbance effects and is unaffected by high or low disturbance noise values. Similarly comparison of Figure 6.7 with Figure 6.8 suggests that the track over the ground is unaffected by the degree or amount of measurement noise. Figures 6.4 to 6.8 show that the filter is capable of providing good estimates of position through very noisy measurements when the disturbance noise has zero mean conditions.

In Figures 6.9 through to 6.12 the mean values of disturbance noise are returned. These are a mean current of 0.669 m/s (1.3 knots) in direction 3.65 radian (209 degrees) clockwise from true north, with a mean wind speed of 10.29 m/s (20 knots) in a direction 3.929 radian (225 degrees) from north. All directions are taken as away from the ship. Comparison of Figure 6.5 with Figure 6.9 where disturbance and measurement noise are both high suggest that the mean values affect the track over the ground, but do not affect the filtering. Similarly the effect of reducing the measurement noise, as in Figure 6.10, does not affect the filtering. In Figure 6.11 the random disturbance noise is zero, whilst the measurement noise is high. In this run the true and filtered tracks diverge slightly as the run progresses, whereas if a low level of random disturbance noise is re-introduced (Figure 6.12) then the divergence of true and filtered tracks is less marked.

To summarise, Figures 6.4 through to 6.12 indicate that the Kalman Filter is capable of operating through noisy measured values and will have its greatest effect upon the measurement noise. Large values of random disturbance noise do not affect the position plot, while the presence of mean values of the disturbances do not decrease the effect of the filter. Alternatively, the disturbances can be looked upon as having mean values with superimposed random fluctuations, thus allowing the Kalman Filter theory to be applied. Grimble, Patton and Wise (1980b) suggest that the wind can be modelled as a disturbance signal and a white noise signal, whilst Medditch (1969) refers to a Gaussian white sequence with a mean value. The mean values can then be treated as a separate disturbance input to the random values used in the filter calculations. In Figures 6.13 and 6.14 the mean values, random disturbance noise and measurement noise are all returned to the normal values used in Figure 6.3. In Figure 6.13 the Kalman Filter gain is only recalculated for every 10 sample times (50 seconds in real time), whilst in Figure 6.14 the gain is recalculated after 50 sampling intervals (250 seconds of real time). It is seen that there is no significant difference between these runs and the first run in this series (Figure 6.3), suggesting that the gain of the filter does not have to be recalculated during each sample time. This fact was to be of significant use later when the physical model software was being developed.

Figure 6.15 illustrates the situation when the off-diagonal terms (3,5) and (5,3) of the measurement covariance matrix are given small values to simulate cross- correlation between the x and the y position measurements.

6.3 The TREMAYNE Model with Optimal Controller

Once the validity of the filter had been established using the Mariner hull characteristics and a simple controller, the next stage was to change to the model of a twin screw car ferry, with optimal controller, to simulate such a vessel approaching the Port of Plymouth and moving along the navigable channel into the harbour. Since this thesis was concerned wth the automatic pilotage of large ships it was intended that the ship followed, automatically, a predetermined track, the co-ordinates of which would be held in an on-board computer. It has already been stated that the car ferry model used was defined by the physical model, CENTAUR, used in later tests on a reservoir, and hence the TREMAYNE model is defined by the non-dimensionalised coefficients derived for CENTAUR and scaled up appropriately to represent a full sized ship such as the QUIBERON, a French car ferry which, at the time of the research, was regularly using Plymouth. (See Frontispiece).

Since the vessel is to be automatically piloted along the predetermined path, this implied that a track controller was to be used. In fact the optimal controller was both a track and a heading controller. As these two requirements could at times conflict the optimal weightings were such that the track control dominated, except at times when an alteration of course became necessary, when the weightings were changed so that the heading control predominated.

In all these later digital computer simulations an outline chart of Plymouth Sound was drawn using subroutine PLYM, which is described in Appendix 6. This gives the position of the breakwater and the principal buoys which outline the navigable channel. The vessel was assumed to be at or close to the demanded track, at its southerly end, at the commencement of each run, with the completion being to the East of Drake's Island. In Figures 6.16 to 6.22 the demanded values are plotted in black, the measured values in green, the true values in blue and the estimated values in red. Figure 6.16 shows a run with the normal set of measurement noise standard deviations referred to in Table 6.1. Hitherto the values of the transition matrices used in the mathematical model to simulate the ship were also used in the filter calculations. For the remaining simulations these values were calculated twice for each sample time; firstly in the mathematical model of the ship when the true values of the state and control vectors were used in the calculations, secondly in the filter calculations. In the latter case only those states available, i.e the estimated and measured values were used, thus adding to the realism of the simulation and allowing the mathematical model used for the ship itself to differ from the mathematical model used in the filter. In Figure 6.16 the values of the Kalman filter gains were recalculated only when the course error exceeded 30 degrees. As with previous runs the true and filtered tracks are almost co-incident with the vessel following very closely the recommended track for deep draft vessels in the approaches to the port. Figure 6.17 illustrates the situation when speed measurement noise is increased. The forward and lateral speed graphs showed this noise with the filtered values unchanged from the previous run. The track plot was identical to that of Figure 6.16 showing no deterioration of the filtered track, or of any of the states plotted out. In Figure 6.18, where the position standard deviations were increased to 200 metres to simulate a night time approach using the Decca Navigator, the Kalman Filter gains were still only re-calculated when the course error exceeded 30 degrees. In this case, although the measured track was somewhat unrealistic, the filtered values still followed closely the true values.

Leaving aside the mean values of wind and tide, Figure 6.19 illustrates a run where the random fluctuations of these quantities were increased. The current standard deviations were increased to 0.6 knots and 30 degrees, thus simulating a bad weather approach to the port. By comparison with the standard conditions of Figure 6.16 there are greater variations in the speeds, yaw rate and heading, but in all cases the true and estimated values are very close. Bearing in mind that both the wind and the tide are from a south westerly direction the track plot does show the vessel off-track during the second and third legs, with the filtered track dangerously close to the starboard side of the navigable channel. However, during the fourth leg the ship is seen to be returning to the demanded track, with the filtered values again close to the true values. Figure 6.20 shows the situation in a night approach in bad weather with the filtered track rather more in error, although still following the true track. In this run the position standard deviation was increased to 200 metres and the speed standard deviation to 2 m/s again showing the ability of the filter to output signals which would enable the optimal controller to effectively guide the vessel along the predetermined track.

Turning now to the mathematical model used in the filter and looking at a typical graph of some of the elements in the continuous time matrix, F (Figure 6.21) it is seen that these elements are reasonably constant except in an alteration of course. It will be shown later, when deriving the filter equations for use in the Centaur model, that the elements are largely functions of forward speed, lateral speed and yaw rate, in which case they would be expected to change whenever speed and/or heading changes. All the coefficients are shown in Equation set 3.28 and are defined in Appendix 3. It is seen from the plots that the values do change at the alter course points but most values remain reasonably constant between alterations of course and speed.

Figures 6.22 and 6.23 show the results when errors appear in the transition matrix. In Figure 6.22 the $\underline{A}$ matrix is scaled by a factor of 1.1 at time k = 50. For the first two legs of the passage the track keeping is as good as for previous runs, but during the second leg the true and filtered tracks are seen to diverge. At the start of the fourth leg the true and filtered tracks are again co-incident, because the state, control and disturbance matrices in the filter are regaining their correct values. In Figure 6.23 the $\underline{A}$ matrix is scaled by a factor of 1.5 after 50 sampling periods. The variations are much greater as would be expected, showing clearly that the filter requires to model the actual system accurately.

These results, together with others carried out earlier, showed quite clearly that if the state, control and disturbance matrices were not frequently updated the accuracy of the mathematical model used in the filter was reduced and the efficiency of the filter fell off rapidly. Moreover, it was found unnecessary to recalculate the filter gains during every sampling instant. This in turn suggested that the filter itself might not be necessary, but later work with the physical model showed this was not so.

6.4 Summary

A full analysis of the mainframe digital computer simulations with emphasis on the filter gains is given in Chapter 7, but the results given in this chapter show that the Kalman filter was able to give accurate estimates of the eight states given very noisy conditions, provided the mathematical model of the ship in the filter was accurate. The results further showed that the random disturbance had little or no effect on the filter and fixed values of wind and tide did not degrade the ability of the filter to feed accurate estimates of the states to the optimal controller.

a) Measurement Noise Standard Deviation

Rudder Angle	0.002 rad
Engine Revolutions	0.002 rad/s
Position	25 metres
Speed	0.025 m/s
Heading	0.017 rad
Yaw Rate	0.00399 rad/s

b) Disturbance Noise Standard Deviations

Current Speed	0.2 m/s (0.39 knots)
Current Direction	0.35 rad (20 degrees)
Wind Speed	3.0 m/s (5.83 knots)
Current Direction	0.35 rad (20 degrees)

c) Disturbance Mean Values

Current Speed	0.669 m/s (1.3 knots)
Current Direction	3.665 rad (209 degrees)
Wind Speed	10.29 m/s (20 knots)
Wind Direction	3.927 rad (225 degrees)

All directions were taken as away from the ship.

Table 6.1 Standard Conditions for Disturbance and Measurement Noise

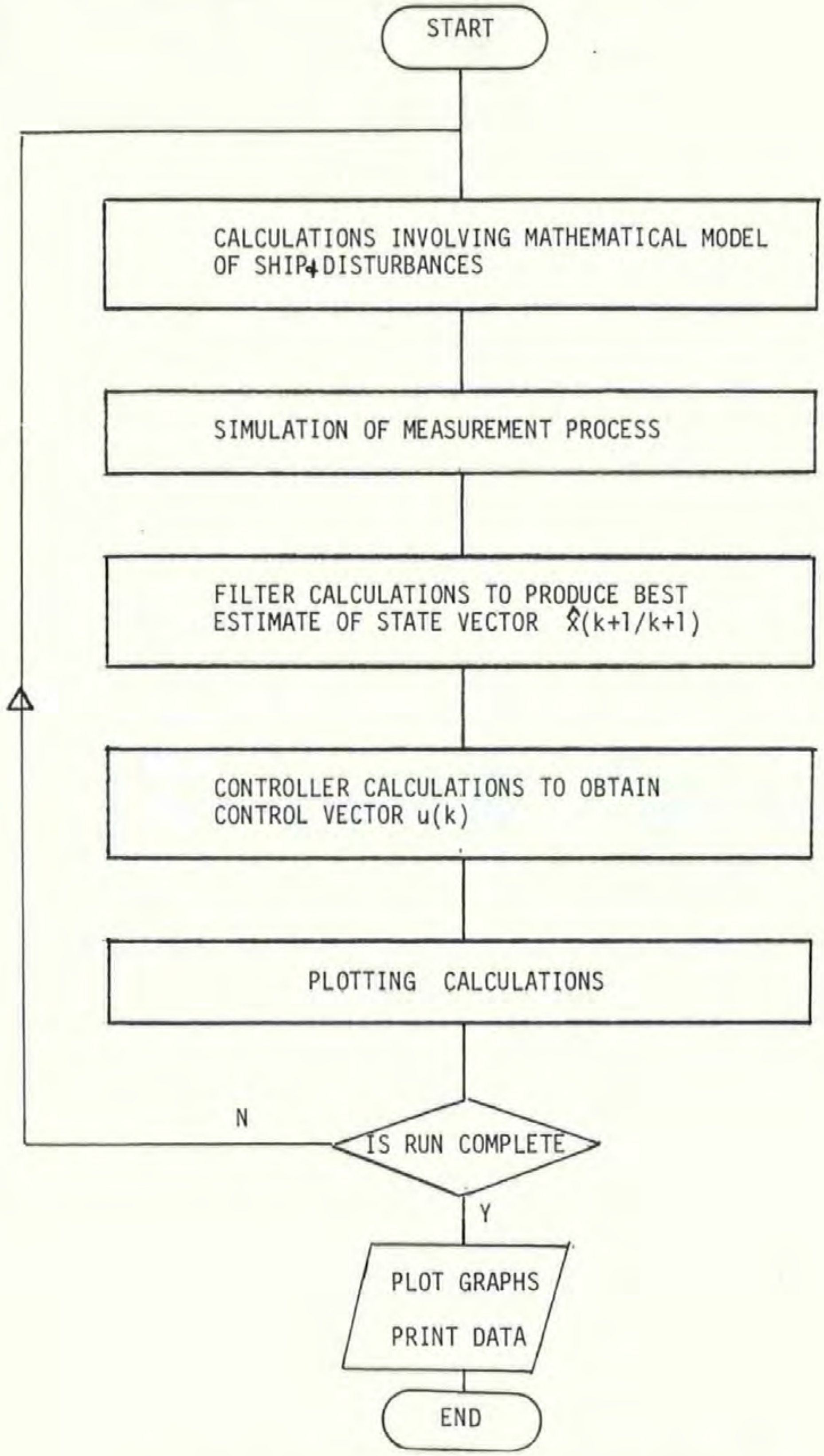

FIG 6.1 Algorithm Of Digital Computer Simulation

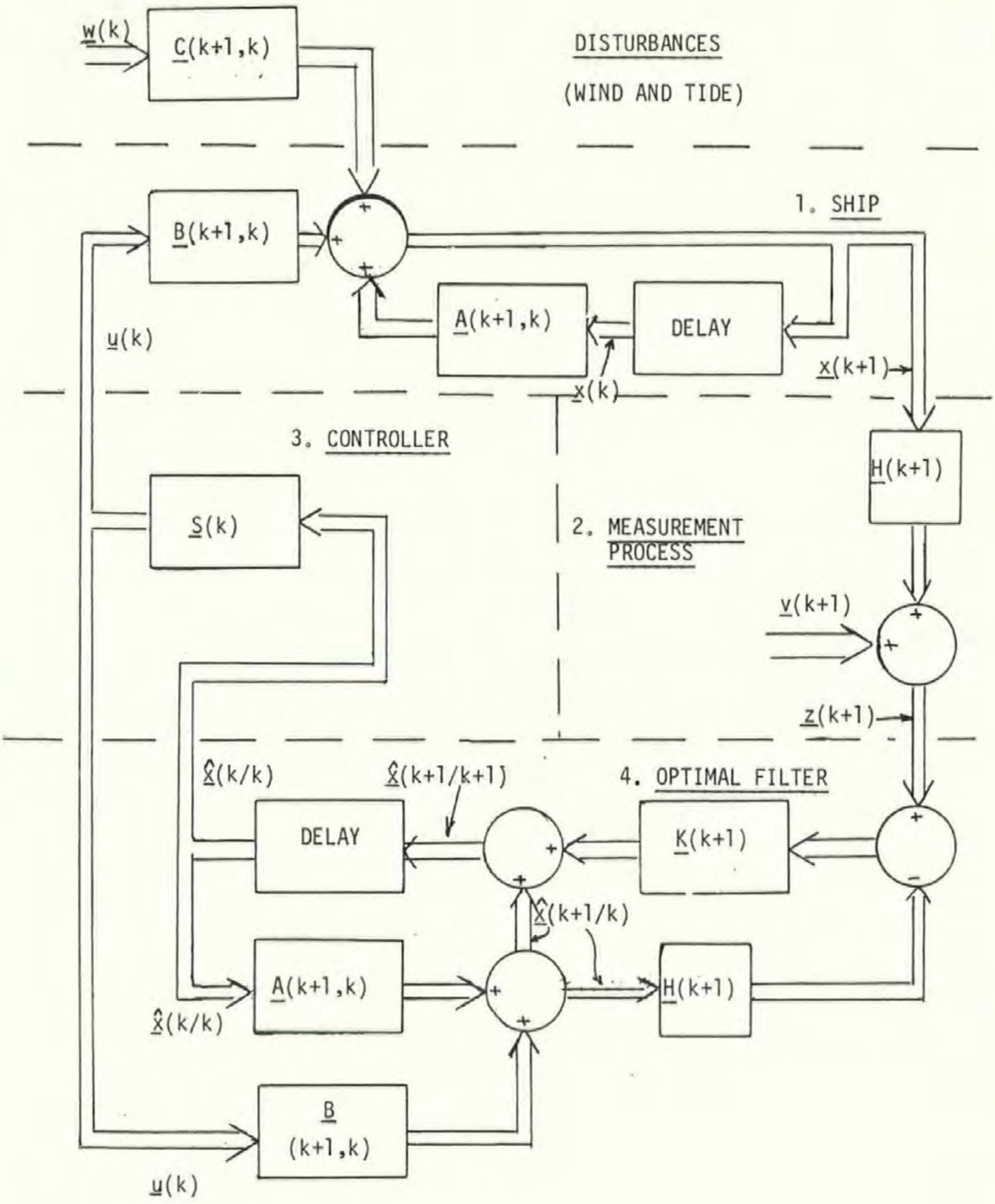

FIG 6.2 Optimal Control System

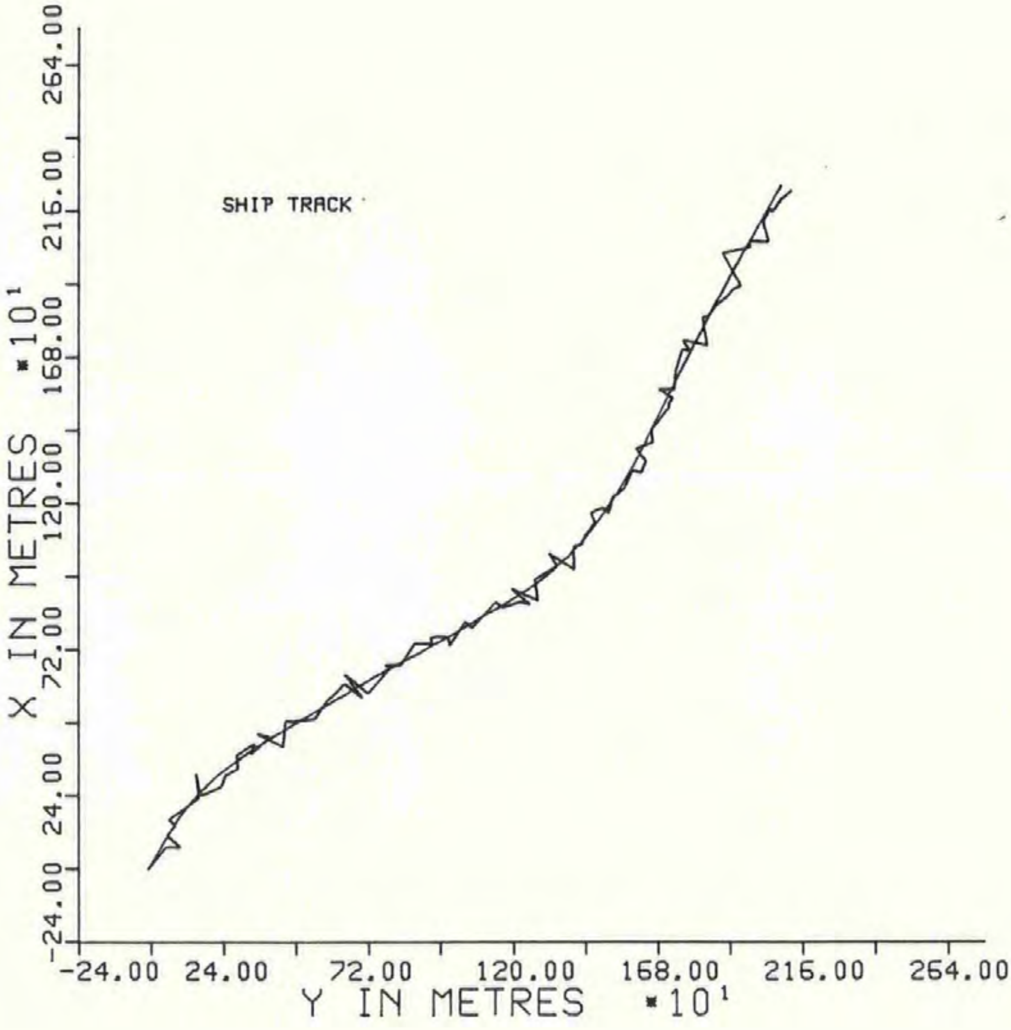

FIG 6.3 Standard Conditions

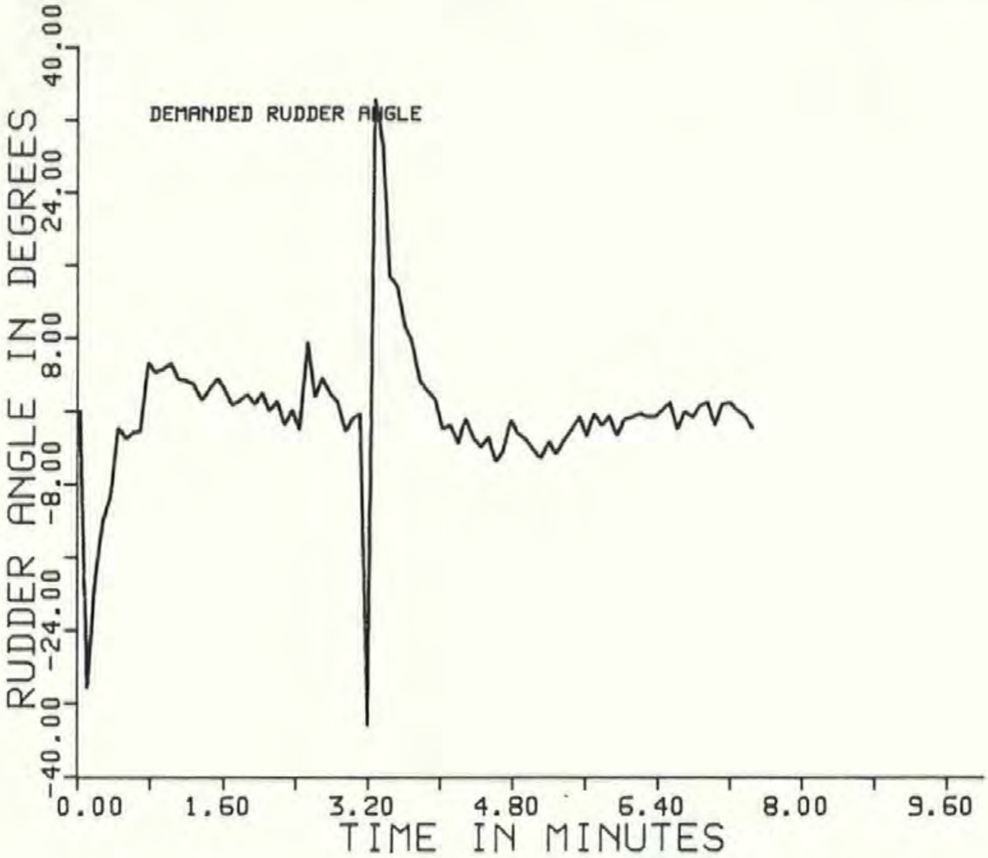
DEMANDED RUDDER ANGLE
RUDDER ANGLE IN DEGREES
40.00
24.00
8.00
-8.00
-24.00
-40.00
0.00
1.60
3.20
4.80
6.40
8.00
9.60
TIME IN MINUTES

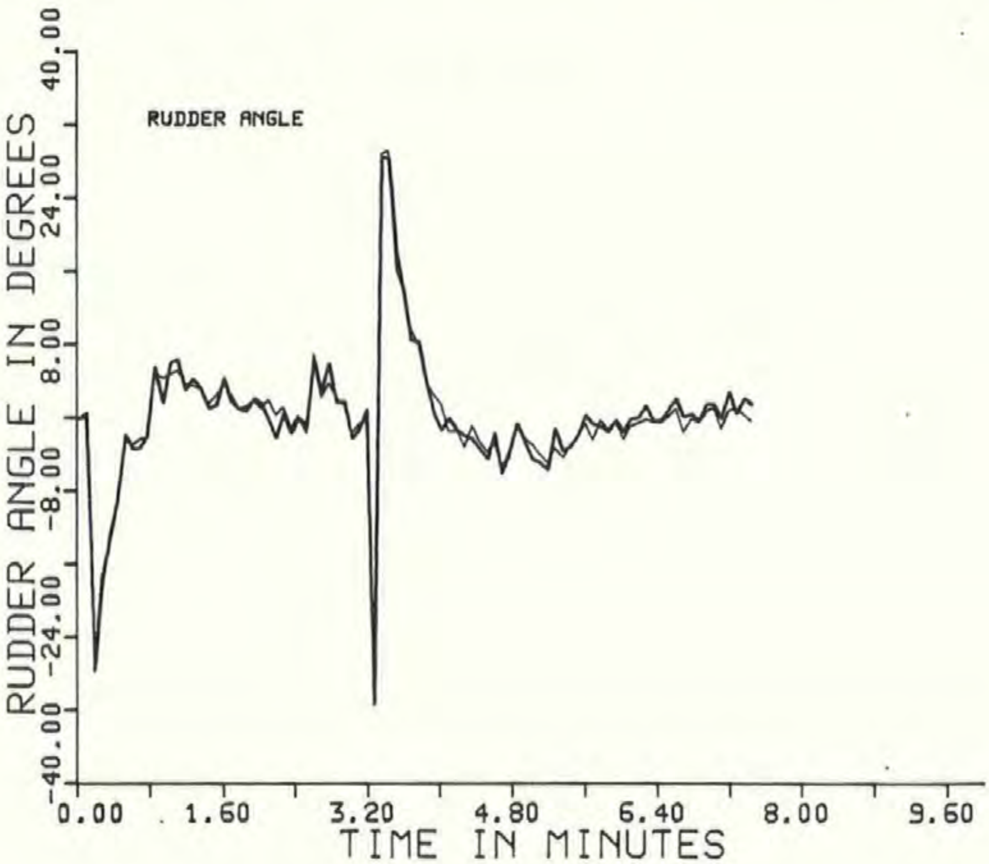
RUDDER ANGLE
RUDDER ANGLE IN DEGREES
40.00
24.00
8.00
-8.00
-24.00
-40.00
0.00
1.60
3.20
4.80
6.40
8.00
9.60
TIME IN MINUTES

FIG 6.3


LATERAL SPEED OF SHIP
LATERAL SPEED IN M/SEC
1.20
0.80
0.40
0.00
-0.40
-0.80
0.00
1.60
3.20
4.80
6.40
8.00
9.60
TIME IN MINUTES

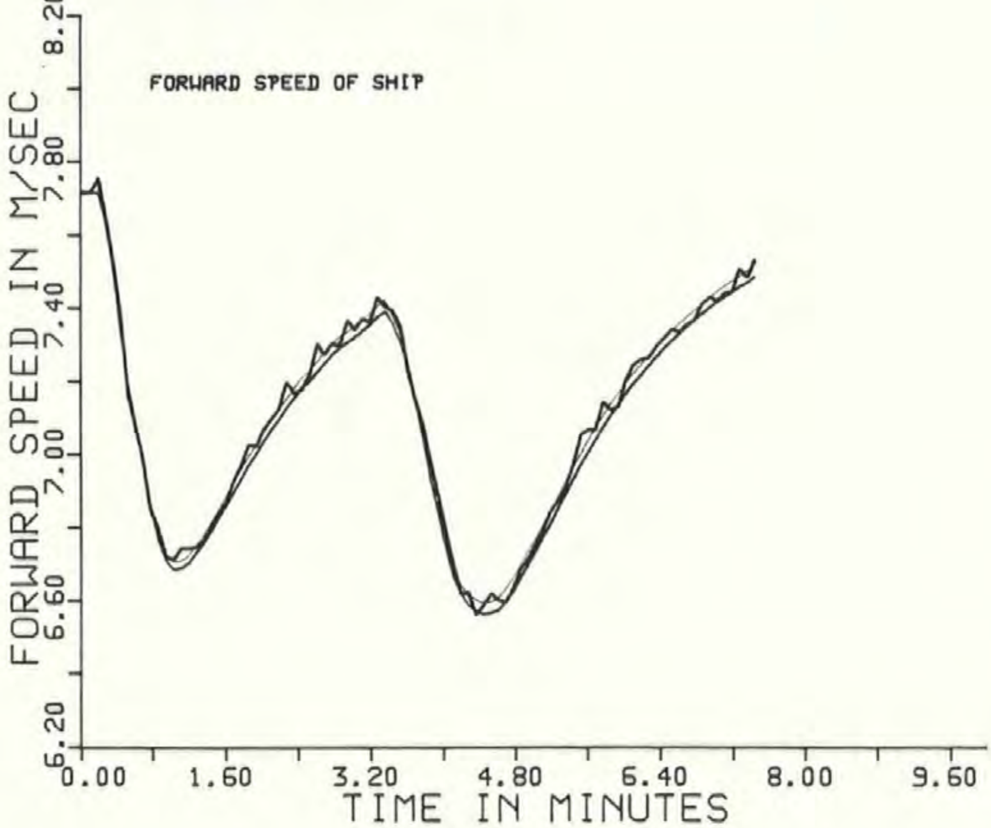
FORWARD SPEED OF SHIP
FORWARD SPEED IN M/SEC
8.20
7.80
7.40
7.00
6.60
6.20
0.00
1.60
3.20
4.80
6.40
8.00
9.60
TIME IN MINUTES

FIG 6.3

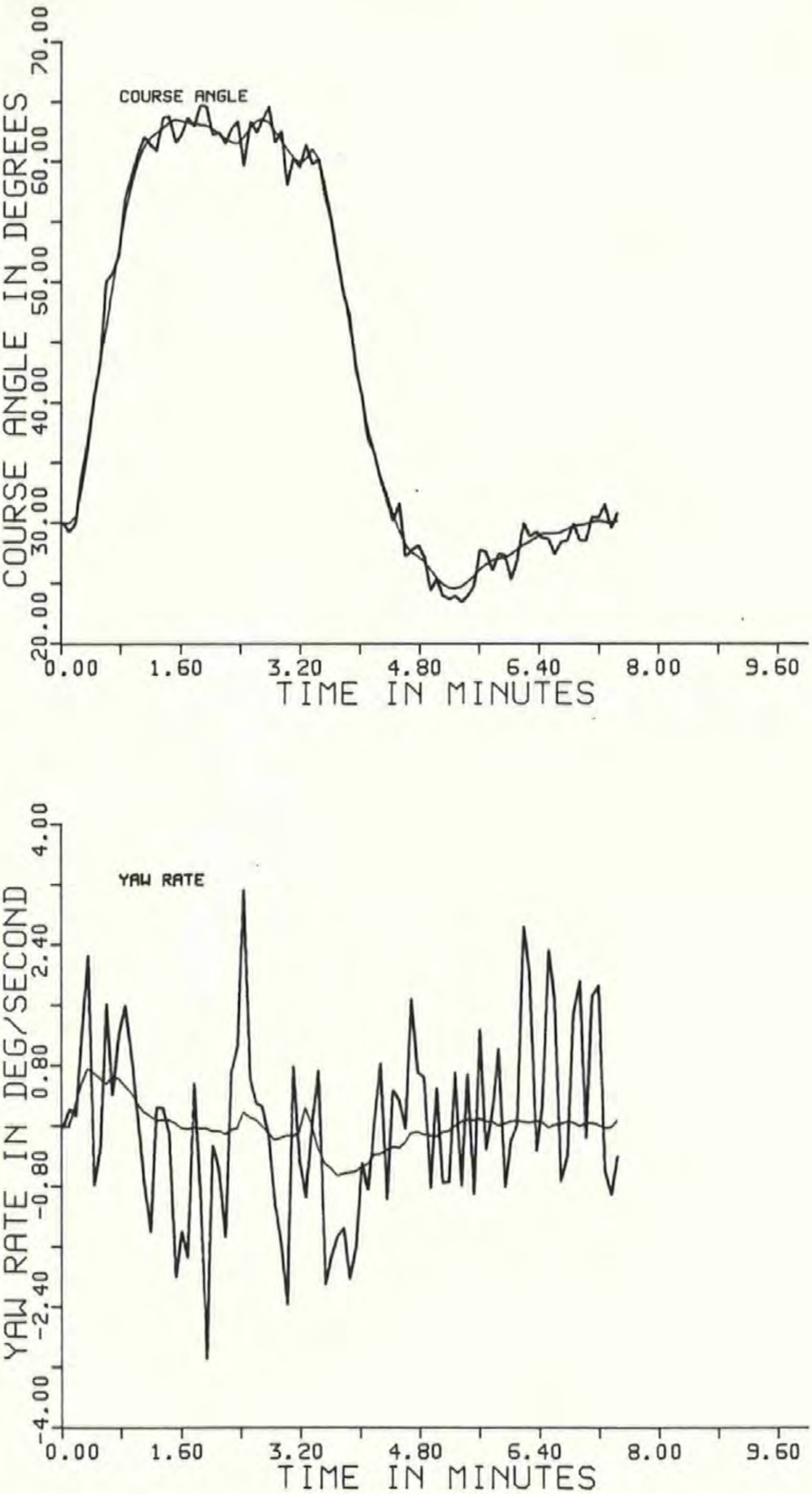
COURSE ANGLE
COURSE ANGLE IN DEGREES
20.00
30.00
40.00
50.00
60.00
70.00
0.00
1.60
3.20
4.80
6.40
8.00
9.60
TIME IN MINUTES
YAW RATE
YAW RATE IN DEG/SECOND
-4.00
-2.40
-0.80
0.80
2.40
4.00
0.00
1.60
3.20
4.80
6.40
8.00
9.60
TIME IN MINUTES

FIG 6.3

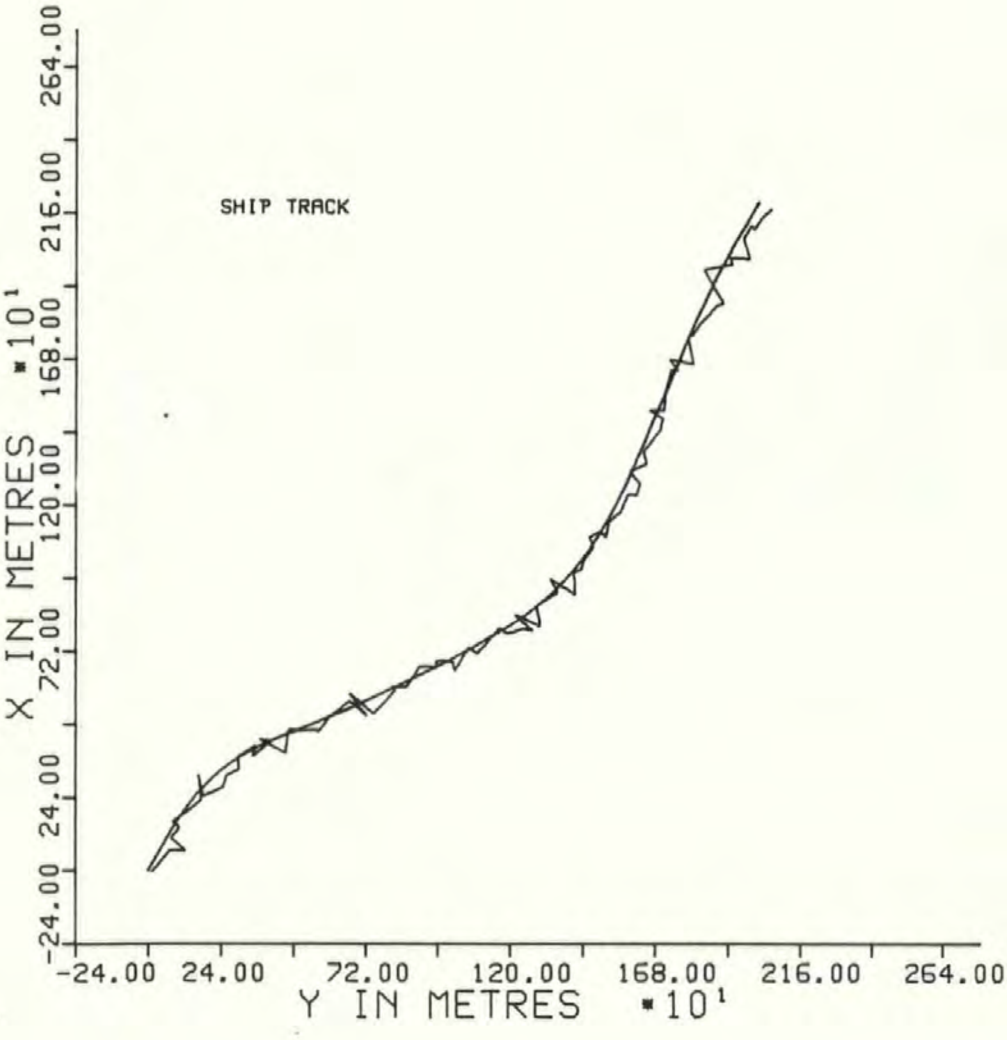

FIG 6.4 Standard Conditions Without Mean Values for Wind and Tide

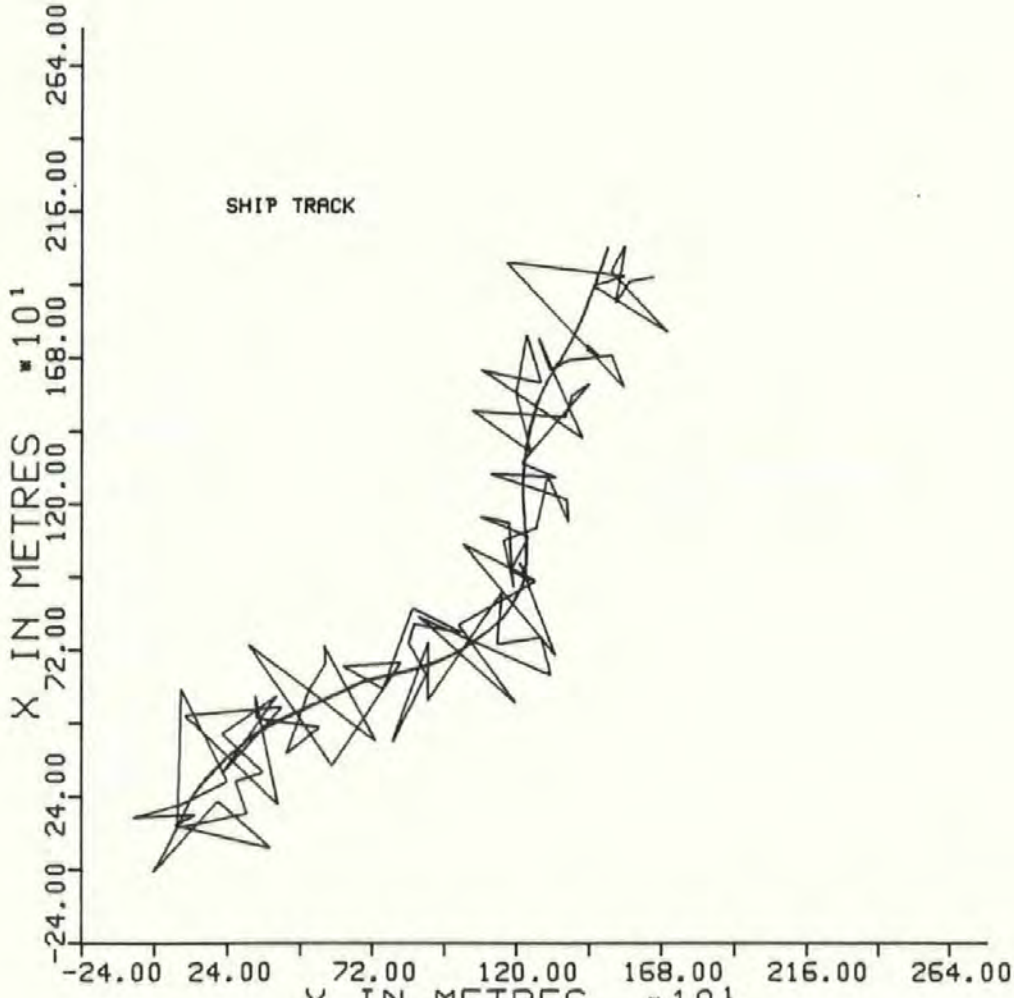

FIG 6.5 Increased Disturbance and Measurement Noise Without Wind and Tide Mean Values

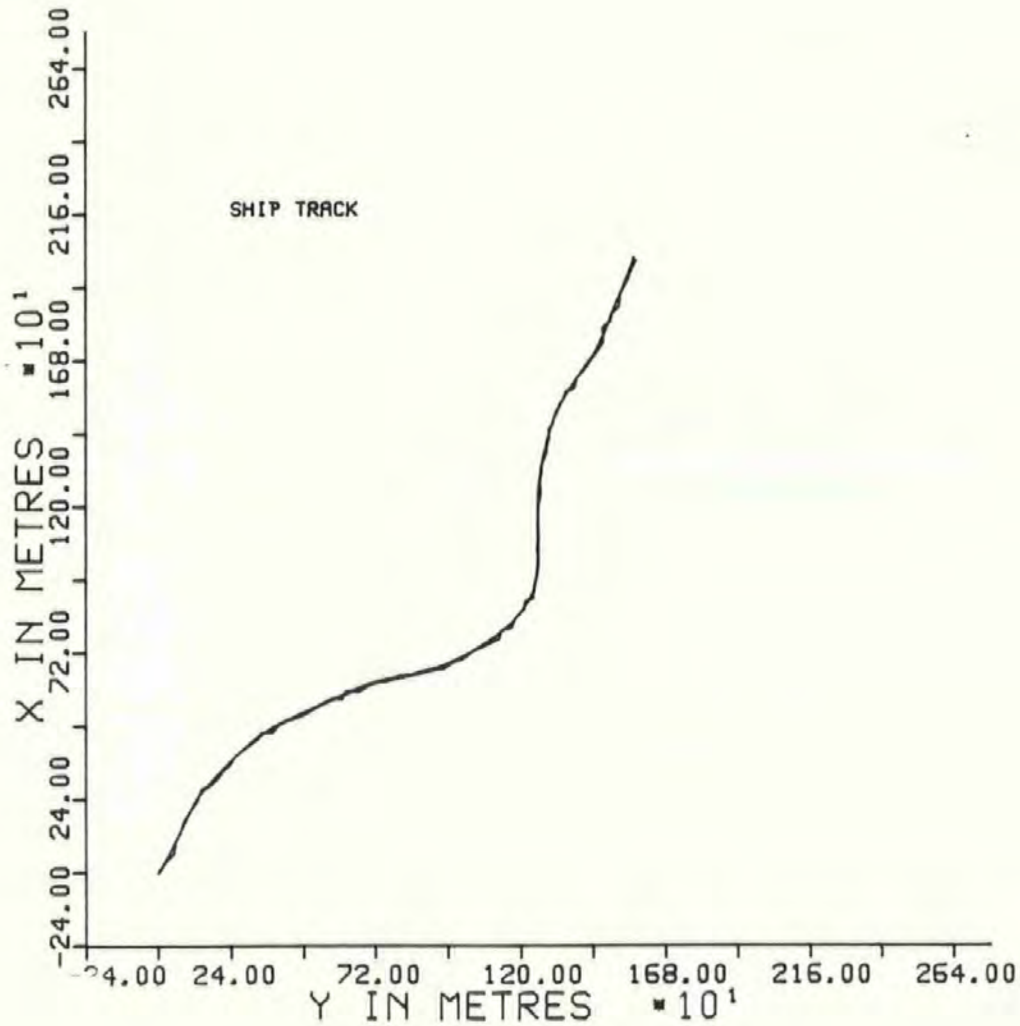

FIG 6.6 Reduced Measurement Noise With Standard Disturbance Noise and Without Wind and Tide Mean Values

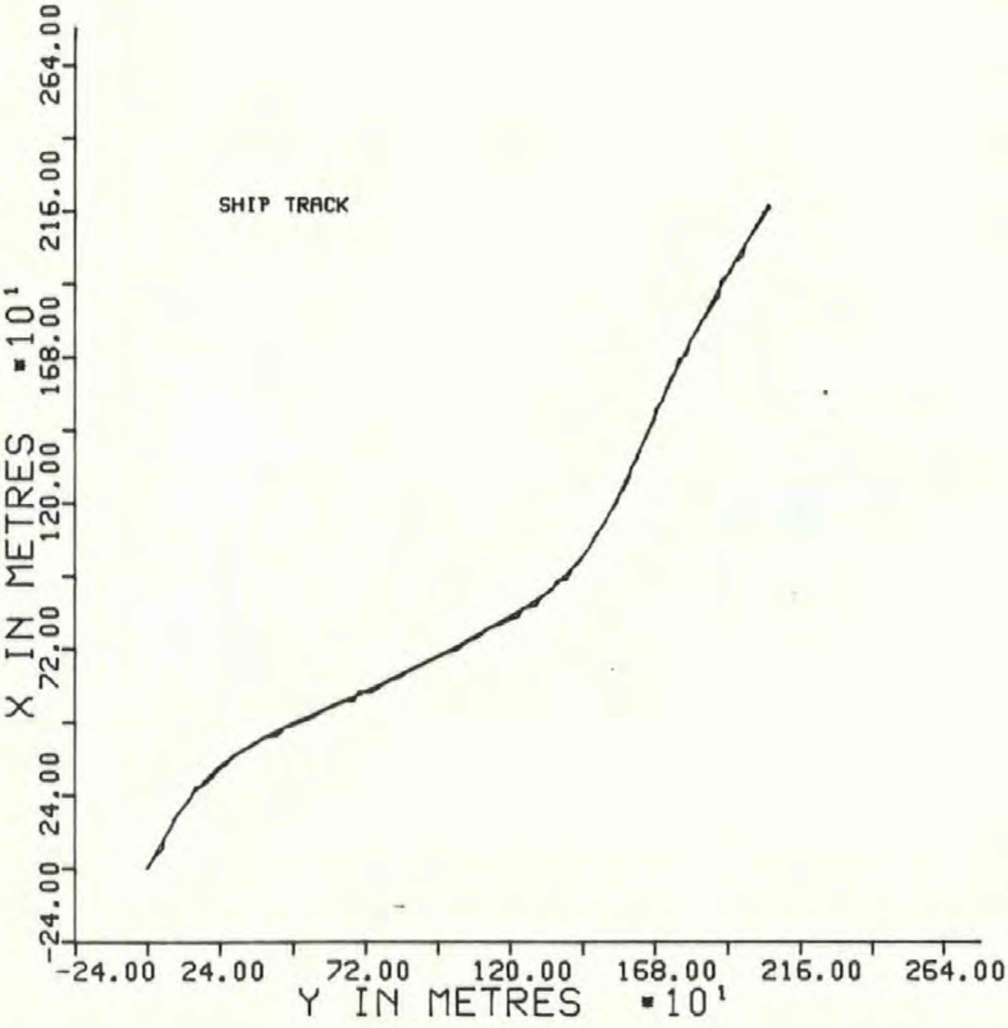

FIG 6.7 Reduced Measurement and Disturbance Noise Without Wind and Tide Mean Values

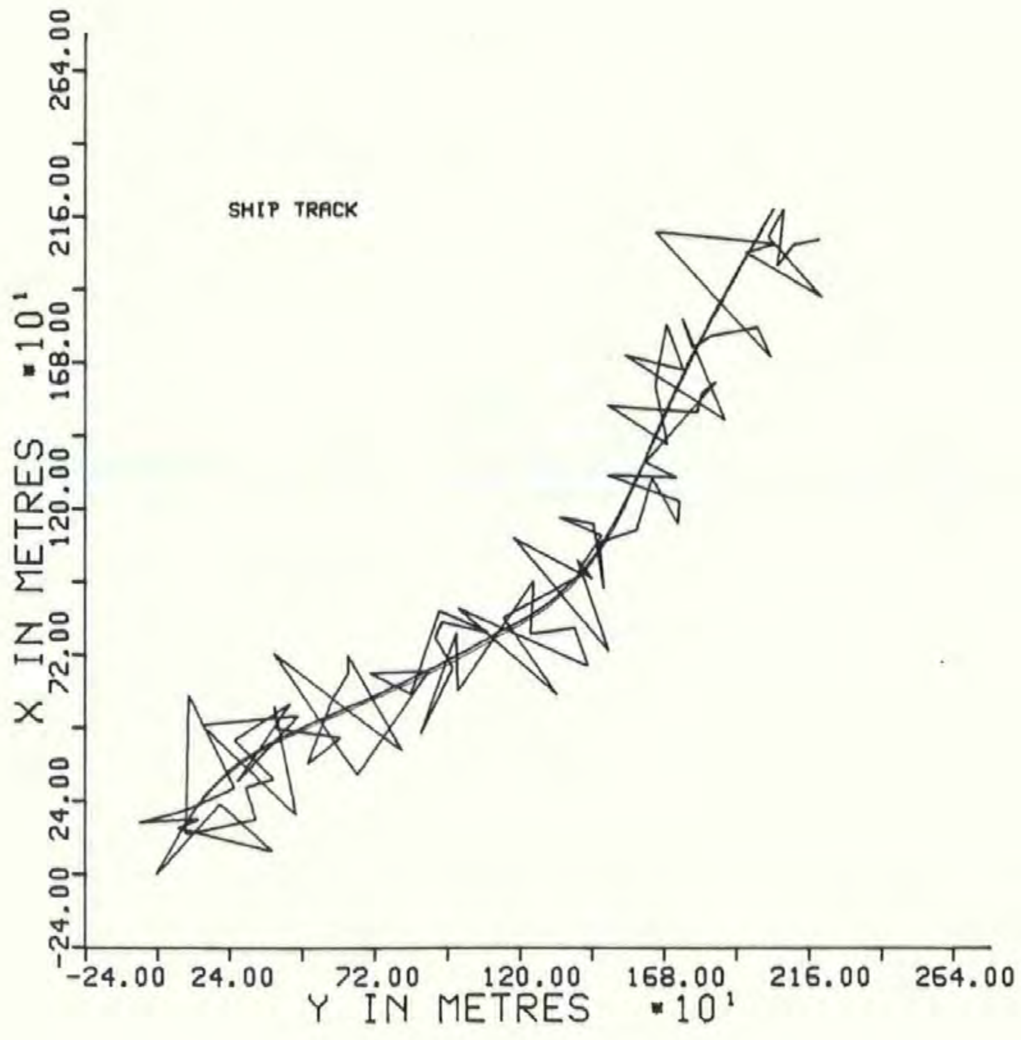

FIG 6.8 Increased Measurement Noise With Reduced Disturbance Noise and Without Wind and Tide Mean Value

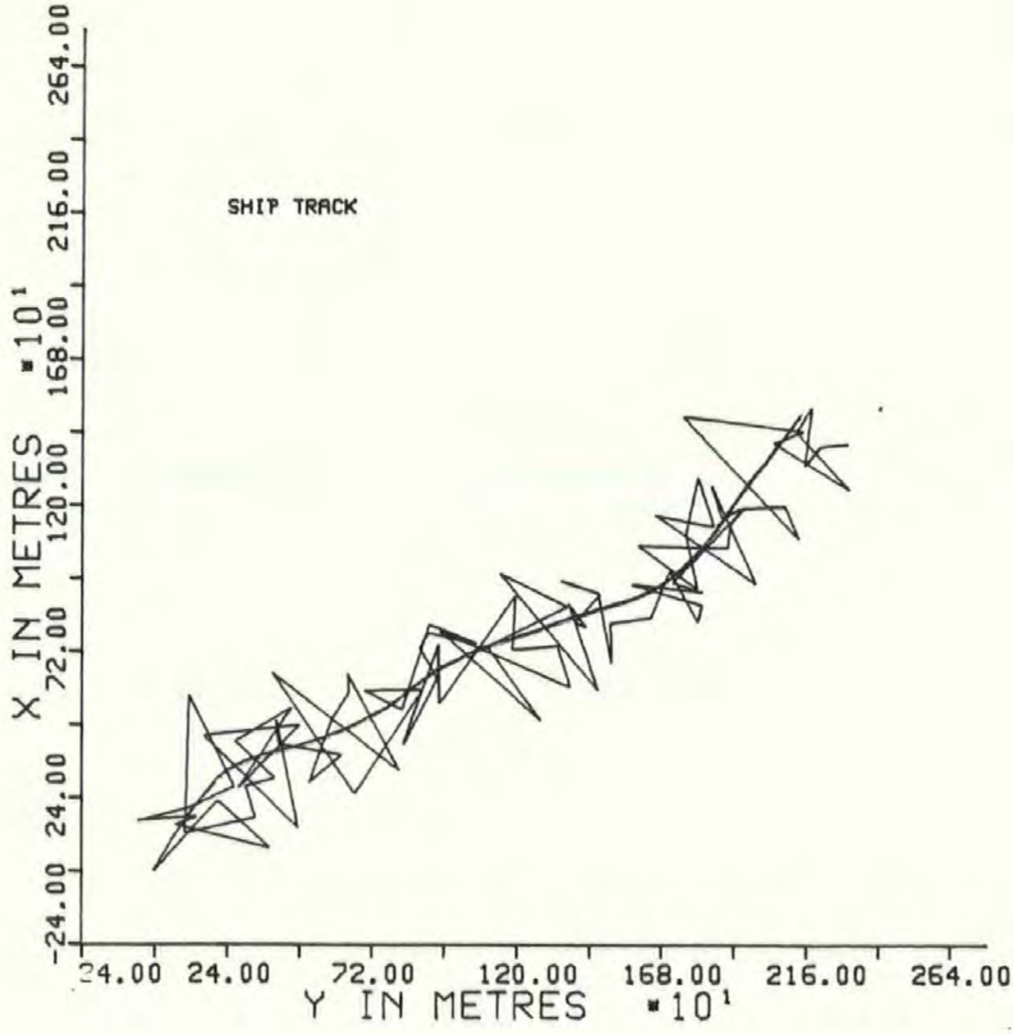

FIG 6.9 Increased Measurement and Disturbance Noise

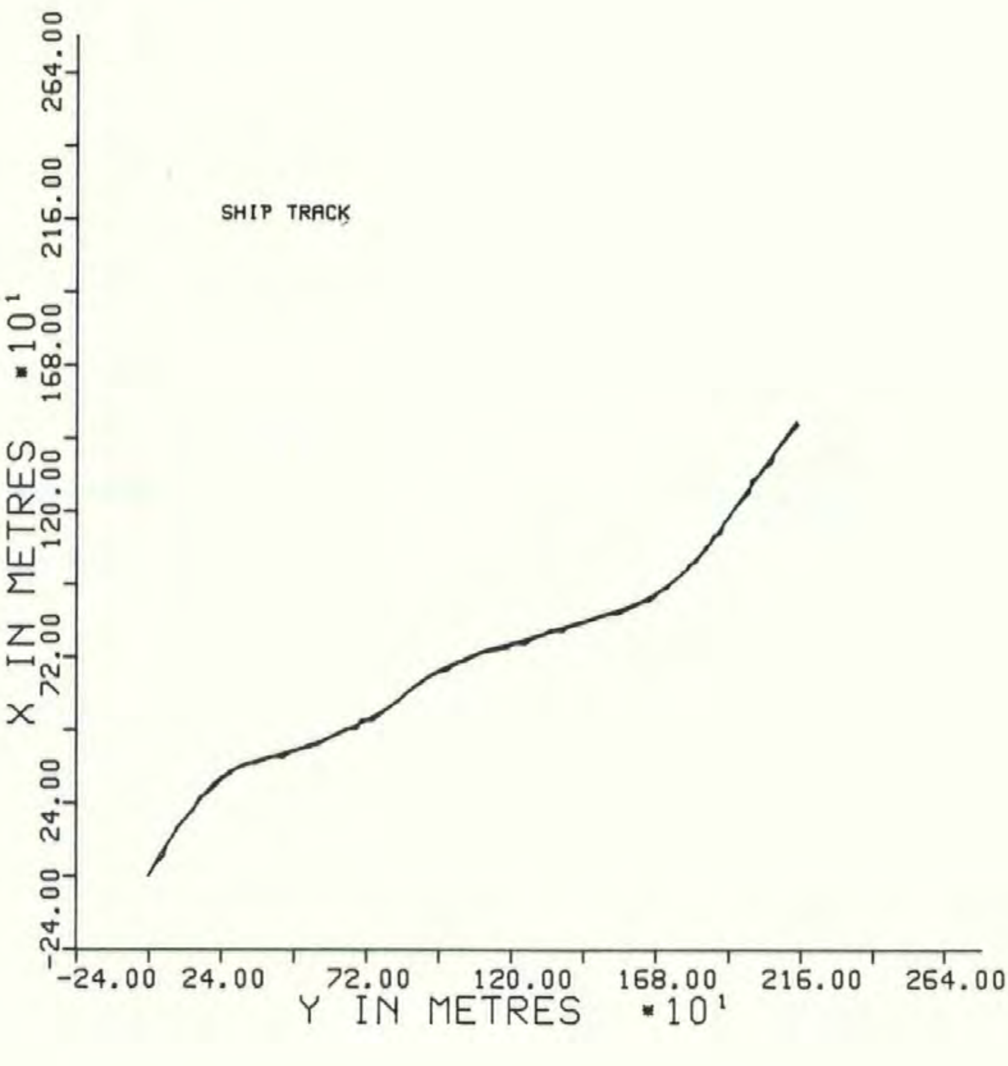

FIG 6.10 Reduced Measurement Noise with Increased Disturbance Noise

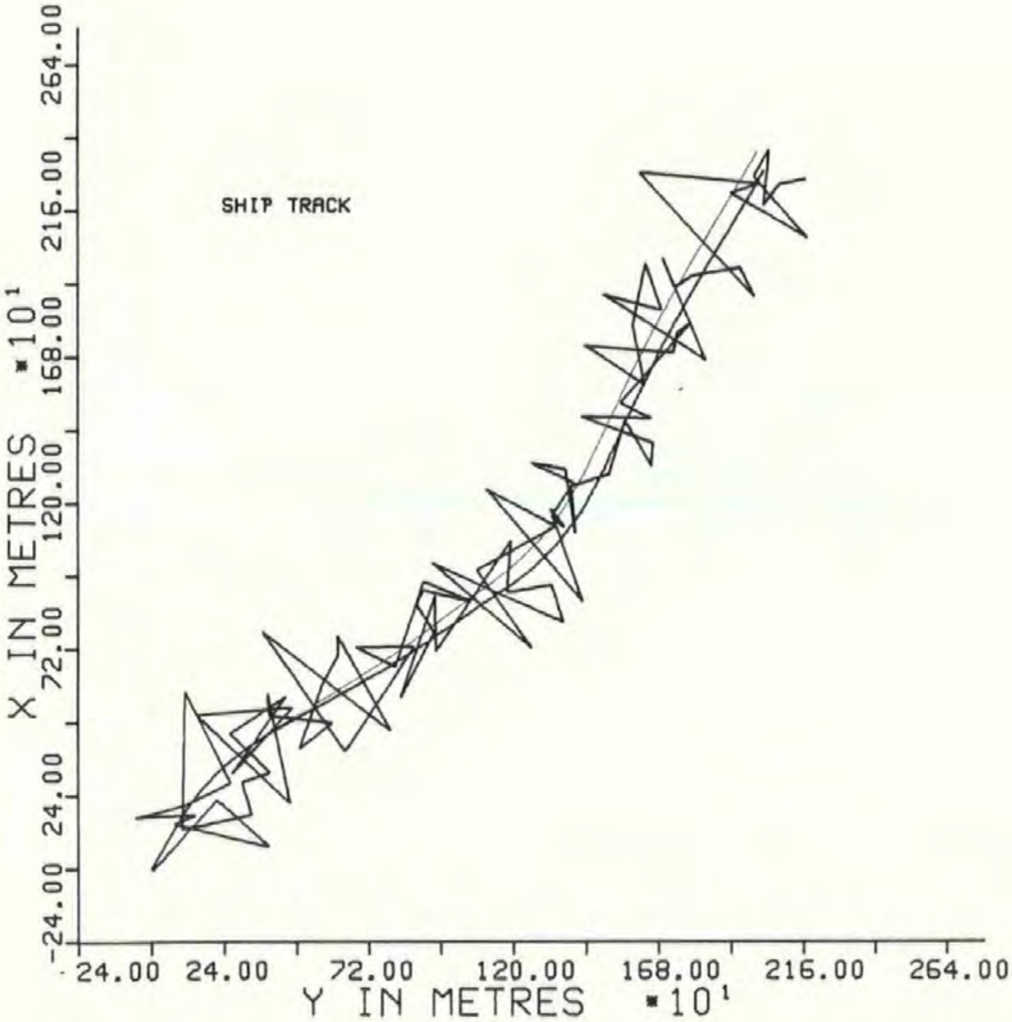

FIG 6.11 Increased Measurement Noise With Zero Disturbance Noise

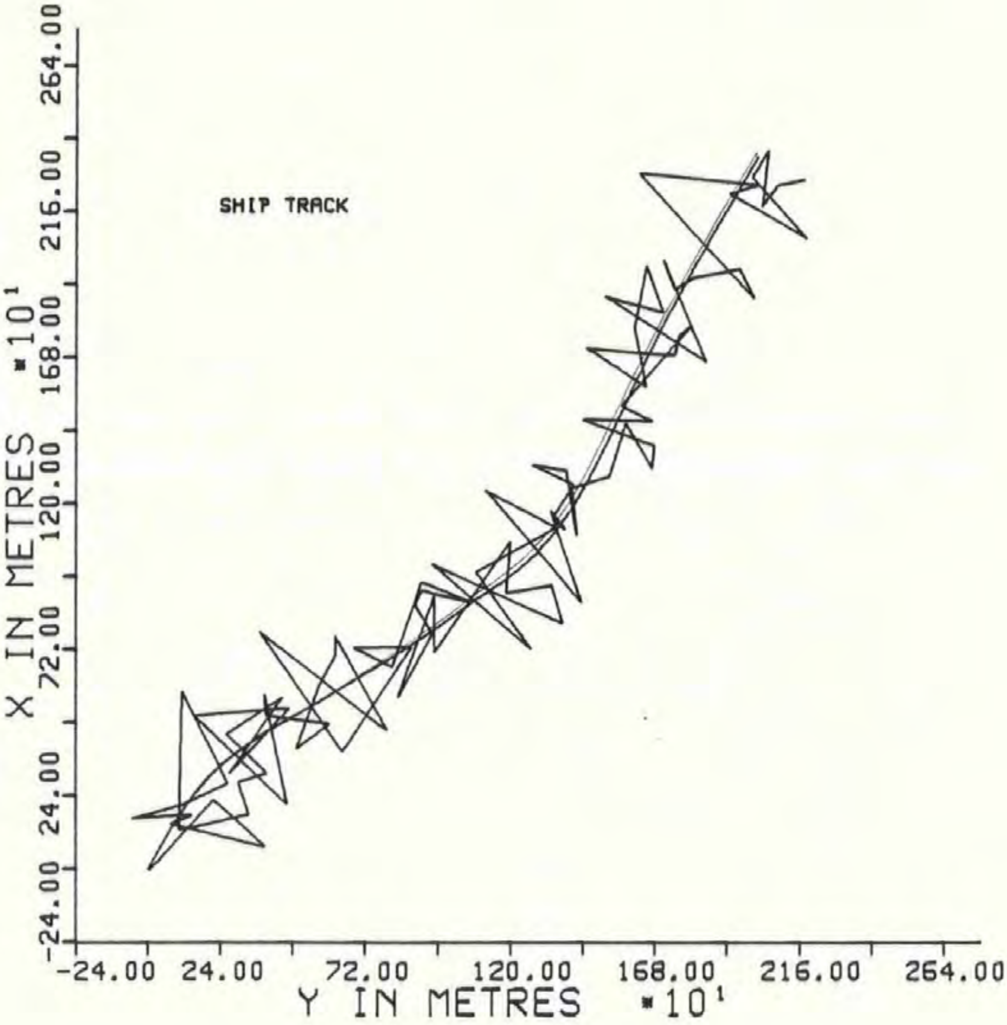

FIG 6.12 Increased Measurement Noise With Reduced Disturbance Noise

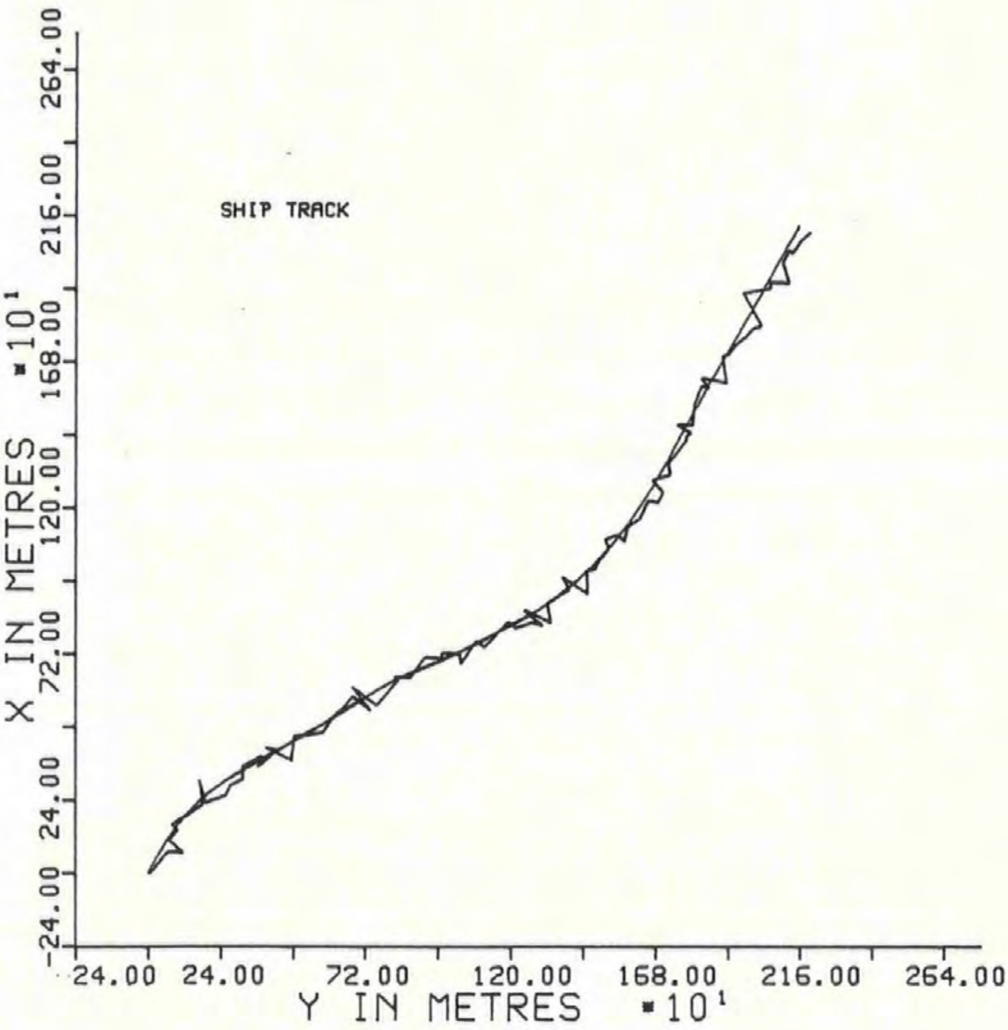

FIG 6.13 Filter Gain Calculations Every 50 Seconds

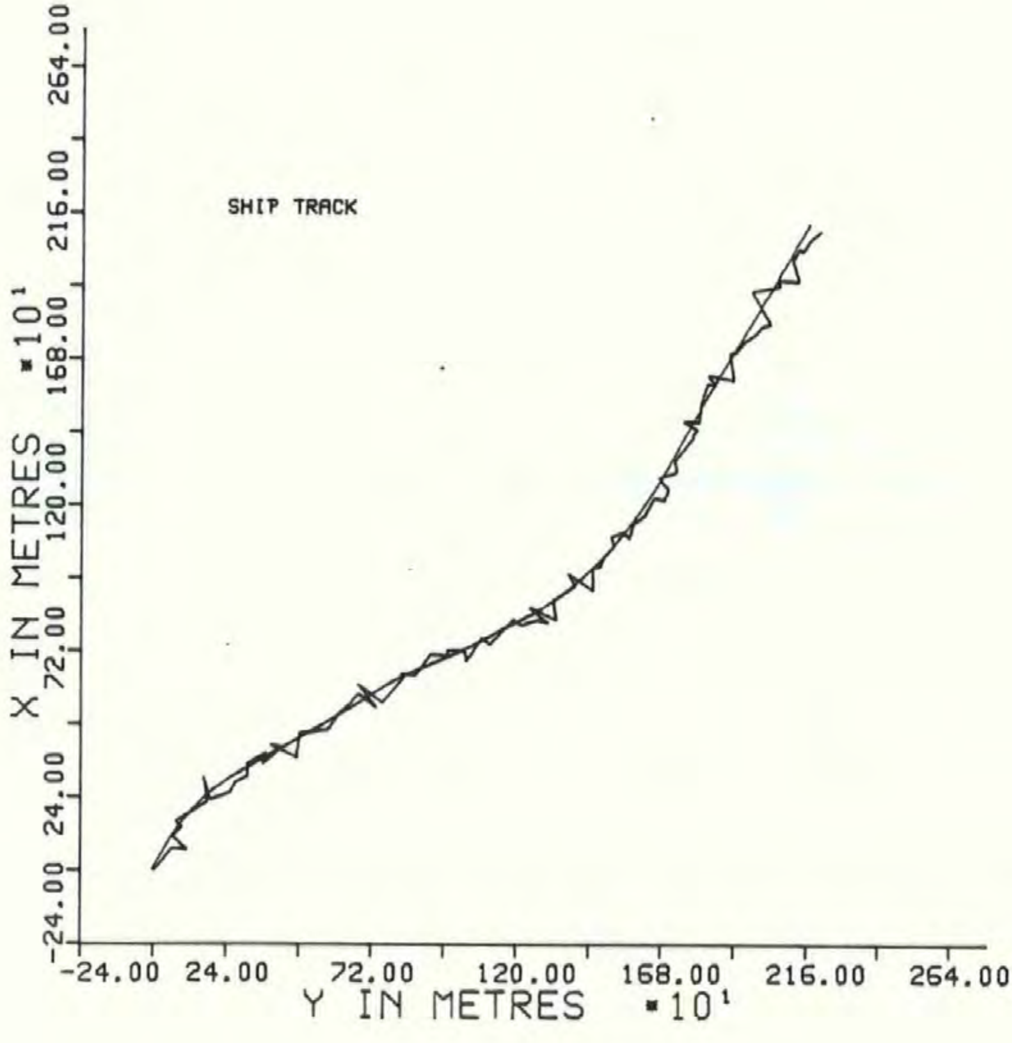

FIG 6.14 Filter Gain Calculations Every 250 Seconds

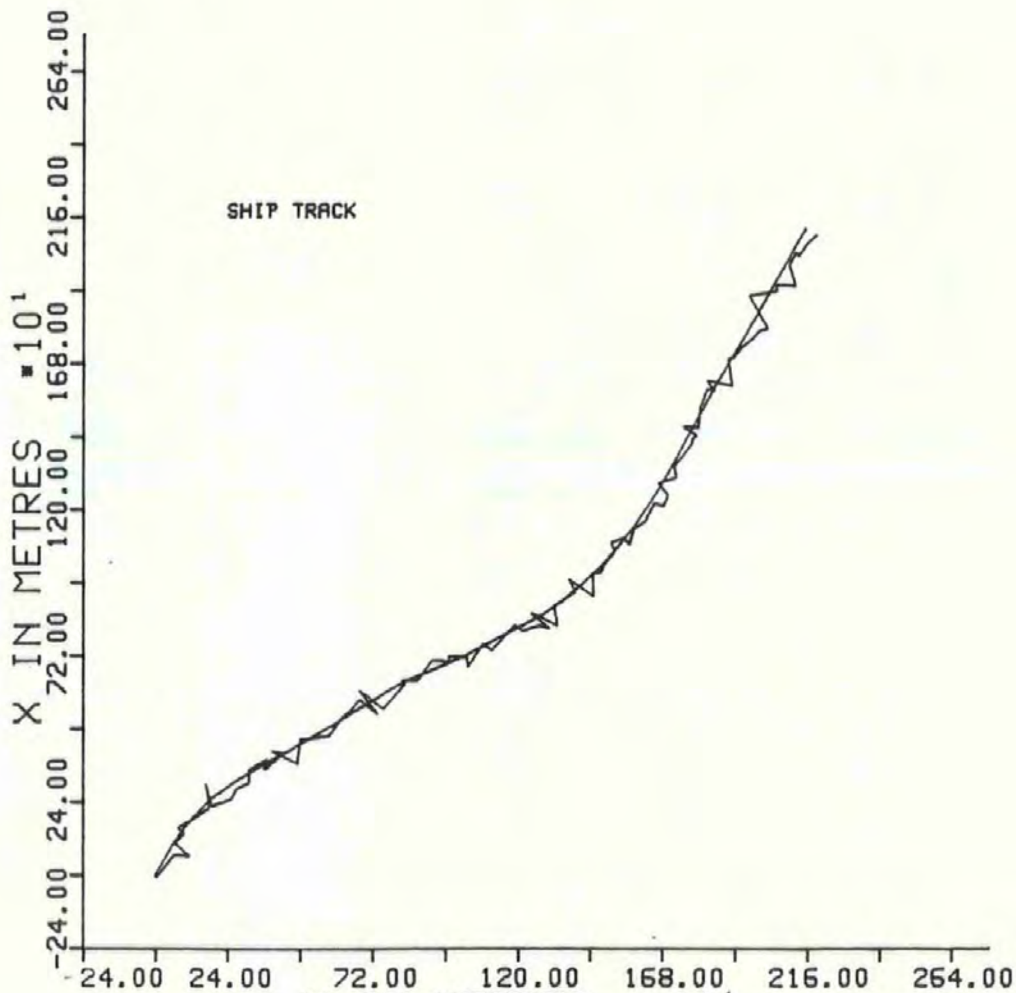

FIG 6.15 Cross Correlation Between x and y Position Measurements

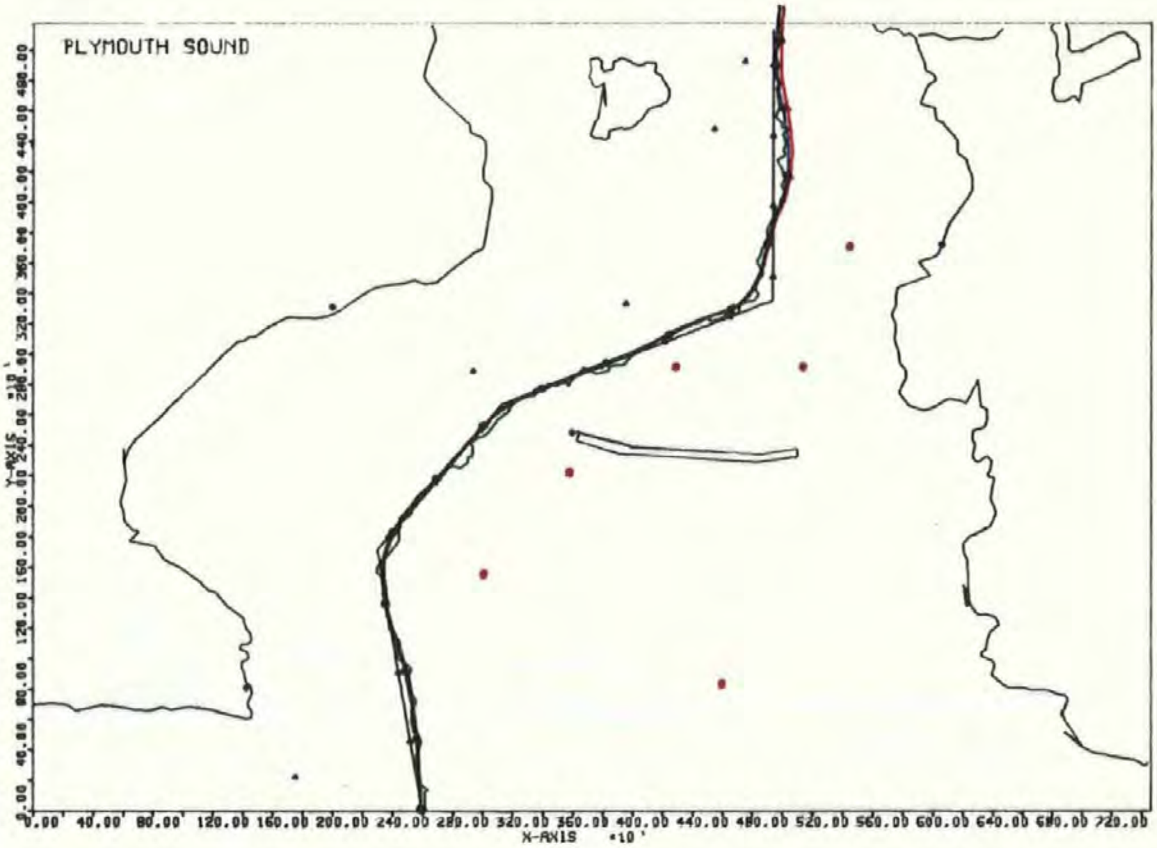

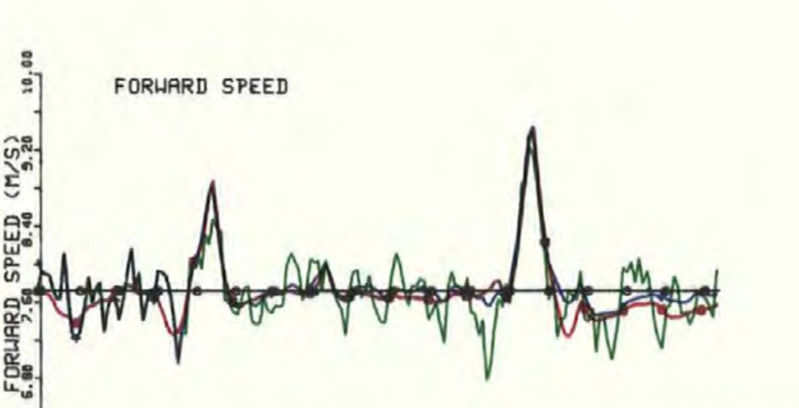

FIG 6.16 DECCA NAVIGATOR- DAYLIGHT CONDITIONS

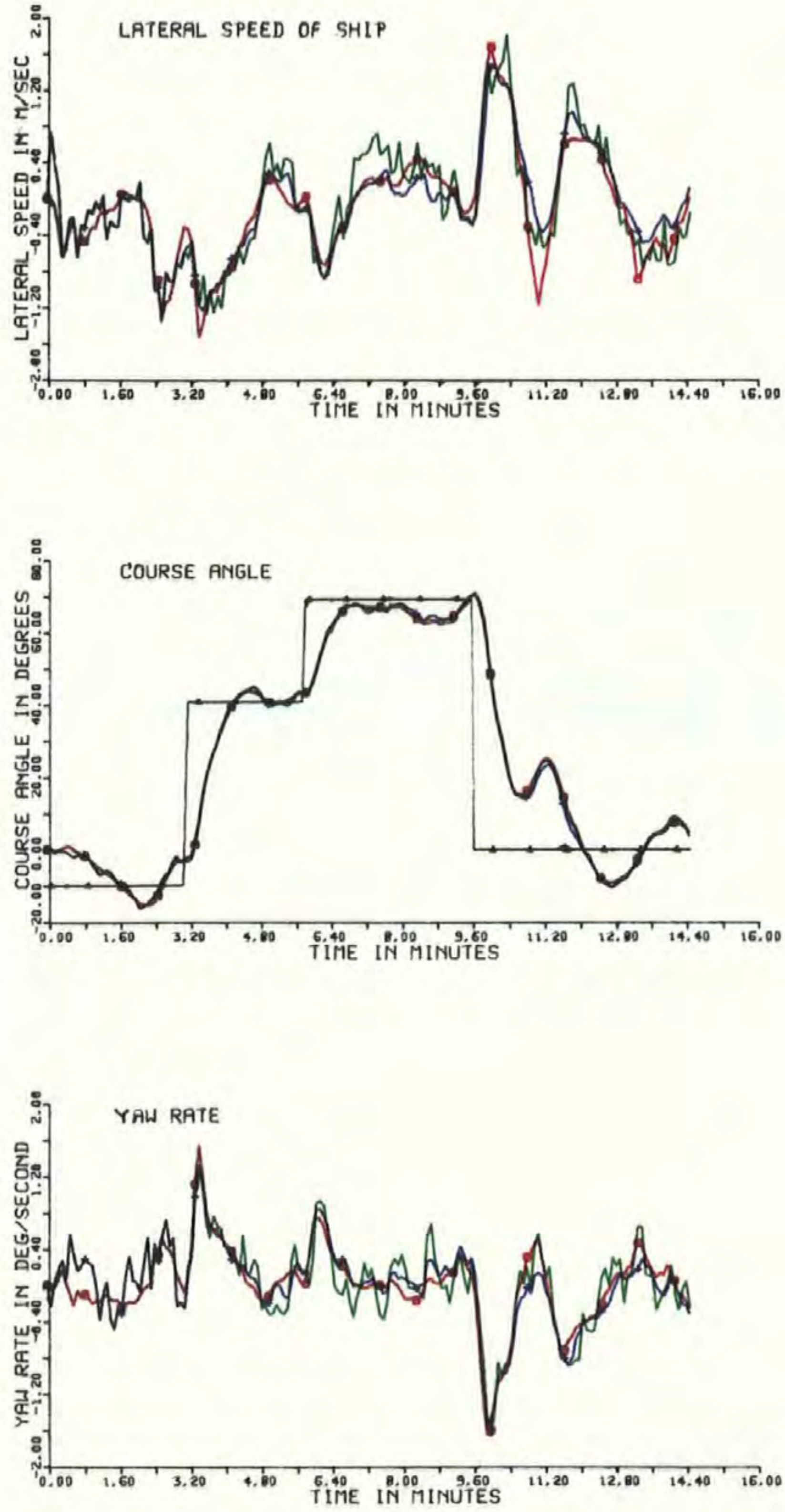
LATERAL SPEED OF SHIP
LATERAL SPEED IN M/SEC
TIME IN MINUTES
COURSE ANGLE
COURSE ANGLE IN DEGREES
TIME IN MINUTES
YAW RATE
YAW RATE IN DEG/SECOND
TIME IN MINUTES

FIG 6.16

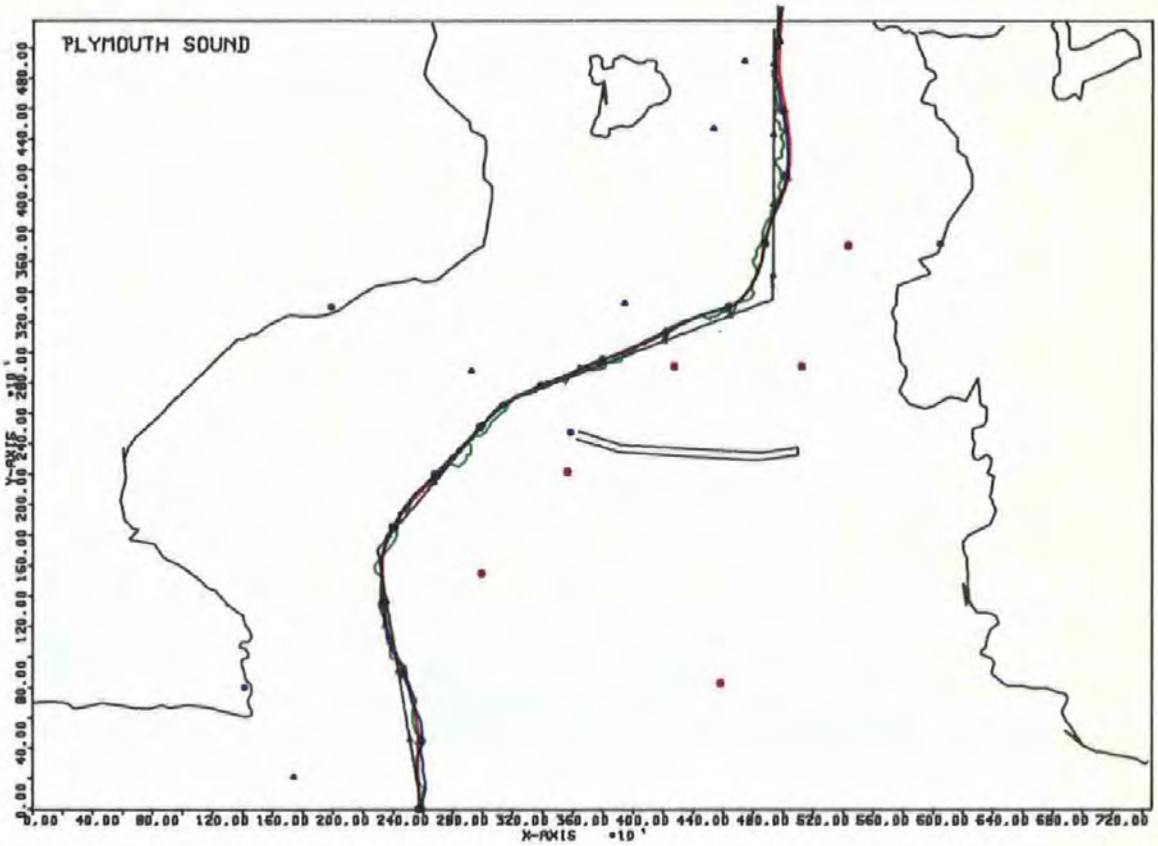

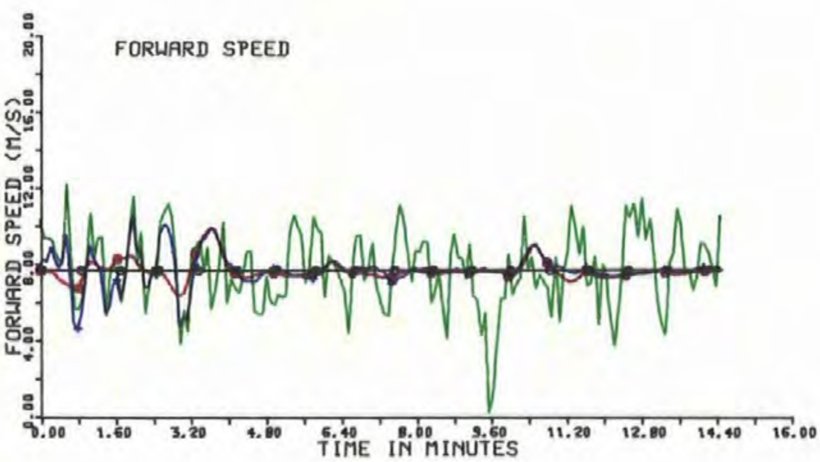

FIG 6.17 NOISEY SPEED MEASUREMENTS

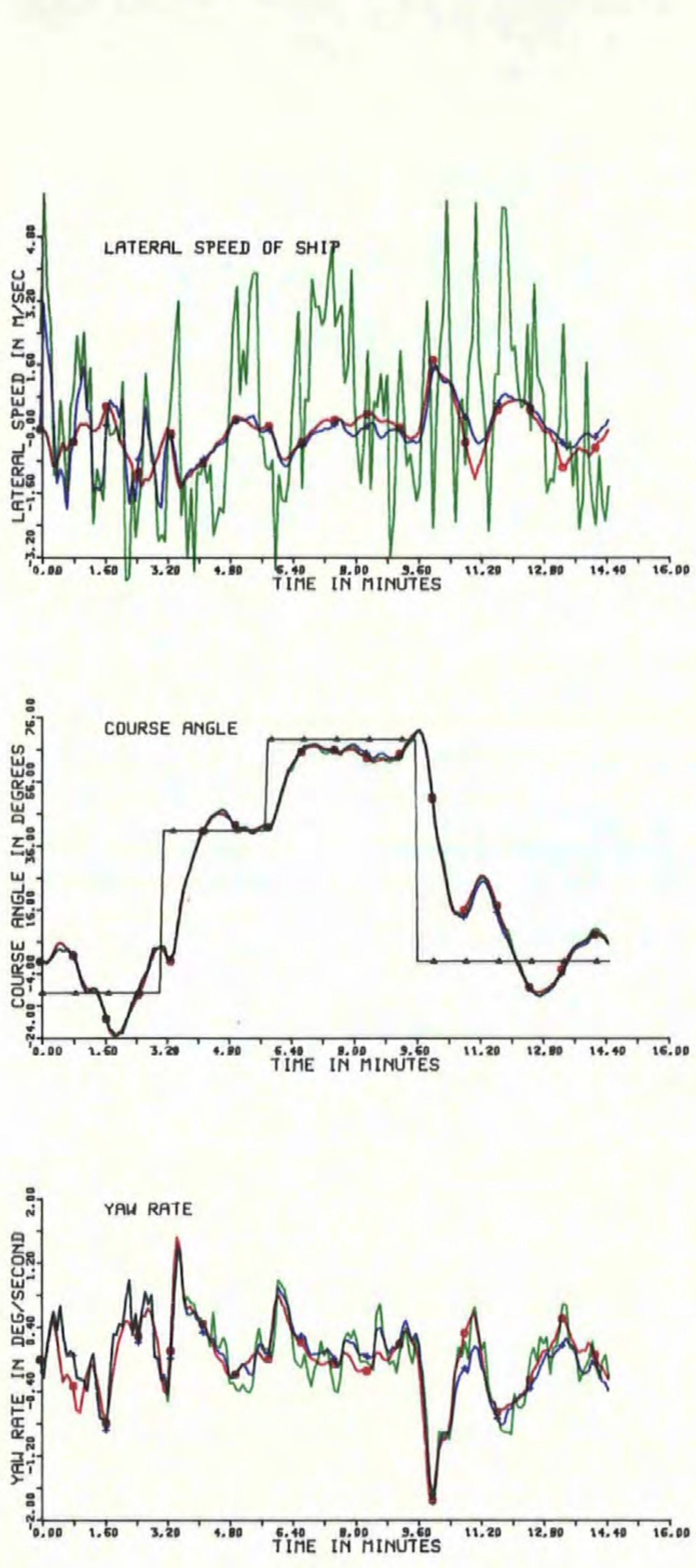
LATERAL SPEED OF SHIP
LATERAL SPEED IN M/SEC
TIME IN MINUTES
COURSE ANGLE
COURSE ANGLE IN DEGREES
TIME IN MINUTES
YAW RATE
YAW RATE IN DEG/SECOND
TIME IN MINUTES

FIG 6.17

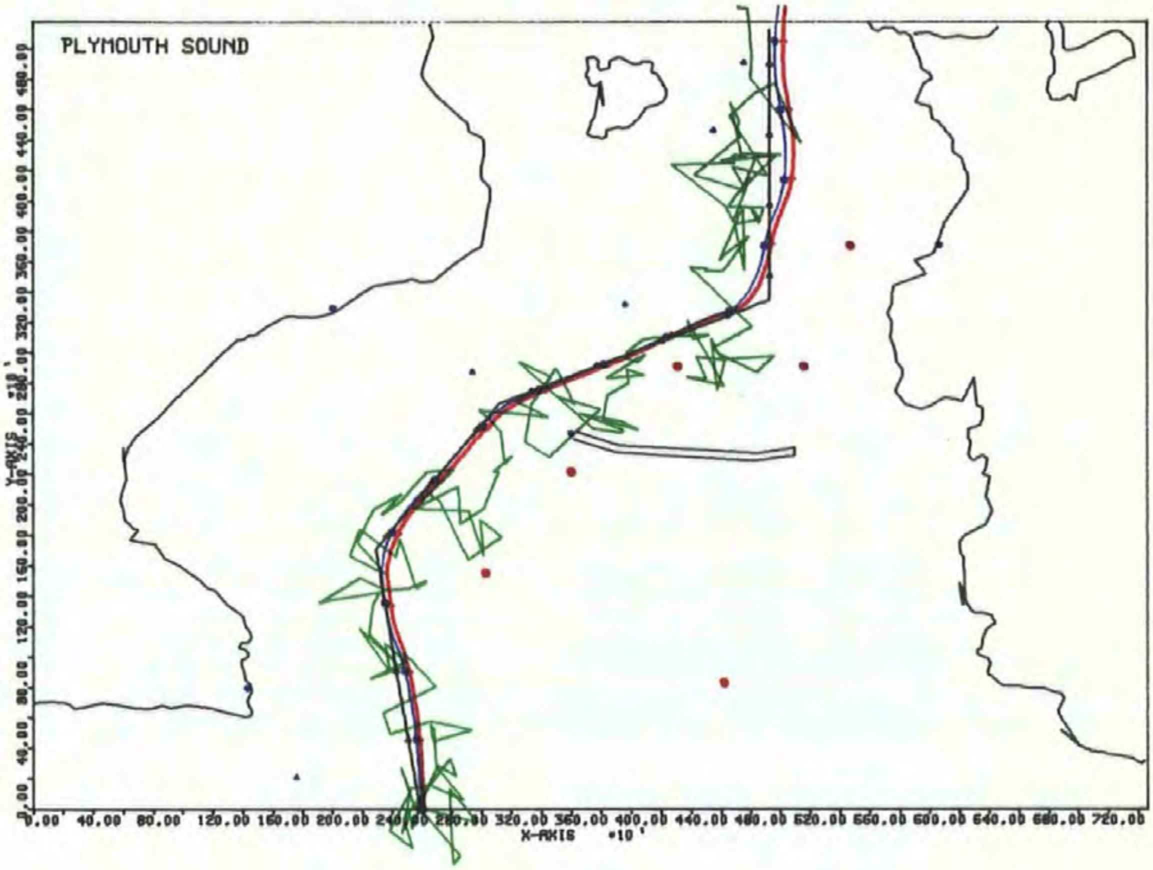

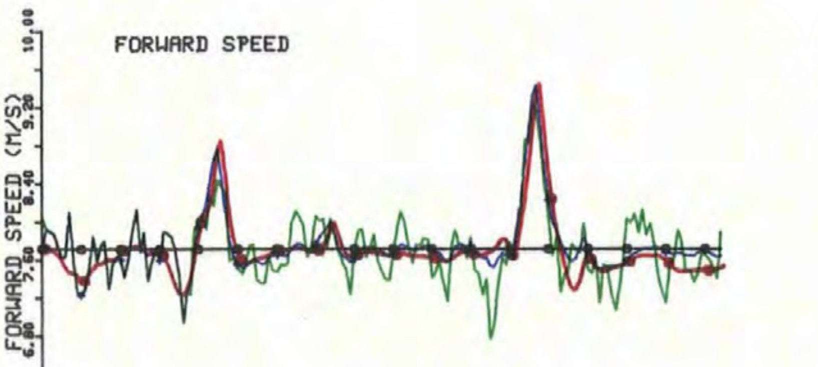

FIG 6.10 DECCA NAVIGATOR- NIGHT APPROACH

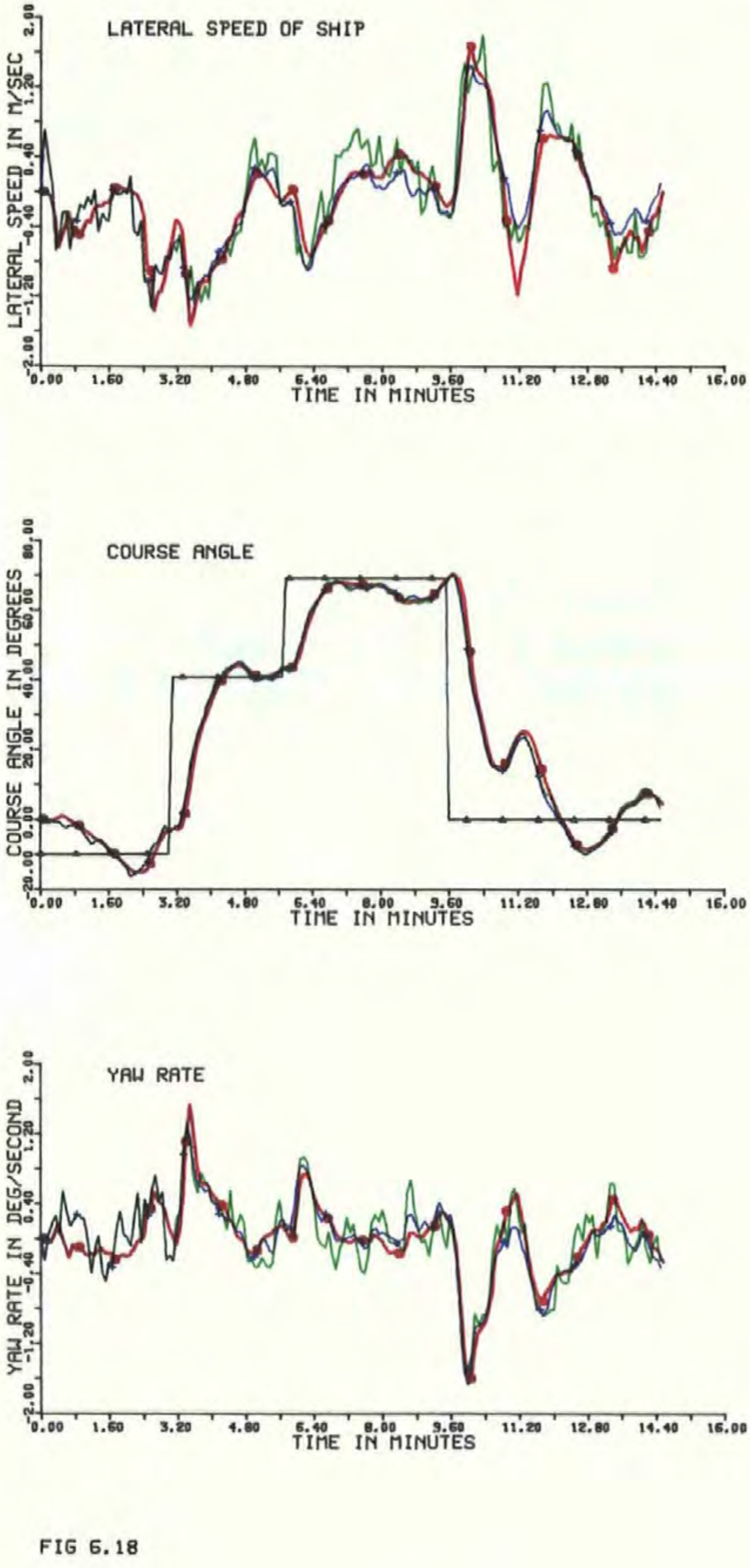
LATERAL SPEED OF SHIP
LATERAL SPEED IN M/SEC
TIME IN MINUTES
COURSE ANGLE
COURSE ANGLE IN DEGREES
TIME IN MINUTES
YAW RATE
YAW RATE IN DEG/SECOND
TIME IN MINUTES
0.00 1.60 3.20 4.80 6.40 8.00 9.60 11.20 12.80 14.40 16.00

FIG 6.18

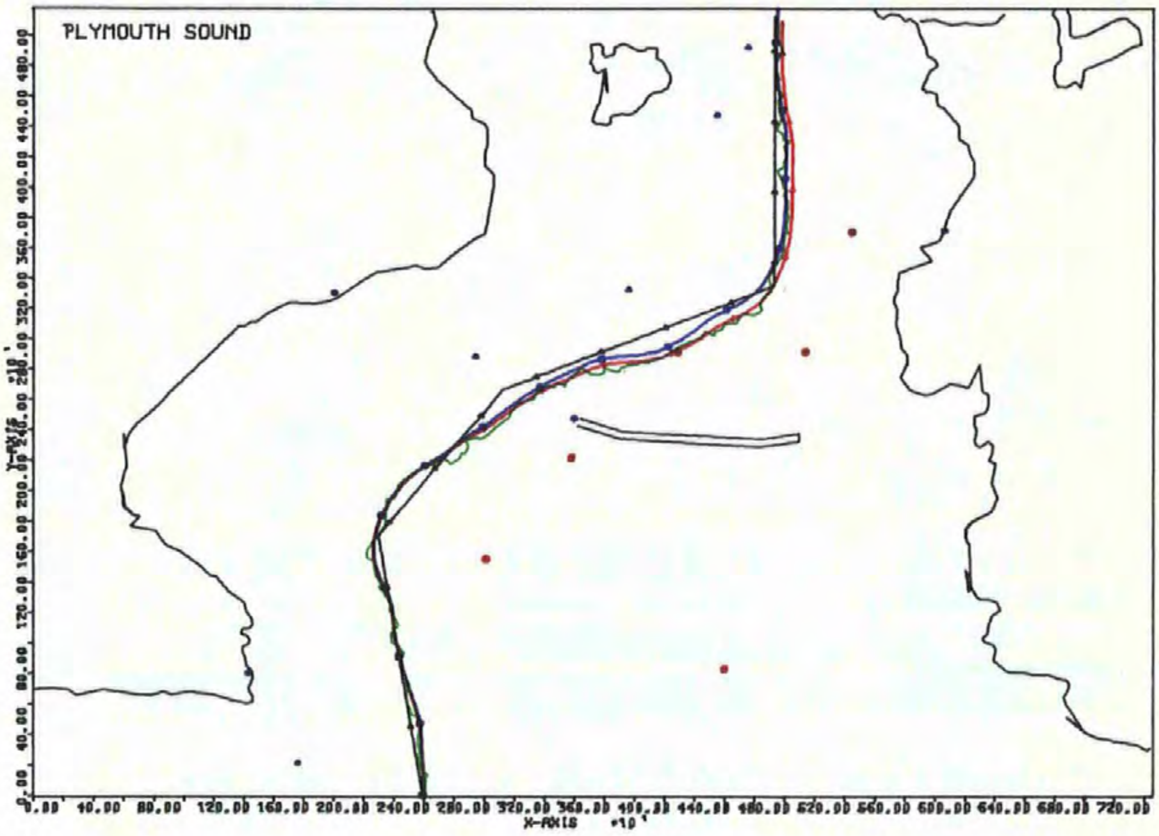

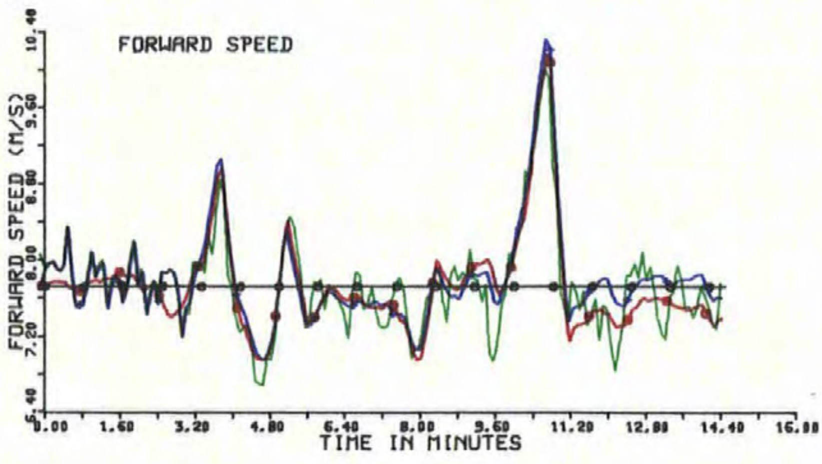

FIG 6.19 BAD WEATHER APPROACH

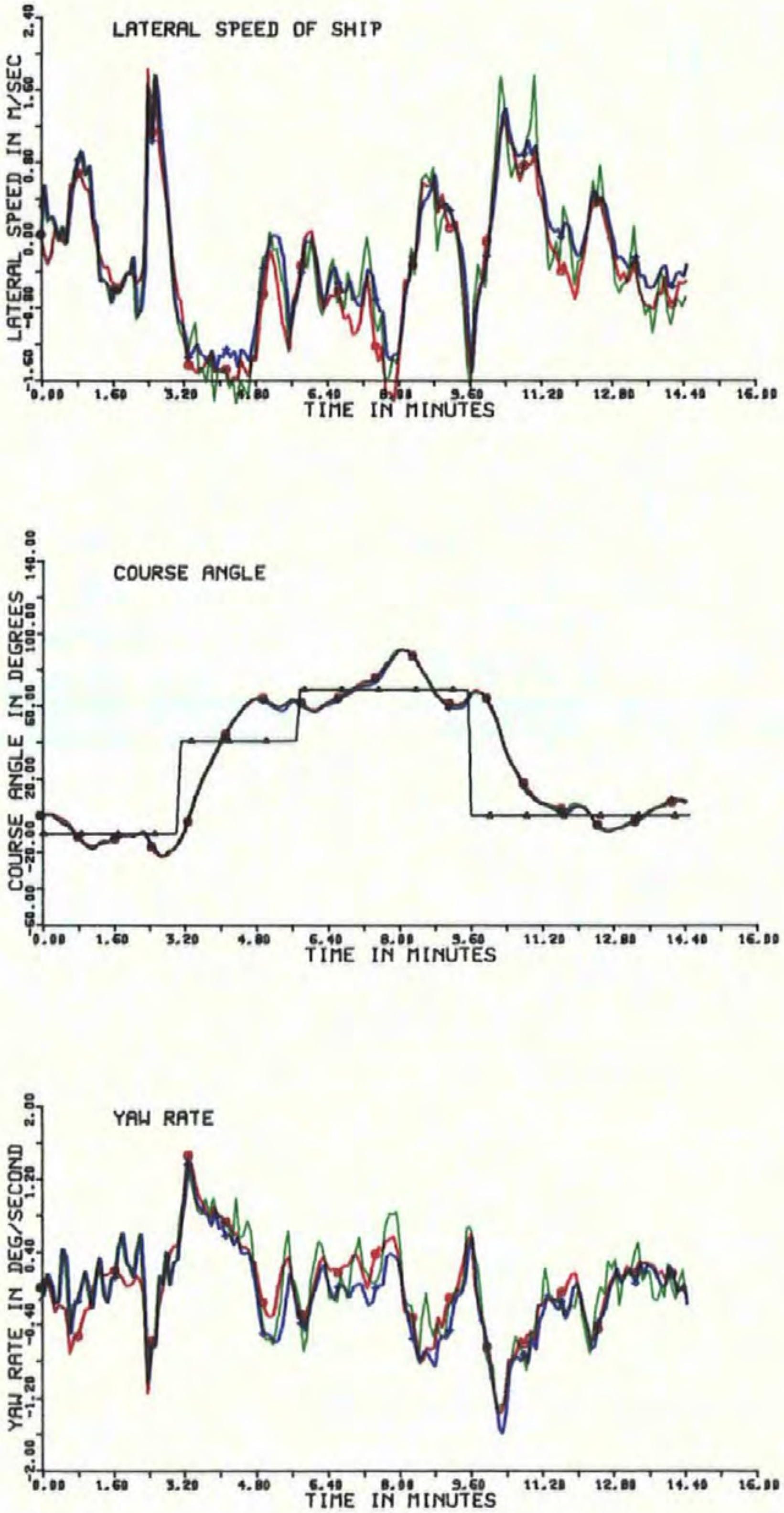

LATERAL SPEED OF SHIP
LATERAL SPEED IN M/SEC
TIME IN MINUTES
COURSE ANGLE
COURSE ANGLE IN DEGREES
TIME IN MINUTES
YAW RATE
YAW RATE IN DEG/SECOND
TIME IN MINUTES

FIG 6.19

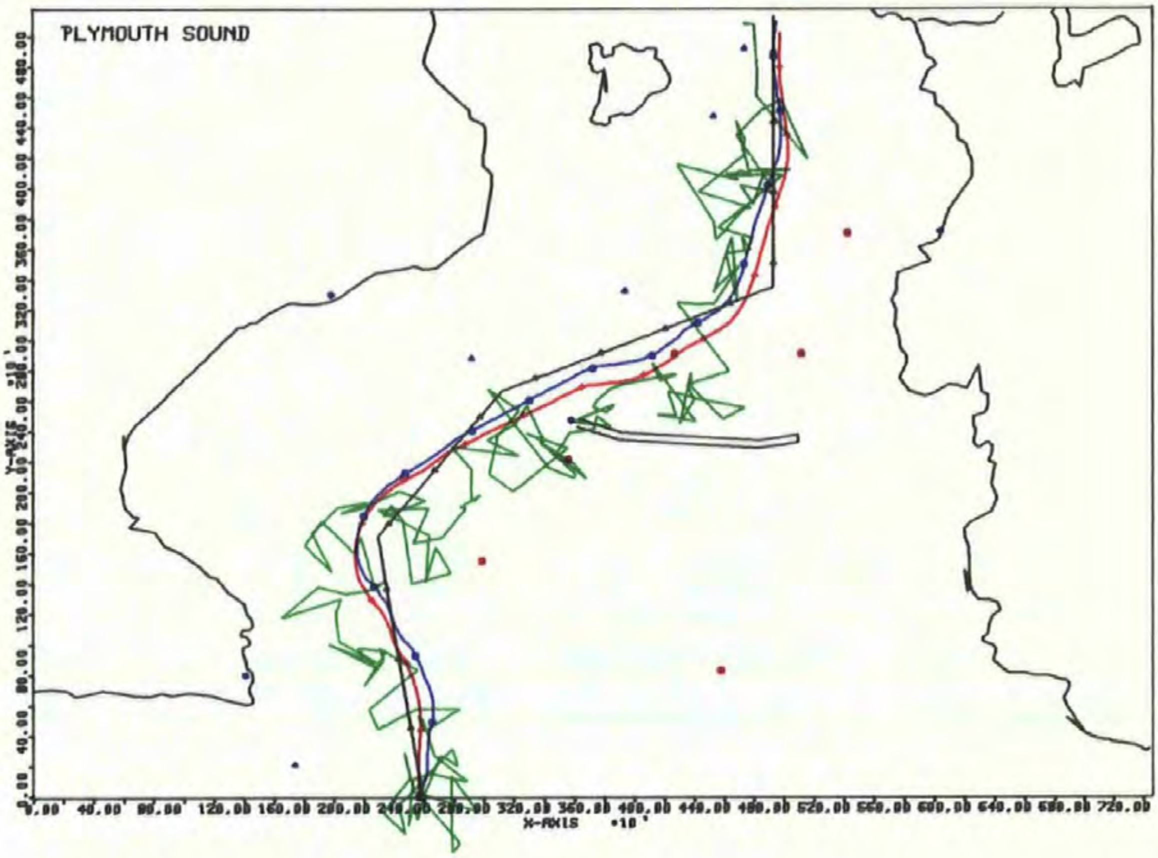

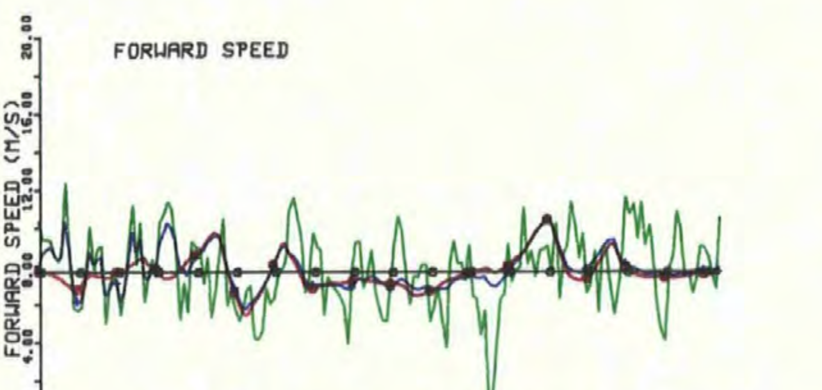

FIG 6.20 BAD WEATHER NIGHT APPROACH

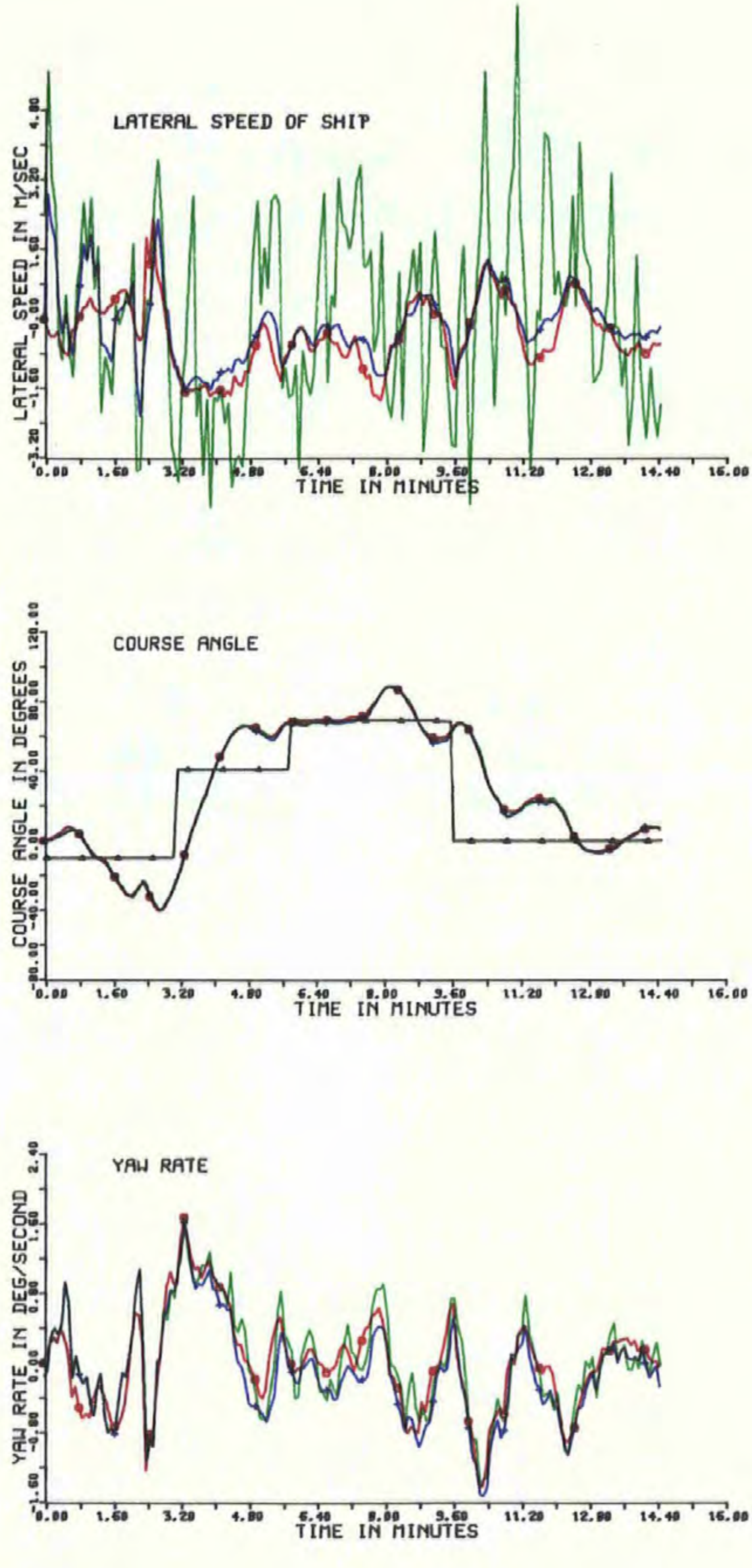

LATERAL SPEED OF SHIP
LATERAL SPEED IN M/SEC
TIME IN MINUTES
COURSE ANGLE
COURSE ANGLE IN DEGREES
TIME IN MINUTES
YAW RATE
YAW RATE IN DEG/SECOND
TIME IN MINUTES

FIG 6.20

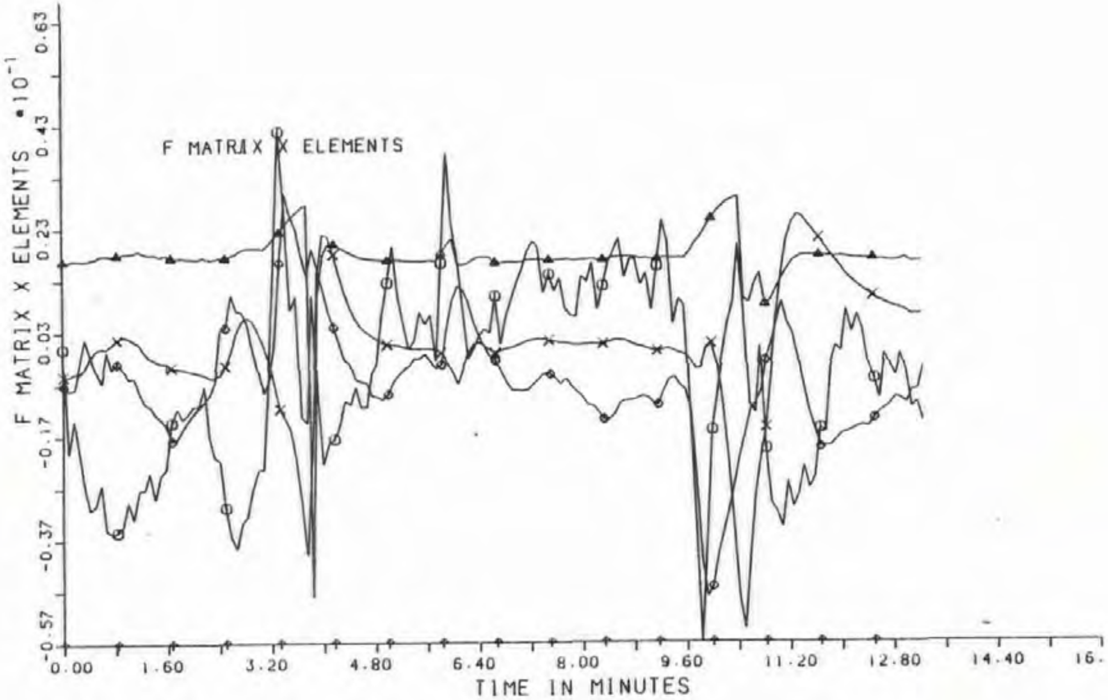

FIG 6.21 Variations of the X Coefficients of the F Matrix

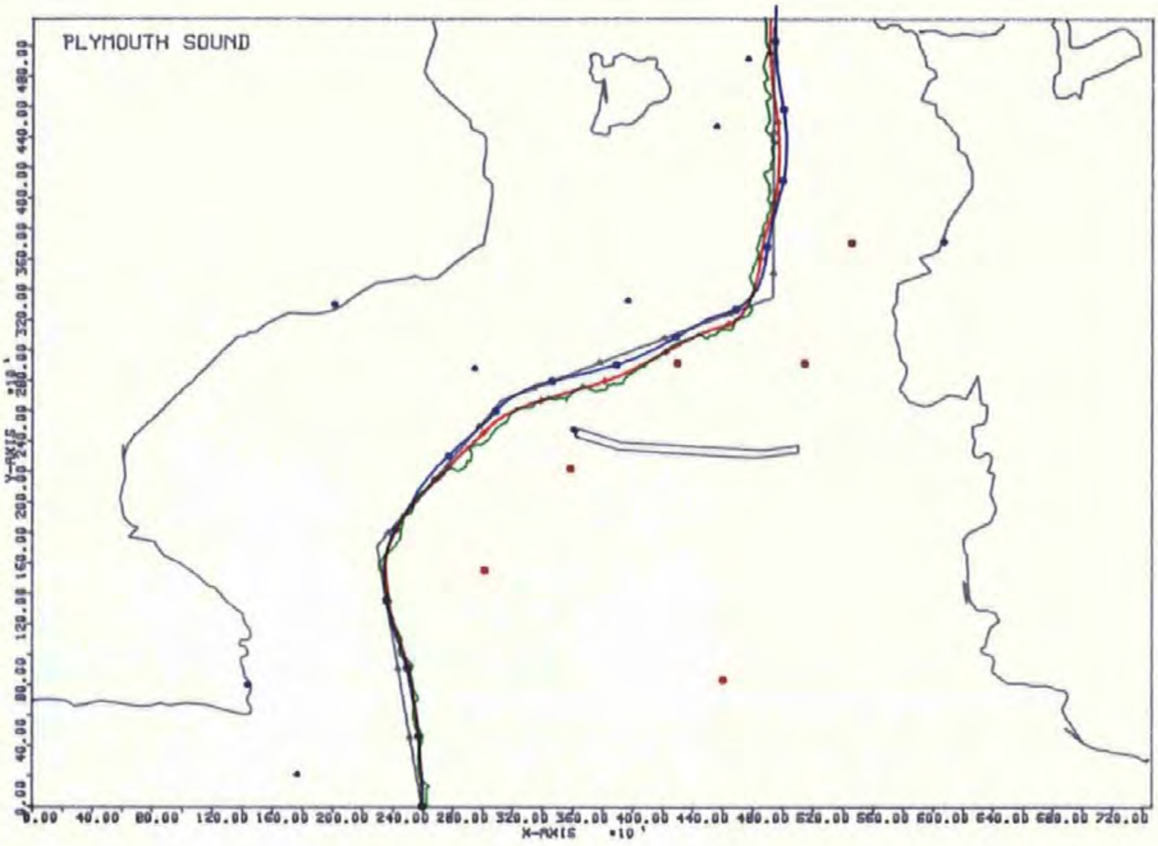

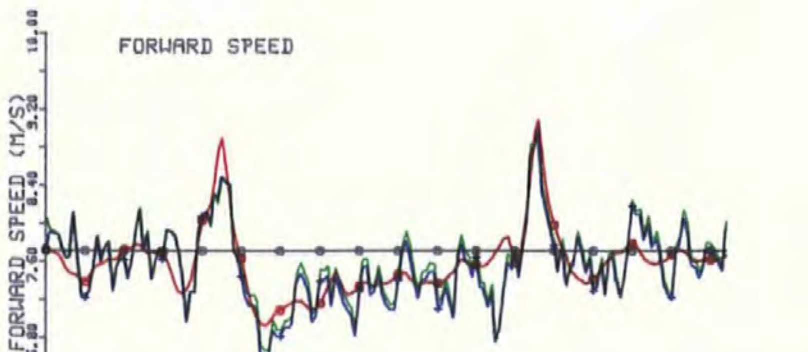

FIG 6.22 REDUCED FILTER

LATERAL SPEED OF SHIP
LATERAL SPEED IN M/SEC
TIME IN MINUTES

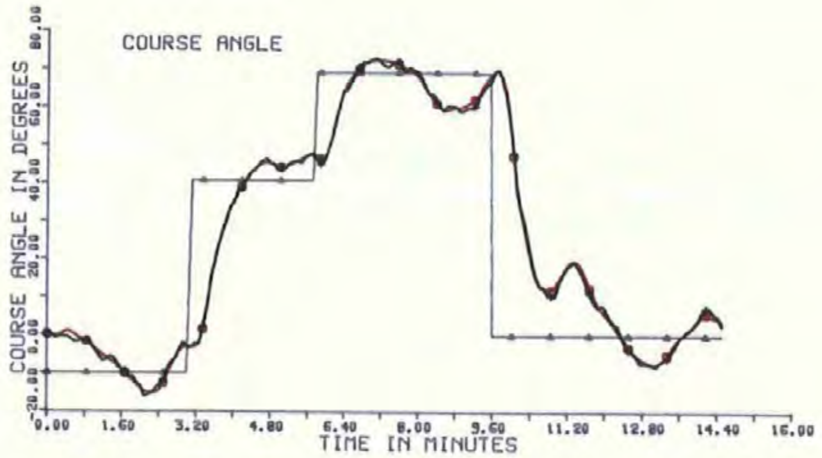

COURSE ANGLE
COURSE ANGLE IN DEGREES
TIME IN MINUTES

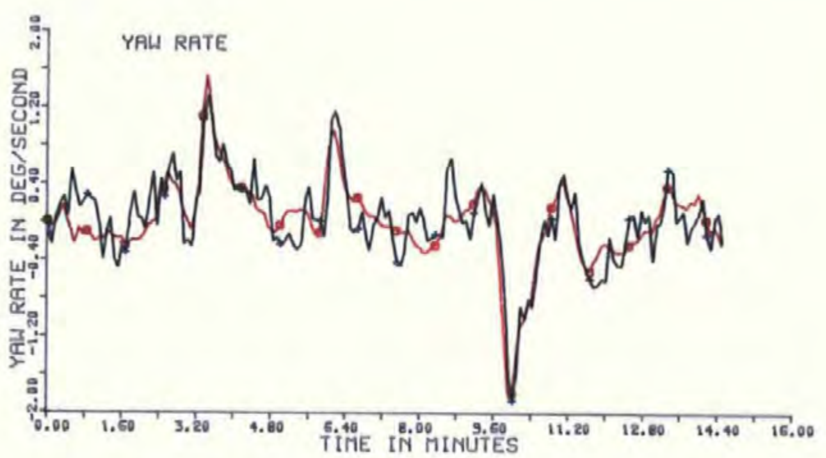

YAW RATE
YAW RATE IN DEG/SECOND
TIME IN MINUTES

FIG 6.22

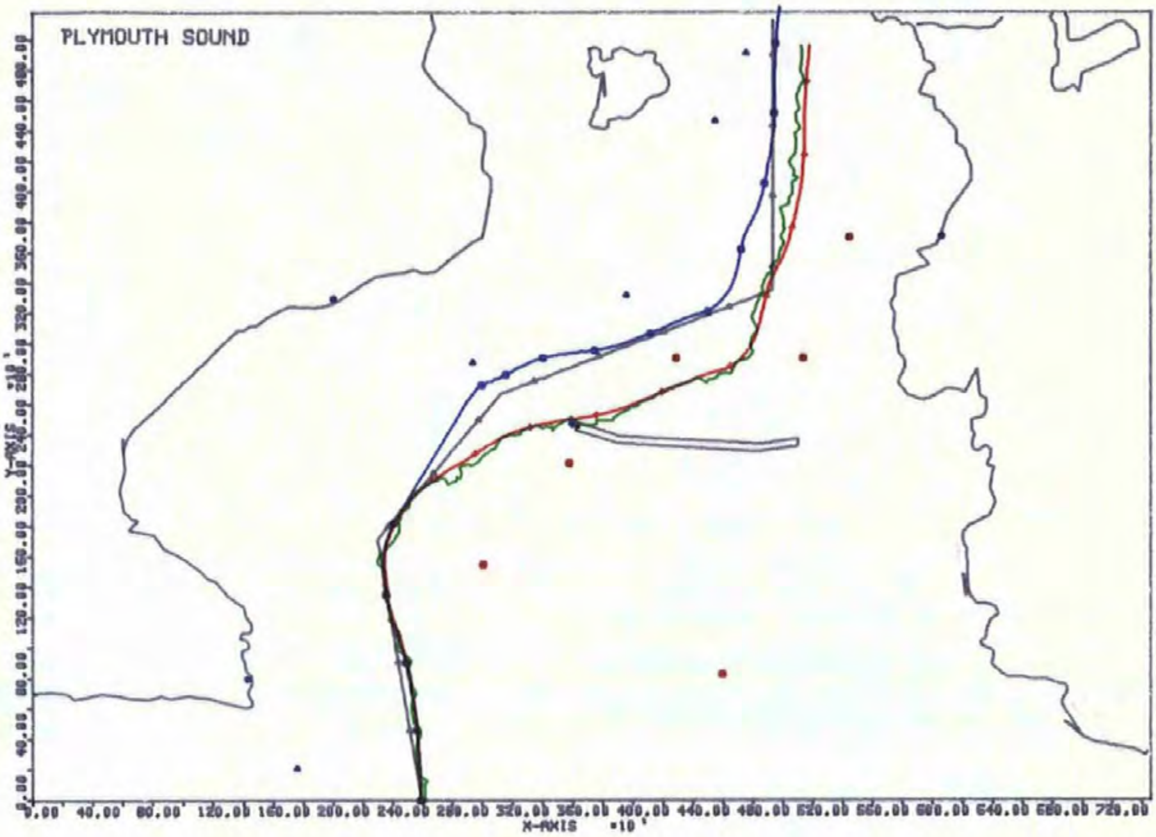

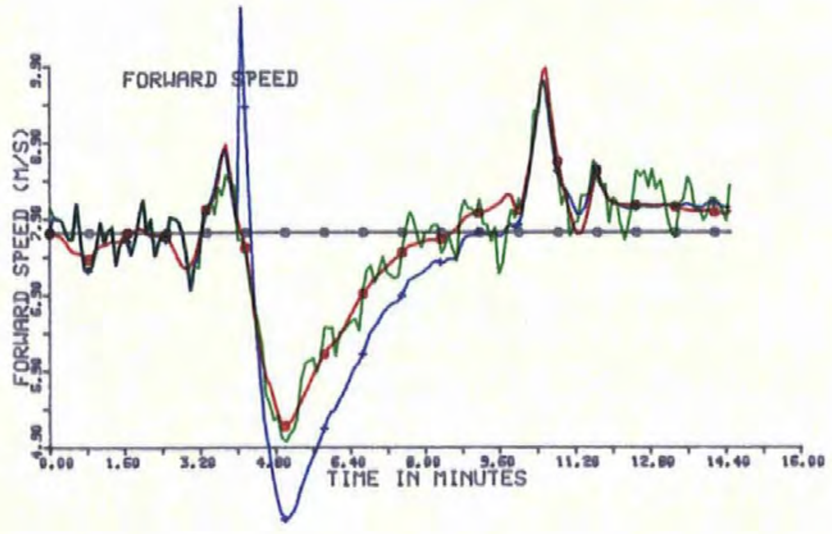

FIG 6.23 REDUCED FILTER

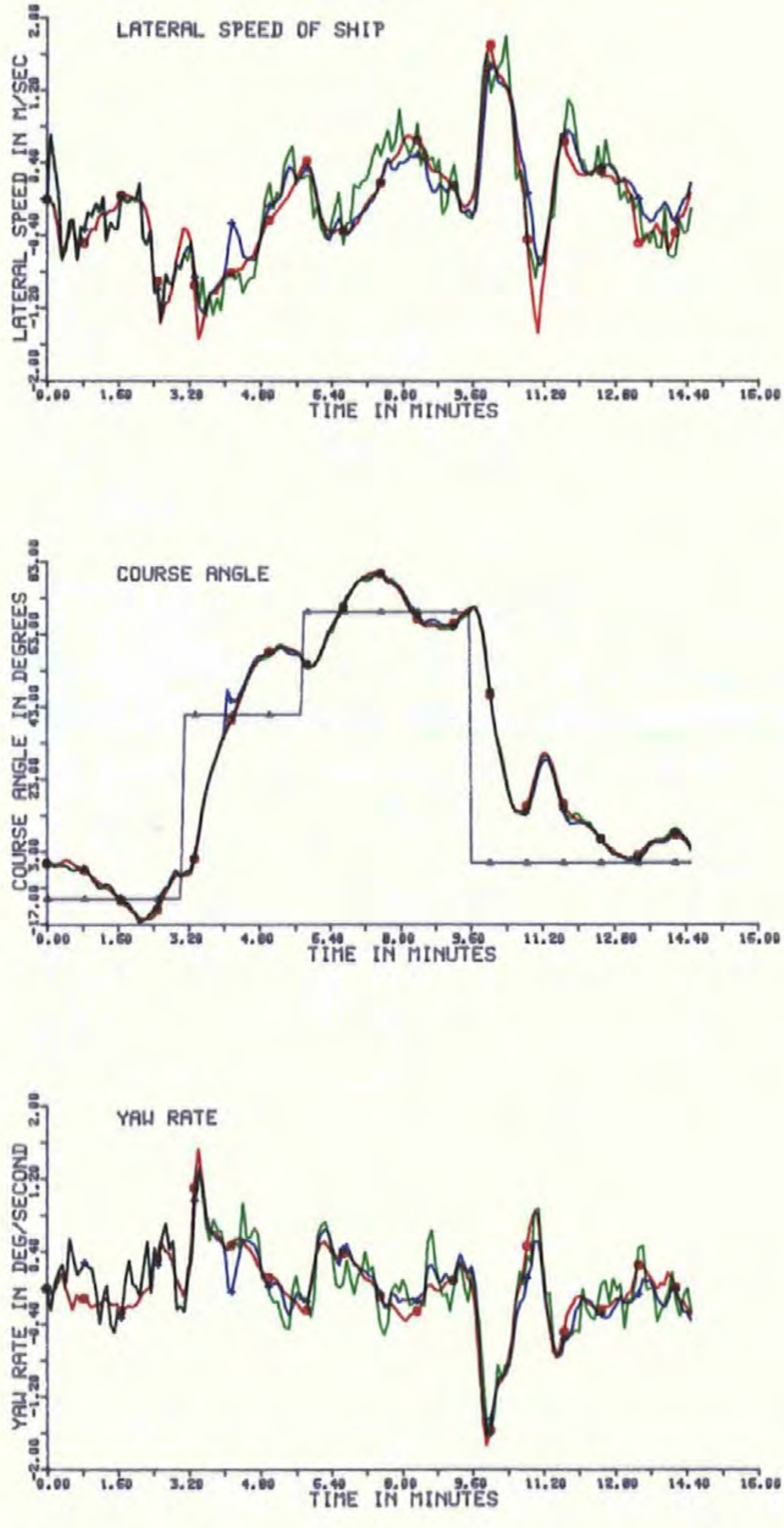
LATERAL SPEED OF SHIP
LATERAL SPEED IN M/SEC
TIME IN MINUTES
COURSE ANGLE
COURSE ANGLE IN DEGREES
TIME IN MINUTES
YAW RATE
YAW RATE IN DEG/SECOND
TIME IN MINUTES

FIG 6.23

CHAPTER 7

DIGITAL COMPUTER SIMULATIONS

DISCUSSION OF RESULTS

7.1 Qualitative Discussion of the Kalman Filter Gains.

Before analysing the factors which govern the filter gains some qualitative comments are made. In a system where there was no measurement or disturbance noise the model states would be in line with those of the vessel and the filter gains would be zero. If there was disturbance noise and no measurement noise, any difference between ship and model would be due to the perturbations of the system caused by random disturbance noise inputs. Without measurement noise the measured values would be correct leading to high filter gains. In this situation the input to the filter reflects the random perturbations due to disturbance. The high filter gains would approach unity as the output from the filter would only be required to add the disturbance effects to the model. Even if a small amount of measurement noise was present the filter gains would still be high. The continuing assumption is made, of course, that there is no correlation between individual measurement systems and reference is then only made to the leading diagonal terms of the filter gain matrix. Even if a small amount of measurement noise is present the filter gains would be expected to approach unity.

If now the measurement noise was high and the disturbance noise low the model states would be correct, but the measurements incorrect, leading to low filter gains so that each output component from the filter would only make a small change to its appropriate model state. In the full scale digital simulations described in the previous chapter there are four disturbance components whereas the measurement vector has eight elements, corresponding to the eight states, but the foregoing does suggest that if the ratio of disturbance noise to measurement noise is high the filter gains will be high, but if the ratio is small, the gains will be low. As some measurement noise values are high and others low this suggests that the elements of the gain matrix may differ widely.

7.2 Analysis of the Kalman Filter Gains.

Before attempting any quantitative analysis of the gains obtained in the digital computer simulations, the matrix equations used in the filter calculations are restated in algebraic form. The first computer equation defines the intermediate or predicted system error covariance matrix given by:-

$$\underline{P}(k+1/k) = \underline{A}(k+1,k)\underline{P}(k/k)\underline{A}^T(k+1,k) + \underline{C}(k+1,k)\underline{N}(k)\underline{C}^T(k+1,k) \qquad (7.1)$$

$\underline{P}(k/k)$ is the system error covariance matrix which has been calculated during the previous sampling instant. In the full scale models it is an 8*8 matrix. During each set of calculations an intermediate value $\underline{P}(k+1/k)$ is calculated from equation 7.1 using the state transition matrix $\underline{A}(k+1,k)$ and its transpose, the disturbance transition matrix $\underline{C}(k+1,k)$ its transpose and the disturbance noise covariance matrix $\underline{N}(k)$ in addition to $\underline{P}(k,k)$.

This predicted error covariance is then used in the calculation of the

Kalman Filter gain matrix $\underline{K}(k+1)$ as follows:-

$$\underline{K}(k+1) = \underline{P}(k+1,k)\underline{H}^{T}(k+1)\left[\underline{H}(k+1)\underline{P}(k+1/k)\underline{H}^{T}(k+1)+\underline{M}(k+1)\right]^{-1} \qquad (7.2)$$

The filter gains therefore depend upon the previous values of the error covariance matrix, the state and disturbance transition matrices, the measurement matrix $\underline{H}(k+1)$ and its transpose, the disturbance noise covariance matrix and the measurement noise covariance matrix $\underline{M}(k+1)$. Finally a new value $\underline{P}(k+1/k+1)$ is obtained from:-

$$\underline{P}(k+1/k+1) = \left[\underline{I}-\underline{K}(k+1)\underline{H}(k+1)\right]\underline{P}(k+1/k) \qquad (7.3)$$

This new value of the error covariance matrix is then available for the next set of filter calculations.

Unless otherwise stated the figures quoted in this section refer to the standard set of conditions set out in Table 6.1 and described in Chapter 6. Table 7.1 and 7.2 gives values for a predicted system error covariance matrix at the beginning and towards the end of a run where the filter gain was calculated for each value of the sample time, and the model matrices were re-calculated in a similar manner. It can be seen from this table that the elements vary from such large numbers as 24.88, PKP1(3,3) at beginning of the run to 0.0000000327, PKP1 (8,2) at the end of the run. It can also be seen that the majority of terms in the matrix are small numbers or zero (typically about 75% are less than 1), brought about by the small numbers in the $\underline{A}$ and $\underline{C}$ matrices. As the elements of the $\underline{C}$ matrix are mainly very small numbers themselves the contribution of the disturbance noise covariance matrix $\underline{N}$ tends to be minimised, but including the term $\underline{C}*\underline{N}*\underline{C}^{T}$ in equation 7.1 acknowledges the deterioration in knowledge of the states that occur due to the effect of random disturbances in each sample time.

The calculation of the filter gains (equation set 7.2) included a matrix inversion. $\underline{H}$, and hence $\underline{H}^T$, were taken as identity matrices and $\underline{P}(k+1/k)$ was thus effectively added to the measurement noise covariance matrix $\underline{M}$, after which the matrix inversion took place. To test the validity of the matrix inversion the original and inverted matrices were multiplied together to give the identity matrix.

When the inverted matrix is multiplied, effectively, by $\underline{P}(k+1/k)$ to give the filter gain matrix then the leading diagonal terms are close to 1 for low measurement noise values and much smaller for high measurement noise values, with the great majority of the off-diagonal terms close to zero, (Table 7.3). When the position standard deviations were increased to 200 metres (to simulate a winter's night approach using the Decca Navigator), then the (3,3) and (5,5) elements of the filter gains were further decreased by a factor of 64. It is interesting to note that this corresponds to a 62.5 factor of increase for the appropriate covariance term in $\underline{M}$. Typical values of the filter gains are given in Table 7.4.

Increase in M(3,3)	=	2002/252 = 64
	=	Increase in M(5,5)
K(3,3) for 25 metres SD	=	0.004026536
K(3,3) for 200 metres SD	=	0.00006342497
Ratio	=	63.48
K(5,5) for 25 metres SD	=	0.004536094
K(5,5) for 200 metres SD	=	0.00008394379
Ratio	=	54

These figures confirm the statements made in 7.1 namely that the filter gains depend largely upon the measurement noise, being low for noisy signals and high for low values of measurement noise, although the disturbance noise does have to be taken into consideration.

The results of Chapter 6 showed quite clearly the ability of the filter to take noisy signals from the eight measured states and provide best estimates which were close to the true values. It has to be borne in mind that the results of simulation are usually better than those achievable in the real world. This is principally due to the similarity between system dynamics, noise colourations and other factors contained both in the Kalman filter equations and the simulation models, a difficult situation to avoid with the normal lack of knowledge of real-world dynamics and stochastic processes. However some differences were obtained by using only true values in the simulation models and either estimated or measured values in the filter equations.

Another problem was the need to transform between co-ordinate systems. In effect three co-ordinate systems were used. The first two were related to the ship and the earth respectively, and when plotting the ship's track relative to earth it was necessary to transform the x and y co-ordinates relative to the ship axes to earth axes. This was unrealistic in that an electronic position fixing system would almost certainly give position co-ordinates in some hyperbolic system. These would then have to be transformed to cartesian co-ordinates relative to the earth. Again this was a limitation of the simulation employed. However rudder angle, speed and yaw rate were measured relative to the ship axes whilst heading was one of the links between the two co-ordinate systems.

A third co-ordinate system was used to define track error. A way point was defined and the position error related to the distance along track and the distance off track (track error). This latter system was primarily to simplify the optimal controller.

0.00673	0.0	-0.0118	-0.00355	0.05902	0.01569	-0.00217	-0.00057
0.0	0.00673	0.00528	0.00151	0.00002	0.00001	0.0	0.0
-0.00181	0.00528	0.00249	0.04669	-0.53231	-0.10927	-0.18566	-0.02907
-0.00355	0.00151	4.66975	0.91377	-0.24973	-0.05965	-0.10611	-0.01672
0.05902	0.00002	-0.53231	-0.24973	34.74558	8.42338	14.58034	2.30938
0.01569	0.00001	-0.10927	-0.05965	8.42338	2.35974	5.22462	0.82947
-0.00217	0.0	-0.18566	-0.10611	14.58034	5.22463	17.42164	2.61496
-0.00057	0.0	-0.02907	-0.01672	2.30938	0.82947	2.61496	0.41641

Table 7.1 Predicted Error Covariance (PKP1) at Start of Run

0.00673	0.0	-0.00555	-0.00146	0.06177	0.01679	-0.00224	-0.00060
0.0	0.00673	0.00669	0.00192	-0.00002	-0.00001	0.0	0.0
-0.00555	-0.00669	24.97807	4.69605	0.21	0.03091	0.12139	0.01989
0.00146	0.00192	4.69605	0.92003	0.12624	0.0283	0.06874	0.01119
0.06177	-0.00002	0.21	0.12624	34.7166	8.39009	14.01015	2.26452
0.01679	-0.00001	0.03091	0.02823	8.39009	2.33597	5.11093	0.82806
-0.00224	0.0	0.12139	0.6874	14.01015	5.11094	18.00821	2.76437
-0.00061	0.0	0.01989	0.01119	2.26452	0.82806	2.76437	0.44931

Table 7.2 Predicted Error Covariance (PKP1) at End of Run

0.99937	0.0	0.0	0.0	0.0	0.00001	0.0	-0.00003
0.0	0.9941	0.0	0.0	0.0	0.0	0.0	0.0
0.35409	-0.36601	0.00403	0.04763	-0.00002	-0.05528	-0.00003	0.02809
-0.01621	0.01831	0.00047	0.93403	0.0	0.00089	0.0	-0.00008
-3.38426	-0.00295	-0.00002	0.02807	0.00454	4.88049	0.00223	-0.03996
0.20291	-0.00038	0.0	0.00089	0.00049	0.92181	0.00095	0.13599
0.00004	0.0	0.0	0.0	0.0	0.0	0.99971	0.00173
-0.00012	0.0	0.0	0.0	0.0	0.00003	0.0001	0.99929

Table 7.3 Typical Kalman Filter Gains

CHAPTER 8

DESIGN OF A MINIMUM VARIANCE FILTER FOR THE PHYSICAL MODEL

8.1 Introduction

Prior to installing the optimal filter and controller in the physical model (CENTAUR) it was decided to simulate them using the mainframe computer. In accordance with the nomenclature of Chapter 3 the computer model of the physical car ferry model was named HEATHMORE. Restrictions were imposed by the instrumentation package installed in the model, which consisted of three accelerometers, a gyro and a yaw rate gyro, but eventually the reduced non-linear model of equation set (3.29) was decided upon.

Limitations of the Texas Instruments microcomputer memory necessitated modification of the computer programs, leading to considerable simplification in the optimal controller and optimal filter. Like all previous mainframe simulations the FORTRAN language was used, but the programs were converted to BASIC for use in the on board computer, in which they were finally burned into an EPROM chip. As with the instrumentation package these decisions were governed by the hardware available

8.2 Development of the Discrete Reduced Non-Linear Model

With the same disturbances as for the full scale models, namely wind and current components along the ship x and y axes, the set of four first order differential equations to represent the model in continuous time were given in equation set (3.29). As with the previous simulations, measurements were taken at discrete time intervals leading to a set of first order difference equations relating the states at one instant to the states at some other instant. These are expressed as:-

$$\begin{bmatrix} u(k+1) \\ v(k+1) \\ \psi(k+1) \\ r(k+1) \end{bmatrix} = \begin{bmatrix} A_{11} & A_{12} & 0 & A_{14} \\ A_{21} & A_{22} & 0 & A_{24} \\ 0 & 0 & A_{33} & A_{34} \\ A_{41} & A_{42} & 0 & A_{44} \end{bmatrix} \begin{bmatrix} u(k) \\ v(k) \\ \psi(k) \\ r(k) \end{bmatrix} + \begin{bmatrix} B_{11} & B_{12} \\ B_{21} & B_{22} \\ 0 & 0 \\ B_{41} & B_{42} \end{bmatrix} \begin{bmatrix} \delta_A(k) \\ n_A(k) \end{bmatrix}$$

$$+ \begin{bmatrix} C_{11} & C_{12} & 0 & 0 \\ 0 & 0 & C_{23} & C_{24} \\ 0 & 0 & 0 & 0 \\ 0 & 0 & C_{43} & C_{44} \end{bmatrix} \begin{bmatrix} u_c(k) \\ u_a(k) \\ v_c(k) \\ v_a(k) \end{bmatrix} \tag{8.1}$$

This in turn led to the following mathematical model in the filter:-

$$\begin{bmatrix} u(k+1) \\ v(k+1) \\ \psi(k+1) \\ r(k+1) \end{bmatrix} = \begin{bmatrix} A_{11} & A_{12} & 0 & A_{14} \\ A_{21} & A_{22} & 0 & A_{24} \\ 0 & 0 & A_{33} & A_{34} \\ A_{41} & A_{42} & 0 & A_{44} \end{bmatrix} \begin{bmatrix} u(k) \\ v(k) \\ \psi(k) \\ r(k) \end{bmatrix} + \begin{bmatrix} B_{11} & B_{12} \\ B_{21} & B_{22} \\ 0 & 0 \\ B_{41} & B_{42} \end{bmatrix} \begin{bmatrix} \delta_A(k) \\ n_A(k) \end{bmatrix} \tag{8.2}$$

The various components of the $\underline{A}$, $\underline{B}$ and $\underline{C}$ matrices were obtained from their continuous time equivalents in equation set 3.29 using the methods described in Chapter 3, and employing subroutine NAB.

8.3 The HEATHMORE Model

To simplify the physical model tests it was decided to undertake them under conditions of zero, or near zero disturbance, but to overcome the practical programming problems small values of disturbance noise covariances were used in the filter calculations. Calculation of the filter gains involves an iterative process, and a test for non-convergency has hitherto been used. In the HEATHMORE tests this process was followed for only the first set of filter calculations. Thereafter the values were calculated only once for each sampling interval. It has already been shown in Chapter 6 that the filter gains remain reasonably constant for a given run. It was therefore reasoned that this assumption did not reduce the effectiveness of the filter.

In laboratory tests the accelerometers gave very noisy signals whereas the gyro compass and the yaw rate gyro noise values were low. In the simulations the standard deviations were treated in a similar manner. Bearing in mind that the forward and lateral velocities in the CENTAUR model would be obtained by integrating the measured forward and lateral accelerations, the appropriate standard deviations in the HEATHMORE simulations were initially kept high (1m/s), whilst those of the third and fourth state vector were set low (0.017 rad and 0.00399 rad/s).

Four tests were carried out under these conditions to test the validity of the filter model and the need to re-calculate the filter gains during each sampling period. These are illustrated in Figures 8.1 to 8.4 inclusive. In Figure 8.5 the filter gains and the transition matrices for the filter are re-calculated during each sample time. In addition to plotting each state against time, a set of position plots for true, measured and filtered values are shown. As with earlier graphs the demanded values are in black, the measured values in green with the true values in blue and the filtered values in red. Position values are calculated in the same way as for the full - scale simulations.

The ship was initially stationed 4 metres to the right of the initial demanded position with an initial forward speed of 0.75 m/s, with zero lateral speed, heading and yaw rate. After 56 seconds (the sampling interval was 1 second) the demanded heading was changed to + 90 degrees. From Figure 8.1 it is seen that, in spite of the very noisy position signals the filtered track followed closely the true track, with a slight overshoot, but after 35 seconds the system anticipated the alteration course (the helm over position) and the rudder was driven to starboard so that the vessel started to move around to her new track. At this point the controller was a heading controller and continued to be so until the heading error was reduced to less than 30 degrees, when the track controller again dominated. During the test run, and in spite of the very noisy speed measurements, it is seen that the ship settles down to her new course and track with only a very small overshoot. Turning now to the speed time graphs it is seen that again the filtered and true values are very close, and close to the demanded value for the forward speed. During the turn the vessel's forward speed decreased and the lateral speed increased, although the latter is shown as negative on the lateral speed plot because of the sign convention adopted. Similarly, the course angle and yaw rate plots give good correlation between true and filtered values.

In Figure 8.2 the filter gains are calculated only at the commencement of the run. Comparison of Figures 8.1 and 8.2 shows no difference in the plots. In Table 8.1 a comparison of gains is made at the beginning, middle and end of a run where they are calculated for each sampling interval. Comparisons show that AK(1,1) and AK(2,2) remain as very small numbers throughout, AK(3,3) decreases from 1.161 to 0.02485 to 0.005921, whilst AK(4,4) remains as a small number. This is in keeping with the qualitative conclusions of the previous chapter. For AK(4,4) the small value is attributed to the low ratio between disturbance and measurement noise. A single calculation of the filter gains, together with a constant $\underline{S}$ matrix used in the optimal filter was to be a significant factor in the software development in CENTAUR, where the re-calculation of all the relevant matrices with the sampling time of 1 second was impossible using the available hardware.

8.4 Simplification of the Filter Mathematical Model

In the full-scale computer simulations a ~~time constant~~ sample time of 5 seconds was used. This was mainly due to the requirement that the duration of the sampling interval should be approximately one tenth of the dominant time constant of the controlled object. Zuidweg (1970) quotes the dominant time constant for the Mariner hull as 56.52 seconds and uses a sample time of 5.65 seconds. For the physical model of the car ferry a sample time was reduced to 1 second, primarily to comply with the one tenth rule quoted above, but also for practical purposes concerned with the model itself. It was felt that a sample time of say 5 seconds would be too large and allow too few measurements in a model run, which was limited to around 2 minutes by such factors as the need to re-charge the model batteries at frequent intervals. Bearing all these factors in mind a sample time of 1 second was chosen. This meant that all the on-board computer calculations would have to be completed within one second, so that each value was available for the next set of calculations. This presented difficulties in the microcomputer to be installed in the physical model so that simplification of controller and filter design was necessary in order to complete each set of calculations in the sample time.

The process of calculating the state, control and disturbance matrices is in itself a lengthy process demanding a great deal of computing time. Once the sampling time of 1 second had been fixed for the CENTAUR model it was necessary to ensure that all necessary calculations were completed within that time interval. Mention of the difficulties was made in Chapter 3, page 33, for the values of these matrices would require recalculation for each sampling interval and early laboratory tests using the microprocessor to be installed in CENTAUR showed that it was incapable of undertaking all the recurrent calculations within one second. Details of these calculations are given in Appendix 7, where the appropriate mainframe computer subroutine NAB is discussed. Referring to equations 3.15 and 3.16 it is seen that $\underline{A}$, $\underline{B}$ and $\underline{C}$ are again obtained by using a power series and the number of terms, L', of the series approximation is decided beforehand. A value of 20 was used in the mainframe computation in order to ensure the power series equations were sufficiently accurate. First thoughts were to reduce the calculation time in the microcomputer by reducing the number of terms. Figures 8.3A and 8.3B show the plots for a reduction in L' to 5 and 1 respectively. Only when the number of terms decreases below 5 does the accuracy of the track plot degrade sufficiently to cause concern. It must be pointed out that these figures only apply to the filter model, that is the full calculations still took place in connection with the model of the ship.

With the calculation times still over one second it was decided to attempt a further simplification of the equations governing the $\underline{A}$ and $\underline{B}$ matrices. By plotting values of the components in the matrices against forward speed and yaw rate Burns (1984) showed that there was a linear relationship between the matrix component and either or both of the states referred to above, with the rudder angle being an additional consideration in the control matrix. For the HEATHMORE and CENTAUR models the equations are shown in Table 8.2.

The equations are set out in the form in which they were used in the computer programs. AA is the 4*4 state transition matrix whilst BB is the 4*2 control transition matrix. The disturbance transition matrix is not used in the filter calculations. Figure 8.4 shows the result of these changes to the calculations of the $\underline{A}$ and $\underline{B}$ matrices in the filter. The filtered values of speed (forward and lateral) follow closely their respective true values whilst heading and yaw rate were less coincident, with the measured values. This in turn led to a track plot which showed the vessel rather too far to the left of the demanded track when the alteration of course commenced.

This condition had already shown up in Figure 8.3B. It confirms that as the $\underline{A}$ and $\underline{B}$ matrices in the filter become dissimilar to the A and B matrices in the ship, the true and filtered tracks diverge because the true and filtered headings diverge.

It has to be remembered that position is not a state in the reduced models, and is calculated from speed and heading, which are states, so that any discrepancy in either of these would cause errors in the track plot. From the data available it was clear that the filter was operating correctly through the noisy speed signals, but rather less efficiently for the low noise heading and yaw rate measurements.

In the qualitative discussion of Chapter 7 (Section 7.1) it was reasoned that a filter gain approaching unity would be required if there was disturbance noise but no measurement noise. But this assumed the filter model was an accurate representation of the system. If the filter model differed from the real model the error might be minimised, although not eliminated by using an artificially high gain in the appropriate position in the filter gain matrix. To test the theory a filter gain of 1.0 was assigned to each of the relevant components of the gain matrix, AK(3,3) and AK(4,4). This did not change the track plot as can be seen when comparing Figures 8.4 and 8.4A. Furthermore, when the normal filter calculations were re-introduced (Figure 8.5) there was no difference to any of the filtered states when compared with the standard conditions of Figure 8.1. This led to further consideration of the Kalman Filter gains and to the possibility of using state plus state estimation feedback to the optimal controller. Figure 8.4 shows the result of these changes to the calculation of $\underline{A}$ and $\underline{B}$ in the filter.

The high noise values associated with the accelerometers and the low noise of the gyro-compass and yaw-rate gyro led in turn to consideration of whether the low noise signals could be fed directly to the controller (state feedback) leaving only the noisy signals to be processed in the filter. Before making these modifications all four measured states were used as inputs to the controller as a "control" experiment. This is illustrated in Figure 8.6 which shows that although the true and filtered tracks are very close the vessel does not follow the demanded track, indicating the need for filtering the measured states prior to their use as inputs to the optimal controller.

Turning now to consideration of state plus state estimation feedback, Grimble (1980a) suggests that the assumption in many industrial control problems is that none of the states can be measured directly, in which case the Kalman Filter has the same dimensions as the plant state space description, often resulting in such a high order controller so that the scheme is impracticable. He goes on to suggest that this is often unrealistic since some state variables can be measured with a high degree of accuracy. This is the case with the system used in CENTAUR. The concept of measurable and unmeasurable state referred to by Grimble is not followed here, but rather the subset of high noise states is fed to the filter. In the mainframe digital simulations using the HEATHMORE model no attempt was made to modify the filter, but from Figure 8.7 it was seen that there was a substantial improvement over the previous case when measured signals were fed directly to the controller. Although the speed noise values have been increased in Figures 8.6 and 8.7 the state plus state estimation feedback compares favourably with Figure 8.1 when only filtered values were fed back to the controller.

Traditionally the mariner has been very dependent upon his instruments. Without an accurate chronometer for example it is impossible to obtain a fix using the well-proven methods of astro-navigation, and without a compass all sense of direction is soon lost when out of sight of land. Whilst chronometers and compasses were reliable the loss of heading information in the approaches to a port could be disastrous. However one of the functions of a Kalman filter is the ability to produce an estimate of an unmeasurable state, so that in the event of a malfunction of one or more of the measurement sub-systems an estimate of that state can still be given. Thus an approach would not have to be aborted in the event of say a gyro breakdown during the passage into a port.

Figure 8.8 shows the effect of a gyro compass reading remaining at zero throughout a run. Although the measured values contain only the superimposed gyro noise the vessel follows the correct path and the estimated values of position, speed, heading and yaw rate remain close to the true values. Particularly interesting is the course angle-time graph which shows the filter giving a reading close to the true course.

In Figure 8.9 a gyro malfunction takes place after 65 seconds, whilst the yaw rate gyro develops a fault after 95 seconds. In Figure 8.10 the lateral speed measurement fails at 65 seconds and the rate gyro at 95 seconds. These points are marked A and B respectively on Figures

8.9 and 8.10. In both of these cases the filtered track is seen to follow closely the true track although after the second measurement system failure of Figure 8.9 the two tend to diverge from the demanded track towards the end of the Figure 8.10 run. Whilst these results are not conclusive they do indicate the ability of a four-state system to accept a malfunction of one of the measurement sub-systems without degrading the overall performance of the system, whereas with errors in two measurement sub-systems the system was still capable of automatic track keeping although the system performance did start to fall off after the rate-gyro ceased to function.

In Figures 8.8 and 8.9 the gyro was made to function incorrectly because it was reasoned that the loss of a low noise measurement would be more harmful to system performance than the loss of the high noise accelerometers. Furthermore the loss of the gyro would have the greatest effect upon the harbour approach and without an integrated system using Kalman filter techniques could lead to the vessel grounding in the Fairway.

8.5 Optimal Filter Specification for CENTAUR

The mainframe simulations carried out on the reduced non-linear car ferry model confirmed the earlier conclusions (Chapter 6) that the recalculation of the filter gains for each sample period was unnecessary and that the values need only be calculated once for a given run or series of runs. It was also confirmed that the mathematical model of the ship used in the filter needed to be a good representation of the plant and would need frequent updating because some of the elements of the $\underline{A}$ and $\underline{B}$ matrices were dependent upon time-varying values. However it was possible to obtain a linear relationship as in Table 8.2. Finally by feeding the measured values of heading and yaw rate directly to the controller it was seen that the automatic track keeping capabilities of the vessel were not impaired.

These conclusions led to the following specifications for the filter software in the physical model:-

i) Using standard deviations obtained in physical model tests the filter gain matrix will be calculated off-line. These values to be used throughout a set of runs but arrangements to be made to change them prior to any individual run.

ii) The equations of Table 2 are to be used to recalculate the state and control transition matrices for use in the filter calculations.

iii) Allow choice of state or state estimation feedback for each of the measured states.

a) Gains at Beginning of Run (AK Matrix)

0.1078E-03	0.0000E 00	0.0000E 00	0.0000E 00
0.0000E 00	0.2384E-19	-0.3380E-09	-0.1624E-14
0.0000E 00	-0.9769E-13	0.1161E-01	0.6656E-08
0.0000E 00	-0.2585E-19	0.3666E-09	0.1761E-14

b) Gains in Middle of Run (AK Matrix)

0.4940E-05	-0.4342E-06	-0.1701E-01	0.5317E-02
-0.4343E-06	0.3814E-07	0.1495E-02	-0.4670E-03
-0.4917E-05	0.4319E-06	0.2485E-01	-0.5289E-02
0.8465E-07	-0.7435E-08	-0.2914E-03	0.9104E-04

c) Gains at End of Run (AK Matrix)

0.6477E-07	-0.4435E-08	0.3510E-03	0.1901E-03
-0.4435E-08	0.3037E-04	-0.2403E-04	-0.1301E-04
0.1014E-06	-0.6946E-08	0.5921E-02	0.2977E-03
0.3026E-08	-0.2072E-09	0.1640E-04	0.8879E-05

Table 8.1 Comparison of Filter Gains for Figure 8.1

```
AA(1,1)=1.0-0.041*XHAT(1)-0.021*XHAT(4)

AA(1,2)=1.067*XHAT(4)

AA(1,3)=0.0

AA(1,4)=0.014*XHAT(4)

AA(2,1)=-0.446096*XHAT(4)

AA(2,2)=0.995-0.1593785*XHAT(1)-2.05168*ABS(XHAT(4))

AA(2,3)=0.0

AA(2,4)=0.05+0.028376*XHAT(1)-0.02429*ABS(XHAT(4))

AA(3,1)=0.015758*XHAT(4)

AA(3,2)=-0.01-0.101248*XHAT(1)+0.6868*ABS(XHAT(4))

AA(3,3)=1.0

AA(3,4)=0.989-0.195818*XHAT(1)

AA(4,1)=0.03377*XHAT(4)

AA(4,2)=-0.0295-0.17164*XHAT(1)+1.29186*ABS(XHAT(4))

AA(4,3)=0.0

AA(4,4)=0.967-0.35436*XHAT(1)
```

Where XHAT(1) = forward speed (estimated)

XHAT(4) = yaw rate (estimated)

Table 8.2A Linearised A Matrix

```
BB(1,1)=-0.0316267*U(1)

BB(1,2)=-0.000195+0.0000065*U(2)+0.000478*ABS(XHAT(4))

BB(2,1)=-0.0195+0.071189*XHAT(1)-0.0045258*ABS(U(1))

BB(2,2)=0.0

BB(3,1)=0.017-0.059506*XHAT(1)-0.001464*ABS(U(1))

BB(3,2)=0.0

BB(4,1)=0.0315-0.1130267*XHAT(1)

BB(4,2)=0.0
```

```
   Where   XHAT(1) = forward speed (estimated)

           XHAT(4) = yaw rate (estimated)

              U(1) = rudder angle
```

Table 8.2B Linearised B Matrix

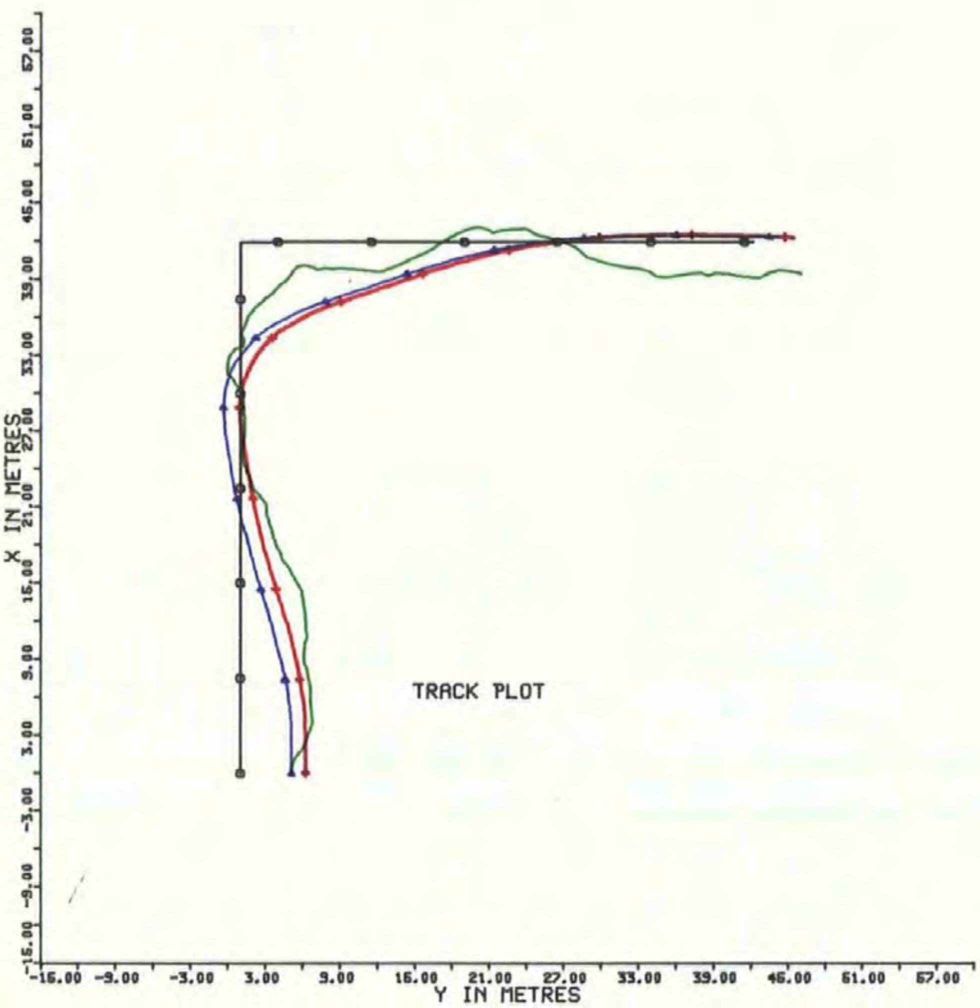

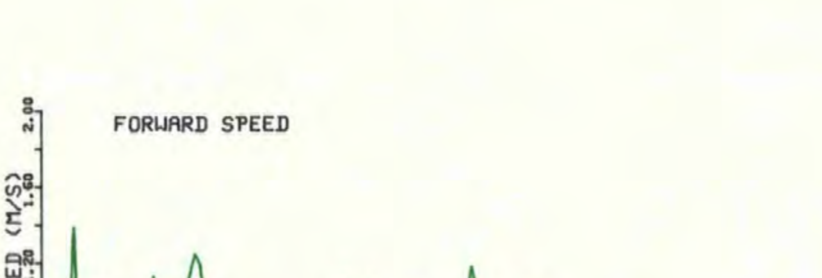

FIG 8.1 STANDARD CONDITIONS

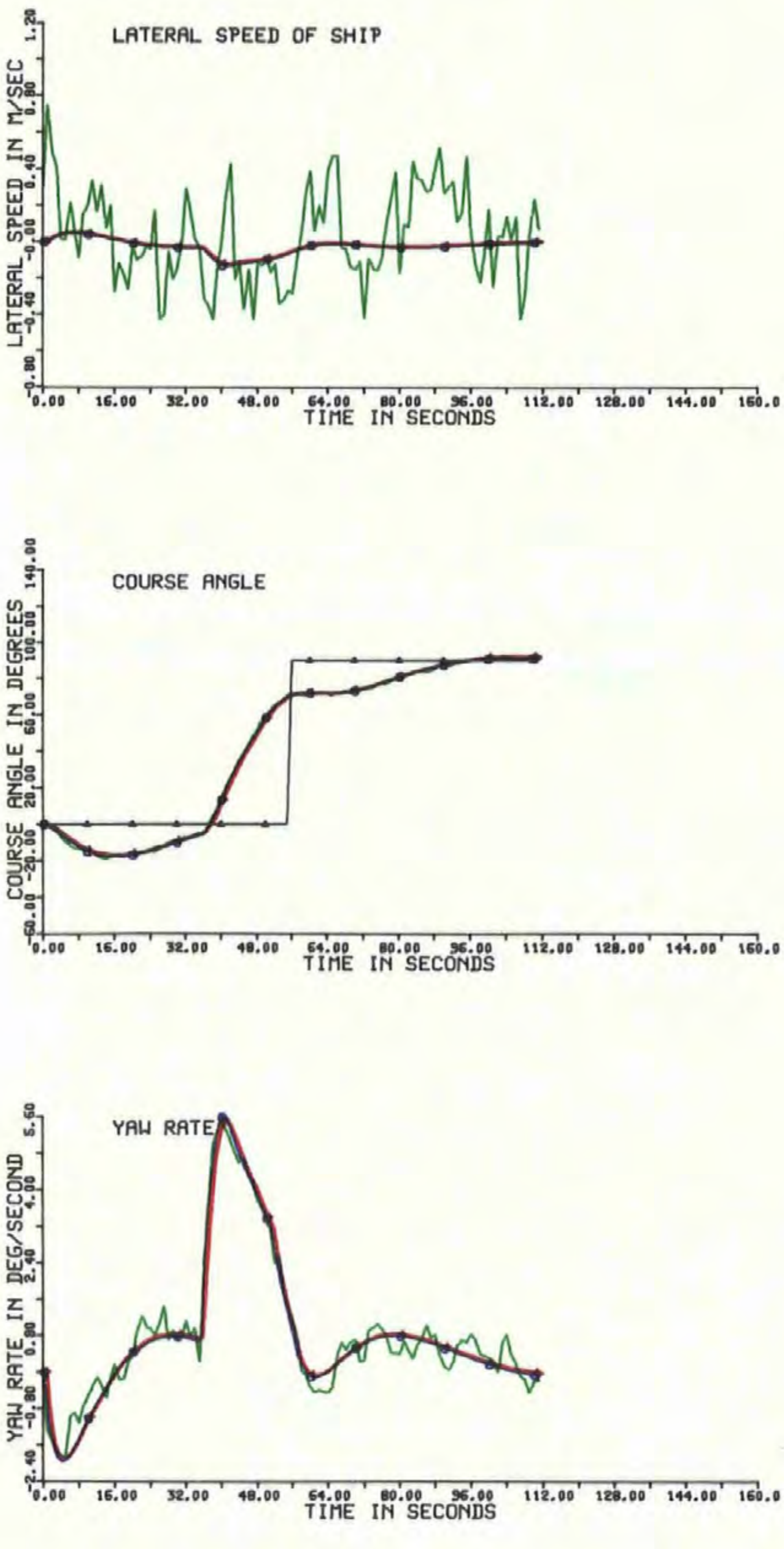
LATERAL SPEED OF SHIP
LATERAL SPEED IN M/SEC
TIME IN SECONDS
COURSE ANGLE
COURSE ANGLE IN DEGREES
TIME IN SECONDS
YAW RATE
YAW RATE IN DEG/SECOND
TIME IN SECONDS

FIG 8.1

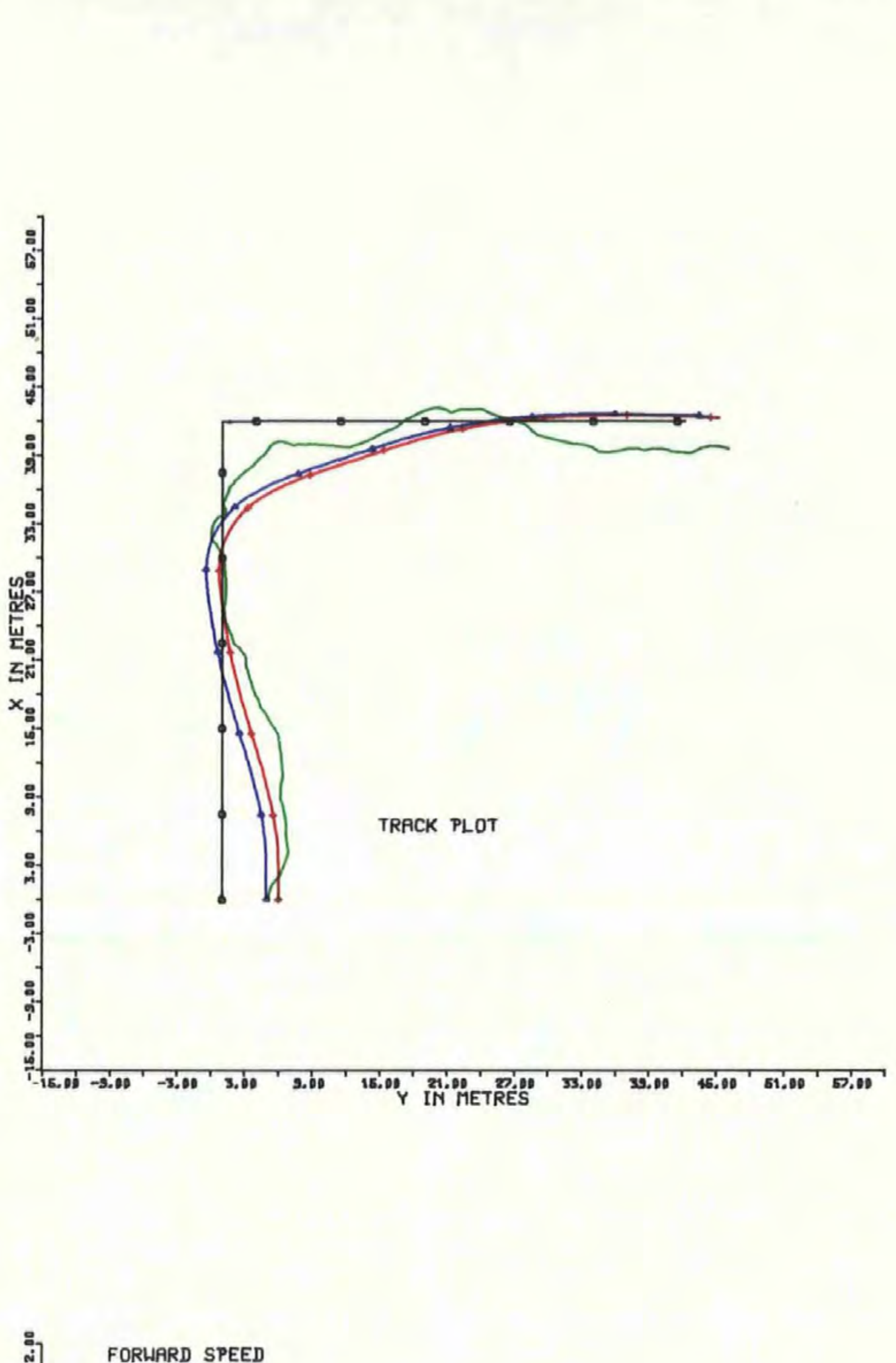

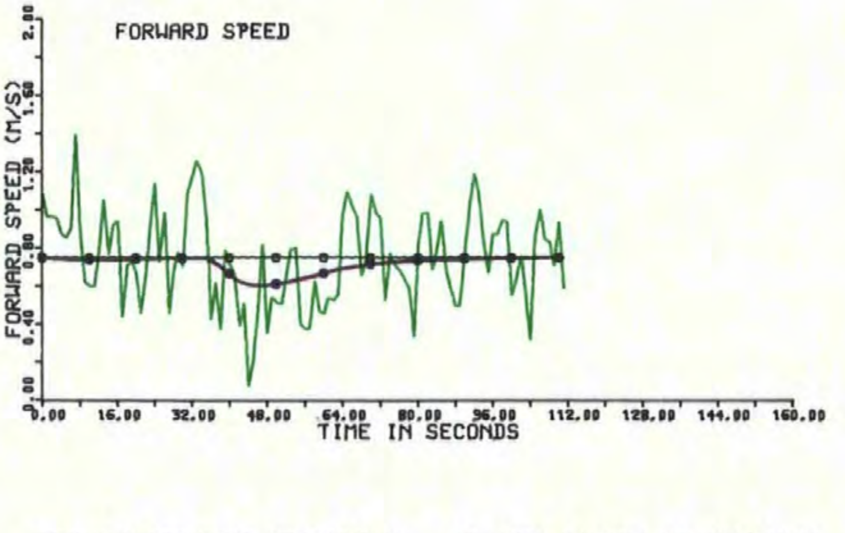

FIG 8.2 STANDARD CONDITIONS LIMITED FILTER CALCULATIONS

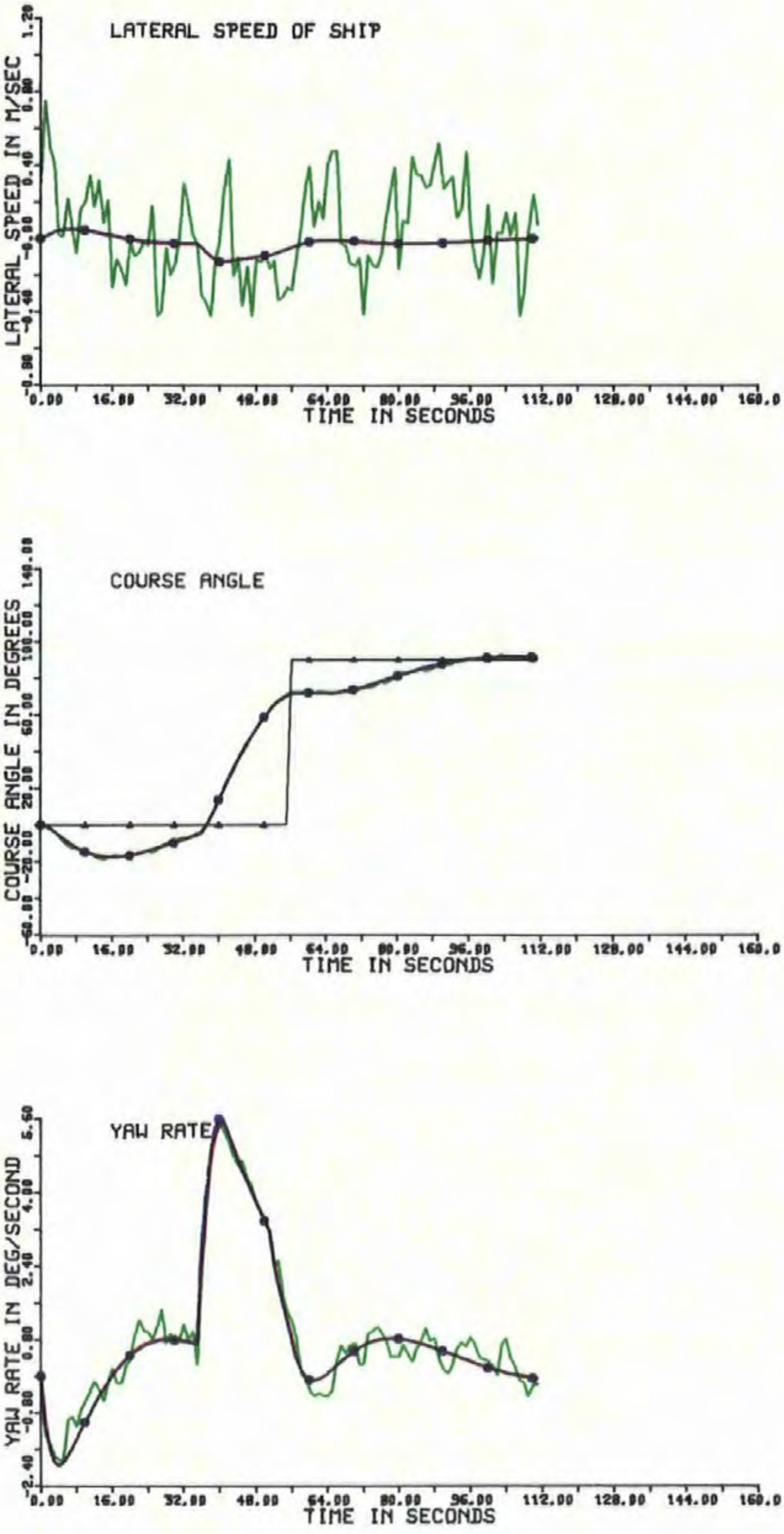
LATERAL SPEED OF SHIP
LATERAL SPEED IN M/SEC
TIME IN SECONDS
COURSE ANGLE
COURSE ANGLE IN DEGREES
TIME IN SECONDS
YAW RATE
YAW RATE IN DEG/SECOND
TIME IN SECONDS

FIG 8.2

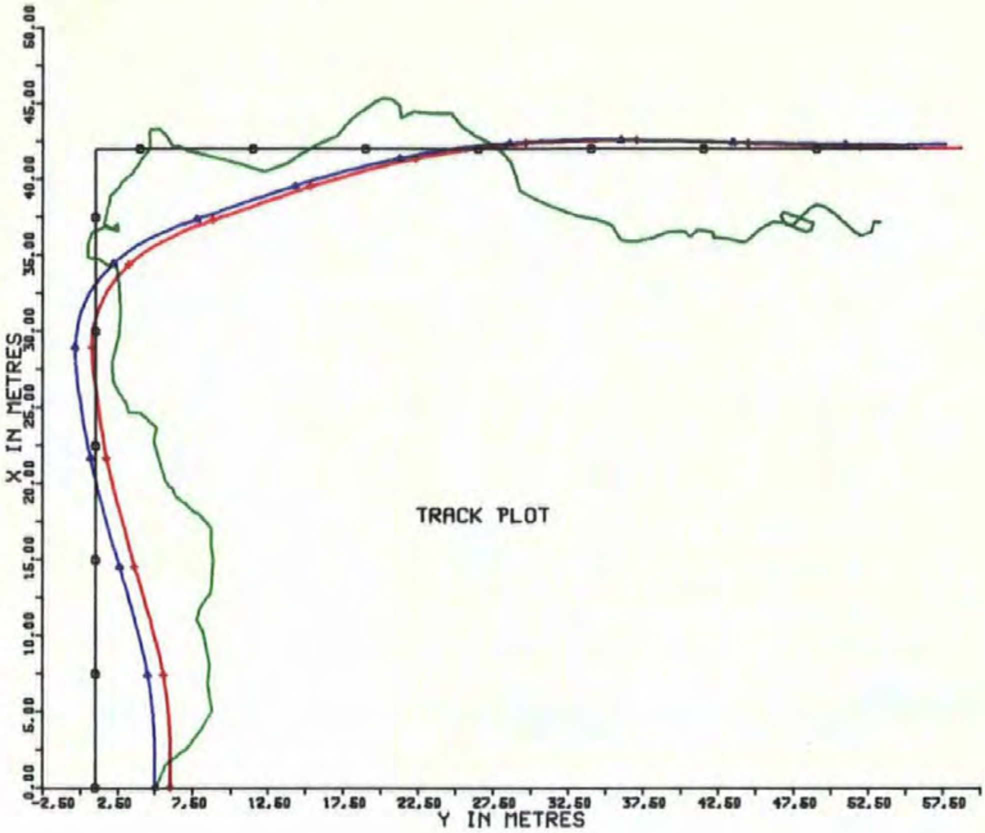

FIG 8.3A REDUCED FILTER CALCULATIONS (POWER=5)

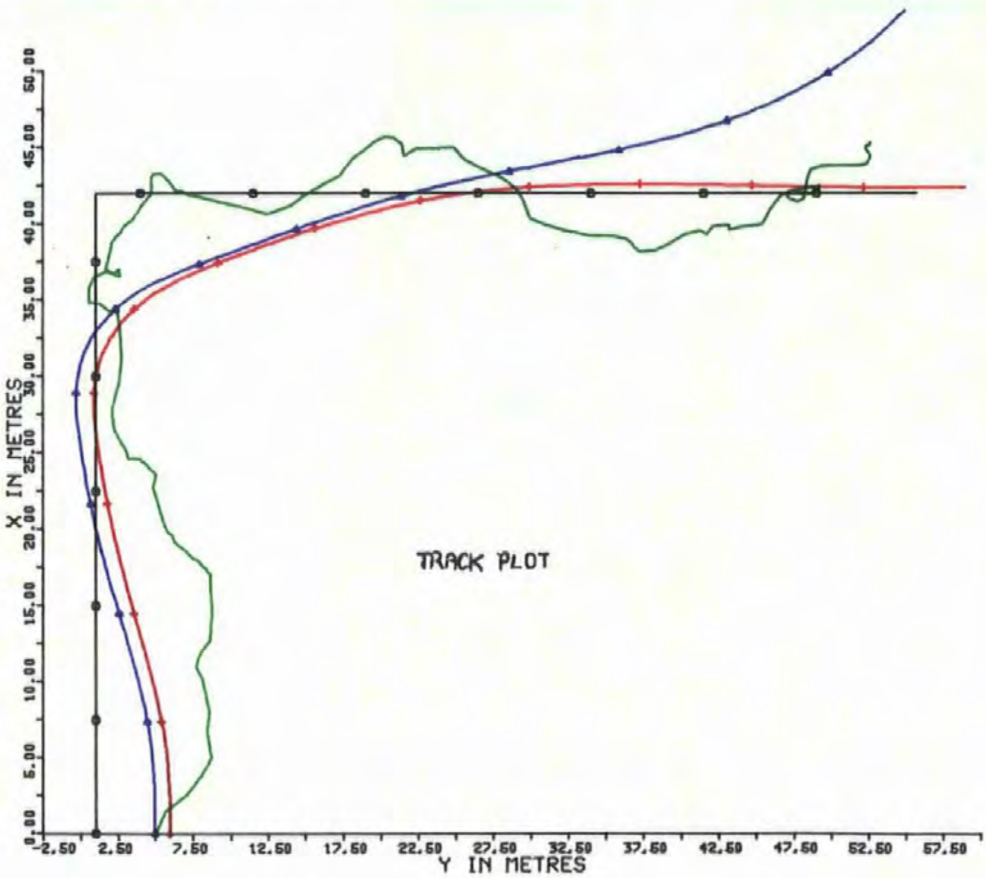

FIG 8.3B REDUCED FILTER CALCULATIONS (POWER=1)

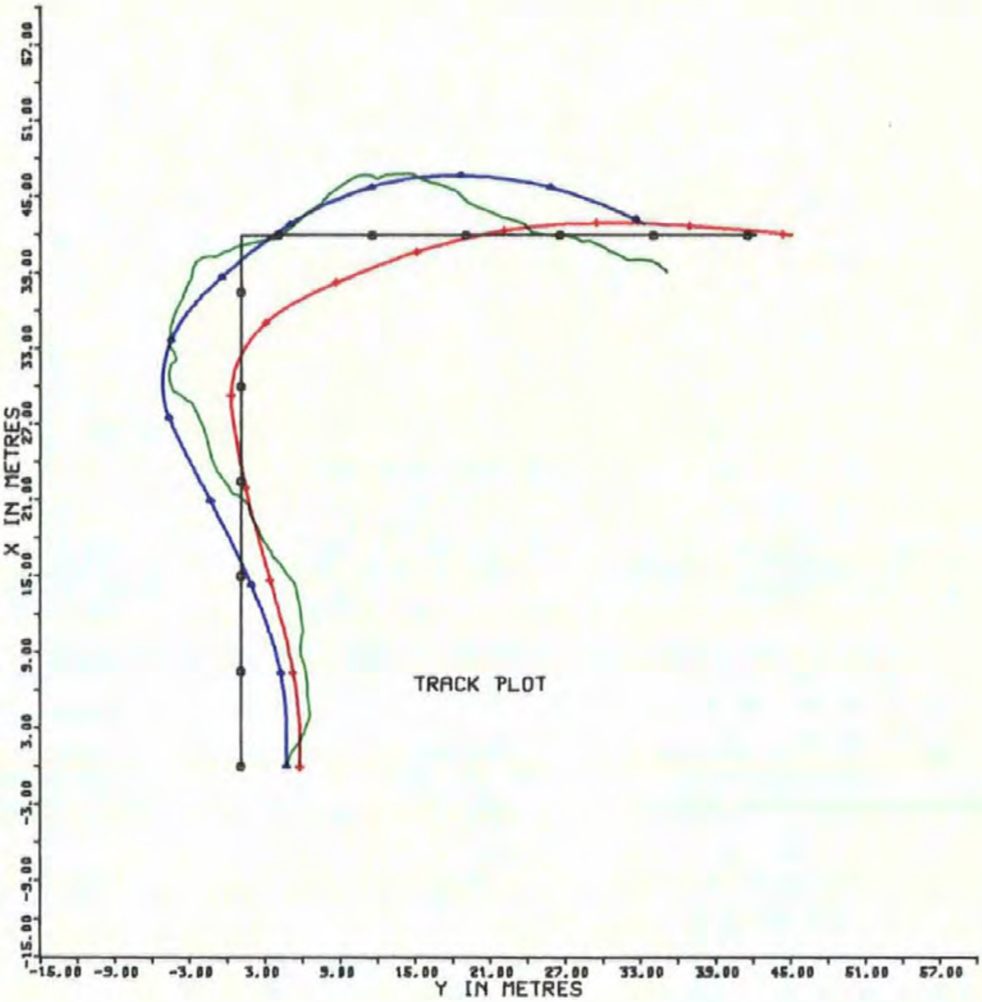

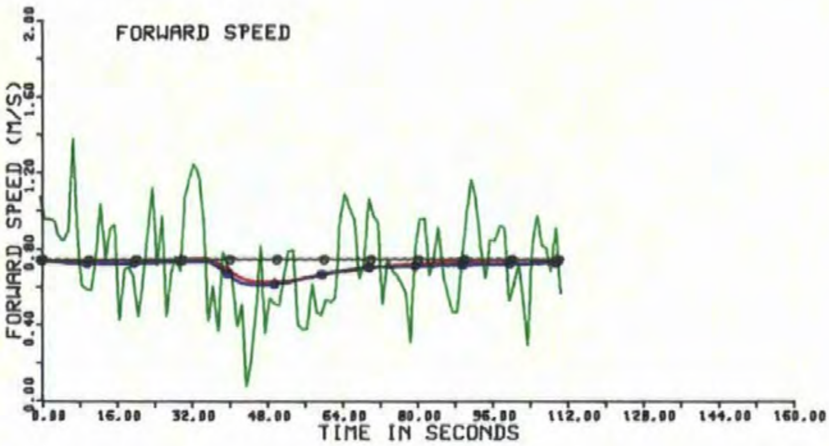

FIG 8.4 STANDARD CONDITIONS LINEARISED MATRICES

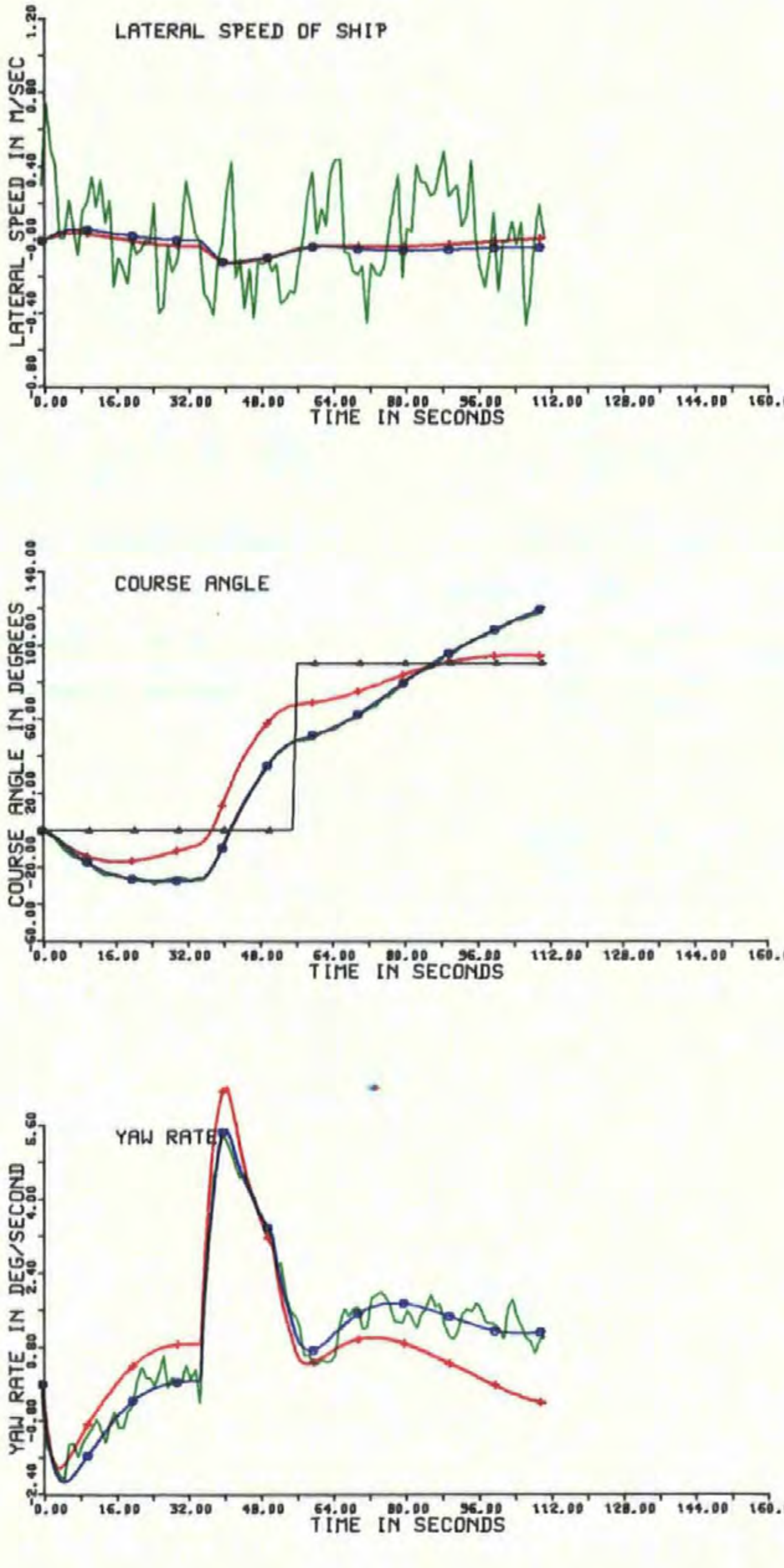
LATERAL SPEED OF SHIP
LATERAL SPEED IN M/SEC
TIME IN SECONDS
COURSE ANGLE
COURSE ANGLE IN DEGREES
TIME IN SECONDS
YAW RATE
YAW RATE IN DEG/SECOND
TIME IN SECONDS

FIG 8.4

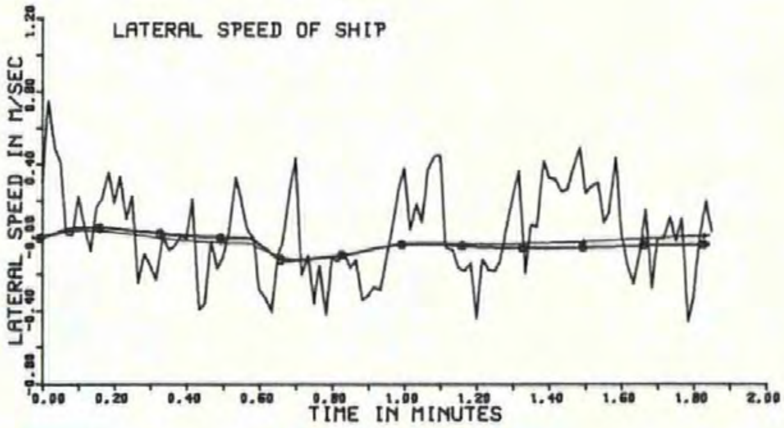

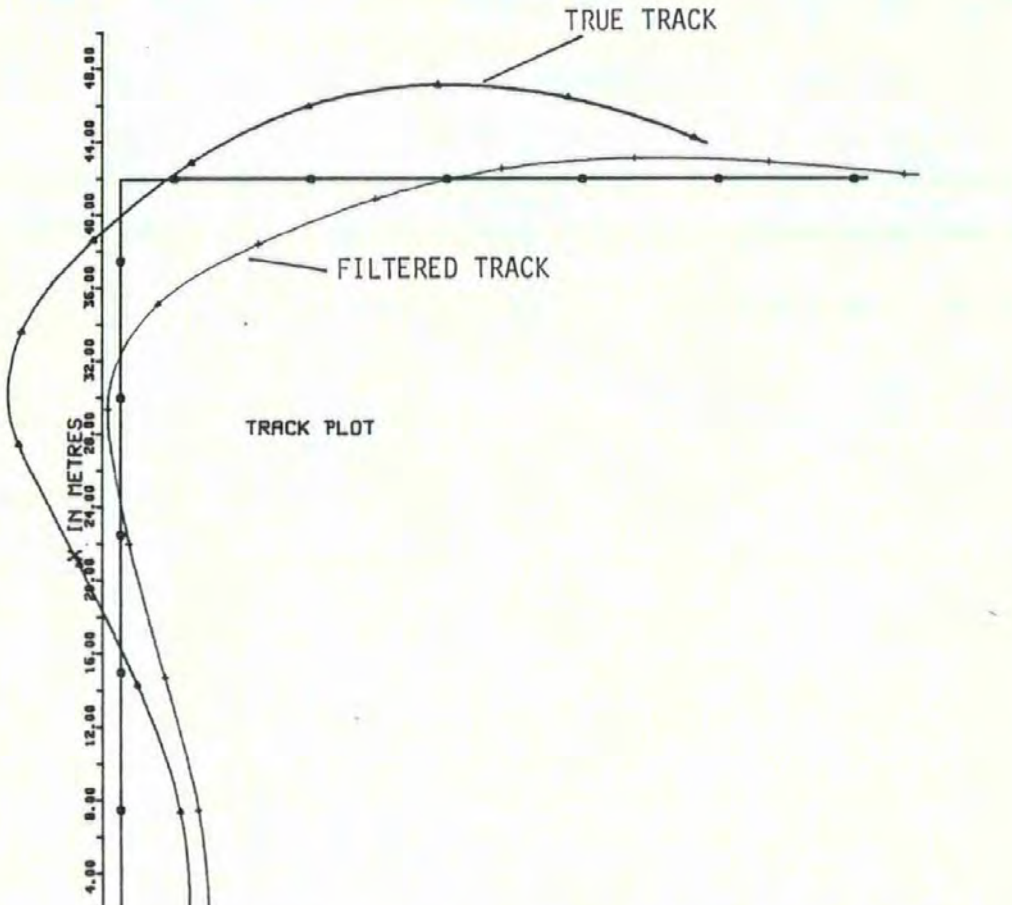

FIG 8.4A <u>Linearised Matrices with AK(3,3) and AK(4,4) Set at Unity</u>

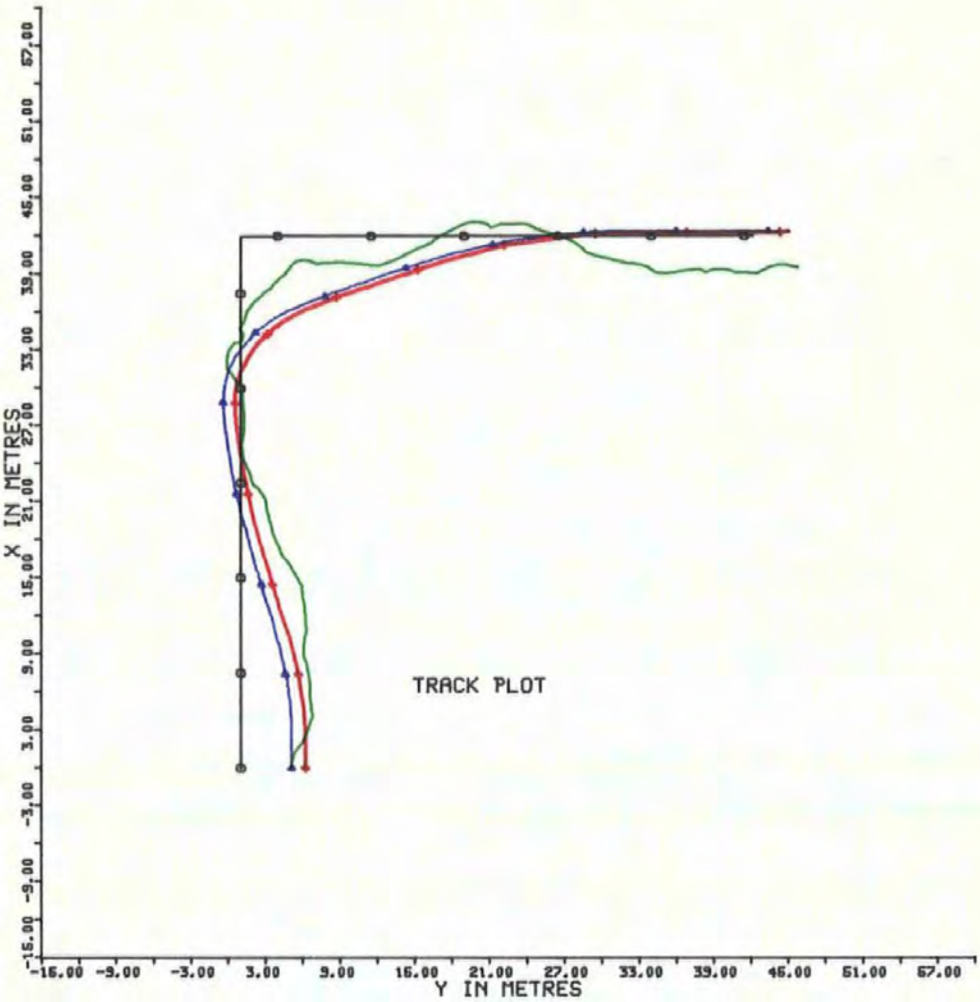

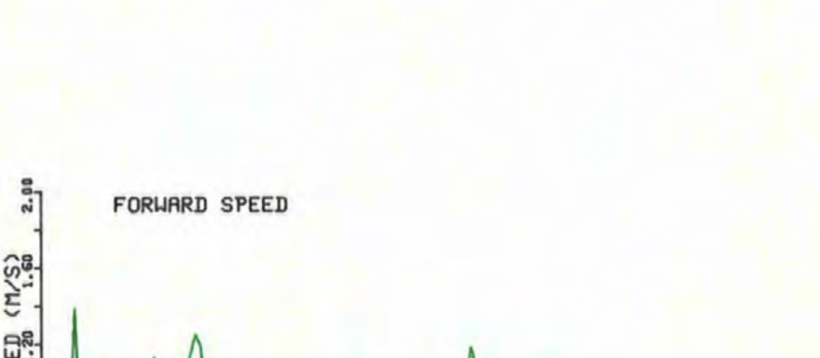

FIG 8.5 <u>REDUCED FILTER</u>

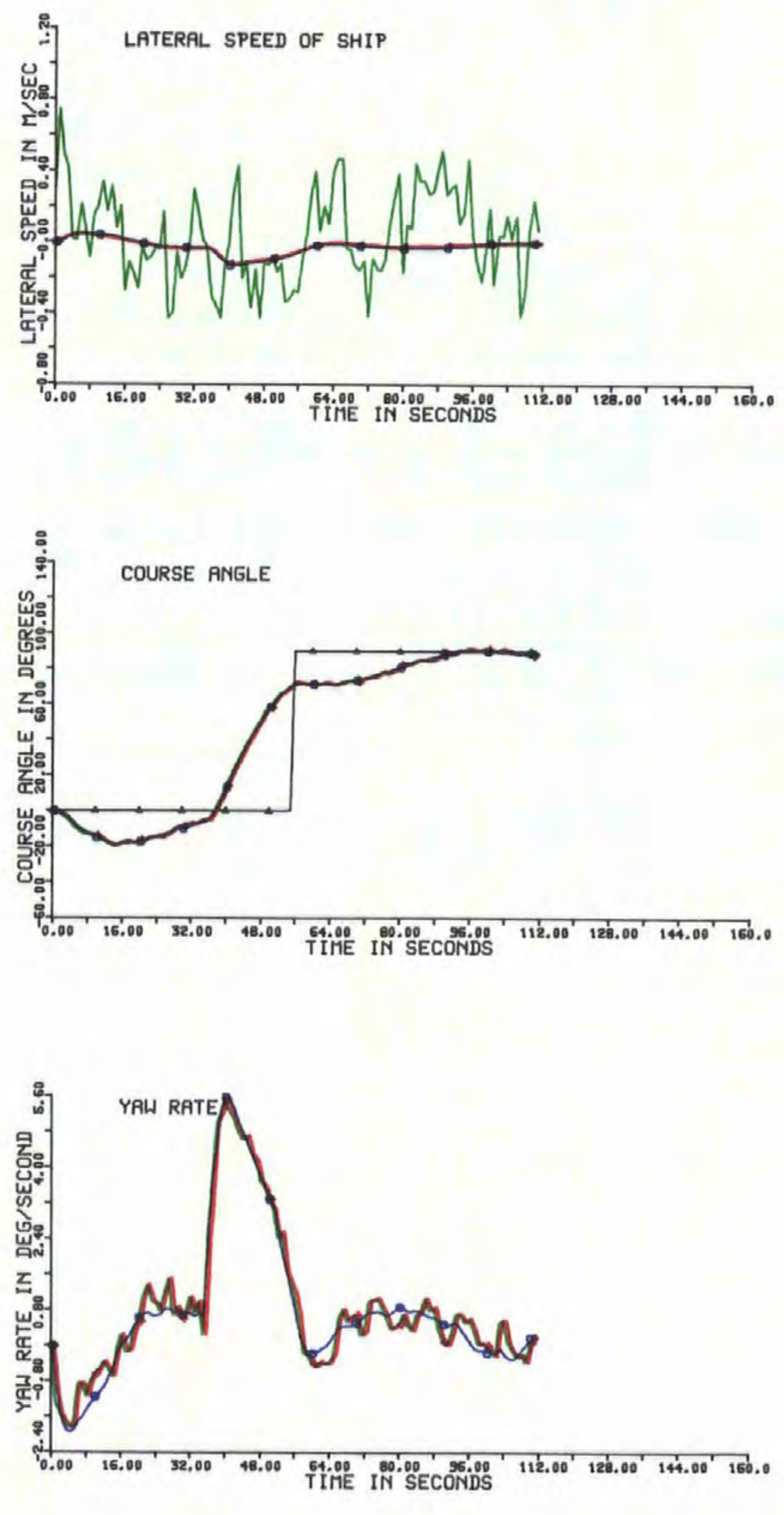
LATERAL SPEED OF SHIP
LATERAL SPEED IN M/SEC
TIME IN SECONDS
COURSE ANGLE
COURSE ANGLE IN DEGREES
TIME IN SECONDS
YAW RATE
YAW RATE IN DEG/SECOND
TIME IN SECONDS

FIG 8.5

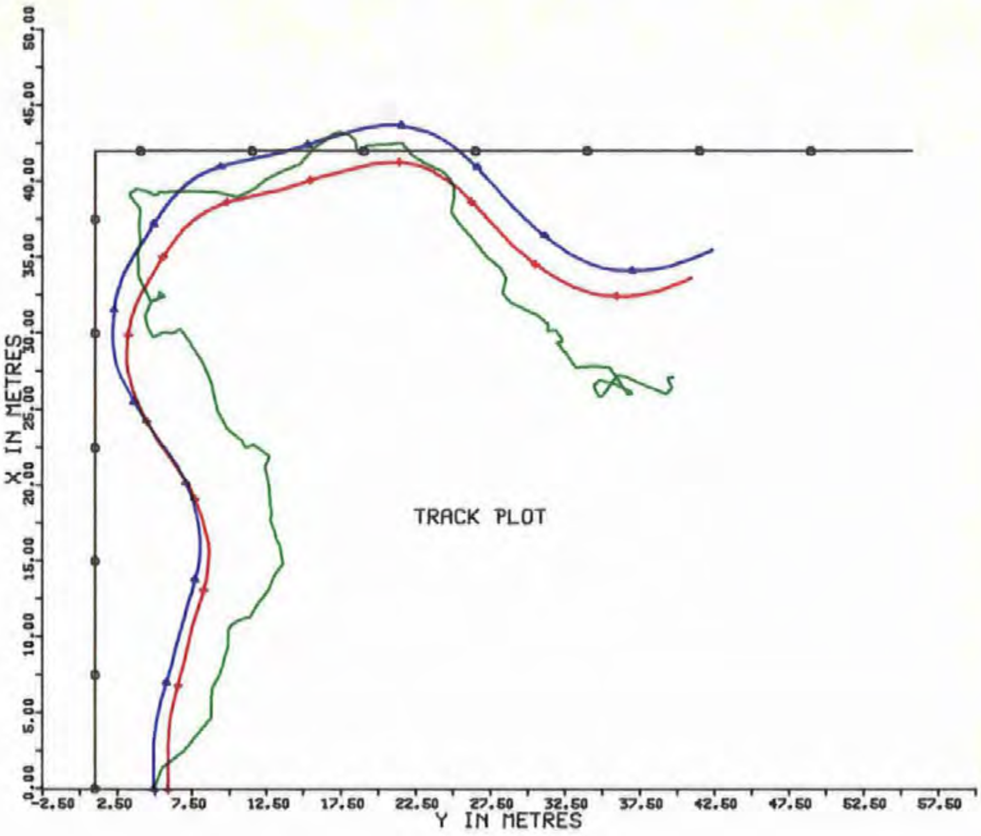

FIG 8.6 <u>STATE FEEDBACK (ALL STATES)</u>

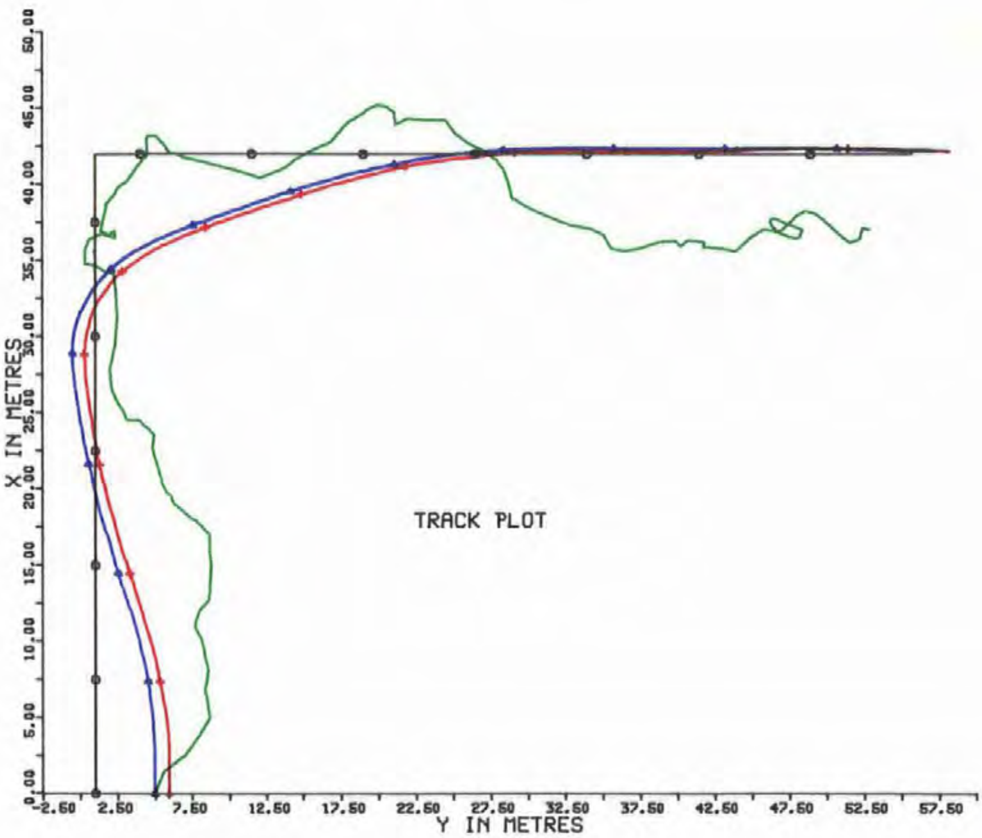

FIG 8.7 <u>STATE FEEDBACK (SPEED ONLY)</u>

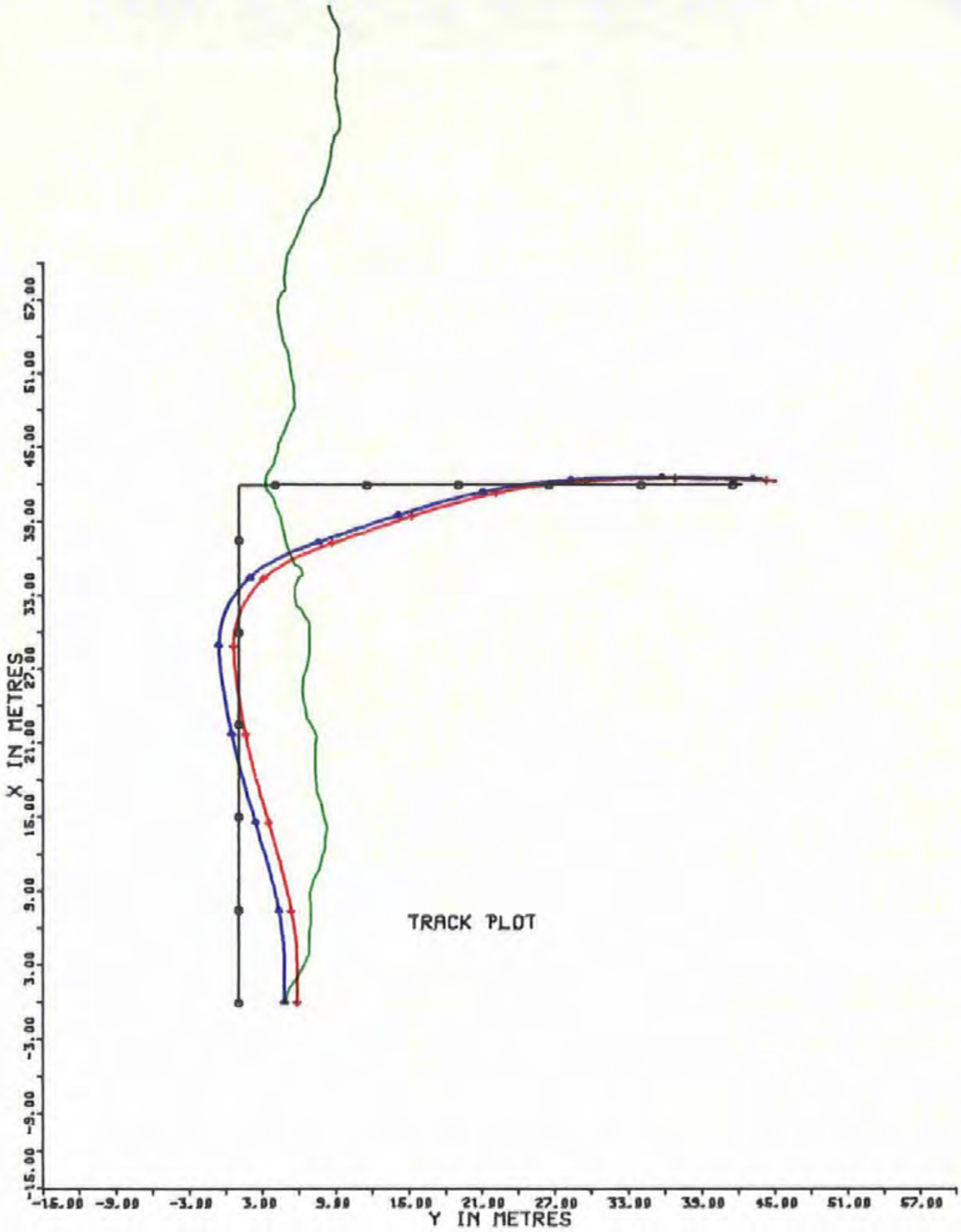

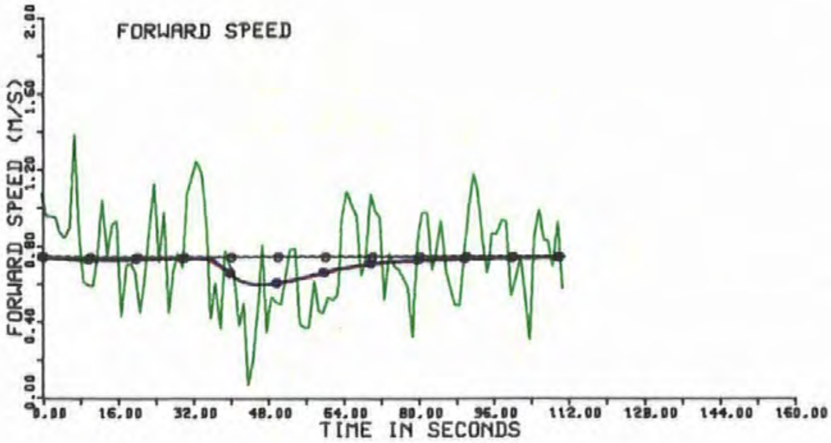

FIG 8.8 GYRO MALFUNCTION

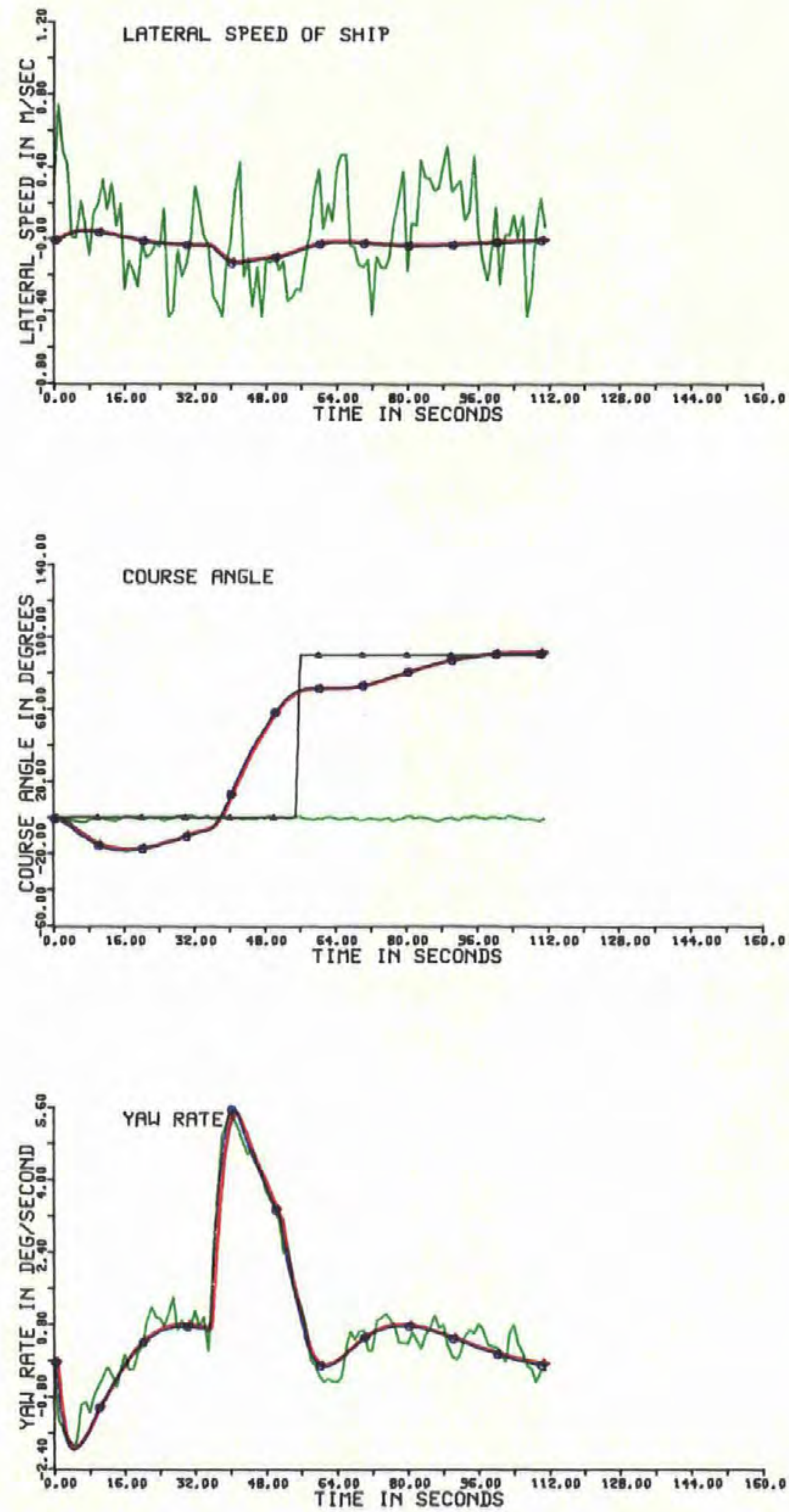
LATERAL SPEED OF SHIP
LATERAL SPEED IN M/SEC
TIME IN SECONDS
COURSE ANGLE
COURSE ANGLE IN DEGREES
TIME IN SECONDS
YAW RATE
YAW RATE IN DEG/SECOND
TIME IN SECONDS

FIG 8.8

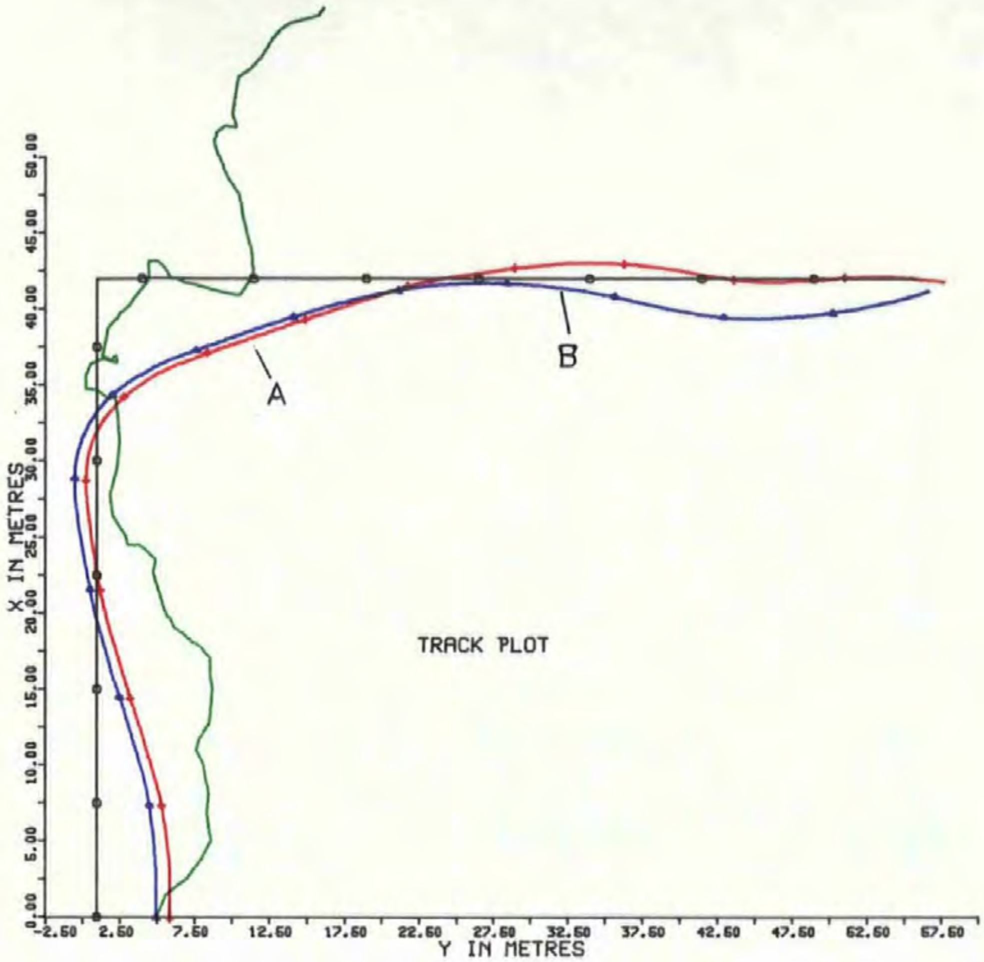

FIG 8.9 GYRO AND RATE GYRO MALFUNCTION

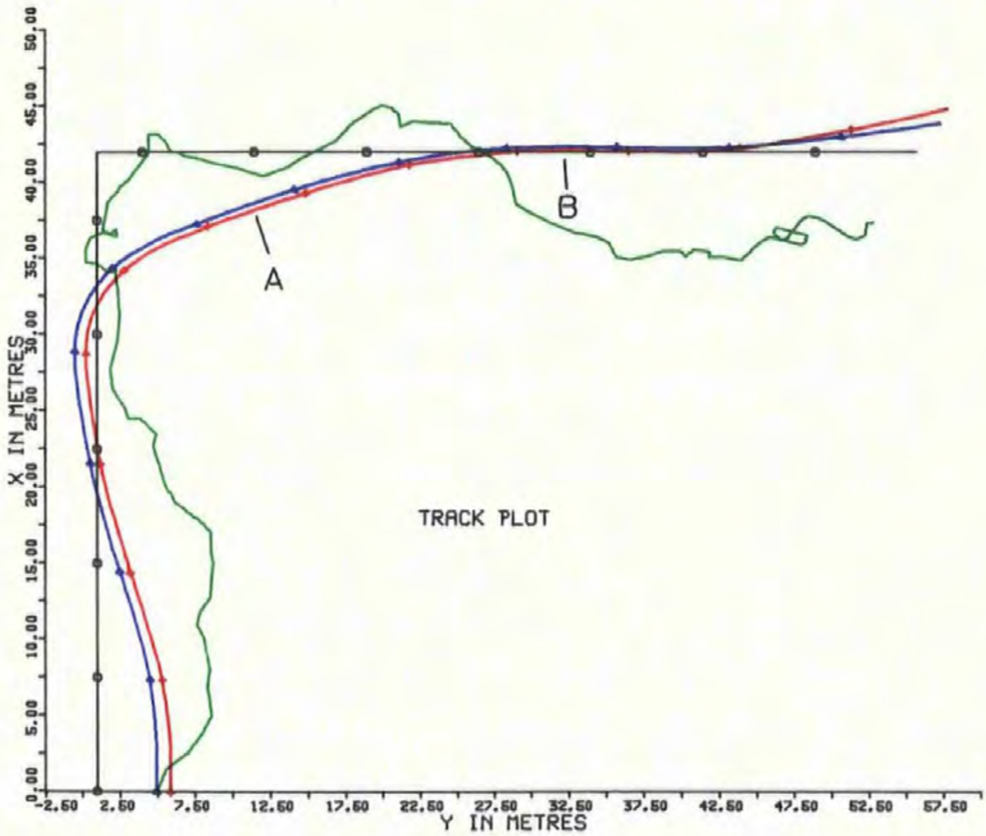

FIG 8.10 LOG AND RATE GYRO MALFUNCTION

CHAPTER 9

THE PHYSICAL MODEL TESTS

9.1 Introduction

Early in the research programme a physical model of a twin screw car ferry was borrowed from the National Maritime Institute. Tank tests were carried out at the NMI to obtain the non-dimensionalised hydrodynamic coefficients of the model. These are illustrated in Figure 9.1. The model was then fitted out with propulsion unit, measurement systems and finally the microprocessor for the optimal filter and optimal controller. Details of the model, together with its hydrodynamic coefficients are given in Appendices 4 and 5. Figures 9.3 and 9.4 show the internal layout of the instrumentation, microprocessor and rudder controls, whilst Figure 9.5 shows the model afloat on Crownhill Reservoir, Plymouth.

During each test run the measured and filtered states, together with position, were recorded in the on-board computer memory. These were printed out on the conclusion of each run. Data was transferred to the mainframe computer and for comparison purposes an identical simulation run was performed using the HEATHMORE model. Where necessary CENTAUR and HEATHMORE results were then plotted on common axes.

The position co-ordinates were obtained from the filtered values of speed and heading and can thus be compared with the estimated position plots from the computer simulations, which were obtained in a similar manner. Additionally the four states were each plotted against time. In each case these were the states fed to the controller, in most cases the filtered values, although in some cases where the measured values of heading and yaw rate were used as inputs to the controller these values are plotted on the appropriate graph.

Unless otherwise stated the HEATHMORE and CENTAUR models were identical with the optimal filter in the physical model conforming to the specifications written in Section 8.5 of the previous Chapter. The Kalman filter gains were calculated off-line and burned into an Eprom chip, with a provision for changing any gain prior to a run. The equations of Table 8.2 were used in the recalculation of the state transition and control matrices in the filter and a choice of estimated or measured state was provided for.

9.2 Details of Test Runs

The afloat tests were undertaken, in the main, in calm weather conditions. A typical set of plots for these conditions is given in Figure 9.6, and the photographs of Figure 9.2 show typical test runs underway. From the track plot it is seen that both the simulated and actual models follow the demanded track closely until the "helm over" position is reached after 35 seconds (0.58 minutes). At this point the course keeping control dominates. 42 seconds after the commencement of the run the new demanded course comes into operation and after 56 seconds the track control again dominates. In this run the filter transition matrices were calculated from the equations of Table 8.2, all the controller inputs were filtered and the filter gain matrix AK was modified by making AK(3,3) and AK)4,4) equal to 1. All other filter gains were as given in Table 9.1. Table 9.1 also gives a set of typical filter gains calculated during a simulation run. Comparison of the filtered states shows remarkable similarity between the simulation and model gains. It must be remembered however that the physical model gains were calculated off-line.

A similar run, but with the models initially offset by four metres is illustrated in Figure 9.6A. Again both the simulated and actual models pull in from their original positions, then follow similar paths until they each settle down close to the new demanded track. Looking at the forward speed plots of Figures 9.6 and 9.6A, there was some concern at the simulation model's increase after the turn was completed. Similarly the lateral speeds of the simulation showed increases towards the end of the run. When the simulation run was repeated (Figure 9.7) with the simulation model filter transition matrices being recalculated for each value of k (using the subroutines described in Appendix 7) the forward speed settled down after the turn to starboard. These differences are explained by the simplification techniques used in the software and the difference between simulation and real models by the differences in the mathematical models used in the filters. Comparison between Figures 9.6 and 9.7 showed the similarity, in all other respects between simulated and actual models, and the differences serve to illustrate the problems of producing an accurate computer model of ship for use in the Kalman Filter calculations. However it can be seen from Tables 9.2 and 9.3 that the values of the state control matrix (AA) and the control transition matrix (BB), using the simplification technique (Table 8.2), do not differ greatly from those obtained using the full software routines.

The run illustrated in Figure 9.8 took place under windy conditions with some gusts during the duration of the test. The run is included to give an indication of the ability of the system to operate in such conditions, although the wind strength was probably equivalent, under scaled conditions, to winds up to Force 8 or more. Towards the end of the run the wind strength increased and the rudder servos were unable effectively to control the vessel, but the results show the filter continuing to operate successfully. In this test the simulated model used the linearised filter equations to obtain the transition matrices, with AK(3,3) and AK(4,4) of the filter gain matrix each changed to 1.0.

For control purposes a test run where all the measured values were fed to the controller was carried out. Results from this run are shown in Table 9.4. With forward speed between +1.0 m/s and -2.0 m/s and with lateral speeds varying between 0 and -12.0 m/s the requirement for filtering, at least in the speed measurements, was clearly demonstrated. These results were not plotted because of the wide variations in speed. A sideways speed of 12 m/s (24 knots) from a model moving at 0.75 m/s was obviously a major error.

In another test run (Figure 9.9) with a breeze at 45 degrees to the initial and final tracks the "helm over" was delayed from 35 to 42 seconds after commencement of the run and the track change to 56 seconds after commencement of the run. Other changes were the use of the measured values of heading and yaw rate giving the state feedback terms whilst the filtered values of speed gave the state estimation terms. Prior to the turn the track plots were similar, but after completing the turn the actual model is seen to diverge from the demanded track.

Comparison of this set of results with those given in Figure 9.8 suggests that the use of state–feedback of heading and yaw rate together with state-estimated feedback of the noisy speed signals was a valid proposition. An interesting point to note here is the increase in measured values of speed with time. This was to be expected for speed measurements were obtained by integrating the accelerometer outputs. Even so the filtered values compare favourably with the computer model estimated values demonstrating once more the ability of the filter to successfully operate under adverse conditions.

Staying with the concept of partial filtering Figure 9.10 shows the results of a straight run with the filter gains as in Table 9.1 and the filtered speeds and unfiltered heading and yaw rate as inputs to the controller. In this experiment the filter gains for AK(3,3) and A(4,4) were set at 1. Starting from a position 5 metres to the right of the demanded track the actual model is seen to overshoot before starting to return to track at the end of the run. This oscillating motion is seen in the forward speed and course angle graphs whereas the computer model motion is damped down much more effectively. A similar run (Figure 9.11) with the vessel offset by 5 metres to the left of the demanded track at the commencement of the test run, but with all the estimated values fed to the controller, showed no overshoot of either real or computer model tracks. Comparison of Figure 9.8 through to 9.11 suggest that, with the measurement systems installed in the vessel, there is little difference between feeding back only the estimated values or by using a combination of filtered and measured states, but that the tuning of the controller is an important feature.

9.3 Analysis of CENTAUR Results

As with the computer simulations described in previous chapters the test runs carried out with the actual model demonstrate the ability of the optimal filter to provide useful estimated values from noisy measurement systems. Computer memory in the on-board microprocessor precluded test runs in excess of two minutes, but the results illustrated here show quite clearly that the combination of an optimal filter with an optimal controller guides the vessel effectively along, or close to, a predetermined track. In comparing the filtered HEATHMORE and CENTAUR tracks it must be remembered that the computer simulations took place under the ideal conditions of no wind or tide, assumed the vessel was in deep water and without any effects from a nearby bank. Although test conditions on the reservoir were as near to ideal as possible no allowance was made for any movement of the water, or possible bank effects when the model came close to the side of the reservoir, as it did during the initial leg of many of the runs, particularly when it overshot the demanded track. It must also be pointed out that no allowance was made for air movement which, however slight, would if both model and wind had been scaled to full size, have represented a considerable wind strength. However these small effects did indicate an ability of the filter to deal with changing disturbance patterns.

A further factor which must be emphasised was the need to simplify the filter and controller in order to meet the constraints of the hardware available. Initially it was hoped to use a shore-mounted Doppler Sonar position measuring system, but when costs dictated the use of an on-board simple inertial navigation system, which was already available, it was shown that the filter was able to deal adequately with the very noisy signals from the accelerometers. As can be seen from Table 9.4 the errors in the accelerometer increased rapidly over the period of each test run.

Mention has frequently been made of the limitations of the computer memory. Whilst other microprocessors were available, space in the actual model was at a premium. These factors were in no small way the reasons why simplifications were carried out but the results given here indicate that the simplifications were justified.

a) Kalman Gains For CENTAUR Filter (AK Matrix)

0.00006816	4.478E-09	-0.0000912	-0.0000644
7.876E-08	5.174E-12	-1.058E-07	-7.442E-08
-4.443E-09	-2.93E-13	0.01189	4.325E-09
-1.099E-08	-7.226E-13	1.516E-08	1.039E-08

b) Typical Kalman Gains For HEATHMORE Filter (AK Matrix)

0.5784234E-04	-0.4476441E-07	0.4847845E-02	0.5620660E-06
-0.2283896E-05	0.1767490E-08	-0.1914155E-03	-0.2219289E-07
0.6128203E-05	-0.4742605E-08	0.1133951E-01	0.5954870E-07
0.1427616E-05	-0.1104826E-08	0.1196500E-03	0.1387233E-07

c) Typical Standard Deviations For Measurement Systems

-0.0253202130	-0.0435451213	-0.000602608622	-0.00552354216

TABLE 9.1 Comparison of Filter Gains Used in HEATHMORE and CENTAUR

a) State Transition Matrix (AA Matrix in Filter)

0.9684997E 00	-0.2755902E-02	0.0000000E 00	-0.4347411E-04
0.1107663E-02	0.8723869E 00	0.0000000E 00	0.2699842E-01
-0.6346549E-04	-0.8781582E-01	0.1000000E 01	0.8383893E 00
-0.1552967E-03	-0.1615462E 00	0.0000000E 00	0.6942202E 00

b) State Control Matrix (Δ,B Matrix in Filter)

-0.1307270E-03	0.3029091E-03
0.3486306E-01	0.1753552E-06
-0.2839876E-01	-0.5740591E-08
-0.5470808E-01	-0.1953357E-07

TABLE 9.2 Typical Transition Matrices - Simplified Linear Method

a) State Transition Matrix (AA Matrix in Filter)

0.9658080E 00	-0.1173969E-01	0.0000000E 00	-0.1540872E-03
0.4907031E-02	0.8386499E 00	0.0000000E 00	0.2855152E-01
-0.1733371E-03	-0.8743246E-01	0.1000000E 01	0.8246310E 00
-0.3714682E-03	-0.1593637E 00	0.0000000E 00	0.6695514E 00

b) State Control Matrix

-0.3976045E-03	0.3103837E-03
0.4019890E-01	0.0000000E 00
-0.3296753E-01	0.0000000E 00
-0.6337422E-01	0.0000000E 00

TABLE 9.3 Typical Transition Matrices - Full Software Routines

TIME	FORWARD SPEED	LATERAL SPEED	HEADING	YAW RATE
Sec.	m/s	m/s	Deg.	m/s
0	0.639	-0.127	0.52	4.28
5	0.560	-0.143	1.40	2.52
10	0.802	-0.215	-14.12	-3.63
15	0.535	-1.091	-16.55	0.97
20	-0.715	-2.967	-14.95	5.13
25	-0.775	-4.145	-24.12	-3.95
30	-0.879	-4.877	-30.53	0.17
35	-1.270	-5.696	-38.62	8.04
40	-1.162	-6.265	-37.18	4.23
45	-1.871	-8.918	-39.24	9.11
50	-1.413	-8.711	-42.53	-0.46
55	-1.084	-8.869	-50.42	-3.38
60	-1.370	-9.400	-57.35	10.65
65	-1.786	-11.047	-55.63	9.22
70	-1.496	-11.253	-46.70	3.67
75	-1.489	-11.846	-47.03	2.23
80	-1.098	-12.009	-46.99	1.78

Table 9.4 Measured States Fed to the Controller in Control Run

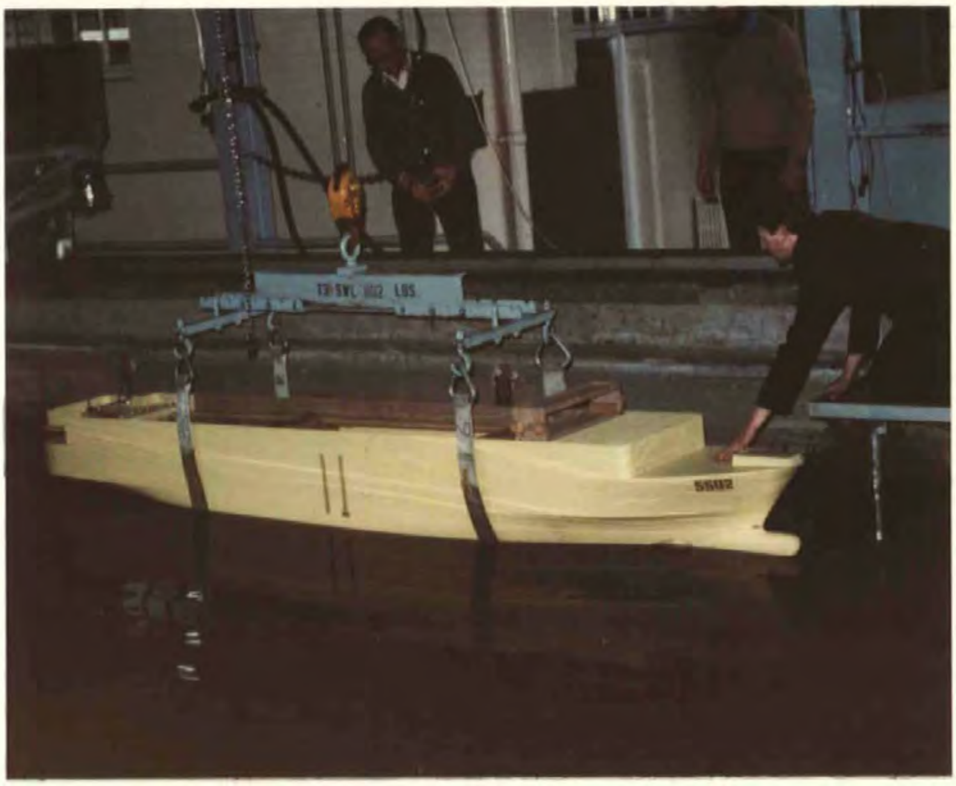

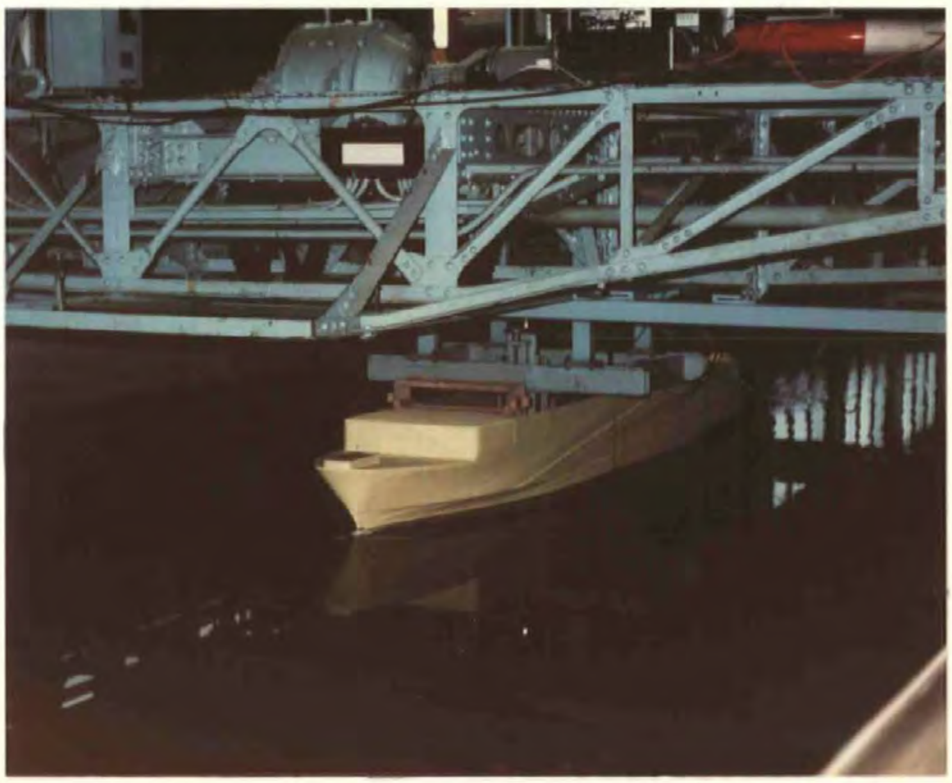

Fig 9.1 NMI Tests

Fig 9.2 Reservoir Tests

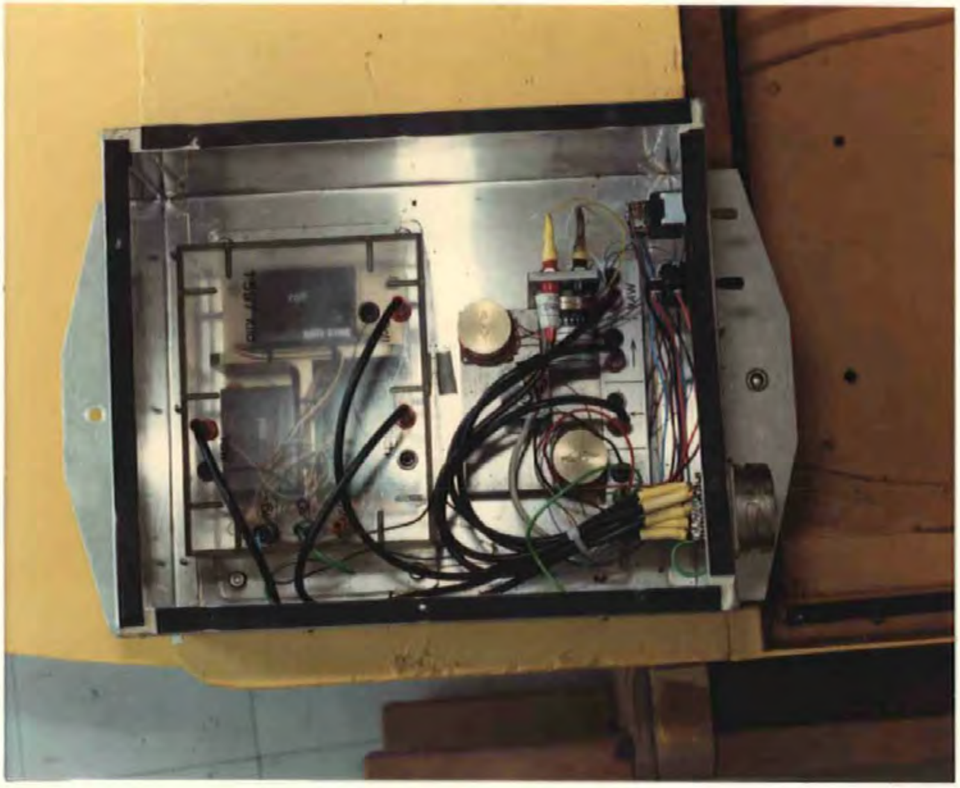

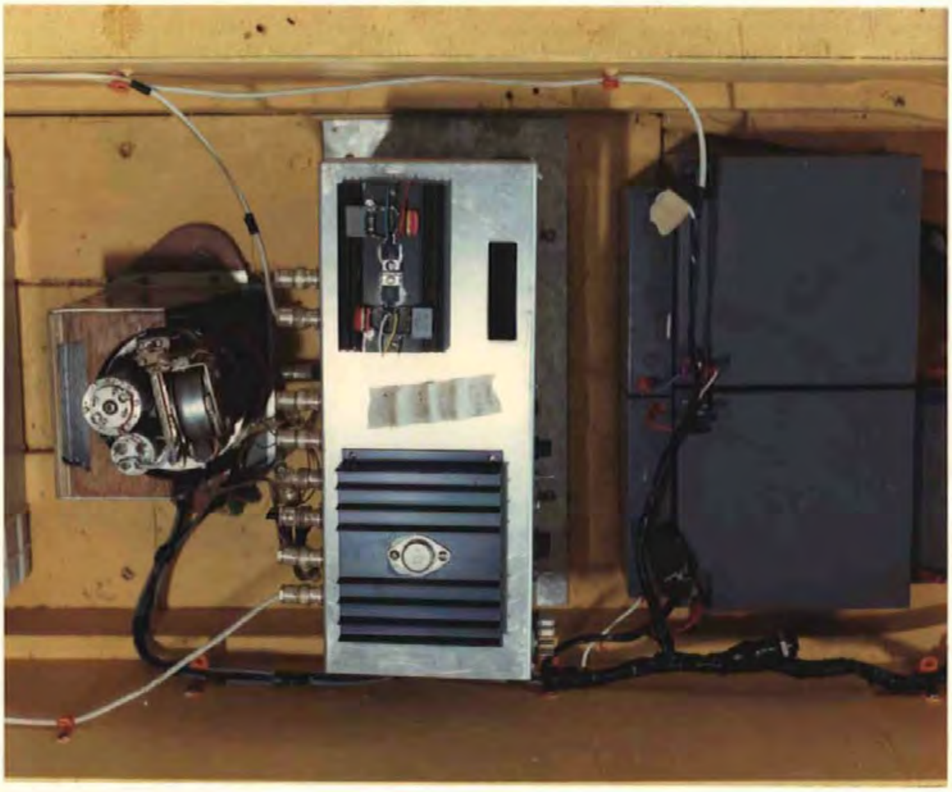

Fig 9.3 Measurement Systems (Top)

Microprocessor (Bottom)

A identifies the Actual Plot and S the Computer Simulation in Figures 9.6 to 9.11

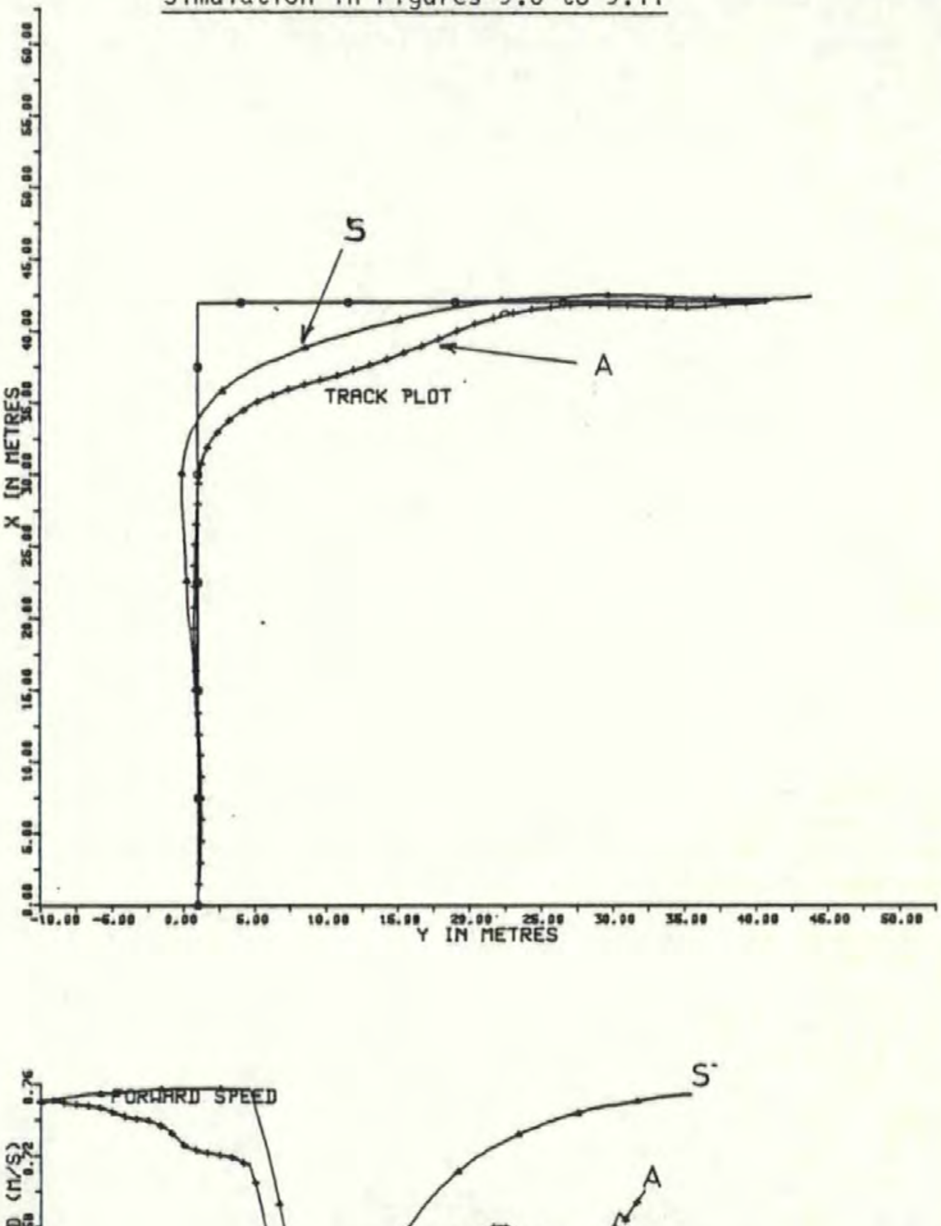

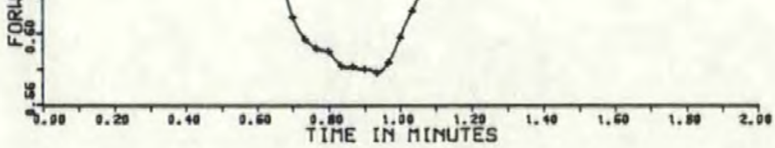

FIG 9.6 CENTAUR COMPARED WITH LINEARISED MATRICES

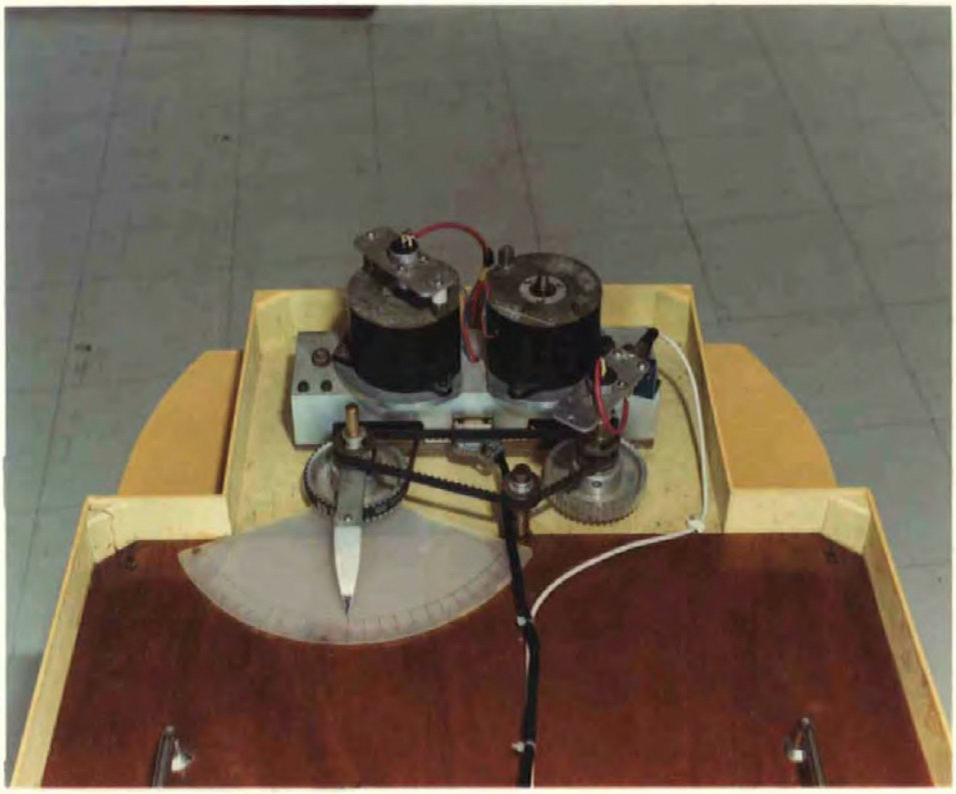

Fig 9.4 Rudder Controls

Fig 9.5 Model Underway on Reservoir

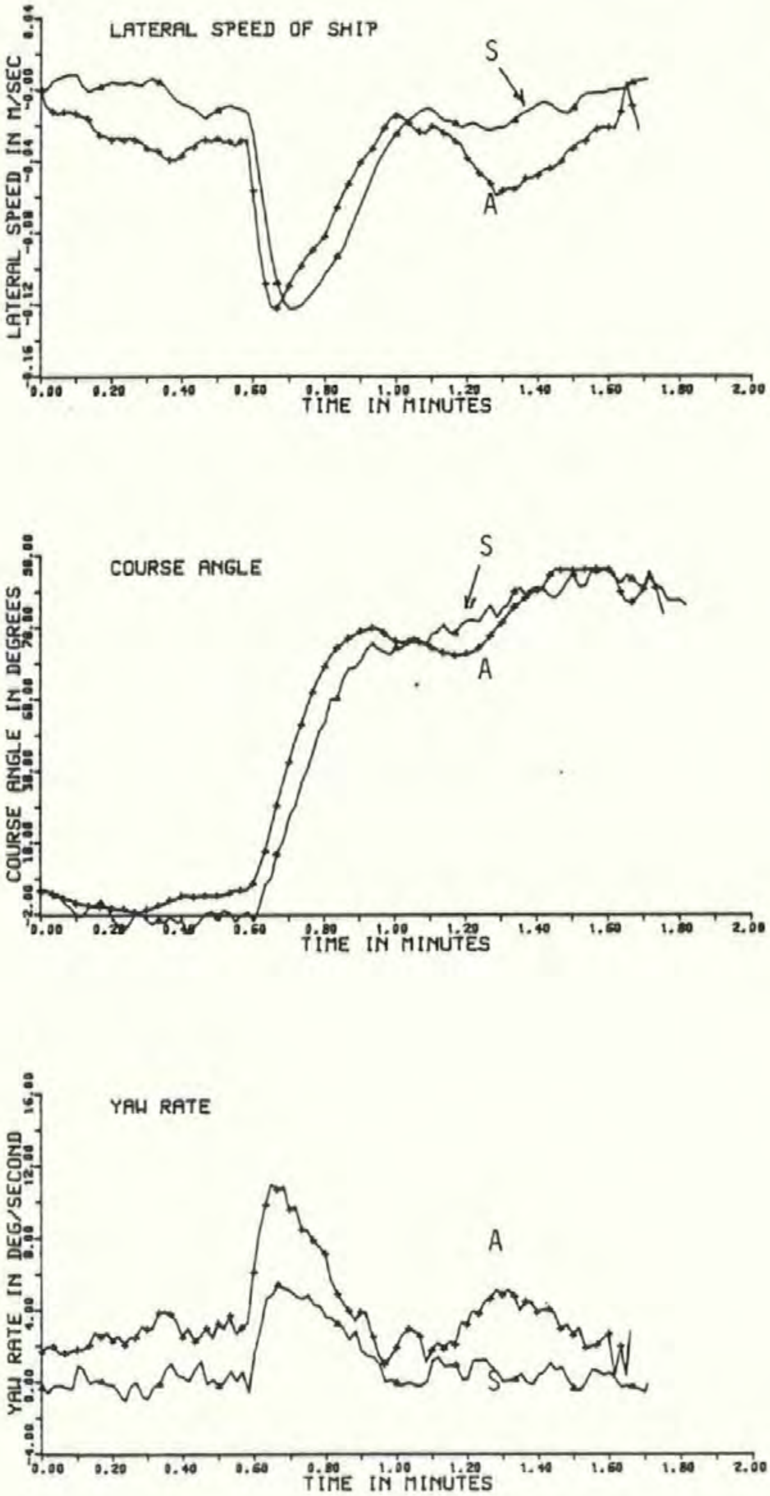
LATERAL SPEED OF SHIP
LATERAL SPEED IN M/SEC
TIME IN MINUTES
S
A
COURSE ANGLE
COURSE ANGLE IN DEGREES
TIME IN MINUTES
S
A
YAW RATE
YAW RATE IN DEG/SECOND
TIME IN MINUTES
A
S

FIG 9.6

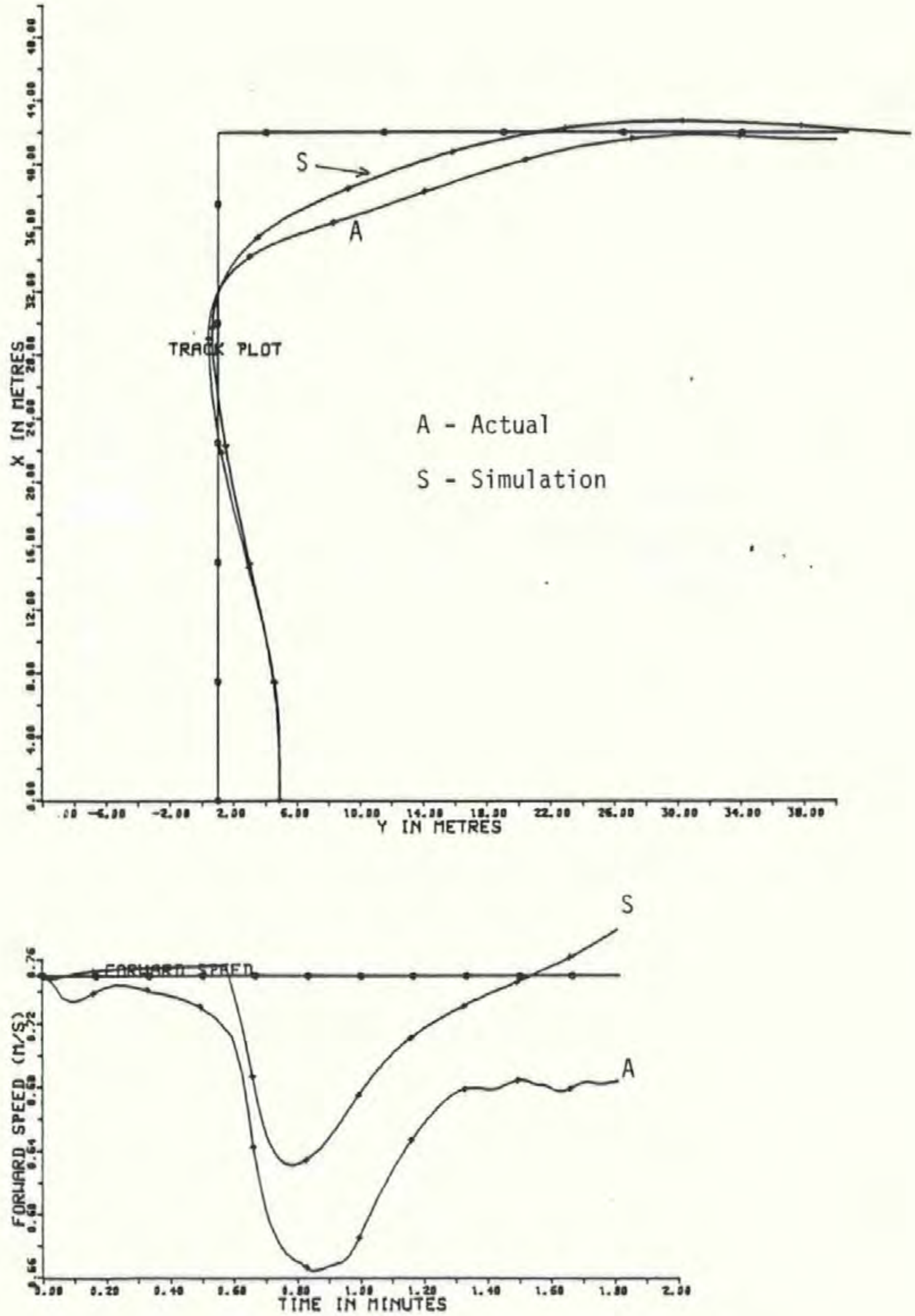

Fig 9.6A Test Run With Model Initially Offset By 4 Metres

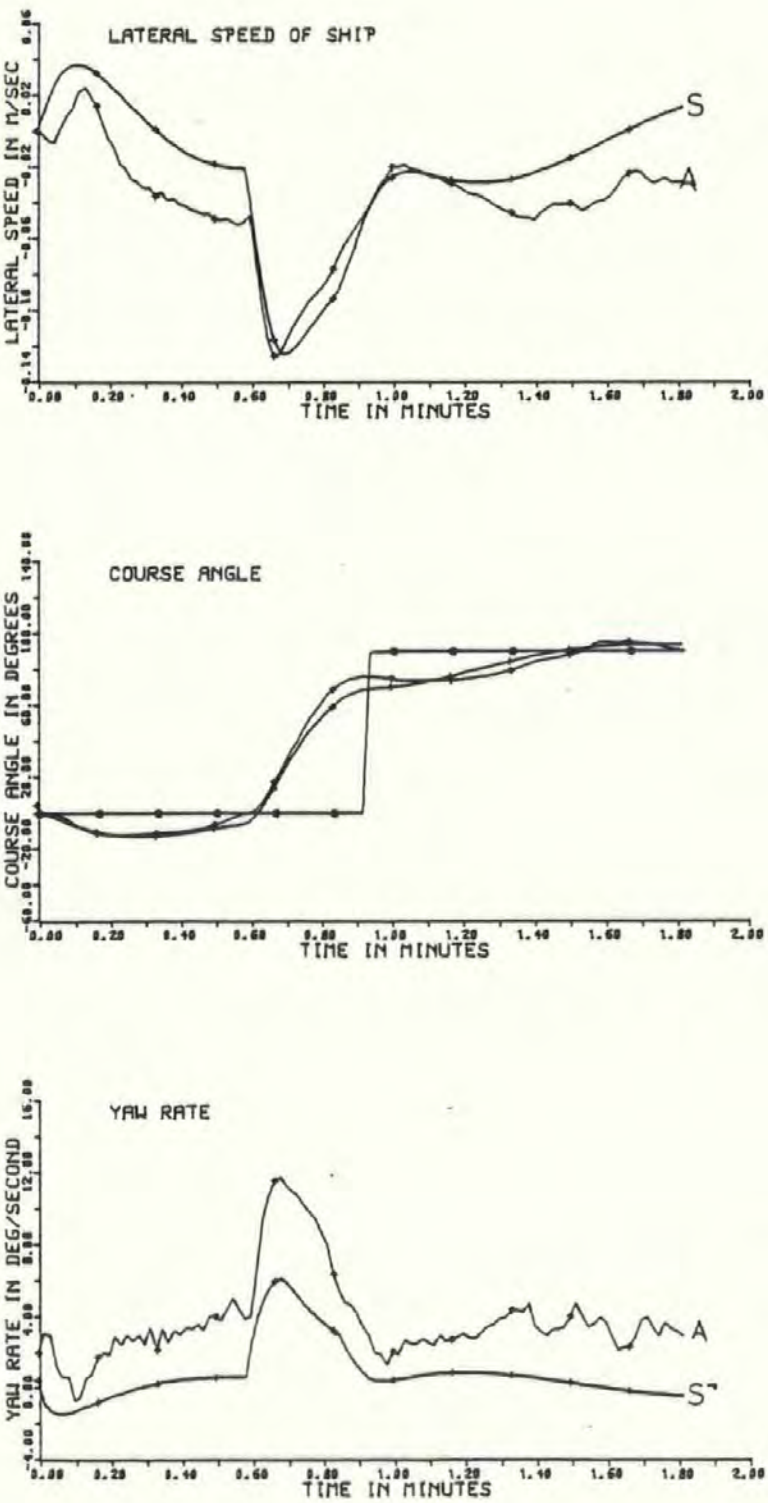
LATERAL SPEED OF SHIP
LATERAL SPEED IN M/SEC
TIME IN MINUTES
S
A
COURSE ANGLE
COURSE ANGLE IN DEGREES
TIME IN MINUTES
YAW RATE
YAW RATE IN DEG/SECOND
TIME IN MINUTES
A
S

Fig 9.6A

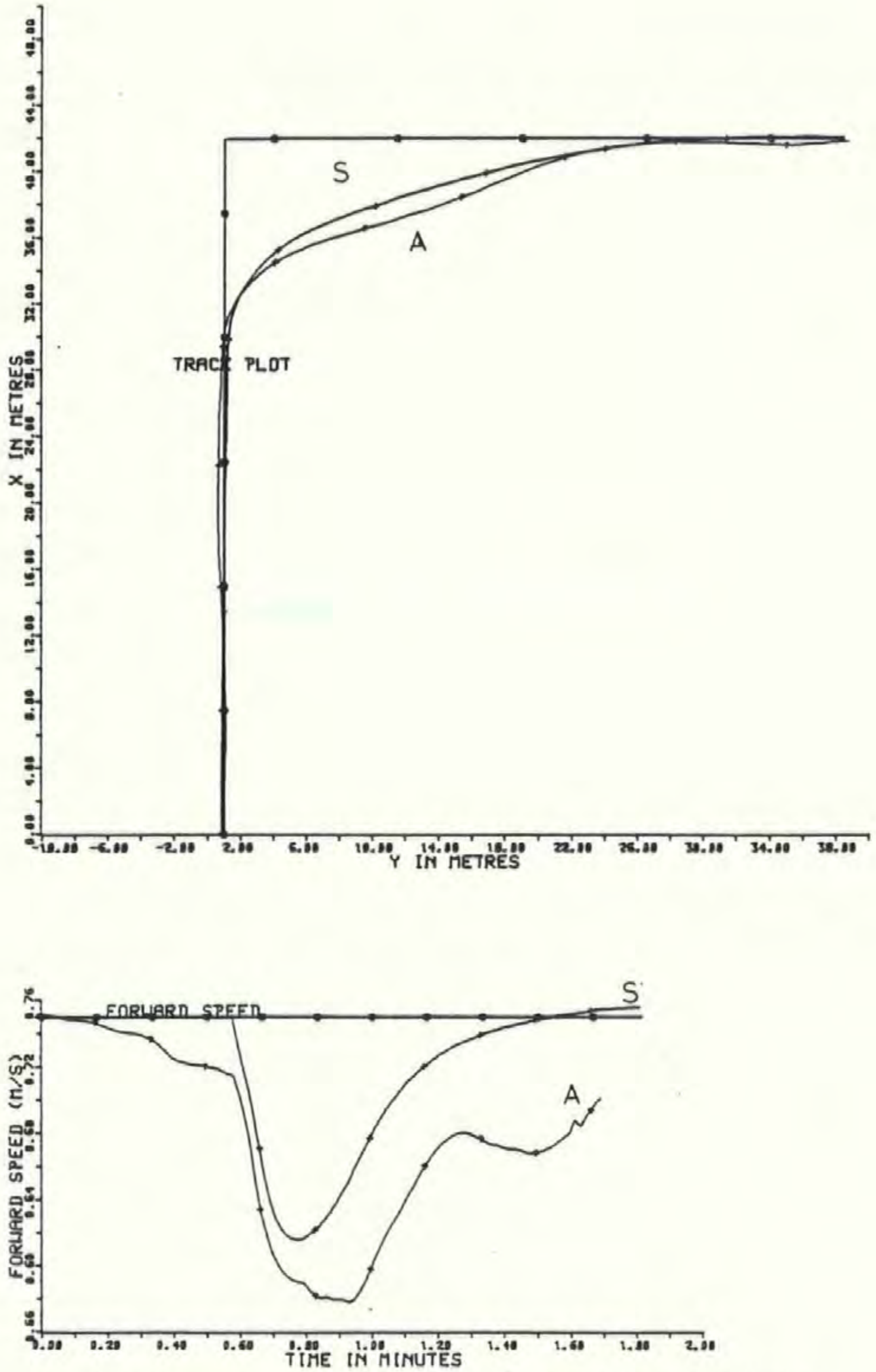

Fig 9.7 Comparison of Actual Model with Simulated Model Using Full Filter Calculations

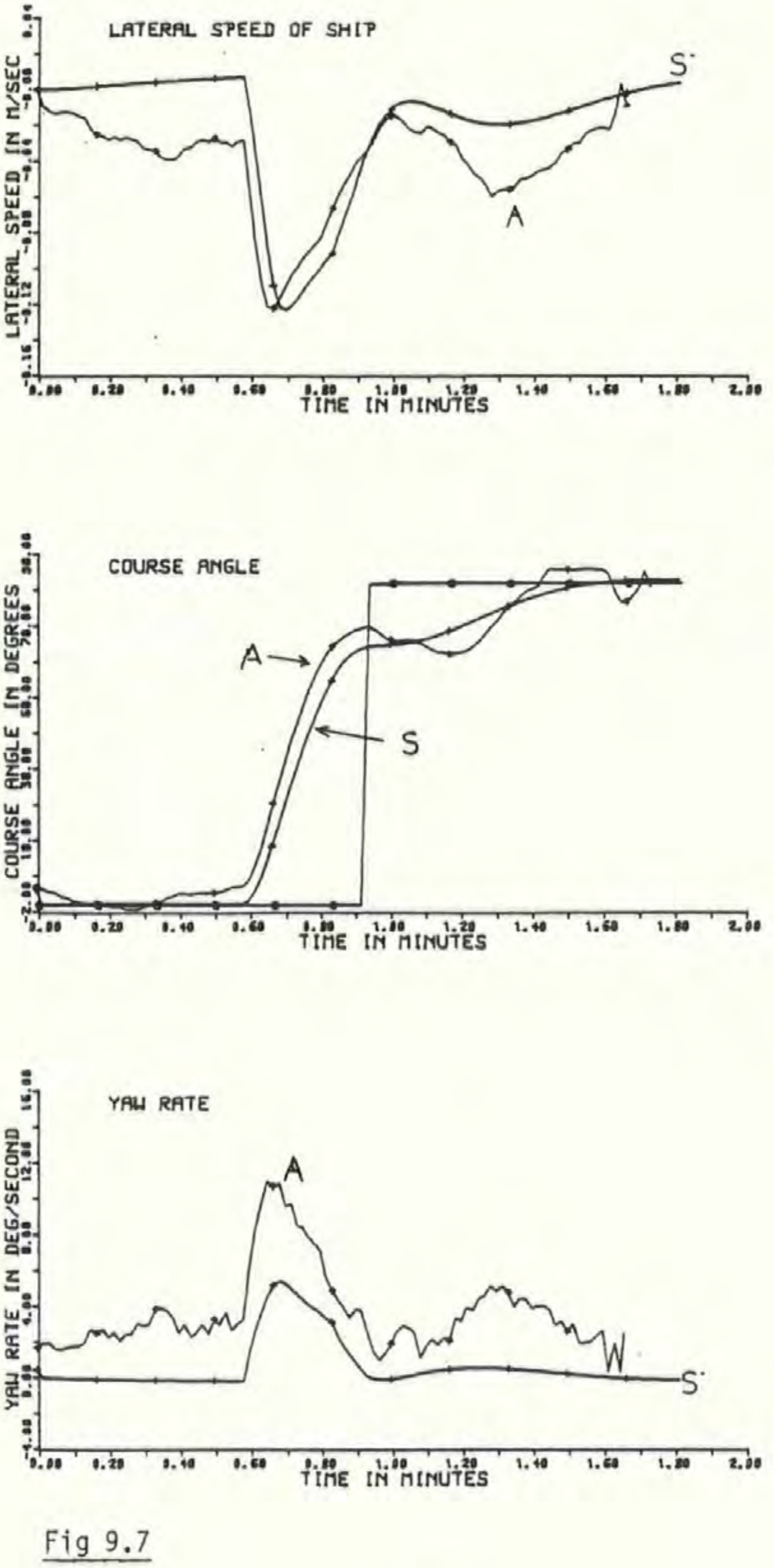
LATERAL SPEED OF SHIP
LATERAL SPEED IN M/SEC
TIME IN MINUTES
S
A
COURSE ANGLE
COURSE ANGLE IN DEGREES
TIME IN MINUTES
A
S
YAW RATE
YAW RATE IN DEG/SECOND
TIME IN MINUTES
A
W
S

Fig 9.7

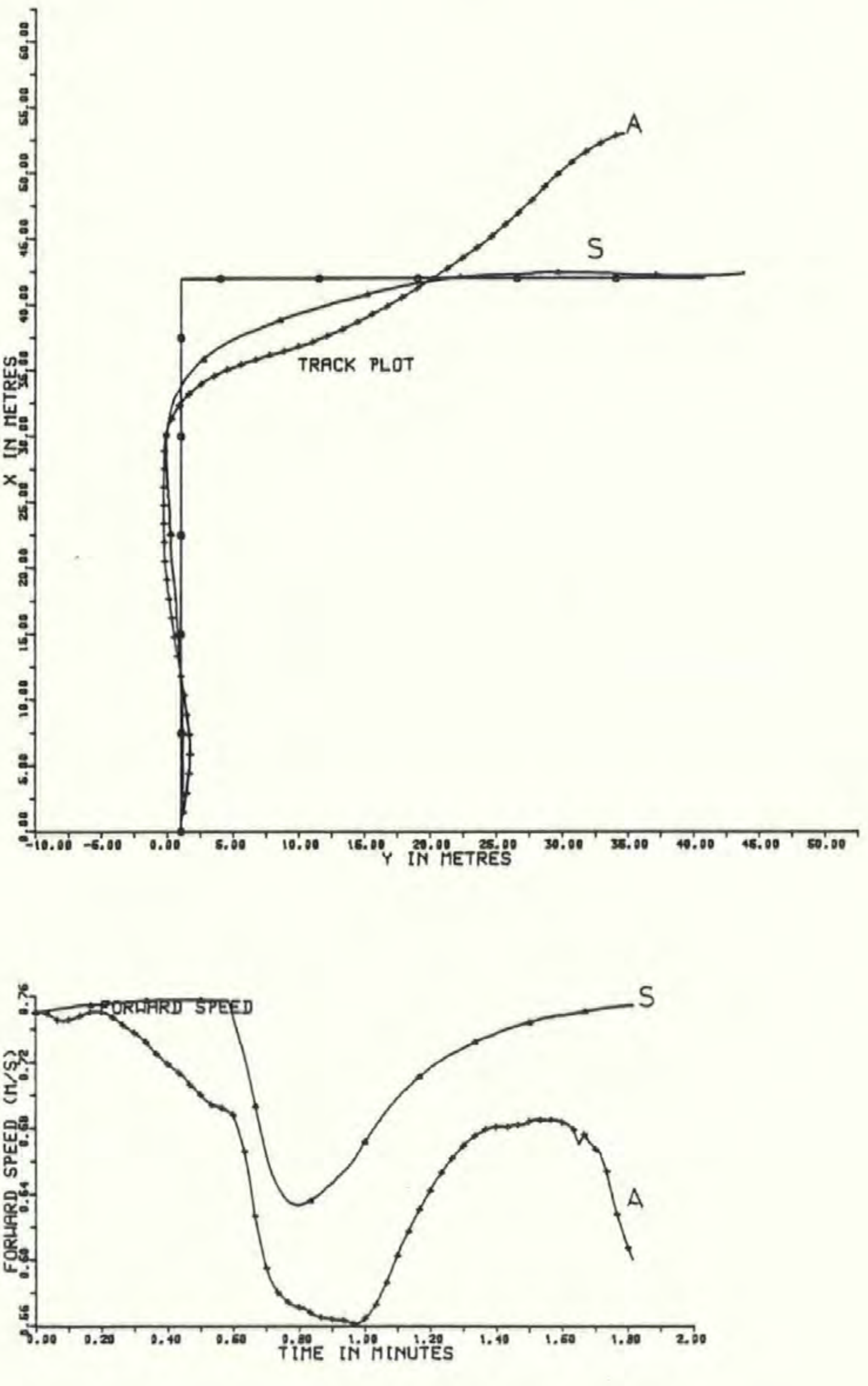

FIG 9.8 CENTAUR COMPARED WITH LINEARISED MATRICES IN WIND

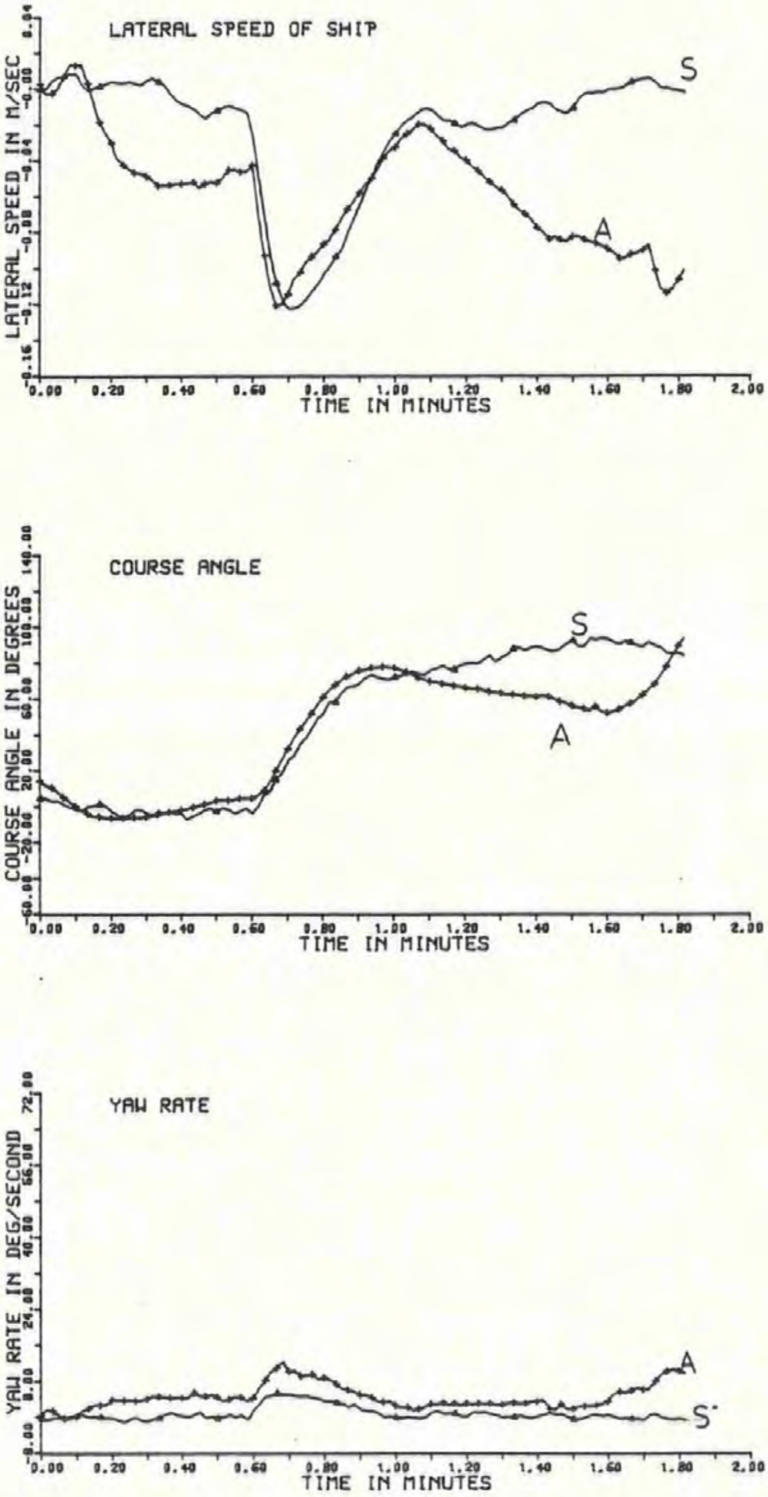
LATERAL SPEED OF SHIP
LATERAL SPEED IN M/SEC
S
A
TIME IN MINUTES
COURSE ANGLE
COURSE ANGLE IN DEGREES
S
A
TIME IN MINUTES
YAW RATE
YAW RATE IN DEG/SECOND
A
S
TIME IN MINUTES

FIG 9.8

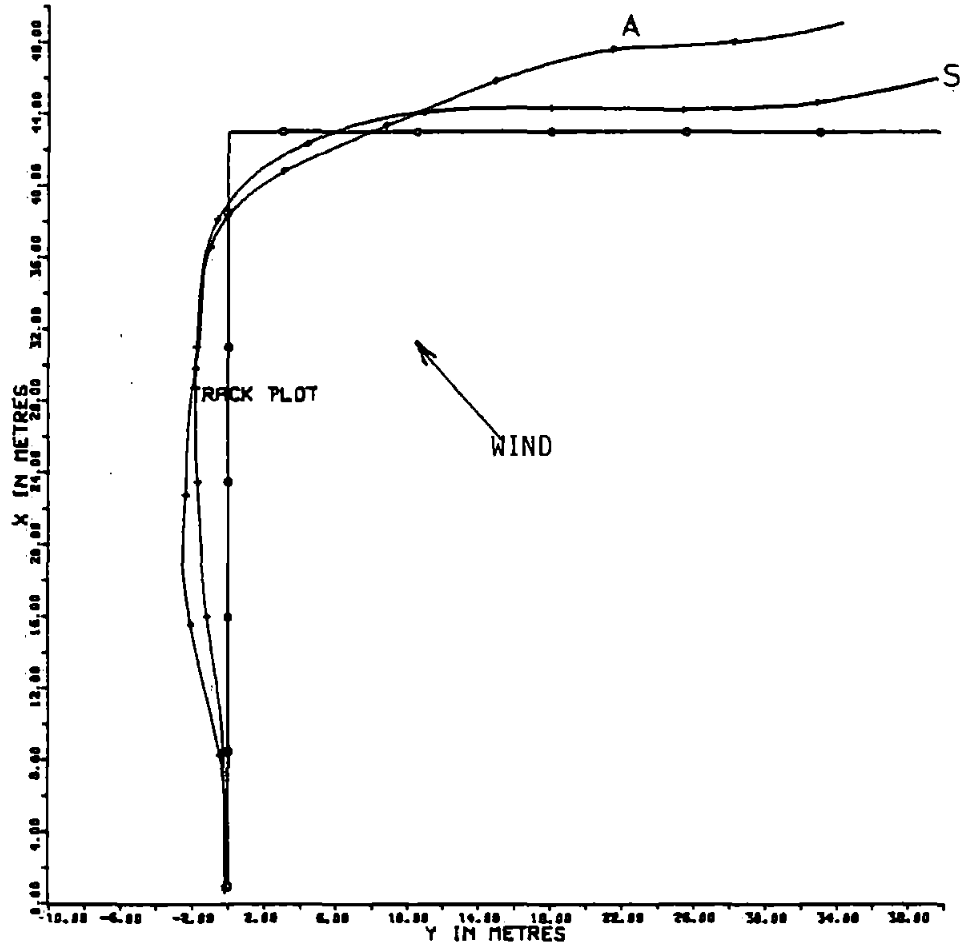

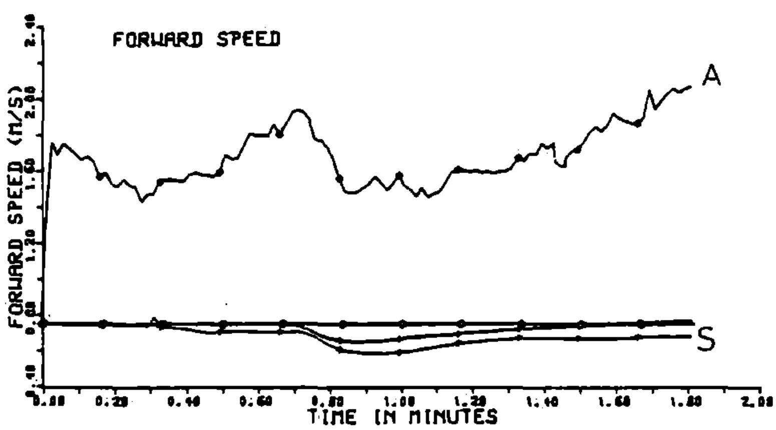

Fig 9.9 Test Run with Wind at 45 Degrees to Initial and Final Tracks

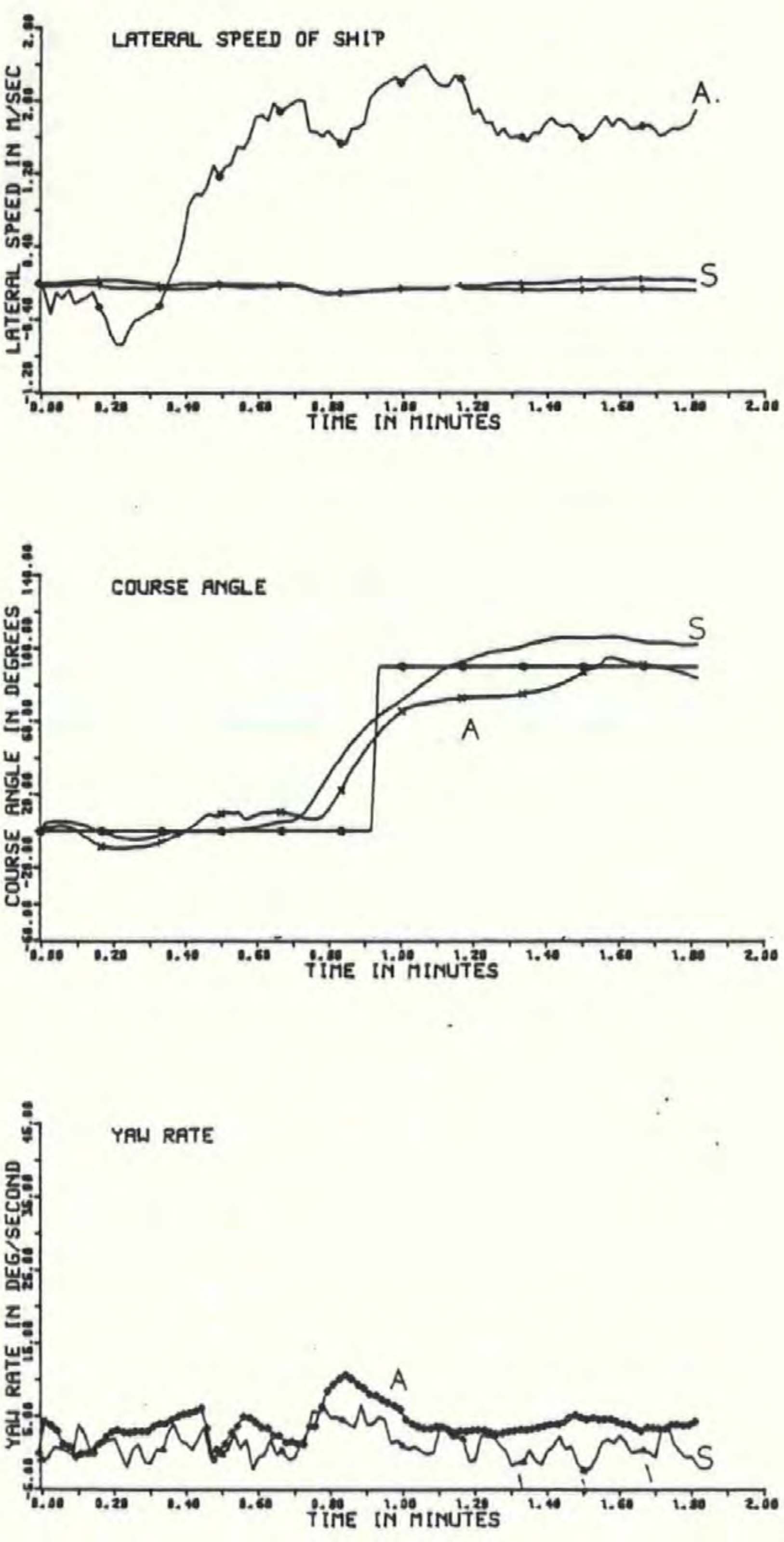
LATERAL SPEED OF SHIP
LATERAL SPEED IN M/SEC
A.
S
TIME IN MINUTES
COURSE ANGLE
COURSE ANGLE IN DEGREES
S
A
TIME IN MINUTES
YAW RATE
YAW RATE IN DEG/SECOND
A
S
TIME IN MINUTES

Fig 9.9

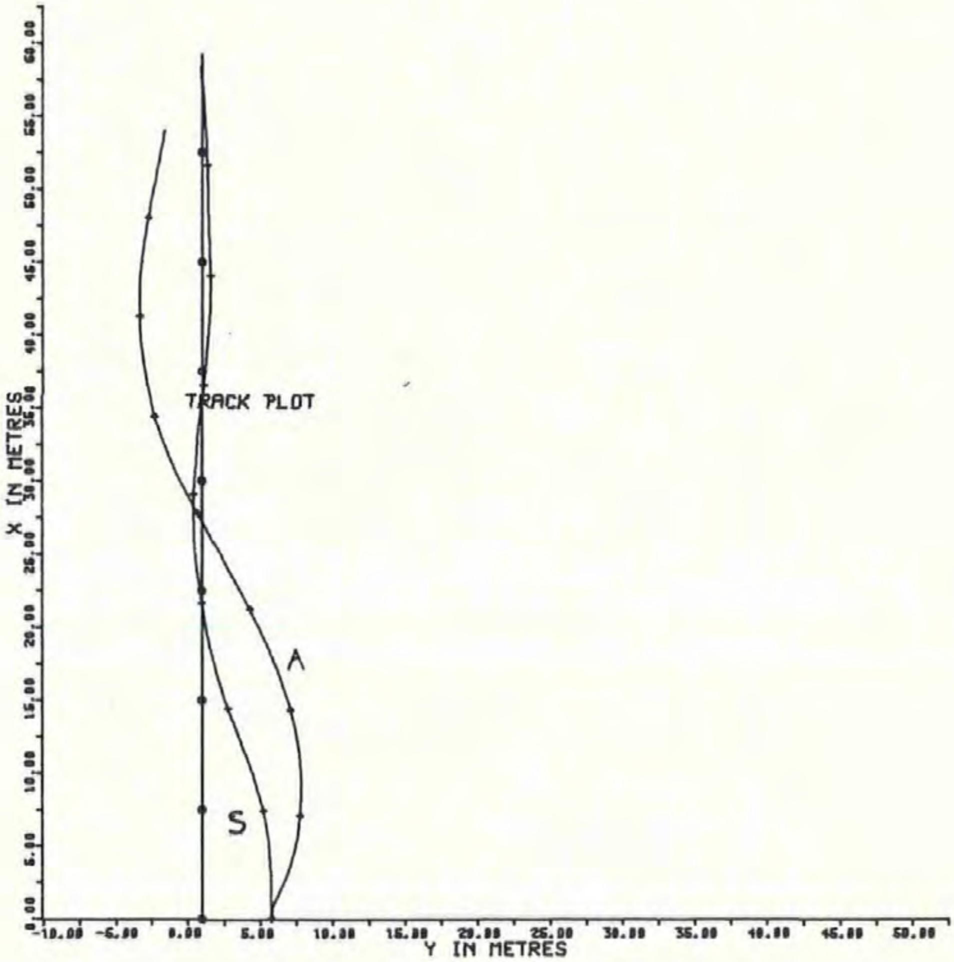

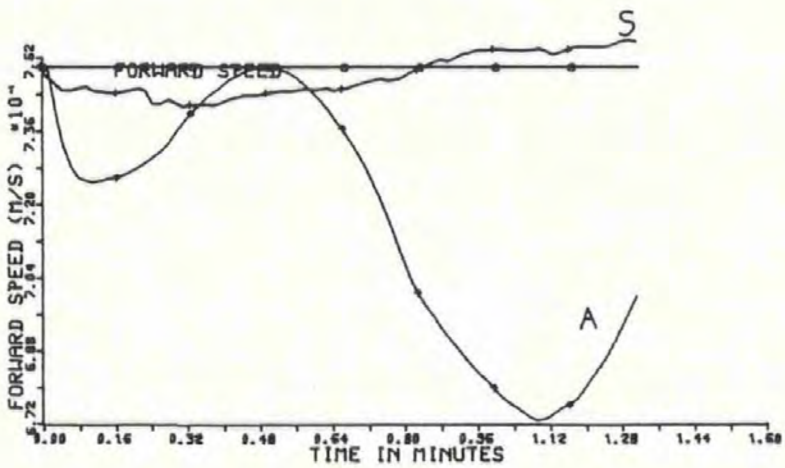

Fig 9.10 State and State Estimation Feedback

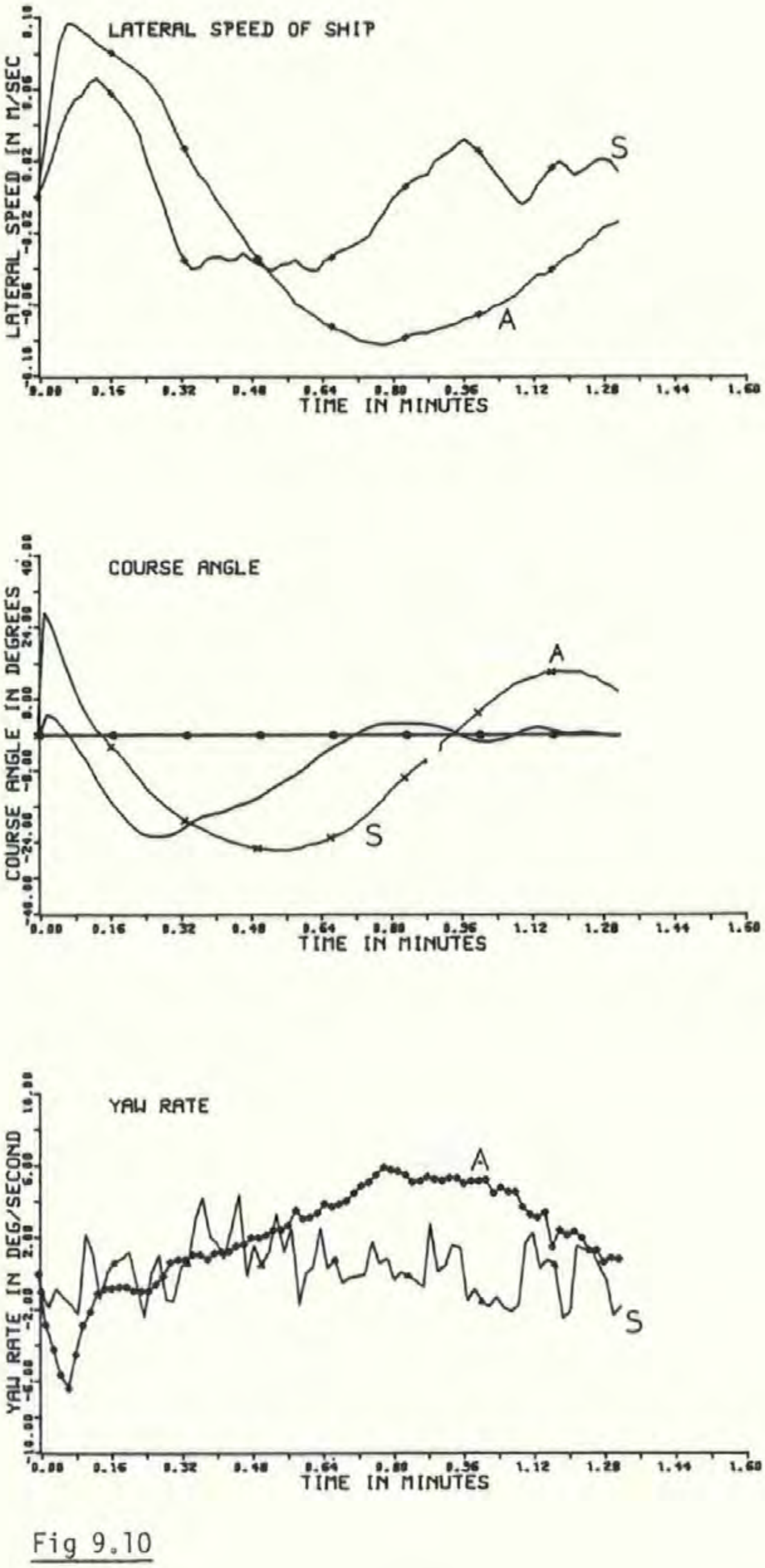
LATERAL SPEED OF SHIP
LATERAL SPEED IN M/SEC
TIME IN MINUTES
S
A
COURSE ANGLE
COURSE ANGLE IN DEGREES
TIME IN MINUTES
A
S
YAW RATE
YAW RATE IN DEG/SECOND
TIME IN MINUTES
A
S

Fig 9.10

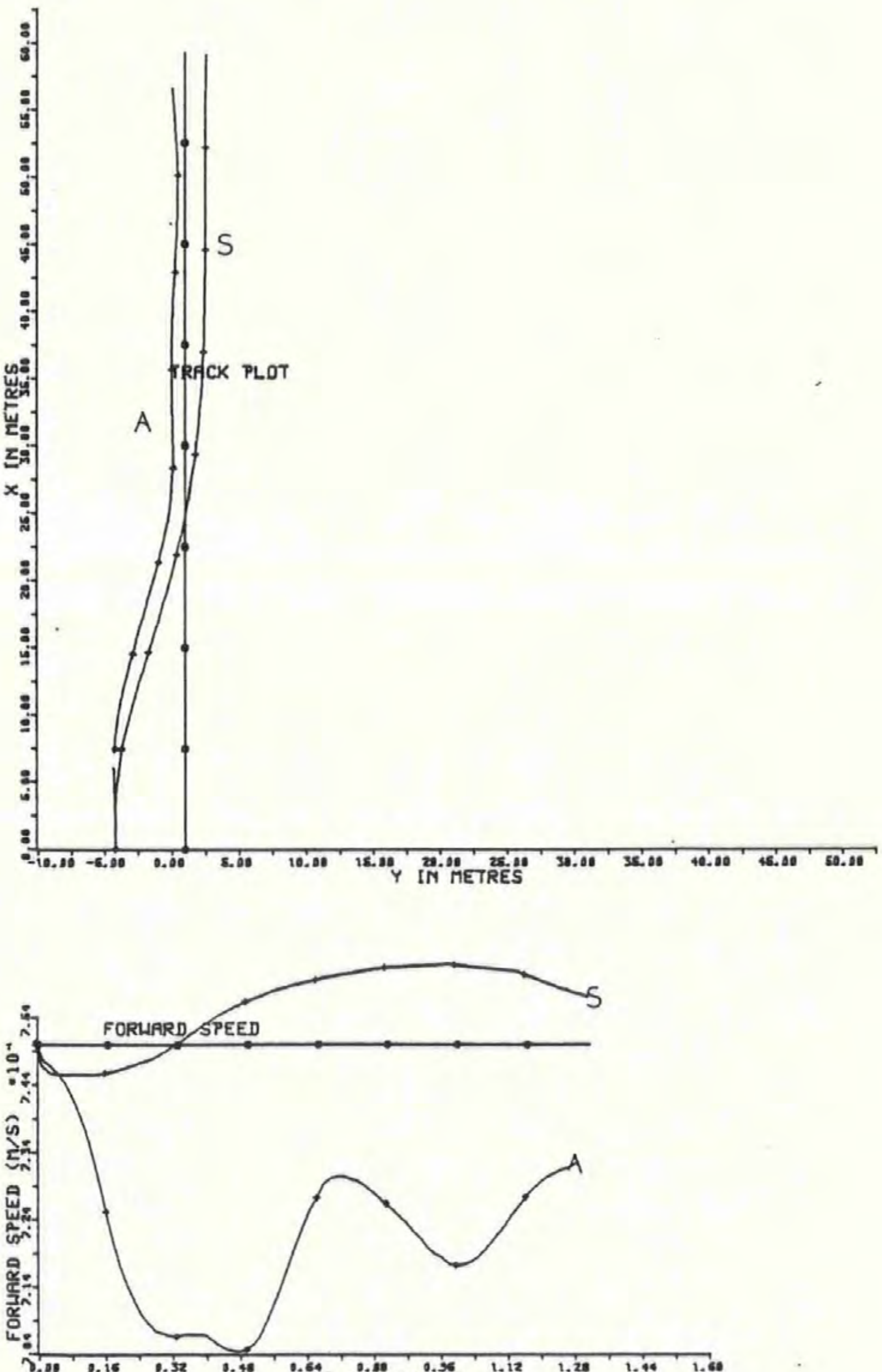

Fig 9.11 Full Filtering in Operation

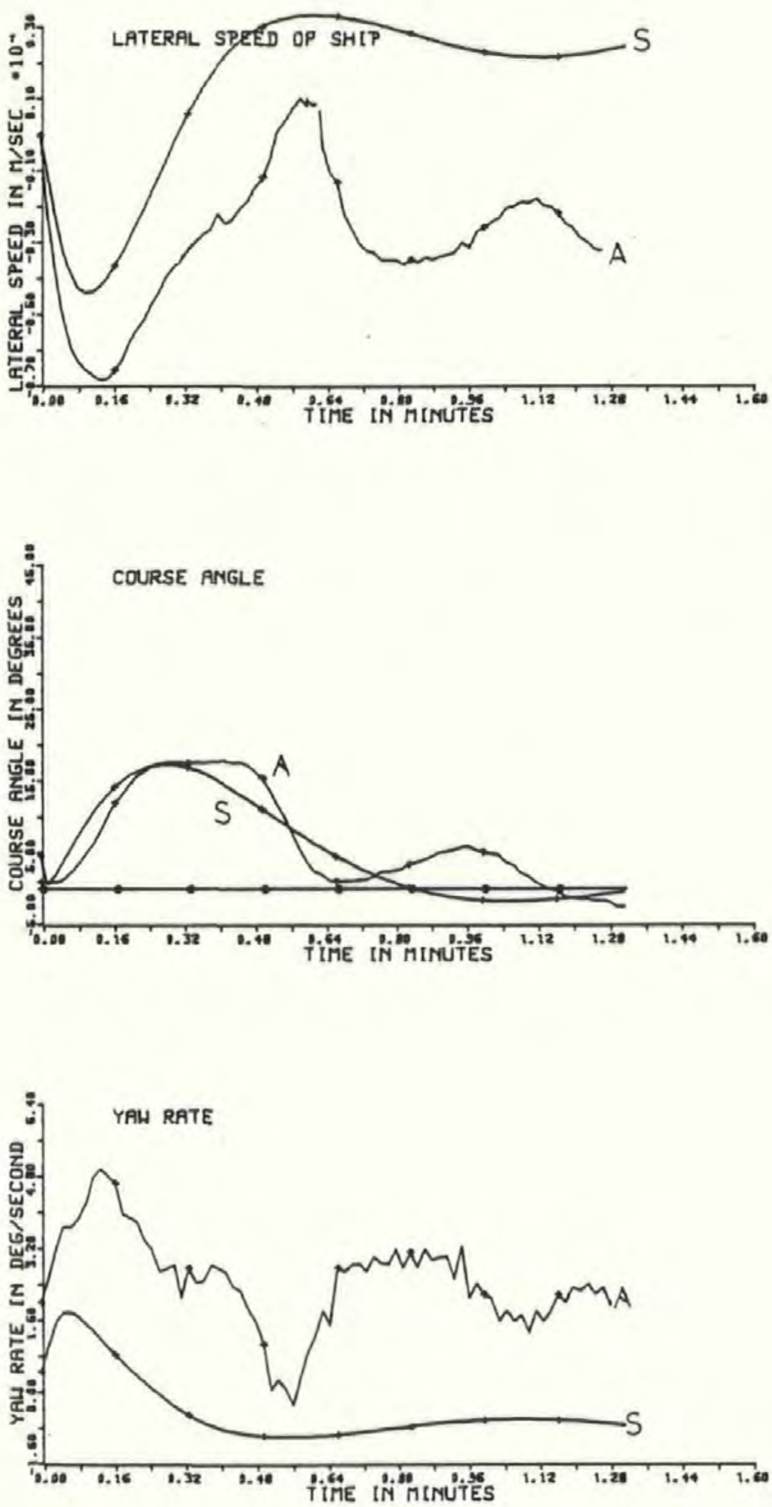
LATERAL SPEED OF SHIP
S
A
LATERAL SPEED IN M/SEC
TIME IN MINUTES
COURSE ANGLE
A
S
COURSE ANGLE IN DEGREES
TIME IN MINUTES
YAW RATE
A
S
YAW RATE IN DEG/SECOND
TIME IN MINUTES

Fig 9.11

CHAPTER 10

CONCLUSIONS AND RECOMMENDATIONS

10.1 Discussion of Results

This research project has been aimed at designing and developing a suitable digital filter for use in conjunction with an optimal controller so that a large ship can be automatically guided along the correct channel into, or out of, a port. This entailed extensive mathematical modelling using the state - space concepts largely associated with control engineering and resulted in a non–linear model which compared very favourably when turning circle and zig-zag tests were compared with those of a full-size vessel.

In the simulations which followed it was shown that the optimal filter would have enabled a twin-screw car ferry to be brought into Plymouth automatically, even though the measurement systems were, in some cases, extremely noisy. In all cases it was assumed that the vessel's demanded engine revolutions were constant. It was also assumed that there were no other vessels in the fairway or likely to cause disruption to the planned passage. Under these circumstances the results clearly show that the eight filtered states, give an extremely accurate input to the controller. Within the sampling interval of 5 seconds all relevant calculations were carried out, and hence the data was updated 12 times in each minute. No officer of the watch would be able to undertake observations this frequently, or with the same precision. He would therefore be forced to err on the side of safety.

In the system under test the filtered and true tracks are remarkably similar and follow very closely to the recommended track for deep draft vessels in the approach to the port. Certainly they are well within the limits imposed by the width of the navigable channel showing clearly that the full system, using measurements from widely fitted navigation aids, has the potential to guide the vessel automatically along the predetermined track.

The reduced non-linear computer model was used to simplify the system bearing in mind the limitations imposed by the physical model. Using the full capabilities of the filter, with transition matrices being calculated for each sampling period, the system was shown to navigate accurately through very noisy conditions.

Finally it was shown that the optimal filter for the reduced non-linear car ferry model (HEATHMORE) worked effectively when installed in the physical model (CENTAUR). In a series of test runs carried out on Crownhill Reservoir, it was shown that CENTAUR was pulled into the demanded track, the helm was then automatically put over at the appropriate time and the vessel came round to the new track at 90 degrees to the original. Computer simulations and test runs showed that without the use of the filter the control system was unable to keep the vessel on her demanded track, although in some runs the heading and yaw rate were unfiltered, giving a degree of control compatible with the fully filtered system. The photographs in Figure 9.2, which were taken during test runs under full filtered control, show how effectively the model was controlled.

10.2 Conclusions

A comprehensive digital simulation of a ship's dynamics has been set up and used to observe the time domain response of a ship in the approaches to a port when the associated track control system employed an optimal digital estimator/filter in conjunction with an optimal controller. The simulation was then used in the design of an optimal filter for installation in a physical model of a car ferry. Tests undertaken with the physical model then confirmed the results obtained in the digital simulations, leading to a proposed automatic guidance system for use in the approaches to a port. Use of this system would make it possible to improve the safety standards in the approaches to a port particularly in conditions of bad weather, making it possible to enter harbour in conditions when the prudent Master would hitherto have remained "hove to" outside the port limits. In the case of a car ferry this would improve the service offered to the passenger and enable already tight schedules to be adhered to more efficiently.

Throughout the research it has been assumed that the ship was under automatic control using a closed loop feedback system. Operated purely in the open loop navigation mode using say a digital display to give along-track and off-track positions and velocities together with an analogue display to show ownship's position relative to the surroundings (and other ships) data would be continuously available to the Master, thus providing an important addition to the safety of the ship operating in restricted waters and narrow waterways.

Important factors to emerge from research may be summarised as follows:-

i) The mathematical model of the ship used in the filter needs to be an almost identical replica of the real vessel.

ii) Using state-space methods and assuming the state variables are constant during each sampling period means the equation can be treated as linear, during each sample period. This allows the linear Kalman Filter theory to be applied, but it does mean that extensive calculations to obtain new transition matrices have to be completed during each sample time and this imposes severe restrictions on the microprocessor to be used. However this restriction need not apply in a ship-fitted system, or in any situation where a more powerful microcomputer is available.

iii) Re-calculation of the filter gains need not take place during each sample time. However, filter gains do change as the transition matrices change so that re-calculation at least during course and speed changes is desirable.

iv) Whilst no simplification of the filter gain equations is possible the state and control transition matrices used in the filter can be derived from the linear equations which would have to be obtained for any given model. These equations are principally functions of speed, yaw rate and rudder angle.

v) The filter was able to handle disturbances with non-zero means. Correlation between individual disturbances or individual measurements was also acceptable provided the correlation was small.

For example an x position measurement could not be completely independent of a y position measurement.

vi) Limited tests showed the ability of the reduced simulation model to follow the correct track with faults in up to 2 of the 4 measurement sub-systems.

10.3 Future Research

Kalman Filter techniques are now being used extensively in marine applications, particularly in the positioning of specialist vessels working in the offshore oil industry and in hydrographic survey work. Much still needs to be done in connection with the physical model however. The present work assumes a set of linearised equations for re-calculations of the state transition and control matrices in the filter. This was necessary due to the limitations of the on – board micro-computer. It was also shown that the more accurate heading and yaw rate signals could be sent directly to the controller, leaving only the more noisy signals to be filtered. Although this was classified as state plus state-estimation feedback no effort was made to change the filter equations, so that the filter gain and the state transition matrices were still 4 * 4 matrices.

By suitable partitioning of the matrices of equation set 8.2 it should be possible to reduce the filter mathematical model, thus allowing the reduction of the time taken in the full calculations of the $\underline{A}$ and $\underline{B}$ matrices, and a reintroduction of subroutine NAB, and in turn the use of a subroutine KBFLTR to recalculate the filter gains at least during alterations of course and speed.

An alternative is to consider the direct measurement of the vessel's parameters using system identification methods together with open loop tests to improve the mathematical model of the car ferry to be used in the filter.

Another possibility would be to enhance the computer facility in the model to allow for a large memory with a faster speed.

Further work will entail the design and development of a system to be installed in one of the craft attached to the Faculty of Maritime Studies. A more powerful microprocessor will be used and after development of the appropriate software in the laboratory, the hardware/software package will be interfaced with electronic position fixing systems, already installed in the vessel, to give an automatic track keeping system. These include Radar, Doppler Sonar, Decca Navigator and Decca Hi-fix electronic position fixing system.

Further work will entail the addition of a hazard-avoidance system. Davis (1981) and Colley et al (1984) have undertaken extensive research programmes to investigate the behaviour of shipping in hazardous situations. These computer simulations have involved the mathematical modelling of the International Regulations for Avoidance of Collision at Sea. This work will lead to the addition of an automatic hazard-avoidance system to the automatic track keeping system so that the vessel will be guided automatically along some predetermined track, but will also undertake the correct avoiding action when risk of collision and/or grounding exists.

All of this work will be brought together by the Ship Dynamics and Control Research Group at Plymouth Polytechnic in an integrated research programme with the following aims:-

i) Improve mathematical modelling using System Identification Techniques and open loop tests on marine craft available. Real time methods of system mathematical model identification and parameter estimation, without the need for physical model testing, will be investigated, thus bringing together identification, optimal control and estimation techniques - Burns, Dove and Bouncer (1982).

ii) Investigate the further use of State plus State Estimation Feedback to the Controller

iii) Development of a complete track and hazard avoidance controller for installation in a suitable marine vehicle. Investigation will also be carried out to ensure that the system stability and integrity remain high when one or more navigation aids become inoperative.

10.4 Concluding Remarks

The operators of today's ocean-going and specialist vessels have several electronic aids available. The traditional role of each navigation aid has been one of a stand-alone unit with the mariner, by his experience and training, co-ordinating the data from all the sources available to him in order to optimise vessel performance. As casualty statistics indicate however, when under stress or at times of peak work load, he is a poor co-ordinator of the information available to him, particularly when that information is from a number of different sources. Furthermore the application of microelectronics to ships has been progressing for many years so that the traditional role of the mariner referred to in Chapter 1 has been changing.

Microelectronics has also been a contributing factor to the changing pattern of the navigation equipment, and the Kalman Filter techniques used throughout this project have found a variety of uses in marine navigation. Dove (1977) suggests the use of Kalman Filter techniques at sea and four recent papers highlight the recent developments in this area. Daniel (1984) points out their uses in the off-shore oil industry where dynamic positioning of survey and supply ships is an important illustration of the use of control technology to maintain a stationary position. Grover-Brown and Hwang (1984) give details of the use of Kalman Filter techniques for precision geodesy whilst Liang et al (1984) describe the operational features and certain software and hardware configuration of a low-cost marine integrated navigation system designed to enhance navigational accuracy, operational reliability and position reporting efficiency of marine vessels. This system uses Kalman Filter techniques. Danson and Kibble (1984) are concerned with the precise navigation of a vessel in the pilotage and berthing stages of a voyage. These papers highlight the so-called "media technology" including satellite communications, which is bringing about a revolution in the mode of ship operations. In the field of modern marine operations there is a need to bring together the new Information Technology, which combines the disciplines of computing and telecommunications, with modern control engineering techniques and naval architecture.

This research programme has, it is hoped, made some small contribution to the developments in this area by applying some of these techniques to the problem of automatically piloting a ship in the approaches to a port, an area where the mariner is likely to be at maximum stress and where there is maximum probability of collision and/or grounding.

The need for improvement to the control of large ships in the approaches to a port was highlighted in a recent Department of Tranport Report (1984) of a Court of Inquiry on the collision of the car ferries European Gateway and Speedlink Vanguard off Harwich in December 1982, when each Master believed the other would alter course to let him past. The report goes on to state, "It is our belief that this collision occurred because of a degree of over complacency on the bridge of both vessels in the performance of what may have appeared routine and unexacting navigation." New traffic arrangements have now been introduced in the Harwich deep-water channel where the collision occurred, but if the European Gateway had been in the correct position in the deep water channel such a collision might not have happened. One of the functions of the system developed in this research is to <u>ensure that each ship is in the correct position at the correct time</u>.

REFERENCES

ABKOWITZ M.A. (1964)

Lectures on Ship Hydrodynamics - Steering and Manoeuvrability

Hydro Og Aerodynamisk Laboratorium Report No. HY-5, December 1964.

BECH M.I. (1972)

Some Aspects of the Stability of Automatic Course Control of Ships.

International Symposium on Directional Stability and Control of Bodies Moving in Water.

I.Mech.E. April 1972.

BOZIC S.M. (1979).

Digital and Kalman Filtering.

Edward Arnold (Publishers) Ltd.

BROWN S.H. and ALVESTAD R. (1974)

Hybrid Computer Simulation of Manoeuvring During Underway Replenishment.

International Shipbuilding Progress. 1974/75, pp 259-275.

BURNS R.S., DOVE M.J. and BOUNCER T.H. (1982).
Automatic Pilotage of Large Ships in Confined Waters - A Multivariable Approach.
Institute of Measurement and Control.
International Symposium on Multivariable Control Systems.
R.N. Engineering College, Plymouth.

BURNS R.S. (1984).
The Control of Large Ships in Confined Waters.
Ph.D. Thesis. CNAA, Plymouth Polytechnic.

CADZOW J.A. and MARTENS, H. R. (1970).
Discrete Time and Computer Control Systems.
Prentice Hall Inc.

COCKCROFT A.N. (1978).
Statistics of Ship Collisions.
J. Nav. Vol.31, No. 2.

COCKCROFT A.N. (1981).
A Comparison of Safety Records.
J. Nav. Vol.36, No. 3.

COLDWELL T.G. (1981).
Marine Traffic Flow and Casualties on the Humber.
J. Nav. Vol.34, No. 1.

COLLEY B.A., CURTIS R.G., and STOCKEL C.T. (1984).
On Marine Traffic Flow and Collision Avoidance Computer Simulation.
J. Nav. Vol.37, No. 2, pp. 232-250.

Conference on "Mathematical Aspects of Marine Traffic" (1971). Chelsea College, London. September 1977.
Organised by the Institute of Mathematics and its Applications and published by Academic Press in 1979.

COOK, C.E. (1983).
The Present Status of Navstar.
J. Nav. Vol.36, No. 3.

DANIEL J.J.S. (1984).
Dynamic Positioning Systems.
J. Nav. Vol.37, No.2. May 1984, p. 264.

DAVIS P.V., DOVE M.J., STOCKEL C.T. (1982).
A Computer Simulation of Multi-Ship Encounters.
J. Nav. Vol.35, pp. 347-352.

DAVIS P.V. (1981).
Computer Modelling of Marine Traffic Behaviour.
Ph.D. Thesis, CNAA, Plymouth Polytechnic.

DANSON G.F.S., and KIBBLE P. (1984).

Precise Positioning for Port Navigation and Berthing.

J. Nav. Vol.37, No.2, May 1984, p. 286.

DECCA NAVIGATOR CO. LTD.(1976)

The Decca Navigator System - Principles and Performance.

DECCA NAVIGATOR CO. LTD. (1973).

Distribution of Decca Errors, the Probability Ellipses and Root Mean Square Error.

(Internal Memo Plan 103).

DEPARTMENT OF TRANSPORT (1984)

Report on the Collision of European Gateway and Speedlink Vanguard off Harwich in December 1982.

Daily Telegraph 4 August 1984

DOVE M.J. (1974).

Automatic Control of Large Ships in Pilotage and Berthing.

J. Nav. Vol.27, No. 4.

DOVE M.J. (1977).

Kalman Filter Techniques in Marine Integrated Navigation Systems.

J. Nav. Vol.30, No. 1.

DOVE M.J. and FORTESCUE, P.W. (1977).
A Mathematical Model of the Design/Evaluation of Automatic Pilotage and Berthing Systems for Large Ships.
Symposium on Data and Information Processing in Navigation Systems.
Brunel University, September 1977. Organised by Institute Measurement and Control.

EDA H. (1965).
Steering Characteristics of Ships in Calm Waters and Waves.
Presented at the Annual S.N.A.M.E. Meeting, New York, 11-12 November 1965.

FENNESSY, Sir Edward (1979).
Radio Aids to Navigation: The Pioneer Days.
J. Nav. Vol.32, No. 1

FUJII Y. (1982).
Recent Trends in Traffic Accidents in Japanese Waters.
J. Nav. Vol.35, No. 1.

FUJII Y. and SHIOBARA R. (1971).
The Analysis of Traffic Accidents.
J. Nav. Vol.24, No. 4.

GILL A.D. (1976).

The Identification of Manoeuvring Equations for Ship Trials Results.

Trans. R.I.N.A. Vol.118, 1976.

GILL A.D. (1977).

Mathematical Modelling of Ship Manoeuvring.

Conference on "Mathematical Aspects of Marine Traffic", Chelsea College, London. September 1977.

GRIMBLE M.J. (1980) (a)

A Combined State and State Estimate Feedback Solution to the Ship Positioning Control Problem.

Optimal Control Applications and Methods. Vol.1, pp. 55-57

GRIMBLE M.J., PATTON R.J. and WISE D.A. (1980) (b)

The Design of Dynamic Ship Positioning Control Systems Using Stochastic Optimal Control Theory.

Optimal Control Applications and Methods. Vol.1, pp. 167-202.

GRIMBLE M.J., PATTON R.J. and WISE D.A. (1980). (c)

Use of Kalman Filtering Techniques in Dynamic Ship Positioning Systems.

Proc. IEE. Vol.127, Pt.D. No. 3. May 1980, pp. 93-102.

GROVER-BROWN R. and HUANG P.Y.C. (1984).

A Kalman Filter Approach to Precision GPS Geodesy.

Navigation, Vol.30, No. 4. Winter 1983-84.

GUNCKEL T.L. and FRANKLIN G.F. (1963).
A General Solution for Linear Sampled Data Control.
J. Basic Eng., Vol.85, p. 197.

HEALEY M. and MacKINNON D.J. (1975).
Design of a Digital Self-Alignment Controller for a Ship's Inertial Navigation System at Sea.
Proc. I.E.E. Vol.122, No. 1. January 1975.

HENDERSON D.W. and STRADA J.A. (1980).
Navstar Field Test Results.
Global Positioning System, ION, 1980.

HOLDER L.A. (1975).
Training for Automated Vessels.
Symposium in Nautical Education and Training.
City University, London. (Organised by Nautical Institute).

IMO Accuracy Standards for Navigation (1983).
J. Nav. Vol.37, No. 2. May 1984, p. 300.

International Symposium on "Vessel Traffic Services (1981).
Bremen, Germany 1981.

JONES R.V. (1975).
Navigation and War.
J. Nav. Vol.28, No. 1.

JOSEPH P.D. and TOU J.T. (1961).
On Linear Control Theory.
Trans. A.I.E.E. pt.II, Vol.80, p. 193.

KALMAN R.E. and BUCY R.S. (1961).
New Results in Linear Filtering and Prediction Theory.
J. Basic Eng. March 1961.

KALMAN R.E. and KOEPCKE R.W. (1958).
Optimal Synthesis of Linear Sampling Control Systems Using Generalised Performance Indices.
Trans. ASME, Vol.80, p. 1820.

KIRK D.E. (1970).
Optimal Control Theory - An Introduction.
Prentice Hall Inc., New Jersey.

KOYAMA T. (1972).
An Improvement of Course Stability by Subsidiary Automatic Control.
International Shipbuilding Progress, April 1972.

KUEBLER W. and SOMMERS S. (1982).
A Critical Review of the Fix Accuracy and Reliability of Electronic Marine Navigation Systems.
Navigation. Vol.29, No. 2.

LEWISON G.R.G. (1973).

The Development of Ship Manoeuvring Equations.

NPL Report, Ship 176, December 1973.

LIANG D.F., McMILLAN J.C., VINNIS M.F., FICKO A., FLETCHER B.G., and MASKELL C.A. (1984).

Low Cost Integrated Marine Navigation System.

Navigation. Vol.37, No. 2. May 1984, p. 232.

MacKINNON D.J. (1972).

A Study of the Application of Stochastic Control Theory to the Self-Alignment of a Ship's Inertial Navigator at Sea.

Ph.D. Thesis. University of Wales, University College, Cardiff.

MANEN J.D. van and HOOFT J.P. (A Three Dimensional Simulator for Manoeuvring of Surface Ships.

J. Nav. Vol.23, No. 3.

MATTIN R.B. (1982).

Understanding Kalman Filters.

Aerospace Dynamics (1982, Issue 7)

(Technical Journal of the British Aerospace Dynamics Group).

MEDITCH J.S. (1969).

Stochastic Optimal Linear Estimation and Control.

McGraw Hill Book Co. 1969.

MILLERS H.F. (1973).

Modern Control Theory Applied to Ship Steering.

Ship Operation Automation - IFAC/IFIP Symposium Oslo July 1973.

MORSE R.V. and PRICE D. (1961).

Manoeuvring Characteristics of the Mariner Type Ship (USS COMPASS ISLAND) in Calm Seas.

Sperry Polaris Management, Sperry Gyroscope Co. New York.

NATIONAL PORTS COUNCIL (1972).

Navigational Aids in Harbours and Port Approaches.

NATIONAL PORTS COUNCIL (1976).

Analysis of Marine Incidents in Ports and Harbours.

O'SULLIVAN J.P. (1982).

The Development of Electronic Navigation Systems.

J. Nav. Vol.35, No. 3.

PANEL ON HUMAN ERROR IN MERCHANT MARINE SAFETY (1976).

Human Error in Merchant Marine Safety.

National Academy of Science, Washington D.C.

ROBINS A.J. (1982).

The Extended Kalman Filter and its Use in Estimating Aerodynamic Derivatives.

Aerospace Dynamics. Issue 9 September 1982. p. 16.

SAGE G.F. and LUSE J.D. (1983).

Integration of Transit, Omega and Loran-C for Marine Navigation.

Navigation, Vol.30, No. 1.

SCOVELL G., ABBOTT J. and GENT C. (1980).

A Guided Tour Through the Implementation of a Kalman Filter.

The Bosworth Course Lectures, University of Birmingham, Department of Electronic and Electrical Engineering.

STRATTON A. and SILVER W.E (1970).

Operational Research and Cost-Benefit Analysis on Navigation with Particular Reference to Marine Accidents.

J. Nav. Vol.23, No. 4.

STROM-TEJSEN J. (1965).

A Digital Computer Technique for Prediction of Standard Manoeuvres of Surface Ships.

Department of Navy Research and Development Report No. 2130.

Washington D.C.

SUAREZ A. (1963).

Rotating Arm Experimental Study of a Mariner Class Vessel.

Davidson Laboratory Note No. 696. June 1963.

THOM H. (1980).

Theoretical and Experimental Modelling of Ship Dynamics.

Proceedings of a Conference on Ship Steering Automatic Control.

Genova, Italy. June 1980.

ZUIDWEG J.K. (1970).

Automatic Guidance of Ships as a Control Problem.

Ph.D. Thesis, Delft Technological University, Holland.

APPENDIX 1

NOTATION

a) Matrices and Vectors

$\underline{A}$	Discrete State Transition Matrix
$\underline{B}$	Discrete Control Matrix
$\underline{C}$	Discrete Disturbance Matrix
$\underline{D}$	Discrete Reverse Transition Matrix
$\underline{E}$	Discrete Reverse Control Matrix
$\underline{F}$	Continuous Time System Matrix
$\underline{G_C}$	Continuous Time Control Matrix
$\underline{G_D}$	Continuous Time Disturbance Matrix
$\underline{H}$	Measurement Matrix
$\underline{K}$	Kalman Gain Matrix
$\underline{M}$	Covariance of Measurement Noise
$\underline{M}'$	Reverse Time State Vector
$\underline{N}$	Covariance of Disturbance Noise
$\underline{N}'$	Residual Vector
$\underline{P}$	State Error Covariance Matrix
$\underline{Q}$	State Error Weighting Matrix
$\underline{R}$	Control Weighting Matrix
$\underline{r}$	Desired State Vector
$\underline{S}$	Feedback Gain Matrix
$\underline{u}$	Control Vector

$\underline{V}$ Command Matrix

$\underline{v}$ Noise Vector

$\underline{W}$ Ricatti Coefficient Matrix

$\underline{w}$ Disturbance Vector

$\hat{\underline{x}}$ State Vector

$\hat{\underline{X}}$ Best Estimate of State Vector

$\underline{z}$ Measured State Vector

b) Scalar Symbols

A,B,C State Equation Coefficients

I_z Moment of Inertia About Z Axis (kg m_2)

J Performance Index

k,i Integer Counters

L Length of Ship Between Perpendiculars (m)

L' Number of Terms in Power Series

m Mass of Ship (kg)

n_A, n_D Actual and Demanded Engine Speeds (rad/s)

N Total Moment Applied to Ship (Nm)

N_u, N_r, etc. Yaw Hydrodynamic Coefficients

$r, \dot{r}$ Angular Velocity and Acceleration of Ship about Z Axis

T Sampling Time Interval (s)

t Time (s)

T_N Time constant of Main Engines (s)

T_R Time constant of Rudder Servo (s)

U Track Velocity (m/s)

u Forward Velocity of Ship (m/s)

u_a, u_c Forward Components of Wind and Current Velocities (m/s)

v Lateral Velocity of Ship (m/s)

v_a, v_c Lateral Components of Wind and Current Velocities (m/s)

x_s, y_s, z_s Ship Related Cartesian Co-ordinates (m)

X Total Force on Ship in Forward Direction (N)

$X_u, X_r,$ etc. Surge Hydrodynamic Coefficients

x_o, y_o, z_o Earth Related Cartesian Co-ordinates (m)

Y Total Lateral Force on Ship (N)

$Y_u, Y_r,$ etc Sway Hydrodynamic Coefficients

c) Greek Symbols

$\beta, \hat{\beta}$ Transpose of Augmented State Transition Matrix and Best Estimate

δ_A, δ_D Actual and Demanded Rudder Angles (rad)

ρ Density of Water (kg/m$_3$)

ψ_A, ψ_D Actual and Demanded Heading of Ship (rad)

APPENDIX 2.

QUASI-LINEAR MODEL COEFFIENTS

Equation set (3.7) represents the quasi-linear form of the mathematical model used in the main frame computer simulations. The terms K, L, and M were obtained in the process of rearrangement and are defined below.

a) K Coefficients

$$K_2 = \frac{X_a}{m - X_{\dot{u}}}$$

$$K_4 = \frac{X_u}{m - X_{\dot{u}}}$$

$$K_6 = \frac{mr}{m - X_{\dot{u}}}$$

$$K_{w1} = K_4$$

$$K_{w3} = \frac{X_{ua}}{m - X_{\dot{u}}}$$

b) L Coefficients

$$L_1 = \frac{Y_1 + Y_{88} N_1}{1 - Y_{88} N_{66}}$$

$$Y_1 = \frac{Y_\delta}{m - Y_{\dot{v}}}$$

$$Y_{88} = \frac{Y_{\dot{r}}}{m - Y_{\dot{v}}}$$

$$N_1 = \frac{N_\delta}{I_z - N_{\dot{r}}}$$

$$N_{66} = \frac{N_{\dot{v}}}{I_z - N_{\dot{r}}}$$

$$L_2 = \frac{Y_2 + Y_{88} N_2}{1 - Y_{88} N_{66}}$$

$$Y_2 = \frac{Y_r}{m - Y_{\dot{v}}}$$

$$N_2 = \frac{N_a}{I_z - N_{\dot r}}$$

$$L_4 = \frac{Y_4}{1 - Y_{88} N_{66}}$$

$$Y_4 = \frac{-mr}{m - Y_{\dot v}}$$

$$L_6 = \frac{Y_6 + Y_{88} N_6}{1 - Y_{88} N_{66}}$$

$$Y_6 = \frac{Y_v}{m - Y_{\dot v}}$$

$$N_6 = \frac{N_v}{I_z - N_{\dot r}}$$

$$L_8 = \frac{Y_8 + Y_{88} N_8}{1 - Y_{88} N_{66}}$$

$$Y_8 = \frac{Y_r}{m - Y_{\dot v}}$$

$$N_8 = \frac{N_r}{I_z - N_{\dot r}}$$

$$L_{w2} = \frac{Y_{w2} + Y_{88} N_{w2}}{1 - Y_{88} N_{66}}$$

$$Y_{w2} = Y_6$$

$$N_{w2} = N_6$$

$$L_{w4} = \frac{Y_{w4} + Y_{88} N_{w4}}{1 - Y_{88} N_{66}}$$

$$Y_{w4} = \frac{Y_{va}}{m - Y_{\dot v}}$$

$$N_{w4} = \frac{N_{va}}{I_z - N_{\dot r}}$$

c) M Coefficients

$$M_1 = \frac{N_1 + N_{66} Y_1}{1 - N_{66} Y_{88}}$$

$$M_2 = \frac{N_2 + N_{662}}{1 - N_{66} Y_{88}}$$

$$M_4 = \frac{N_{66} Y_4}{1 - N_{66} Y_{88}}$$

$$M_6 = \frac{N_6 + N_{66} Y_6}{1 - N_{66} Y_{88}}$$

$$M_8 = \frac{N_8 + N_{66} Y_8}{1 - N_{66} Y_{88}}$$

$$M_{w2} = \frac{N_{w2} + N_{66} Y_{w2}}{1 - N_{66} Y_{88}}$$

$$M_{w4} = \frac{N_{w4} + N_{66} Y_{w4}}{1 - N_{66} Y_{88}}$$

APPENDIX 3

NON-LINEAR MODEL COEFFICIENTS

Equation set (3.28) represents the non linear form of the mathematical model used in the main frame computer simulations. The X, B, and C, coefficients were obtained from the non dimensionalised hydrodynamic derivatives,

a) X Coeffients

$$X_1 = \frac{\bar{X}_{\delta\delta}\,\delta_A}{m - X_{\dot{u}}} \qquad \bar{X}_{\delta\delta} = 1/2\ X_{\delta\delta}$$

$$X_2 = \frac{X_{un}u + \bar{X}_{nn}\,n_A}{m - X_{\dot{u}}} \qquad \bar{X}_{nn} = 1/2\ X_{nn}$$

$$X_4 = \frac{X_u + \bar{X}_{uu}u + \bar{X}_{uuu}u^2}{m - X_{\dot{u}}} \qquad \bar{X}_{uu} = 1/2\ X_{uu}$$

$$\bar{X}_{uuu} = 1/6\ X_{uuu}$$

$$X_6 = \frac{\bar{X}_{vv}v + mr}{m - X_{\dot{u}}} \qquad \bar{X}_{vv} = 1/2\ X_{vv}$$

$$X_8 = \frac{\bar{X}_{rr}r}{m - X_{\dot{u}}} \qquad \bar{X}_{rr} = 1/2\ X_{rr}$$

$$X_{w1} = K_{w1}$$

$$X_{w3} = K_{w3}$$

b) B Coefficients

$$B_1 = \frac{Y_1 + Y_{88}\,N_1}{1 - Y_{88}\,N_{66}}$$

$$Y_1 = \frac{Y_\delta + \bar{Y}_{\delta\delta\delta}\,\delta_A^2}{m - Y_{\dot{v}}} \qquad \bar{Y}_{\delta\delta\delta} = 1/6\ Y_{\delta\delta\delta}$$

$$Y_{88} = \frac{Y_{\dot{r}}}{m - Y_{\dot{v}}}$$

$$N_1 = \frac{N_\delta + \bar{N}_{\delta\delta\delta}\,\delta_A^2}{I_z - N_{\dot{r}}} \qquad \bar{N}_{\delta\delta\delta} = 1/6\ N_{\delta\delta\delta}$$

$$N_{66} = \frac{N_{\dot v}}{I_z - N_{\dot r}}$$

$$B_2 = \frac{Y_2 + Y_{88} N_2}{1 - Y_{88} N_{66}}$$

$$Y_2 = \frac{\overline{Y}_{nn}\, n_\theta}{m - Y_{\dot v}} \qquad \overline{Y}_{nn} = 1/2\ Y_{nn}$$

$$N_2 = \frac{\overline{N}_{nn}\, n_\theta}{I_z - N_{\dot r}} \qquad \overline{N}_{nn} = 1/2\ N_{nn}$$

$$B_4 = \frac{Y_4}{1 - Y_{88} N_{66}}$$

$$Y_4 = \frac{-mr}{m - Y_{\dot v}}$$

$$B_6 = \frac{Y_6 + Y_{88} N_6}{1 - Y_{88} N_{66}}$$

$$Y_6 = \frac{Y_v + \overline{Y}_{rvv} rv + \overline{Y}_{vvv} v^2 + \overline{Y}_{\delta vv} v^2 + \overline{Y}_{\delta vv} \delta_\theta v}{m - Y_{\dot v}}$$

$$\overline{Y}_{rvv} = 1/6\ Y_{rvv}$$

$$\overline{Y}_{vvv} = 1/6\ Y_{vvv}$$

$$\overline{Y}_{\delta vv} = 1/6\ Y_{\delta vv}$$

$$N_6 = \frac{N_v + \overline{N}_{rvv} rv + \overline{N}_{vvv} v^2 + \overline{N}_{\delta vv} \delta_\theta v}{I_z - N_{\dot r}}$$

$$\overline{N}_{rvv} = 1/6\ N_{rvv}$$

$$\overline{N}_{vvv} = 1/6\ N_{vvv}$$

$$\overline{N}_{\delta vv} = 1/6\ N_{\delta vv}$$

$$B_8 = \frac{Y_8 + Y_{88} N_8}{1 - Y_{88} N_{66}}$$

$$Y_8 = \frac{Y_r}{m - Y_{\dot v}}$$

$$N_8 = \frac{N_r}{I_z - N_{\dot r}}$$

$$B_{w2} = L_{w2}$$

$$B_{w4} = L_{w4}$$

c) C Coefficients

$$C_1 = \frac{N_1 + N_{66}\, Y_1}{1 - N_{66}\, Y_{88}}$$

$$C_2 = \frac{N_2 + N_{66}\, Y_2}{1 - N_{66}\, Y_{88}}$$

$$C_4 = \frac{N_{66}\, Y_4}{1 - N_{66}\, Y_{88}}$$

$$C_6 = \frac{N_6 + N_{66}\, Y_6}{1 - N_{66}\, Y_{88}}$$

$$C_8 = \frac{N_8 + N_{66}\, Y_{88}}{1 - N_{66} Y_{88}}$$

$$C_{w2} = M_{w2}$$

$$C_{w4} = M_{w4}$$

APPENDIX 4

HYDRODYNAMIC DERIVATIVES

The various hydrodynamic derivatives which appear in the equations of motion have numerical values which depend upon the geometry of the ship. This involves calculating forces and moments acting upon a given ship with constant forward velocity and also when lateral and angular velocity exist.

The hydrodynamic coefficients for the Mariner hull were taken from published papers such as Morse and Price (1961). For the physical model of the car ferry tests were carried out at the National Maritime Institute's towing tank at Teddington, London, after which open loop tests were undertaken at Plymouth. At Teddington the model was towed along the tank at various angles of attack to the model path. A dynamometer measured the forces and moments experienced by the model. These were plotted against speed, acceleration, engine revolutions and angle of attack to obtain the derivatives. The tank testing techniques and the open loop tests involving turning circles, spiral tests and zig-zag manoeuvres are described in Abkowitz (1964). The non-dimensional coefficients together with the dimensionalising factors are given in this appendix.

DERIVATIVE	CAR FERRY HULL	MARINER HULL	DIMENSIONALISING FACTORS
X'_{s}	0.0	0.0	$0.5\rho L^{2}u^{2}$
X'_{n}	0.0	0.0	$0.5\rho L^{3}(u/2\pi)$
X'_{u}	76.1783 *	-6000.0 *	
X'_{u}	-0.000426	-0.00042	$0.5\rho L^{2}u$
X'_{uu}	-1446.16 *	-1860.436 *	$0.5\rho L^{3}$
X'_{uuu}	-450.1888 *	-272.047 *	
X'_{un}	-39468.78 *	-15155.799 *	
X'_{r}	0.0	0.0	
X'_{ua}	-0.015	-0.0012	$0.5\ \rho_{a}L^{2}u_{a}$
X'_{va}	0.0	0.0	
X'_{vv}	-0.00617	-0.008988	$0.5\rho L^{2}$
X'_{rr}	0.0	0.00018	$0.5\rho L^{4}$
$X'_{\delta\delta}$	-0.00221	-0.000948	$0.5\rho L^{2}u^{2}$
X'_{nn}	7339.8 *	21855.5 *	

* Dimensionalised Coefficient

DERIVATIVE	CAR FERRY HULL	MARINER HULL	DIMENSIONALISING FACTORS
Y'_{a}	0.003418	0.00255	$0.5\rho L^2 u^2$
Y'_{nn}	0.0	2104.307 *	
Y'_{u}	0.0	0.0	
$Y'_{\dot{u}}$	0.0	0.0	
Y'_{v}	-0.0098675	-0.0116	$0.5\rho L^2 u$
$Y'_{\dot{v}}$	-0.007583	-0.00748	$0.5\rho L^3$
Y'_{r}	0.0004926	0.0022	$0.5\rho L^3 u$
$Y'_{\dot{r}}$	-0.0001368	-0.000086	$0.5\rho L^4$
Y'_{ua}	0.0	0.0	
Y'_{va}	-0.0870	-0.0116	$0.5\rho_a L^2 u_a$
Y'_{vvv}	-0.441178	-0.080782	$0.5\rho L^2/u$
Y'_{rvv}	0.022934	0.15356	$0.5\rho L^3/u$
$Y'_{\delta\delta\delta}$	-0.0009569	-0.00082	$0.5\rho L^2 u^2$
$Y'_{\delta vv}$	0.0	0.011896	$0.5\rho L^2$

* Dimensionalised Coefficient

DERIVATIVE	CAR FERRY HULL	MARINER HULL	DIMENSIONALISING FACTORS
N'_{δ}	-0.0016011	-0.001274	$0.5\rho L^3 u^2$
N'_{nn}	0.0	-169291.5	
N'_{u}	0.0	0.0	
N'_{u}	0.0	0.0	
N'_{v}	-0.0043535	-0.002365	$0.5\rho L^3 u$
N'_{v}	-0.000230	-0.000227	$0.5\rho L^4$
N'_{r}	-0.002143	-0.00166	$0.5\rho L^4 u$
N'_{r}	-0.0006952	-0.000437	$0.5\rho L^5$
N'_{ua}	-0.007200	0.0	$0.5\rho_a L^3 u_a$
N'_{va}	-0.002600	-0.002635	$0.5\rho_a L^3 u_a$
N'_{vvv}	-0.0326335	0.016361	$0.5\rho L^3/u$
N'_{rvv}	-0.047235	-0.05483	$0.5\rho L^4/u$
$N'_{\delta\delta\delta}$	0.0007421	0.00041	$0.5\rho L^3 u^2$
$N'_{\delta vv}$	0.0	-0.00489	$0.5\rho L^3$

* Dimensionalised Coefficient

APPENDIX 5

GENERAL DATA FOR MODELS

	URCHIN TRELEVEN VIGILANT	TREMAYNE	HEATHMORE CENTAUR
LENGTH (m)	160.9	150.0	3.419
BEAM (m)	23.17	24.8	0.565
DRAFT (m)	9.07	5.9	0.134
DISPLACEMENT (kg)	17062900.0	14400000.0	166.4
BLOCK COEFFICIENT	0.6	0.64	0.64
PROPELLOR TYPE	RIGHT HAND SINGLE SCREW	TWIN SCREW CONTRA	TWIN SCREW CONTRA
MOMENT OF INERTIA I_z ABOUT MASS CENTRE	36.8115 $*10^9$	24.36395 $*10^9$	149.8937 $*10^9$
RUDDER TIME CONSTANT	2	2	-
ENGINE TIME CONSTANT	2	2	-
SAMPLE TIME (s)	5	5	1

APPENDIX 6

THE COMPUTER PROGRAMS

A 6.1 Mainframe Simulations - Master Segment

To facilitate programming the simulation models were divided into a master segmemt and a series of subroutines. All the mainframe programming was undertaken in FORTRAN IV. The master segment was altered slightly depending upon the desired simulation. The version given in this appendix simulates the passage of a twin screw car ferry into the Port of Plymouth. It was the full-scale non-linear model referred to as Tremayne in the main text. A detailed flow chart is given in Figure A6.1

The following variables are used:-

AK(8,8)	Kalman Filter Gain Matrix
B(8,2)	State Control Matrices
C(8,4)	Disturbance Matrix
DELTO(250)	Actual rudder angle
DELTM(250)	Measured rudder angle
DELTE(250)	Estimated rudder angle
DELTD(250)	Demanded rudder angle
F(8,8)	Continuous Transition Matrix
G(8,6)	Forcing Matrix
H(8,8)	Measurement Matrix
RNO(250), RNM(250)	Actual, measured, estimated

RNE(250), RND(250)	and demanded rudder angles.
PSIO(250), PSIM(250)	Actual, measured, estimated
PSIE(250), PSID(250)	and demanded heading.
Q(8,8), R(2,2)	Weighting matrices used in controller.
RO(250), RM(250),	Actual, measured and
RE(250),	estimated yaw rates
RMINS(250)	Time in Minutes
SDR(8), SDQ(4)	Standard deviation for measurement and disturbance noise
U(2)	Control Vector
USHIP(250), UN(250),	Actual, measured and estimated
UE(250),	components of ship's speed along Fore and Aft line
VSHIP(250), VM(250),	Actual, measured and estimated
VE(250)	lateral ship speeds
XOLD(8), XNEW(8)	Values of state vector at beginning and end of each sample time
XO(250), YO(250)	Actual ship's position
XM(250), YM(250)	Measured position
XE(250), YE(250)	Estimated position
XD(250), YD(250)	Demanded position
ZOLD(8), ZNEW(8)	Measured values of state vector at beginning and end of each sample period

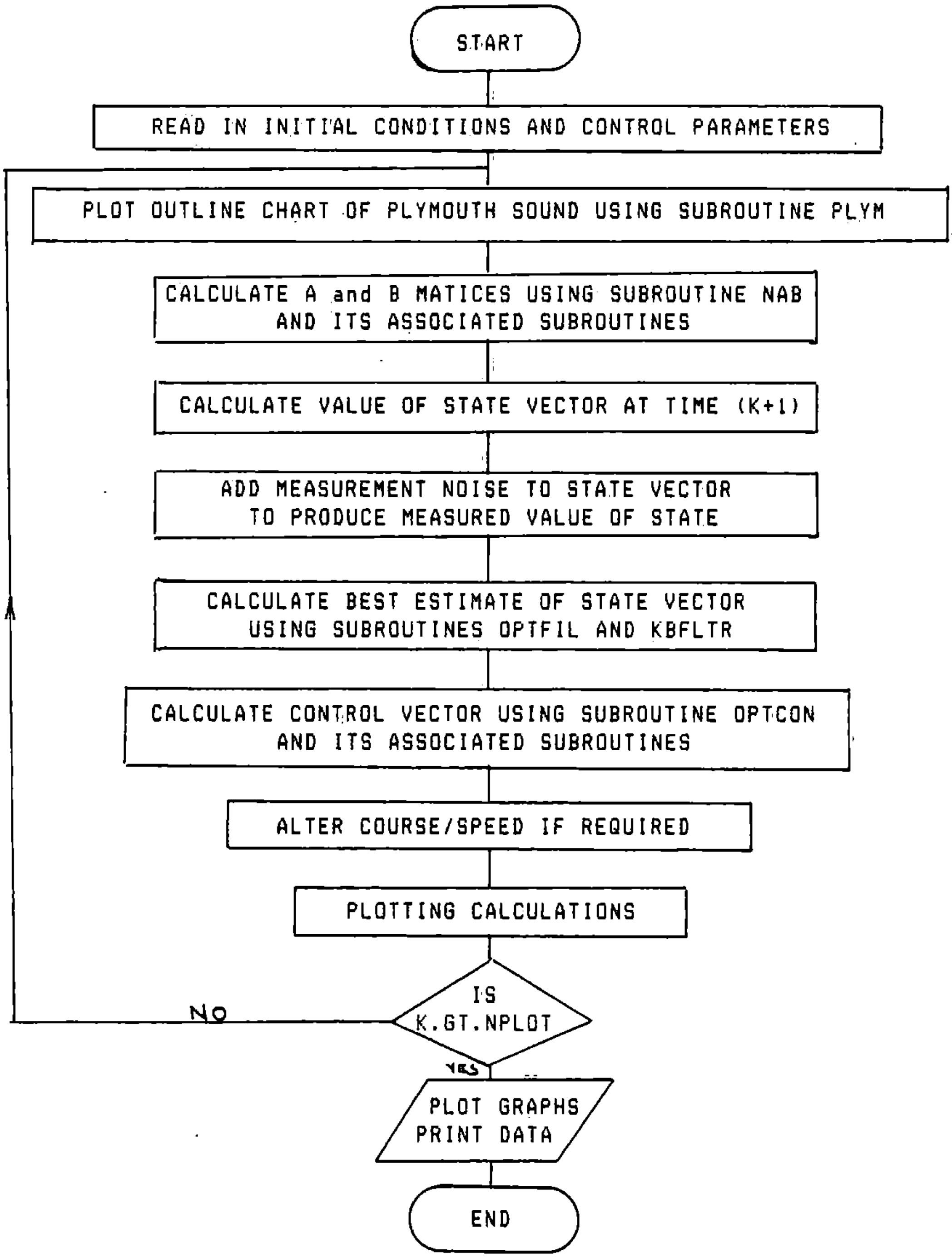

Figure A6.1 Overall Flow Chart

```
C  SHIP OPTIMAL CONTROL SIMULATION PROGRAM SHIP CO-ORDS.....
C          PLUS OPTIMAL FILTER (KALMAN-BUCY)
C              FOR FULL SIZE SHIP
C
C
      REAL*4 A(8,8),AA(8,8),AK(8,8),AXHT(8),AXBU(8),AX(8),
     *       B(8,2),BB(8,2),BBU(8),BU(8),
     *       CWU(8),CC(8,4),C(8,4),
     *       DRUDD(250),DELTO(250),DELTM(250),DELTD(250),
     *       DELTE(250),
     *       F(8,8),
     *       F41X(250),F42X(250),F44X(250),F46X(250),
     *       F48X(250),
     *       F61Y(250),F62Y(250),F64Y(250),F66Y(250),
     *       F68Y(250)
     *       F81N(250),F82N(250),F84N(250),F86N(250),
     *       F88N(250),
     *       G(8,6),GU(8,2),
     *       H(8,8), HXN(8),
     *       PSIO(250),PSIM(250),PSIE(250),PSID(250),
     *       Q(8,8),
     *       RND(250),RNE(250),RNM(250),RNO(250),
     *       RO(250),RE(250),RM(250),RMINS(250),R(2,2),
     *       S(2,8),SDR(8),SDQ(4),
     *       T(250),
     *       U(2),UO(250),UE(250),UM(250),USHIP(250),
     *       UW(200,4),USHID(250),
     *       VO(250),VM(250),VE(250),VSHIP(250),VFOR(2,500),
     *       V(200,8),
     *       W(8,8),WUS(200,4),WP1(8,8),WU(4),WUM(4),
     *       XOLD(8),XNEW(8),XHAT(8),XHAT1(8),XHAT2(8),
     *       XO(250),XD(250),XE(250),XM(250),
     *       YO(250),YD(250),YE(250),YM(250),
     *       ZOLD(8),ZNEW(8),Z1(8),Z2(8),ZDIFF(8),
      REAL KZ(8)
      COMMON RIN(8,500),YOUT(8,250)
C
C PLOT PLYMOUTH SOUND
C
      CALL PLYM(START,DELTA)
C
C
C READ IN CONTROL PARAMETERS
C
      READ(5,101)N,NX,NG,NB,NC,NM,IFIN,MODE,TSAMP
  101 FORMAT(9I5,F10.5)
C
C READ IN IP,IM,& INITIAL VALUE FOR K
C
      IP=NC
      IM=N
      K=1
C
C  CALCULATE STATE TRANSITION MATRIX
C
      CALL MATRED(F,N,N)
```

```
      CALL MATRED(G,N,NG)
      CALL TRNMAC(F,G,AA,BB,CC,N,NG,NB,TSAMP)
      CALL MATRED(Q,N,N)
      CALL MATRED(R,NB,NB)
C
C  READ IN H MATRIX
C
      CALL MATIDN(H,N)
C
C
C XOLD=EXISTING STATE
C XNEW=PREDICTED STATE AFTER TSAMP SECONDS
C CONVENTION:  XOLD(1)=DELTA    XOLD(2)=NA       XOLD(3)=XO
C              XOLD(4)=U        XOLD(5)=YO       XOLD(6)=V
C              XOLD(7)=PSI      XOLD(8)=R
C
C
C
C INITIAL CONDITIONS FOR STATES AND BEST ESTIMATE OF STATES
C
      CALL MATRED(XOLD,N,NX)
      CALL MATEQL(XHAT,XOLD,N,NX)
C
C XO,YO,UO,VO=POSITION AND VELOCITY RELATIVE TO REFERENCE
C CO-ORDINATE SYSTEM
C
C INITIAL POSITION OF SHIP ON REFERENCE COORDINATE SYSTEM
C
      READ(5,103) XO(1),YO(1),PSIO(1),UO(1),VO(1),RO(1)
 103  FORMAT (6F10.5)
C
C  DETERMINE RICCATI FEEDBACK MATRIX AND COMMAND MATRIX
C
      CALL RICAL(F,G,GU,AA,BB,Q,R,S,W,XD,YD,VFOR,TSAMP
     &,N,NB,NM,NN,IFIN)
      NPLOT=175
      NPLOT1=NPLOT+1
      NPLOT2=NPLOT+2
      T(1)=0.0
      UVEL=SQRT((XOLD(4)**2)+(XOLD(6)**2))
C
C  READ IN DISTURBANCE VECTOR WITH STANDARD DEVIATIONS
C   WU(1)=UCURRENT(MEAN)
C   WU(2)=VECTOR ANGLE ALPHA(MEAN)
C   WU(3)=UAIR(MEAN)
C   WU(4)=VECTOR ANGLE PHI(MEAN)
C
      CALL MATRED(WU,NC,NX)
      CALL MATRED(WUS,200,4,400)
C
C CORRECTION FACTORS FOR DISTURBANCE NOISE
C
      CD1=1.0
      CD2=CD1
      CD3=1.0
      CD4=CD3
```

```
C
C DISTURBANCE NOISE STANDARD DEVIATIONS
C
      SDQ(1)=0.2*CD1
      SDQ(2)=0.35*CD2
      SDQ(3)=3.0*CD3
      SDQ(4)=0.35*CD4
C
C CORRECTION FACTORS FOR MEASUREMENT NOISE
C
      C1=1.0
      C2=1.0
      C3=1.0
      C4=1.0
      C5=1.0
      C6=1.0
      C7=1.0
      C8=1.0
C
C READ IN MEASUREMENT NOISE WITH STANDARD DEVIATIONS
C
      CALL MATRED(V,200,8,400)
C
      SDR(1)=0.002*C1
      SDR(2)=0.002*C2
      SDR(3)=25.0*C3
      SDR(4)=0.25*C4
      SDR(5)=25.0*C5
      SDR(6)=0.25*C6
      SDR(7)=0.017*C7
      SDR(8)=0.00399*C8
C
C  INITIAL CONDITIONS FOR MEASURED VALUES OF STATE VECTOR
C
      ZOLD(1)=XOLD(1)+V(1,1)*C1
      ZOLD(2)=XOLD(2)+V(1,2)*C2
      ZOLD(3)=XOLD(3)+V(1,3)*C3
      ZOLD(4)=XOLD(4)+V(1,4)*C4
      ZOLD(5)=XOLD(5)+V(1,5)*C5
      ZOLD(6)=XOLD(6)+V(1,6)*C6
      ZOLD(7)=XOLD(7)+V(1,7)*C7
      ZOLD(8)=XOLD(8)+V(1,8)*C8
C
C SET CONSTANTS TO CONVERT SCALES
C
      RADCON=57.2957795
      REVCON=30/3.14159
C
C
      XM(1)=XO(1)
      YM(1)=YO(1)
      XE(1)=XO(1)
      YE(1)=YO(1)
      PSIO(1)=XOLD(7)*RADCON
      PSIM(1)=ZOLD(7)*RADCON
      PSIE(1)=XOLD(7)*RADCON
```

```
      RO(1)=XOLD(8)*RADCON
      RM(1)=ZOLD(8)*RADCON
      RE(1)=XOLD(8)*RADCON
      USHIP(1)=XOLD(4)
      USHID(1)=RIN(4,1)
      UM(1)=ZOLD(4)
      UE(1)=XHAT(4)
      VSHIP(1)=XOLD(6)
      VM(1)=ZOLD(6)
      VE(1)=XHAT2(6)
      RNO(1)=XOLD(2)*REVCON
      RNM(1)=ZOLD(2)*REVCON
      RNE(1)=XHAT(2)*REVCON
      RND(1)=U(2)*REVCON
      PSID(1)=RIN(7,1)*RADCON
      RMINS(1)=0.0
      T(1)=0.0
C
C
      UCURM=WU(1)
      ALPHM =WU(2)
      UAIRM=WU(3)
      PHIM=WU(4)
C
C   START SIMULATION
C
      DO 10 K=1,NPLOT
      KK=(K/50)*50
C
      UVEL=SQRT((XOLD(4)**2)+(XOLD(6)**2))
C
C   COMPONENTS OF UCURRENT AND UAIR IN X AND Y DIRECTIONS
C
      GAMMA=XOLD(7)-((ALPHM+WUS(K,2))*CD2)+1.570796
      WU(1)=(UCURM+WUS(K,1))*SIN(GAMMA)*CD1
      UW(K,1)=WU(1)
      WUM(1)=UCURM*SIN(GAMMA)*CD1
      WU(2)=(UCURM+WUS(K,1))*COS(GAMMA)*CD1
      UW(K,2)=WU(2)
      WUM(2)=UCURM*COS(GAMMA)*CD1
      ANG=((PHIM+WUS(K,4))*CD4)-XOLD(7)
      WU(3)=(UAIRM+WUS(K,3))*COS(ANG)*CD3+XOLD(4)
      UW(K,3)=WU(3)
      WUM(3)=UAIRM*COS(ANG)*CD3+XOLD(4)
      WU(4)=(UAIRM+WUS(K,3))*SIN(ANG)*CD3+XOLD(6)
      UW(K,4)=WU(4)
      WUM(4)=UAIRM*SIN(ANG)*CD3+XOLD(6)
      UA=SQRT(WU(3)**2+WU(4)**2)
C
C   CALCULATE THE SYSTEM DISCRETE-TIME MATRICES A AND B
C
      CALL NAB(A,B,C,N,NX,NG,NB,NC,IFIN,K,LOOP,T,WUM,
     &TSAMP,XOLD,UVEL,UA,F41X,F42X,F44X,F46X,F48X,WU,UD1,UD2,
     &F61Y,F62Y,F64Y,F66Y,F68Y,F81N,F82N,F84N,F86N,F88N)
C
C
```

```
C  COMPUTE OPTIMAL CONTROL LAW
C
      CALL OPTCON(XHAT,K,S,VFOR,UD1,UD2,U,N,NB,NX,NN,TSAMP
     *,DRUDD,MODE,ABCER,CERROR,XE,YE,RIN7,YI,XI,XHAT5)
C
C SIMPLE P+D HEADING CONTROLLER
C
C
C CALCULATE X(K+1)=A*X(K)+B*U(K)+C*W(K) USING SHIP AXES
C
      CALL MATMUL(AX,A,XOLD,N,N,NX)
      CALL MATMUL(BU,B,U,N,NB,NX)
      CALL MATADD(AXBU,AX,BU,N,NX)
      CALL MATMUL(CWU,C,WU,N,NC,NX)
      CALL MATADD(XNEW,AXBU,CWU,N,NX)
C
C  CALCULATE Z(K+1)=H(K+1)*X(K+1)+V(K+1) USING SHIP AXES
C
      CALL MATMUL(HXN,H,XNEW,N,N,NX)
      ZNEW(8)=HXN(8)+V(K+1,8)*C8
      ZNEW(7)=HXN(7)+(V(K+1,7)*C7)
      ZNEW(6)=HXN(6)+V(K+1,6)*C6
      ZNEW(4)=HXN(4)+V(K+1,4)*C4
      BETA=ATAN(ZNEW(6)/ZNEW(4))
      ZNEW(5)=HXN(5)+(V(K+1,5)*C5)
      ZNEW(3)=HXN(3)+(V(K+1,3)*C3)
      ZNEW(2)=HXN(2)+V(K+1,2)*C2
      ZNEW(1)=HXN(1)+V(K+1,1)*C1
      CALL OPTFIL(AA,BB,CC,BU,H,U,Z,N,NB,NC,NX,IP,IM,
     *XHAT2,XHAT,XHAT1,K,CERROR,V,ABCER,RADCON)

C
C CALCULATE SHIP'S ACTUAL POSITION & VELOCITY
C
      XDELT=XNEW(3)-XOLD(3)
      YDELT=XNEW(5)-XOLD(5)
      XDELM=ZNEW(3)-ZOLD(3)
      YDELM=ZNEW(5)-ZOLD(5)
      XDELE=XHAT2(3)-XHAT(3)
      YDELE=XHAT2(5)-XHAT(5)
      XO(K+1)=XO(K)+XDELT*COS(XOLD(7))-YDELT*SIN(XOLD(7))
      YO(K+1)=YO(K)+YDELT*COS(XOLD(7))+XDELT*SIN(XOLD(7))
      XM(K+1)=XM(K)+XDELM*COS(ZOLD(7))-YDELM*SIN(ZOLD(7))
      YM(K+1)=YM(K)+YDELM*COS(ZOLD(7))+XDELM*SIN(ZOLD(7))
      XE(K+1)=XE(K)+XDELE*COS(XHAT(7))-YDELE*SIN(XHAT(7))
      YE(K+1)=YE(K)+YDELE*COS(XHAT(7))+XDELE*SIN(XHAT(7))
      PSIO(K+1)=XNEW(7)*RADCON
      PSIM(K+1)=ZNEW(7)*RADCON
      PSIE(K+1)=XHAT2(7)*RADCON
      UO(K+1)=XNEW(4)*COS(XNEW(7))-XNEW(6)*SIN(XNEW(7))
      VO(K+1)=XNEW(6)*COS(XNEW(7))+XNEW(4)*SIN(XNEW(7))
      RO(K+1)=XNEW(8)*RADCON
      RM(K+1)=ZNEW(8)*RADCON
      RE(K+1)=XHAT2(8)*RADCON
```

```
      DRUDD(K)=U(1)
      DELTD(K)=U(1)*RADCON
      DELTO(K)=XOLD(1)*RADCON
      DELTM(K+1)=ZNEW(1)*RADCON
      DELTE(K+1)=XHAT2(1)*RADCON
      USHIP(K)=XOLD(4)
      USHID(K)=RIN(4,K)
      UM(K+1)=ZNEW(4)
      UE(K+1)=XHAT2(4)
      VSHIP(K)=XOLD(6)
      VM(K+1)=ZNEW(6)
      VE(K+1)=XHAT2(6)
      RNO(K)=(XOLD(2)*REVCON)
      RNM(K+1)=(ZNEW(2)*REVCON)
      RNE(K+1)=(XHAT2(2)*REVCON)
      RND(K)   =(U(2)*REVCON)
      PSID(K)=RIN(7,K)*RADCON
      RMINS(K)=T(K)/60.0
      T(K+1)=T(K)+TSAMP
C
C SPECIFY OUTPUT VECTOR AND UPDATE STATE VECTOR
C
      DO 20 I=1,8
      YOUT(I,K)=XOLD(I)
      XOLD(I)=XNEW(I)
      XHAT(I)=XHAT2(I)
      ZOLD(I)=ZNEW(I)
   20 CONTINUE
   10 CONTINUE
C
C END OF SIMULATION
C

C
C PLOT SHIP TRACK
C
      XD(NPLOT1)=0.0
      XD(NPLOT2)=200.0
      YD(NPLOT1)=0.0
      YD(NPLOT2)=200.0
      XO(NPLOT1)=0.0
      XO(NPLOT2)=200.0
      YO(NPLOT1)=0.0
      YO(NPLOT2)=200.0
      XM(NPLOT1)=0.0
      XM(NPLOT2)=200.0
      YM(NPLOT1)=0.0
      YM(NPLOT2)=200.0
      XE(NPLOT1)=0.0
      XE(NPLOT2)=200.0
      YE(NPLOT1)=0.0
      YE(NPLOT2)=200.0
C
      CALL NEWPEN(1)
      CALL LINE(YD,XD,NPLOT,1,12,2)
      CALL LINE(YM,XM,NPLOT,1,0,0)
```

```
      CALL NEWPEN(2)
      CALL LINE(YO,XO,NPLOT,1,12,3)
      CALL NEWPEN(3)
      CALL LINE(YE,XE,NPLOT,1,12,1)
      CALL NEWPEN(1)
C
C PLOT ACTUAL RUDDER ANGLE
C
      CALL PLOT(50.0,1.0,-3)
      CALL SCALE(RMINS,20.0,NPLOT,1)
      CALL SCALE(DELTM,10.0,NPLOT,1)
      DELTO(NPLOT1)=DELTM(NPLOT1)
      DELTO(NPLOT2)=DELTM(NPLOT2)
      DELTE(NPLOT1)=DELTM(NPLOT1)
      DELTE(NPLOT2)=DELTM(NPLOT2)
      CALL AXIS(0.0,0.0,15HTIME IN MINUTES,-15,
     &20.0,0.0,RMINS(NPLOT1),RMINS(NPLOT2))
      CALL AXIS(0.0,0.0,23HRUDDER ANGLE IN DEGREES,+23,
     &10.0,90.0,DELTM(NPLOT1),DELTM(NPLOT2))
      CALL LINE(RMINS,DELTM,NPLOT,1,0,0)
      CALL NEWPEN(3)
      CALL LINE(RMINS,DELTE,NPLOT,1,10,3)
      CALL NEWPEN(2)
      CALL LINE(RMINS,DELTO,NPLOT,1,10,1)
      CALL NEWPEN(1)
      CALL SYMBOL(2.0,9.5,0.25,12HRUDDER ANGLE,0.0,12)
C
C PLOT DEMANDED RUDDER ANGLE
C
      CALL PLOT(0.0,15.0,-3)
      CALL SCALE(RMINS,20.0,NPLOT,1)
      CALL SCALE(DELTD,10.0,NPLOT,1)
      CALL AXIS(0.0,0.0,15HTIME IN MINUTES,-15,
     &20.0,0.0,RMINS(NPLOT1),RMINS(NPLOT2))
      CALL AXIS(0.0,0.0,23HRUDDER ANGLE IN DEGREES,+23,
     &10.0,90.0,DELTD(NPLOT1),DELTD(NPLOT2))
      CALL SCALE(DELTD,10.0,NPLOT,1)
      CALL LINE(RMINS,DELTD,NPLOT,1,10,5)
      CALL SYMBOL(2.0,9.5,0.25,21HDEMANDED RUDDER ANGLE,
     &0.0,21)
C
C PLOT LATERAL SPEED
C
      CALL PLOT(25.0,-15.0,-3)
      CALL SCALE(RMINS,20.0,NPLOT,1)
      CALL SCALE(VE,10.0,NPLOT,1)
      VSHIP(NPLOT1)=VE(NPLOT1)
      VSHIP(NPLOT2)=VE(NPLOT2)
      VM(NPLOT1)=VE(NPLOT1)
      VM(NPLOT2)=VE(NPLOT2)
      CALL AXIS(0.0,0.0,15HTIME IN MINUTES,-15,
     &20.0,0.0,RMINS(NPLOT1),RMINS(NPLOT2))
      CALL AXIS(0.0,0.0,22HLATERAL SPEED IN M/SEC,+22,
     &10.0,90.0,VM(NPLOT1),VM(NPLOT2))
      CALL LINE(RMINS,VM,NPLOT,1,0,0)
      CALL NEWPEN(3)
```

```
      CALL LINE(RMINS, VE, NPLOT, 1, 10, 3)
      CALL NEWPEN(2)
      CALL LINE(RMINS, VSHIP, NPLOT, 1, 10, 1)
      CALL NEWPEN(1)
      CALL SYMBOL(2.0, 9.5, 0.25, 21HLATERAL SPEED OF SHIP, 0.0, 21)
C
C PLOT YAW RATE
C
      CALL PLOT(0.0, 15.0, -3)
      CALL SCALE(RMINS, 20.0, NPLOT, 1)
      CALL SCALE(RM, 10.0, NPLOT, 1)
      RO(NPLOT1)=RM(NPLOT1)
      RO(NPLOT2)=RM(NPLOT2)
      RE(NPLOT1)=RM(NPLOT1)
      RE(NPLOT2)=RM(NPLOT2)
      CALL AXIS(0.0, 0.0, 15HTIME IN MINUTES, -15,
     &20.0, 0.0, RMINS(NPLOT1), RMINS(NPLOT2))
      CALL AXIS(0.0, 0.0, 22HYAW RATE IN DEG/SECOND, +22,
     &10.0, 90.0, RM(NPLOT1), RM(NPLOT2))
      CALL LINE(RMINS, RM, NPLOT, 1, 0, 0)
      CALL NEWPEN(3)
      CALL LINE(RMINS, RE, NPLOT, 1, 10, 3)
      CALL NEWPEN(2)
      CALL LINE(RMINS, RO, NPLOT, 1, 10, 1)
      CALL NEWPEN(1)
      CALL SYMBOL(2.0, 9.5, 0.25, 8HYAW RATE, 0.0, 8)
C
C PLOT COURSE ANGLE
C
      CALL PLOT(25.0, -15.0, -3)
      CALL SCALE(RMINS, 20.0, NPLOT, 1)
      CALL SCALE(PSIM, 10.0, NPLOT, 1)
      PSIO(NPLOT1)=PSIM(NPLOT1)
      PSIO(NPLOT2)=PSIM(NPLOT2)
      PSIE(NPLOT1)=PSIM(NPLOT1)
      PSIE(NPLOT2)=PSIM(NPLOT2)
      PSID(NPLOT1)=PSIM(NPLOT1)
      PSID(NPLOT2)=PSIM(NPLOT2)
      CALL AXIS(0.0, 0.0, 15HTIME IN MINUTES, -15,
     &20.0, 0.0, RMINS(NPLOT1), RMINS(NPLOT2))
      CALL AXIS(0.0, 0.0, 23HCOURSE ANGLE IN DEGREES, +23,
     &10.0, 90.0, PSIM(NPLOT1), PSIM(NPLOT2))
      CALL LINE(RMINS, PSIM, NPLOT, 1, 0, 0)
      CALL LINE(RMINS, PSID, NPLOT, 1, 10, 2)
      CALL NEWPEN(3)
      CALL LINE(RMINS, PSIE, NPLOT, 1, 10, 3)
      CALL NEWPEN(2)
      CALL LINE(RMINS, PSIO, NPLOT, 1, 10, 1)
      CALL NEWPEN(1)
      CALL SYMBOL(2.0, 9.5, 0.25, 12HCOURSE ANGLE, 0.0, 12)
C
C PLOT F MATRIX VARIATION WITH TIME
C
C X ELEMENTS
C
```

```
      CALL PLOT(0.0,15.0,-3)
      CALL SCALE(RMINS,20.0,NPLOT,1)
      CALL SCALE(F41X,10.0,NPLOT,1)
      CALL SCALE(F42X,10.0,NPLOT,1)
      CALL SCALE(F44X,10.0,NPLOT,1)
      CALL SCALE(F46X,10.0,NPLOT,1)
      CALL SCALE(F48X,10.0,NPLOT,1)
      CALL AXIS(0.0,0.0,15HTIME IN MINUTES,-15,
     &20.0,0.0,RMINS(NPLOT1),RMINS(NPLOT2))
      CALL AXIS(0.0,0.0,19HF MATRIX X ELEMENTS,+19,
     &10.0,90.0,F41X(NPLOT1),F41X(NPLOT2))
      CALL LINE(RMINS,F41X,NPLOT,1,10,1)
      CALL LINE(RMINS,F42X,NPLOT,1,10,2)
      CALL LINE(RMINS,F44X,NPLOT,1,10,4)
      CALL LINE(RMINS,F46X,NPLOT,1,10,5)
      CALL LINE(RMINS,F48X,NPLOT,1,10,6)
      CALL SYMBOL(2.0,9.5,0.25,19HF MATRIX X ELEMENTS,0.0,19)
C
C PLOT X AGAINST TIME
C
      CALL PLOT(25.0,-15.0,-3)
      CALL SCALE(RMINS,20.0,NPLOT,1)
      CALL SCALE(XM,10.0,NPLOT,1)
      XO(NPLOT1)=XM(NPLOT1)
      XO(NPLOT2)=XM(NPLOT2)
      XE(NPLOT1)=XM(NPLOT1)
      XE(NPLOT2)=XM(NPLOT2)
      XD(NPLOT1)=XM(NPLOT1)
      XD(NPLOT2)=XM(NPLOT2)
      CALL AXIS(0.0,0.0,15HTIME IN MINUTES,-15,
     &20.0,0.0,RMINS(NPLOT1),RMINS(NPLOT2))
      CALL AXIS(0.0,0.0,14HX CO-ORDINATES,+14,
     &10.0,90.0,XM(NPLOT1),XM(NPLOT2))
      CALL LINE(RMINS,XM,NPLOT,1,0,0)
      CALL LINE(RMINS,XD,NPLOT,1,10,2)
      CALL NEWPEN(3)
      CALL LINE(RMINS,XE,NPLOT,1,10,3)
      CALL NEWPEN(2)
      CALL LINE(RMINS,XO,NPLOT,1,10,1)
      CALL NEWPEN(1)
      CALL SYMBOL(2.0,9.5,0.25,14HX CO-ORDINATES,0.0,14)
C
C PLOT Y AGAINST TIME
C
      CALL PLOT(0.0,15.0,-3)
      CALL SCALE(RMINS,20.0,NPLOT,1)
      CALL SCALE(YM,10.0,NPLOT,1)
      YO(NPLOT1)=YM(NPLOT1)
      YO(NPLOT2)=YM(NPLOT2)
      YE(NPLOT1)=YM(NPLOT1)
      YE(NPLOT2)=YM(NPLOT2)
      YD(NPLOT1)=YM(NPLOT1)
      YD(NPLOT2)=YM(NPLOT2)
      CALL AXIS(0.0,0.0,15HTIME IN MINUTES,-15,
     &20.0,0.0,RMINS(NPLOT1),RMINS(NPLOT2))
      CALL AXIS(0.0,0.0,14HY CO-ORDINATES,+14,
```

```
     &10.0,90.0,YM(NPLOT1),YM(NPLOT2))
      CALL LINE(RMINS,YM,NPLOT,1,10,1)
      CALL LINE(RMINS,YD,NPLOT,1,10,2)
      CALL NEWPEN(3)
      CALL LINE(RMINS,YE,NPLOT,1,10,3)
      CALL NEWPEN(2)
      CALL LINE(RMINS,YO,NPLOT,1,10,1)
      CALL NEWPEN(1)
      CALL SYMBOL(2.0,9.5,0.25,14HY CO-ORDINATES,0.0,14)
C
C PLOT FORWARD SPEED
C
      CALL PLOT(25.0,-15.0,-3)
      CALL SCALE(RMINS,20.0,NPLOT,1)
      CALL SCALE(UM,10.0,NPLOT,1)
      USHIP(NPLOT1)=UM(NPLOT1)
      USHIP(NPLOT2)=UM(NPLOT2)
      UE(NPLOT1)=UM(NPLOT1)
      UE(NPLOT2)=UM(NPLOT2)
      USHID(NPLOT1)=UM(NPLOT1)
      USHID(NPLOT2)=UM(NPLOT2)
      CALL AXIS(0.0,0.0,15HTIME IN MINUTES,-15,
     &20.0,0.0,RMINS(NPLOT1),RMINS(NPLOT2))
      CALL AXIS(0.0,0.0,19HFORWARD SPEED (M/S),+19,
     &10.0,90.0,UM(NPLOT1),UM(NPLOT2))
      CALL LINE(RMINS,UM,NPLOT,1,0,0)
      CALL LINE(RMINS,USHID,NPLOT,1,10,1)
      CALL NEWPEN(3)
      CALL LINE(RMINS,UE,NPLOT,1,10,3)
      CALL NEWPEN(2)
      CALL LINE(RMINS,USHIP,NPLOT,1,10,1)
      CALL NEWPEN(1)
      CALL SYMBOL(2.0,9.5,0.25,13HFORWARD SPEED,0.0,13)
C
C
      CALL PLOT(12.0,0.0,999)
C
      CALL EXIT
      END
```

A 6.2 Subroutine PLYM

At the beginning of the master segment this subroutine is called to draw an outline chart of Plymouth Sound, including the main navigational marks and buoys.

Variables are:-

START, DELTA   Initial and incremental values for graph plotting

A 6.3 Matrix Package

Subroutine MATADD was used to add a substract two matrices, to produce the identity matrix, MATINV to invert a matrix and MATMUL to multiply two matrices together, MATONE produces a one's matrix whilst MATPRN is used to print out data in rows and columns, with MATRED used to read in data in matrix form, whilst MATSCL is used to multiply a matrix by a scalar, MATRNS to transpose a matrix and MATZER to produce a matrix of 0's.

```
C
C SUBROUTINE TO PLOT PLYMOUTH SOUND
C
      SUBROUTINE PLYM(START,DELTA)
C
      DIMENSION FF1(152),FF2(152),FF3(152),FF4(152),FF5(12),FF6(12)

      DIMENSION FF7(152),FF8(152),TR1(4),TR2(4),FF9(152),FF10(152)

      DIMENSION STX(12),STY(12),PTX(12),PTY(12)
      DIMENSION TR3(4),TR4(4),TR5(4),TR6(4),TR7(4),TR8(4)
      DIMENSION XTOP(4),YTOP(4),XSIDE(4),YSIDE(4)
      REAL LH1(7),LH2(7)
C
C ************ CHECKING A **************
C
C
C ***************************************
C
C
C THIS SUBROUTINE PLOTS PLYMOUTH SOUND
C
      CALL PLOTS(0,0,16)
      CALL FACTOR(0.5)
C
C START IS THE ORIGIN, DELTA IS THE NO OF DATA UNITS   PER CM.
 OF AXIS
C
      START=0.00
      DELTA=200.0
C
C READ IN CO-ORDS FOR WESTERN SIDE OF PLYMOUTH SOUND
C
      READ(5,501)(FF1(M),FF2(M),M=1,104)
 501  FORMAT(10F8.2)
C
C ************** CHECKING B ****************************
C
C
C ******************************************************
C
C
C READ IN CO-ORDS FOR EASTERN SIDE OF PLYMOUTH SOUND
C
      READ(5,502)(FF3(N),FF4(N),N=1,134)
 502  FORMAT(10F8.2)
C
C ****************
C     ***********READ IN CO-ORD FOR NORTHCOAST1*************
C
C
      READ(5,503)(FF7(N),FF8(N),N=1,28)
 503  FORMAT(10F8.2)
C ************** CHECKING Z****************
C ****************************************
C
```

```
C  *****
C **********NORTHCOAST2 *************
C
C
C
      READ (5,503)(FF9(N),FF10(N),N=1,8)
C **************** CHECKING 3 **********************
C
C
C
C **************************************************
C
C OPEN GRAPH PLOTTER FILE
C
      CALL PLOT(0.0,1.0,-3)
      CALL AXIS(0.0,0.0,18HX-AXIS      200.00M,-30,37.3,0.0,
     *START,DELTA)
      CALL AXIS(0.0,0.0,18HY-AXIS      200.00M,+30,25.9,90.0,
     *START,DELTA)
C ****** BOUNDARY DRAWING  ************

C ****  THIS PLOTS THE TOP BOUNDARY    ****
C
      XTOP(1)=0.0
      YTOP(1)=5180.0
      XTOP(2)=7460.0
      YTOP(2)=5180.0
      XTOP(3)=START
      YTOP(3)=START
      XTOP(4)=DELTA
      YTOP(4)=DELTA
      CALL LINE(XTOP,YTOP,2,1,0,0)
C
C ****   THIS PLOTS THE RIGHT SIDE BOUNDARY    *******
C
      XSIDE(1)=7460.0
      YSIDE(1)=5180.0
      XSIDE(2)=7460.0
      YSIDE(2)=0.0
      XSIDE(3)=START
      YSIDE(3)=START
      XSIDE(4)=DELTA
      YSIDE(4)=DELTA
      CALL LINE(XSIDE,YSIDE,2,1,0,0)
C
C *************** END BOUNDARY DRAWING *****************
C
      CALL SYMBOL(1.0,24.9,0.5,14HPLYMOUTH SOUND,0.0,14)

C
C
C ***************** CHECKING 4 ********************
C
C
C ***************************************************
C
```

```
C THIS PLOTS THE WESTERN SIDE OF PLYMOUTH SOUND
C
      FF1(105)=START
      FF2(105)=START
      FF1(106)=DELTA
      FF2(106)=DELTA
      CALL LINE(FF1,FF2,104,1,0,0)
C ****************** CHECKING 5 *********************
C
C
C ****************************************************
C
C THIS PLOTS THE EASTERN SIDE OF PLYMOUTH SOUND
C
      FF3(135)=START
      FF4(135)=START
      FF3(136)=DELTA
      FF4(136)=DELTA
      CALL LINE(FF3,FF4,134,1,0,0)
C ************** CHECKING 6 ***************************
C
C
C *****************************************************
C
C *******    THIS PLOTS NORTHCOAST1&2   *********
C
C
      FF7(29)=START
      FF8(29)=START
      FF7(30)=DELTA
      FF8(30)=DELTA
      CALL LINE(FF7,FF8,28,1,0,0)
C **************** CHECKING 7 ************************
C
C
C ****************************************************
      FF9(9)=START
      FF10(9)=START
      FF9(10)=DELTA
      FF10(10)=DELTA
      CALL LINE(FF9,FF10,8,1,0,0)
C **************** CHECKING 8 ************************
C
C
C ****************************************************
C
C THIS PLOTS THE BREAKWATER
C
      READ(5,503)(FF5(I),FF6(I),I=1,8)
      FF5(9)=START
      FF6(9)=START
      FF5(10)=DELTA
      FF6(10)=DELTA
      CALL LINE(FF5,FF6,8,1,0,0)
C **************** CHECKING 9 ************************
C
```

```
C
C *****************************************************
C
C THIS PLOTS DRAKES ISLAND
C
      READ(5,504)(FF7(M),FF8(M),M=1,50)
 504  FORMAT(10F8.2)
      FF7(51)=START
      FF8(51)=START
      FF7(52)=DELTA
      FF8(52)=DELTA
      CALL LINE(FF7,FF8,50,1,0,0)
C Z*************** CHECKING 99 ***********************
C
C
C *****************************************************
C
C THIS PLOTS STARBOARD HAND BUOYS
C
      READ(5,505)(STX(K),STY(K),K=1,6)
 505  FORMAT(10F8.2)
      CALL NEWPEN(2)
      STX(7)=START
      STY(7)=START
      STX(8)=DELTA
      STY(8)=DELTA
      CALL LINE(STX,STY,6,1,-1,1)
C **************** CHECKING 10 *******************
C
C
C ***************************************************
C
C THIS PLOTS THE PORT HAND BUOYS
C
      READ(5,506)(PTX(J),PTY(J),J=1,5)
 506  FORMAT(10F8.2)
      PTX(6)=START
      PTY(6)=START
      PTX(7)=DELTA
      PTY(7)=DELTA
      CALL NEWPEN(3)
      CALL LINE(PTX,PTY,5,1,-1,2)
C **************** CHECKING 11 *****************
C
C
C ************************************************
C
C THIS PLOTS POSITIONS OF LIGHTS
C
      READ(5,507)(LH1(L),LH2(L),L=1,4)
 507  FORMAT(10F8.2)
      LH1(5)=START
      LH2(5)=START
      LH1(6)=DELTA
      LH2(6)=DELTA
      CALL LINE(LH1,LH2,4,1,-1,14)
```

```
C *************** CHECKING 12 ********************
C
C
C ************************************************
C
C PLOT RECOMMENDED TRACK FOR DEEP DRAUGHT VESSELS
C
      RETURN
      END
```

```
      SUBROUTINE MATADD(A,B,C,N,M,NN)
C
C MATADD A=B+C
C
C N IS THE NUMBER OF ROWS IN B AND C
C M IS THE NUMBER OF COLUMNS IN B AND C
C
      REAL*4 A(N,M),B(N,M),C(N,M)
      DO 10 I=1,N
      DO 10 J=1,M
      A(I,J)=B(I,J)+C(I,J)
   10 CONTINUE
      RETURN
      END


      SUBROUTINE MATEQL(A,B,N,M,NN)
C
C MATEQL A=B
C
C N IS THE NUMBER OF ROWS
C M IS THE NUMBER OF COLUMNS
C
      REAL*4 A(N,M),B(N,M)
      DO 10 I=1,N
      DO 10 J=1,M
   10 A(I,J)=B(I,J)
      RETURN
      END


      SUBROUTINE MATIDN(A,N,NN)
C
C MATIDN PRODUCES A UNITY MATRIX A
C
C N IS THE NUMBER OF ROWS AND COLUMNS
C
      REAL*4 A(N,N)
      DO 10 I=1,N
      DO 10 J=1,N
      A(I,J)=0.0
   10 CONTINUE
      DO 20 I=1,N
      A(I,I)=1.0
   20 CONTINUE
      RETURN
      END
```

```
      SUBROUTINE MATINV(A,N,NA,NN)
      REAL*4 A(NA,N),PIVOT(20),IPIVOT(20),INDEX(20,2)
      EQUIVALENCE (IROW,JROW),(ICOLUM,JCOLUM),(AMAX,T,SWAP)
      IF(N-1)10,5,10
    5 AT=A(1,1)
      A(1,1)=1./AT
      RETURN
   10 DETERM=1.0
   15 DO 20 J=1,N
   20 IPIVOT(J)=0
   30 DO 550 I=1,N
   40 AMAX=0.0
   45 DO 105 J=1,N
   50 IF(IPIVOT(J)-1)60,105,60
   60 DO 100 K=1,N
   70 IF(IPIVOT(K)-1)80,100,740
   80 IF(ABS(AMAX)-ABS(A(J,K)))85,100,100
   85 IROW=J
   90 ICOLUM=K
   95 AMAX=A(J,K)
  100 CONTINUE
  105 CONTINUE
  110 IPIVOT(ICOLUM)=IPIVOT(ICOLUM)+1
  130 IF(IROW-ICOLUM)140,260,140
  140 DETERM=-DETERM
  150 DO 200 L=1,N
  160 SWAP=A(IROW,L)
  170 A(IROW,L)=A(ICOLUM,L)
  200 A(ICOLUM,L)=SWAP
  260 INDEX(I,1)=IROW
  270 INDEX(I,2)=ICOLUM
  310 PIVOT(I)=A(ICOLUM,ICOLUM)
  320 DETERM=-DETERM*PIVOT(I)
  330 A(ICOLUM,ICOLUM)=1.0
  340 DO 350 L=1,N
  350 A(ICOLUM,L)=A(ICOLUM,L)/PIVOT(I)
  380 DO 550 L1=1,N
  390 IF(L1-ICOLUM)400,550,400
  400 T=A(L1,ICOLUM)
  420 A(L1,ICOLUM)=0.0
  430 DO 450 L=1,N
  450 A(L1,L)=A(L1,L)-A(ICOLUM,L)*T
  550 CONTINUE
  600 DO 710 I=1,N
  610 L=N+1-I
  620 IF(INDEX(L,1)-INDEX(L,2))630,710,630
  630 JROW=INDEX(L,1)
  640 JCOLUM=INDEX(L,2)
  650 DO 700 K=1,N
  660 SWAP=A(K,JROW)
  670 A(K,JROW)=A(K,JCOLUM)
  700 A(K,JCOLUM)=SWAP
  710 CONTINUE
  740 RETURN
      END
```

```
      SUBROUTINE MATMUL(A,B,C,N,M,L,NN)
C
C MATMUL A=B*C
C
C N IS NUMBER OF ROWS IN B
C M IS NUMBER OF COLUMNS IN B AND ROWS IN C
C L IS NUMBER OF COLUMNS IN C
C
      REAL*4 A(N,L),B(N,M),C(M,L)
      DO 10 I=1,N
      DO 10 K=1,L
      A(I,K)=0.0
      DO 10 J=1,M
   10 A(I,K)=A(I,K)+B(I,J)*C(J,K)
      RETURN
      END
```

```
      SUBROUTINE MATONE(A,N,M,NN)
C
C PRODUCES A ONE'S MATRIX
C
      REAL*4 A(N,M)
      DO 10 I=1,N
      DO 10 J=1,M
   10 A(I,J)=1.0
      RETURN
      END
```

```
      SUBROUTINE MATPRN(A,N,M,NN,NAME)
C
C PRINTS OUT MATRIX A
C
C N IS NUMBER OF ROWS
C M IS NUMBER OF COLUMNS
C
      REAL*4 A(N,M),NAME(2)
      WRITE(6,30)
      WRITE(6,40)NAME(1),NAME(2),N,M
      DO 10 I=1,N
      WRITE(6,20)(A(I,J),J=1,M)
   10 CONTINUE
   20 FORMAT(1X,8E14.7)
   30 FORMAT(//)
   40 FORMAT(12H REAL MATRIX,3X,2A4,10X,I3,3H X ,I3//)
      RETURN
      END
```

```
      SUBROUTINE MATRED(A,N,M,NN)
C
      REAL*4 A(N,M)
      DO 10 I=1,N
   10 READ(5,20)(A(I,J),J=1,M)
   20 FORMAT(8F10.0)
      RETURN
      END
```

```
      SUBROUTINE MATRNS(A,B,N,M,NN)
C
C A=TRANSPOSE OF B
C
      REAL*4 A(M,N),B(N,M)
      DO 10 I=1,M
      DO 10 J=1,N
      A(I,J)=B(J,I)
   10 CONTINUE
      RETURN
      END
```

```
      SUBROUTINE MATSCL(A,S,B,N,M,NN)
C
C N IS NUMBER OF ROWS,M NUMBER OF COLUMNS
C
      REAL*4 A(N,M),B(N,M)
      DO 10 I=1,N
      DO 10 J=1,M
      A(I,J)=S*B(I,J)
   10 CONTINUE
      RETURN
      END
```

```
      SUBROUTINE MATZER(A,N,M,NN)
C
      REAL*4 A(N,M)
      DO 10 I=1,N
      DO 10 J=1,M
      A(I,J)=0.0
   10 CONTINUE
      RETURN
      END
```

APPENDIX 7

THE MAIN SUBROUTINES

A7.1 Subroutine NAB

This part of the program controls the calculation of the discrete time state, control and disturbance matrices used in the mathematical model of the ship. The routine is called twice for each value of the sampling time. In the first instant it is used to evaluate the equation which represents the ship; in the second it is used in the filter. Starting with the non-dimensional hydrodynamic coefficients NAB calls subroutine DIMEN to dimensionalise the coefficients that correspond to the ship's forward speed. Next subroutine CALXBC is used to compute the coefficients X, B and C used in equation set 3.28 and defined in Appendix 3. From these subroutines FMAT and GMAT are used to form the F and G continuous time matrices of equation set 3.12. It should be noted that G appears as an 8 * 6 matrix in the computer subroutine, whereas it is in fact made up of the two matrices G_C and G_D. After conversion to discrete time form in subroutine TRNMAC the discrete time transition matrices are available for calculations involving the mathematical model of the ship. Figure A7.1 gives the inter-relationship of NAB with its own subroutines.

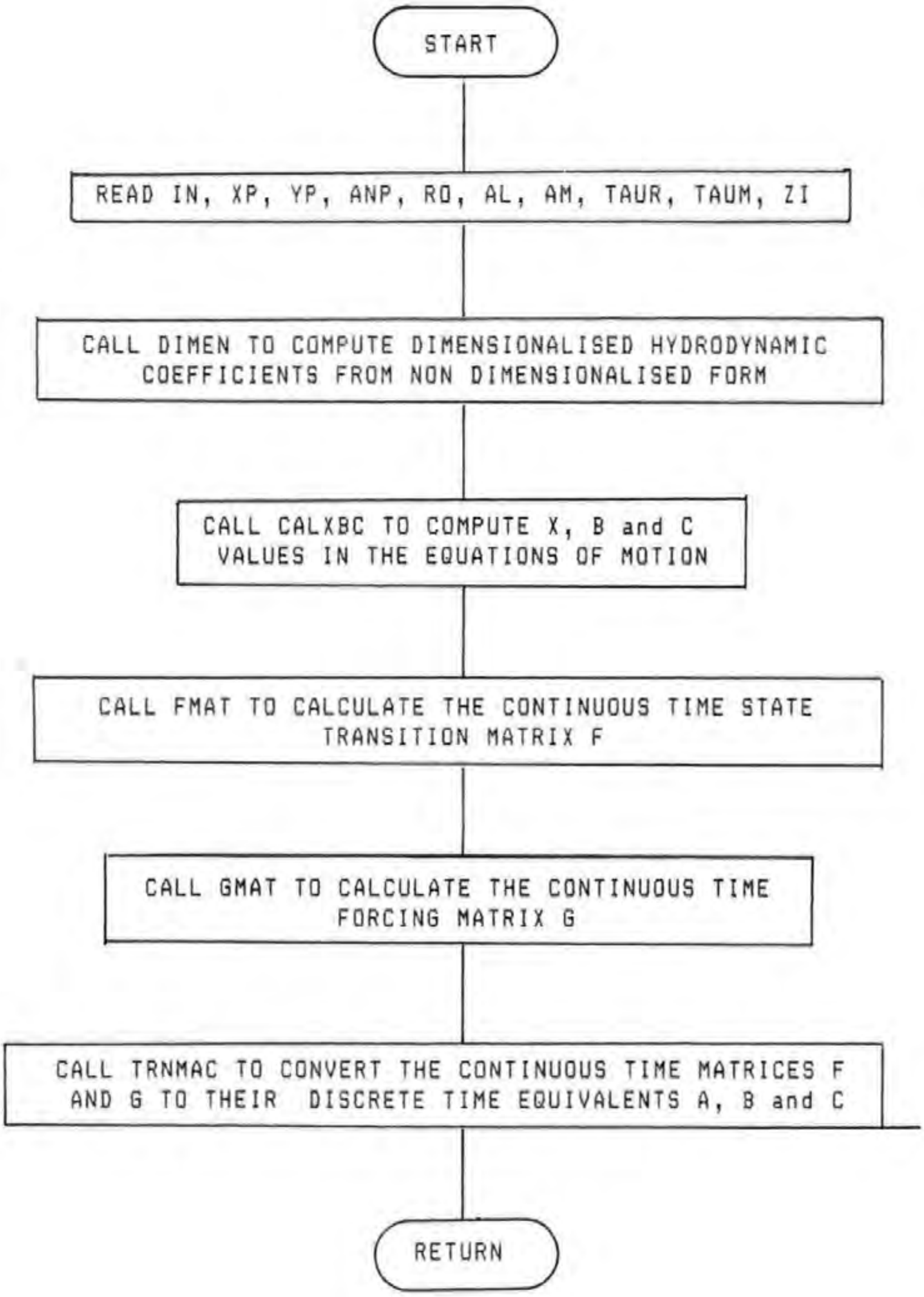

Figure A 7.1 Module Dependency Chart and Flowchart for Subroutine NAB

Variables used in addition to those already defined are:-

XP(14), YP(14), ANP(14)	The non-dimensionalised X, Y and N coefficients
RO	Density of Water
AL	Length of Ship
AM	Mass of Ship
TAUR, TAUN	Time constants of rudder and engine respectively
ZI	Moment of Inertia of ship

```
      SUBROUTINE NAB(A, B, C, N, NX, NG, NB, NC, NN, IFIN, K, LOOP, T, WUM,
     &TSAMP, XOLD, UVEL, UA, F41X, F42X, F44X, F46X, F48X, WU, UD1, UD2,
     &F61Y, F62Y, F64Y, F66Y, F68Y, F81N, F82N, F84N, F86N, F88N)
C
C THIS SUBROUTINE COMMENCES WITH THE NON DIMENSIONALISED
C HYDRODYNAMICCOEFFICIENTS AND CALCULATES THE CONTINUOUS
C TIME STATE AND FORCINGMATRICES. IT THEN CALLS TRNMAT TO
C CONVERT THESE TO THE DISCRETE TIMEMATRICES A & B
C
C
      REAL*4 A(8,8),B(8,2),C(8,4),F(8,8),G(8,6),
     *       F41X(250),F42X(250),F44X(250),F46X(250),
     *       F48X(250),F61Y(250),F62Y(250),F64Y(250),
     *       FF66Y(250),F68Y(250),F81N(250),F82N(250),
     *       F84N(250),F86N(250),F88N(250),
     *       R(250),
     *       ANP(14),XP(14),YP(14),
     *       XOLD(8),T(250),WU(250),WUM(250)
C
      IF(K-1)6,6,7
    6 READ(5,101)RO,AL,AM,TAUR,TAUN,ZI
      IFIM=IFIN+1
      NX=1
C
C READ IN NONDIMENSIONALISED HYDRODYNAMIC DERIVATIVES
C USING MATRED AND PRINT VALUES USING MATPRN
C CONVENTION:
C           XP(1)=XDELT'      YP(1)=YDELT'      ANP(1)=NDELT'
C           XP(2)=XN'         YP(2)=YNN         ANP(2)=NNN
C           XP(3)=XU'         YP(3)=YU'         ANP(3)=NU'
C           XP(4)=XUDOT'      YP(4)=YUDOT'      ANP(4)=NUDOT'
C           XP(5)=XUU'        YP(5)=YV'         ANP(5)=NV'
C           XP(6)=XUUU'       YP(6)=YVDOT'      ANP(6)=NVDOT'
C           XP(7)=XUN'        YP(7)=YR'         ANP(7)=NR'
C           XP(8)=XRDOT'      YP(8)=YRDOT'      ANP(8)=NRDOT'
C           XP(9)=XUA'        YP(9)=YUA'        ANP(9)=NUVA'
C           XP(10)=XVA'       YP(10)=YVA'       ANP(10)=NVA'
C           XP(11)=XVV'       YP(11)=YVVV'      ANP(11)=NVVV'
C           XP(12)=XRR'       YP(12)=YRVV'      ANP(12)=NRVV'
C           XP(13)=XDD'       YP(13)=YDDD'      ANP(13)=NDDD'
C           XP(14)=XNN'       YP(14)=YDVV'      ANP(14)=NDVV'
C
      CALL MATRED(XP,14,1,28)
C
      CALL MATRED(YP,14,1,28)
C
      CALL MATRED(ANP,14,1,28)
C
C
C
C COMPUTE DIMENSIONALISED HYDRODYNAMIC DERIVATIVES
C THAT CORRESPOND TO SHIP FORWARD VELOCITY UVEL
C
    7 CALL DIMEN(RO,AL,XP,YP,ANP,UVEL,XOLD,UA,
     &XDELT,XN,XU,XUDOT,XUU,XUUU,XUN,XRDOT,XUA,XVA,XVV,XRR,
     &XDD,XNN,
```

```
     &YDELT, YNN, YU, YUDOT, YV, YVDOT, YR, YRDOT, YUA, YVA, YVVV, YRVV,
     &YDDD, YDVV,
     &ANDELT, ANNN, ANU, ANUDOT, ANV, ANVDOT, ANR, ANRDOT, ANUA, ANVA,
     &ANVVV, ANRVV, ANDDD, ANDVV)
C
C
C COMPUTE X,B AND C COEFFICIENTS
C
      CALL CALXBC(AM, ZI, XOLD, UVEL, WU, UD1, UD2, K, WUM,
     &XN, XU, XUDOT, XUU, XUUU, XUN, XUA, XVA, XVV, XRR, XDD, XNN,
     &YDELT, YNN, YV, YVDOT, YR, YRDOT, YUA, YVA, YVVV, YRVV, YDDD, YDVV,
     &ANDELT, ANNN, ANV, ANVDOT, ANR, ANRDOT, ANUA, ANVA, ANVVV, ANRVV,
     &ANDDD, ANDVV, X1, X2, X4, X6, X8, XU3, XU5,
     &B1, B2, B4, B6, B8, BU4, BU6,
     &C1, C2, C4, C6, C8, CU4, CU6)
C
C
C COMPUTE F MATRIX
C
      CALL FMAT(TAUR, TAUN, X1, X2, X4, X6, X8, XOLD,
     &B1, B2, B4, B6, B8, C1, C2, C4, C6, C8, F, N)
C
      F41X(K)=F(4,1)
      F42X(K)=F(4,2)
      F44X(K)=F(4,4)
      F46X(K)=F(4,6)
      F48X(K)=F(4,8)
      F61Y(K)=F(6,1)
      F62Y(K)=F(6,2)
      F64Y(K)=F(6,4)
      F66Y(K)=F(6,6)
      F68Y(K)=F(6,8)
      F81N(K)=F(8,1)
      F82N(K)=F(8,2)
      F84N(K)=F(8,4)
      F86N(K)=F(8,6)
      F88N(K)=F(8,8)
C
C COMPUTE G MATRIX
C
      CALL GMAT(TAUR, TAUN, XU3, XU5,
     &BU4, BU6, CU4, CU6, G, N, NG, NN)
C
C
C COMPUTE DISCRETE TIME STATE TRANSITION MATRIX A(T)
C AND DISCRETE TIME FORCING MATRIX B(T)
C
      CALL TRNMAC(F, G, A, B, C, N, NG, NB, TSAMP, NN)
C
    4 RETURN
      END
```

A 7.2 Subroutines DIMEN, CALXBC, FMAT, GMAT

These have been discribed in the previous section. Variables not already defined are:-

RA2	Air density
XDELT, XN, XU, XUDOT XUU, XUUU, XUN, XRDOT XUA, XVA, XVV, XRR XDD, XNN	Dimensionalised X coefficients
YDELT, YNN, YU, YUDOT YV, YVDOT, YR, YRDOT, YUA, YVA, YVVV, YRVV, YDDD, YDVV	Dimensionalised y coefficients
ANDELT, ANNN, ANU, ANUDOT ANN, ANUDOT, ANR, ANRDOT, ANUA, ANVA, ANVVV, ANRVV, ANDDD, ANDVV	Dimensionalised N coefficients
UCOR2	Correction for propeller action
X1 etc, Y1 etc, AN1 etc B1 etc, C1 etc	Coefficients of X, Y and N equations defined in Appendix 3

```
      SUBROUTINE DIMEN(RO, AL, XP, YP, ANP, UVEL, XOLD, UA,
     &XDELT, XN, XU, XUDOT, XUU, XUUU, XUN, XRDOT, XUA, XVA, XVV, XRR, XDD
, XNN,
     &YDELT, YNN, YU, YUDOT, YV, YVDOT, YR, YRDOT, YUA, YVA, YVVV, YRVV, Y
DDD, YDVV,
     &ANDELT, ANNN, ANU, ANUDOT, ANV, ANVDOT, ANR, ANRDOT, ANUA, ANVA, A
NVVV,
     &ANRVV, ANDDD, ANDVV)
      DIMENSION XP(14), YP(14), ANP(14), XOLD(8)
C
C
C X DIMENSIONALISED HYDRODYNAMIC DERIVATIVES
C FOR NON-LINEAR MODEL
C
      RO2=0.5*RO
      RA2=0.5*1.28
C
      XDELT=XP(1)*RO2*AL**2*UVEL**2
      XN=(XP(2)*RO2*AL**3*7.752)/(2.*3.14159)
      XU=XP(3)
      XUDOT=XP(4)*RO2*AL**3
      XUU=XP(5)
      XUUU=XP(6)
      XUN=XP(7)
      XRDOT=0.0
      XUA=XP(9)*RA2*AL**2*UA
      XVA=0.0
      XVV=XP(11)*RO2*AL**2
      XRR=XP(12)*RO2*AL**4
      XDD=XP(13)*RO2*AL**2*UVEL**2
      XNN=XP(14)
C
C Y DIMENSIONALISED HYDRODYNAMIC DERIVATIVES
C FOR NON-LINEAR MODEL
C
      UCOR2=(0.84*UVEL**2-1.257*UVEL*XOLD(2)+2.3359*XOLD(2)**2
)
      YDELT=YP(1)*RO2*AL**2*UCOR2
      YNN=YP(2)
      YU=0.0
      YUDOT=0.0
      YV=YP(5)*RO2*AL**2*UVEL
      YVDOT=YP(6)*RO2*AL**3
      YR=YP(7)*RO2*AL**3*UVEL
      YRDOT=YP(8)*RO2*AL**4
      YUA=0.0
      YVA=YP(10)*RA2*AL**2*UA
      YVVV=(YP(11)*RO2*AL**2)/UVEL
      YRVV=(YP(12)*RO2*AL**3)/UVEL
      YDDD=YP(13)*RO2*AL**2*UCOR2
      YDVV=YP(14)*RO2*AL**2
C
C N DIMENSIONALISED HYDRODYNAMIC DERIVATIVES
C FOR NON-LINEAR MODEL
C
      ANDELT=ANP(1)*RO2*AL**3*UCOR2
```

```
      ANNN=ANP(2)
      ANU=0.0
      ANUDOT=0.0
      ANV=ANP(5)*RO2*AL**3*UVEL
      ANVDOT=ANP(6)*RO2*AL**4
      ANR=ANP(7)*RO2*AL**4*UVEL
      ANRDOT=ANP(8)*RO2*AL**5
      ANUA=ANP(9)*RA2*AL**3
      ANVA=ANP(10)*RA2*AL**3*UA
      ANVVV=(ANP(11)*RO2*AL**3)/UVEL
      ANRVV=(ANP(12)*RO2*AL**4)/UVEL
      ANDDD= ANP(13)*RO2*AL**3*UCOR2
      ANDVV=ANP(14)*RO2*AL**3
C
      RETURN
      END
```

```
      SUBROUTINE CALXBC(AM, ZI, XOLD, UVEL, WU, UD1, UD2, K, WUM,
     1XN, XU, XUDOT, XUU, XUUU, XUN, XUA, XVA, XVV, XRR, XDD, XNN,
     2YDELT, YNN, YV, YVDOT, YR, YRDOT, YUA, YVA, YVVV, YRVV, YDDD, YDVV,
     3ANDELT, ANNN, ANV, ANVDOT, ANR, ANRDOT, ANUA, ANVA, ANVVV, ANRVV,
     4ANDDD, ANDVV, X1, X2, X4, X6, X8, XU3, XU5,
     5B1, B2, B4, B6, B8, BU4, BU6,
     6C1, C2, C4, C6, C8, CU4, CU6)
C
      REAL*4 XOLD(8), WU(4), WUM(4)
C
C
C X COEFFICIENTS
C
      XUDOTM=AM-XUDOT
C
      X1=(XDD*XOLD(1))/XUDOTM
      X2=((XUN*UVEL)+(XNN*XOLD(2)))/XUDOTM
      X4=(XU+XUU*XOLD(4)+XUUU*XOLD(4)**2)/XUDOTM
      X6=(XVV*XOLD(6)+AM*XOLD(8))/XUDOTM
      X8=(XRR*XOLD(8))/XUDOTM
      XU3=(XU+XUU*WU(1)+XUUU*WU(1)**2)/XUDOTM
      XU5=XUA/XUDOTM
C
C Y COEFFICIENTS
C
      YVDOTM=AM-YVDOT
C
      Y1=(YDELT+YDDD*XOLD(1)**2)/YVDOTM
      Y2=(YNN*XOLD(2))/YVDOTM
      Y4=(-AM*XOLD(8))/YVDOTM
      Y6=(YV+YRVV*XOLD(8)*XOLD(6)+YVVV*XOLD(6)**2+YDVV*XOLD(1)
     1     *XOLD(6))/YVDOTM
      Y8=YR/YVDOTM
      Y88=YRDOT/YVDOTM
      YU4=(YV+YRVV*XOLD(8)*WU(2)+YVVV*WU(2)**2+YDVV*XOLD(1)*
     *      WU(2))/YVDOTM
      YU6=YVA/YVDOTM
C
C N COEFFICIENTS
C
      ANRDOI=ZI-ANRDOT
C
      AN1=(ANDELT+ANDDD*XOLD(1)**2)/ANRDOI
      AN2=(ANNN*XOLD(2))/ANRDOI
      AN4=0.0
      AN6=(ANV+ANRVV*XOLD(8)*XOLD(6)+ANVVV*XOLD(6)**2+ANDVV
     *     *XOLD(1)
     1     *XOLD(6))/ANRDOI
      AN66=ANVDOT/ANRDOI
      AN8=ANR/ANRDOI
      ANU4=(ANV+ANRVV*XOLD(8)*WU(2)+ANVVV*WU(2)**2+ANDVV
     *     *XOLD(1)
     &*WU(2))/ANRDOI
C
C * EDA'S TERM
C
```

```
      ANU6=(ANVA+ANUA*WU(3))/ANRDOI
C
C * DISTURBANCE CONTROL TERMS
C
      TC=(XU3*XUDOTM)*WUM(1)
      TA=-(XUA*WUM(3))
      TP=(XUN*UVEL)+(XNN*XOLD(2))
      UD2=(TC+TA)/TP
C
      ANC=-(ANU4*ANRDOI)*WUM(2)
      ANA=-(ANVA+ANUA*WUM(3))*WUM(4)
      ANR=(ANDELT+ANDDD*XOLD(1)**2)
      UD1=(ANC+ANA)/ANR
C
C B COEFFICIENTS
C
      BDEN=1.0-Y88*AN66
C
      B1=(Y1+Y88*AN1)/BDEN
      B2=(Y2+Y88*AN2)/BDEN
      B4=(Y4)/BDEN
      B6=(Y6+Y88*AN6)/BDEN
      B8=(Y8+Y88*AN8)/BDEN
      BU4=(YU4+Y88*ANU4)/BDEN
      BU6=(YU6+Y88*ANU6)/BDEN
C
C C COEFFICIENTS
C
      CDEN=1.0-AN66*Y88
C
      C1=(AN1+AN66*Y1)/CDEN
      C2=(AN2+AN66*Y2)/CDEN
      C4=(AN66*Y4)/CDEN
      C6=(AN6+AN66*Y6)/CDEN
      C8=(AN8+AN66*Y8)/CDEN
      CU4=(ANU4+AN66*YU4)/CDEN
      CU6=(ANU6+AN66*YU6)/CDEN
C
      RETURN
      END
```

```
      SUBROUTINE FMAT(TAUR, TAUN, X1, X2, X4, X6, X8, XOLD,
     1B1, B2, B4, B6, B8, C1, C2, C4, C6, C8, F, N, NN)
C
      REAL*4 F(N, N), XOLD(8)
      CALL MATZER(F, N, N, NN)
      F(1, 1)=(-1. 0)/TAUR
      F(2, 2)=(-1. 0)/TAUN
      F(3, 4)=1. 0
      F(4, 1)=X1
      F(4, 2)=X2
      F(4, 4)=X4
      F(4, 6)=X6
      F(4, 8)=X8
      F(5, 6)=1. 0
      F(6, 1)=B1
      F(6, 2)=B2
      F(6, 4)=B4
      F(6, 6)=B6
      F(6, 8)=B8
      F(7, 8)=1. 0
      F(8, 1)=C1
      F(8, 2)=C2
      F(8, 4)=C4
      F(8, 6)=C6
      F(8, 8)=C8
C
      RETURN
      END
```

```
      SUBROUTINE GMAT(TAUR, TAUN, XU3, XU5,
     1BU4, BU6, CU4, CU6, G, N, NG, NN)
C
      REAL*4 G(N, NG)
      CALL MATZER(G, N, NG, NN)
      G(1, 1)=1.0/TAUR
      G(2, 2)=1.0/TAUN
      G(4, 3)=XU3
      G(4, 5)=XU5
      G(6, 4)=BU4
      G(6, 6)=BU6
      G(8, 4)=CU4
      G(8, 6)=CU6
C
      RETURN
      END
```

A 7.3 Subroutine TRNMAC

A description of the method used to obtain the discrete transition matrices was given in Chapter 3, section 3.2; equations (3.15) and (3.16) describe the computations which take place whenever this subroutine is called.

Variables called and not already defined are:-

POWER	Number of terms of the series approximation given by equations (3.15) and (3.16)
ST(I,J)	FT in equations (3.15) and (3.16)
FPOWR	(L-1), (L-2), etc in equations (3.15) and (3.16)
INTEGA (J,K)	FT/(L-1), FT/(L-2) etc in equations (3.15) and (3.16)
BUD (8,6)	Discrete time transform of G(8,6). This is then split into B(8,2) and C(8,4)

```
      SUBROUTINE TRNMAC(F,G,A,B,C,N,NG,NB,TSAMP,NN)
C
C EVALUATES DISCRETE STATE TRANSITION MATRIX A(T)
C AND DISCRETE FORCING MATRICES B(T) AND C(T)
C
      REAL*4 ST(8,8),F(8,8),A(8,8),INTEGA(8,8)
      REAL*4 BUD(8,6),G(8,6),B(8,2),C(8,4)
      REAL INTEGA
      INTEGER POWER
      NORMFT=0.0
      DO 1 I=1,N
      DO 1 J=1,N
      ST(I,J)=F(I,J)*TSAMP
    1 A(I,J)=ST(I,J)
      POWER=50
      DO 7 I=2,POWER
      FPOWR=POWER-I+2
      DO 5 J=1,N
      DO 3 K=1,N
    3 INTEGA(J,K)=A(J,K)/FPOWR
    5 INTEGA(J,J)=INTEGA(J,J)+1.0
      CALL MATMUL(A,ST,INTEGA,N,N,N,NN)
    7 CONTINUE
      DO 9 J=1,N
      A(J,J)=A(J,J)+1.0
      DO 9 K=1,N
    9 INTEGA(J,K)=TSAMP*INTEGA(J,K)
      CALL MATMUL(BUD,INTEGA,G,N,N,NG,NN)
C
C * SPLIT BUD(8,6) INTO B(8,2) AND C(8,4)
C
      DO 10 I=1,N
      DO 10 J=1,NB
   10 B(I,J)=BUD(I,J)
      DO 20 I=1,N
      DO 20 J=3,NG
      K=J-2
   20 C(I,K)=BUD(I,J)
C
C
      RETURN
      END
```

A 7.4 Subroutine OPTFIL

This subroutine performs two main functions. It models the ideal system, that is one with no disturbances or measurement noise, and calls subroutine KBFLTR from which the Kalman filter gains are obtained. The output is then the best estimate of the state vector which is used as input to the optimal controller. Figure A 7.2 gives a flowchart for this subroutine. The variables used and not already defined are as listed below:-

AA(8,8),BB(8,2)	Transition matrices used in filter equations
XHAT(8), XHAT1(8), XHAT2(8)	Previous, predicted and final.estimates of state vector
ABCED	Absolute value of course error in degrees
CED	Course error in degrees
Z1	Predicted measured state
ZDIFF	Measurement Residual
AK(8,8)	Kalman filter gain matrix

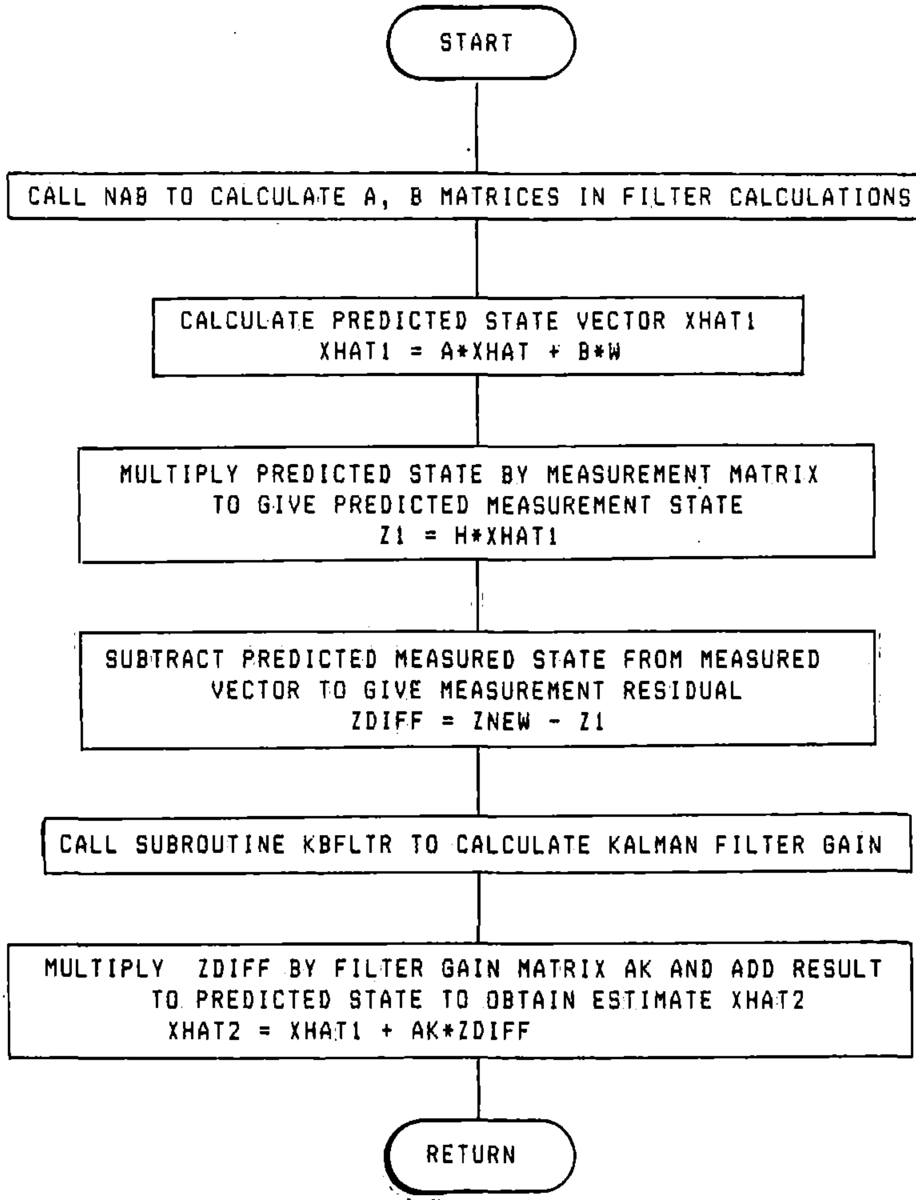

Figure A 7.2 Flow Chart for Subroutine OPTFIL

```
      SUBROUTINE OPTFIL(AA,BB,CC,BU,H,U,Z,N,NB,NC,NX,IP,IM,
     *XHAT2,XHAT,XHAT1,K,CERROR,V,ABCER,RADCON)
C
C This Subroutine calculates the Best Estimate of the STATE VECTOR.
C It solves the equations below & calls KBFLTR.
C KBFLTR calculates the Steady State Kalman-Bucy Filter Gain Matrix K(k+1
C
C xhat(k+1/k)=A(k+1,k)*xhat(k/k)+B(k+1,k)*u(k)
C xhat(k+1/k+1)=xhat(k+1/k)+K(k+1)[ z(k+1)-H(k+1)*xhat(k+1)]
C
C XHAT=xhat(k/k)     XHAT1=xhat(k+1/k)      XHAT2=xhat(k+1/k+1)
C
      REAL*4 V(N,NX)
      REAL*4 AA(N,N),BB(N,NB),CC(N,NC),BU(N,NX),H(N,N),Z(N,NX)
      REAL*4 U(NB,NX),XHAT(N,NX),XHAT1(N,NX),XHAT2(N,NX)
      REAL*4 AK(8,8),KZ(8,1)
      REAL*4 AXHT(8,1)
      REAL*4 Z1(8,1),Z2(8,1),ZDIFF(8,1)
C
C CALCULATE AA,BB,CC MATRICES
C
      ABCED=ABCER*RADCON
      CED=CERROR*RADCON
      UVELE=SQRT((XHAT(4)**2)+(XHAT(6)**2))
      IF (K.GT.1)GOTO 2
      NK=K+1
      CALL NAB(AA,BB,CC,N,NX,NG,NB,NC,NN,IFIN,NK,LOOP,T,WUM,
     *TSAMP,XHAT,UVELE,UA,F41X,F42X,F44X,F46X,F48X,WU,UD1,UD2,
     *F61Y,F62Y,F64Y,F66Y,F68Y,F81N,F82N,F84N,F86N,F88N)
      GO TO 3
    2 IF (ABCED.LT.1.0)GOTO 3
      CALL NAB(AA,BB,CC,N,NX,NG,NB,NC,IFIN,K,LOOP,T,WUM,
     *TSAMP,XHAT,UVELE,UA,F41X,F42X,F44X,F46X,F48X,WU,UD1,UD2,
     *F61Y,F62Y,F64Y,F66Y,F68Y,F81N,F82N,F84N,F86N,F88N)
C
C XHAT1=A*XHAT+B*U
C
    3 IF(K.EQ.49) CALL MATSCL(AA,1.1,AA,N,N,NN)
      CALL MATMUL(AXHT,AA,XHAT,N,N,NX)
      CALL MATMUL(BBU,BB,U,N,NB,NX)
      CALL MATADD(XHAT1,AXHT,BBU,N,NX)
C
C Z1=H*XHAT1
C
      CALL MATMUL(Z1,H,XHAT1,N,N,NX)
C
C ZDIFF=ZNEW-Z1
C
      CALL MATSCL(Z2,-1.0,Z1,N,NX)
      CALL MATADD(ZDIFF,ZNEW,Z2,N,NX)
C
C CALCULATE K(k+1) using KBFLTR
C
      CALL KBFLTR(AA,CC,H,AK,N,NC,NX,IP,IM,K,V,SDQ,SDR)
C
C XHAT2=XHAT1+AK*ZDIFF
C
      CALL MATMUL(KZ,AK,ZDIFF,N,N,NX)
      CALL MATADD(XHAT2,KZ,XHAT1,N,NX)
      RETURN
      END
```

Appendix A 7.5 Subroutine KBFLTR

This subroutine is called from OPTFIL and used to update the error covariance matrix together with the filter gain matrix AK. The action of the filter is described fully in Chapter 4, section 4.6. The software routines used in subroutine KBFLTR are due to MacKinnon (1972) and Healey et al (1975). Figure A 7.3 gives the Kalman filter algorithm.

Variables used and not already defined are:-

CR(8,8)	Disturbance noise covariance matrix
CQ(4,4)	Measurement noise covariance matrix
PK(8,8)	Error covariance Matrix
PKP1(8,8)	Predicted Error Covariance Matrix

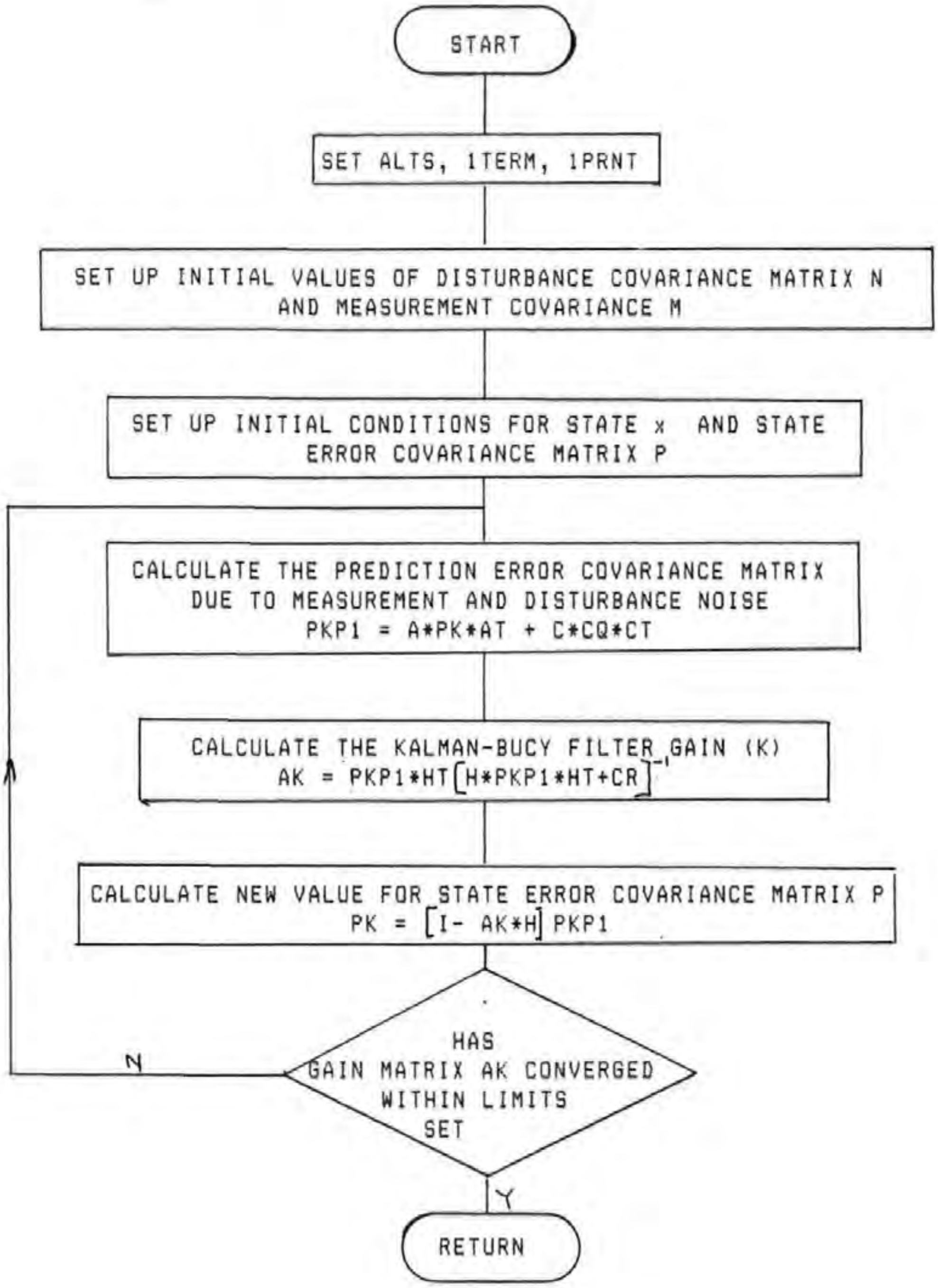

Figure A 7.3 The Kalman Filter Algorithm

```
      SUBROUTINE KBFLTR(A,C,H,AK,N,NN,NC,NX,IP,IM,K,V,SDQ,SDR)
C          CALCULATES STEADY STATE KALMAN-BUCY FILTER GAIN MAT
RIX
C
      REAL*8 DHPHR(8,8),DPH(8,8),WKSPCE(64)
      REAL*8 DUNIT(8,8)
      REAL*4 RHPH(8,8),HPHR(8,8)
      REAL*4 A(N,N),C(N,NC),H(N,N),AK(N,N)
      REAL*4 PASTK(8,8),PK(8,8),PKP1(8,8),CONVER(8,8)
      REAL*4 RR(8,8),SS(8,8),CT(4,8),AT(8,8),HT(8,8)
      REAL*4 CCQ(8,4),PA(8,8),CQC(8,8),APA(8,8),PH(8,8),HPH(8,8)

      REAL*4 AHAK(8,8),AKH(8,8),CQ(4,4),CR(8,8),AH(8,8)
      REAL*4 HKA(8,8),HPPH(8,8)
      REAL*4 V(200,8),SDR(8),SDQ(4)
C
      WRITE(1,74)
 74   FORMAT(' KBF')
C
C
C READ IN ALTS,ITERM,IPRNT
C
      ALTS=1.0
C     IF(K.EQ.1) ALTS=ALTS/100.0
      ITERM=100
      IPRNT=100
C
C KBFLTR REQUIRES A,C,H,CQ,CR SET ON ENTRY
C
C Initial Conditions for Covariances CQ(disturbance) & CR(Nois
e)
C
      CALL MATZER(CR,IM,IM,NN)
      CR(1,1)=SDR(1)**2
      CR(2,2)=SDR(2)**2
      CR(3,3)=SDR(3)**2
      CR(4,4)=SDR(4)**2
      CR(5,5)=SDR(5)**2
      CR(6,6)=SDR(6)**2
      CR(7,7)=SDR(7)**2
      CR(8,8)=SDR(8)**2
C
C STANDARD DEVIATIONS FOR WIND AND CURRENT
C
C     CALL MATPRN(CR,IM,IM,NN,8HCR       )
      CALL MATZER(CQ,IP,IP,NN)
      CQ(1,1)=SDQ(1)**2
      CQ(2,2)=SDQ(2)**2
      CQ(3,3)=SDQ(3)**2
      CQ(4,4)=SDQ(4)**2
C     CALL MATPRN(CQ,IP,IP,NN,8HCQ       )

C L IS THE ITERATION COUNTER,0-IPRINT
C
      ICOUNT=0
      L=0
```

```
      FPZ=0.0
C
C
C
C Read in Initial Conditions for CONVER
C
      CALL MATIDN(CONVER,N,NN)
C
C Read in Initial Conditions for STATE VECTOR Covariance Matri
x(P(k/k)
C
      CALL MATIDN(PK,N,NN)
      IF(K.GT.1) GO TO 299
C     CALL MATPRN(CR,IM,IM,NN,8HCR      )
C     CALL MATPRN(CQ,IP,IP,NN,8HCQ      )
      CALL MATSCL(PK,5.0,PK,N,N,NN)
 299  CONTINUE
C     CALL MATPRN(PK,N,N,NN,8HPK      )
C
C Commence Iteration Loop
C
  300 CONTINUE
      DELS=0.0
      IF(L-IPRNT) 320,310,320
  310 L=0
  320 CONTINUE
C
C Calculate the Prediction Error Covariance Matrix(P(k+1/k))
C
C
C CQC=C*CQ*CT    CT=Transpose of C
C
      CALL MATMUL(CCQ,C,CQ,N,IP,IP,NN)
      CALL MATRNS(CT,C,N,IP,NN)
C     CALL MATPRN(CT,IP,N,NN,8HCT      )
      CALL MATMUL(CQC,CCQ,CT,N,IP,N,NN)
      WRITE(1,106)
 106  FORMAT(1H ,'CQC CALCULATED')
CC    CALL MATPRN(CQC,N,N,NN,8HCQC     )
C
C APA=A*PK*AT   AT=Transpose of A
C
      CALL MATRNS(AT,A,N,N,NN)
C     CALL MATPRN(AT,N,N,NN,8HAT      )
C
C PKP1=P(k+1/k)
C
      CALL MATMUL(PA,PK,AT,N,N,N,NN)
      CALL MATMUL(APA,A,PA,N,N,N,NN)
C     CALL MATPRN(APA,N,N,NN,8HAPA     )
      CALL MATADD(PKP1,APA,CQC,N,N,NN)
      CALL MATPRN(PKP1,N,N,NN,8HPKP1    )
C
C Calculate the KALMAN-BUCY FILTER GAIN
C
C AK=K(k+1)      PASTK=K(k)
```

```
C
C HT=Transpose of H
C
      CALL MATRNS(HT,H,N,N,NN)
C     CALL MATPRN(HT,N,N,NN,8HHT       )
C
C PH=PKP1*HT
C
      CALL MATMUL(PH,PKP1,HT,N,N,N,NN)
C
C PRINT PH MATRIX
C
C
C HPH=H*PKP1*HT
C
      CALL MATMUL(HPH,H,PH,N,N,N,NN)
C     CALL MATPRN(HPH,N,N,NN,8HHPH      )
C
C HPHR=(H*PKP1*HT)+CR
C
      CALL MATADD(HPHR,HPH,CR,N,IM,NN)
      WRITE(1,107)
C
C
      DO 98 I=1,N
      WRITE(1,97) (HPHR(I,J),J=1,N)
 98   CONTINUE
 97   FORMAT(1X,8E14.7)
 107  FORMAT(1H ,'HPHR CALCULATED')
C
C CHANGE TO DOUBLE PRECISION
C
      DO 10 I1=1,N
      DO 20 I2=1,N
      DHPHR(I1,I2)=HPHR(I1,I2)
 20   CONTINUE
 10   CONTINUE
      IFAIL=0
      CALL F01AAF(DHPHR,N,N,DUNIT,N,WKSPCE,IFAIL)
C
C RETURN TO SINGLE PRECISION
C
      DO 30 I1=1,N
      DO 40 I2=1,N
      RHPH(I1,I2)=DUNIT(I1,I2)
 40   CONTINUE
 30   CONTINUE
C     CALL MATINV(HPHR,N,N,NN)
      WRITE(1,108)
 108  FORMAT(1H ,'HPHR INVERTED')
      IF(K.GT.5) GO TO 93
      DO 95 I=1,N
      WRITE(1,94) (RHPH(I,J),J=1,N)
 95   CONTINUE
 94   FORMAT(1X,8E14.7)
      CALL MATMUL(HPPH,HPHR,RHPH,N,N,N,NN)
```

```
      WRITE(1,112)
 112  FORMAT('HPHR*RHPH=IDN')
      DO 113 I=1,N
      WRITE(1,114) (HPPH(I,J),J=1,N)
 113  CONTINUE
 114  FORMAT(1X,8E14.7)
 93   CONTINUE
      CALL MATMUL(AK,PH,RHPH,N,N,N,NN)
      WRITE(1,109)
 109  FORMAT(1H ,'AK CALCULATED')
C
C Calculate P(k+1/k+1)
C
C AKH=AK*H
C
      CALL MATMUL(AKH,AK,H,N,N,N,NN)
      WRITE(1,111)
 111  FORMAT(1H ,'AKH CALCULATED')
C
C AHAK=AH-AKH
C
      CALL MATIDN(AH,N,NN)
      CALL MATSCL(HKA,-1.0,AKH,N,N,NN)
      CALL MATADD(AHAK,AH,HKA,N,N,NN)
      CALL MATMUL(PK,AHAK,PKP1,N,N,N,NN)
C
      WRITE(1,110)
 110  FORMAT(1H ,'PK CALCULATED')
      DO 89 I=1,N
      WRITE(1,88) (PK(I,J),J=1,N)
 89   CONTINUE
 88   FORMAT(1X,8F10.5)
C End of FILTER calculations
C
      ICOUNT=ICOUNT+1
      L=L+1
C     TEST FOR NON-CONVERGENCE OF GAIN MATRIX K(K+1)
      DO 400 I=1,N
      TEST=PK(I,I)
      IF(TEST-FPZ) 400,400,350
  350 CONVER(I,I)=1./SQRT(TEST)
  400 CONTINUE
      CALL MATMUL(RR,CONVER,AK,N,N,IM,NN)
      DO 500 J=1,IM
      DO 500 I=1,N
      TEST=RR(I,J)
      IF(ABS(TEST)-DELS) 500,500,450
  450 DELS=ABS(TEST)
  500 CONTINUE
      CALL MATMUL(SS,CONVER,PASTK,N,N,IM,NN)
      DO 600 I=1,N
      DO 600 J=1,IM
      TEST=RR(I,J)-SS(I,J)
      IF(ABS(TEST)-ALTS*DELS) 600,600,620
  600 CONTINUE
      GO TO 800
```

```
  620 IF(ICOUNT-ITERM) 650,650,2500
  650 CONTINUE
      CALL MATEQL(PASTK,AK,N,IM,NN)
      IF(L-IPRNT) 300,700,300
  700 CONTINUE
      WRITE(6,200) ICOUNT
      CALL MATPRN(AK,N,IM,NN,8HAK(K)    )
      GO TO 300
  800 CONTINUE
C
C  WRITE KALMAN FILTER GAIN & SYSTEM COVARIANCE MATRICES
C
      IF(K.EQ.1) LOOP=0
      IF(K.LT.LOOP) GO TO 4
      LOOP=LOOP+20
      ALTS=ALTS*100.
      WRITE(6,250) ALTS,ICOUNT
      CALL MATPRN(AK,N,IM,NN,8HAK(K)    )
      CALL MATPRN(PK,N,N,NN,8HPK       )
 4    RETURN
 2500 CONTINUE
      WRITE(6,280) ICOUNT
      RETURN
  200 FORMAT(///15X,I5,' ITERATIONS')
  250 FORMAT(///15X,'K(K+1) GAIN MATRIX CONVERGED WITHIN ',E10
.4,
     1' PERCENT AFTER ',I5,' ITERATIONS'/
     215X,'*****************************************************
********')
  280 FORMAT(///15X,'K(K+1) GAIN MATRIX FAILED TO CONVERGE WIT
HIN ',
     1I5,' ITERATIONS'/
     215X,'*****************************************************
********')
      END
```

APPENDIX 8

MEASUREMENT AND DISTURBANCE NOISE MODELS

A8.1 Disturbance Noise

In modelling wind and tide in the digital computer simulations it was assumed that the tests were carried out over a period of up to 15 minutes during the vessel's passage into harbour. As the port chosen for the simulations was Plymouth the tide and wind models were based upon information for that port. From the tide tables the spring tide in the region of the Plymouth breakwater had a value of 1.3 knots (0.669 m/s) in direction 046 degrees at 4 hours before high water on a specific day. These values were taken as the means over the time of each run. It was then assumed that any turbulance was of a stochastic nature.

Based upon the work of Zuidweg (1970) and Millars (1973), Burns (1984) has developed a tidal model used in this work. The equation is:-

$$v_c(k+1) = \delta v_c(k) + (k) \qquad \text{(A8.1)}$$

$$E\left[w(k)\right] = w_m = 0.669 \qquad \text{(A8.2)}$$

For a sampling time of 5 seconds and tidal time constant of 150 seconds the following value for γ is suggsted

$$\gamma = e^{-T/T_c} = e^{-5/150} = 0.967$$

For a sample time of 6 seconds this changes to 0.961

with $\mathrm{Cov}\left\{w_c(k_1),\ w_c(k_2)\right\} = \begin{cases} \ell_c & k_1 = k_2 \\ 0 & k_1 \neq k_2 \end{cases}$

where R_c is a non-negative constant given by

$$\sigma_c = \sqrt{R_c/(1-\gamma^2)} \tag{A8.4}$$

If σ_c, the standard deviation of the current about its mean value, is taken as 0.5 m/s this gives a value of 0.01623 for R_c

Thus

$$v_c(k+1) = 0.967v_c(k) + w(k) \tag{A8.5}$$

Where w(k) has a mean value of 0.0669 m/s and a standard deviation of 0.5 m/s. This was obtained from subroutine STANDEV with values of current magnitude over a 500 second period as inputs. A slight modification was obtained by using a first order filter when the discrete equation is re-written as

$$v_c(k+1) = Av_c(k) + Bw(k) \tag{A8.6}$$

where

UCURR = total tidal rate

UCURS = random tidal rate

UCURM = mean tidal rate

ALPHA = total tidal direction

ALPHS = random tidal direction

ALPHM = mean tidal direction

UAIR = total wind speed

UAIRS = random wind speed

UAIRM = mean wind direction

PHI = total wind direction

PHIS = random wind direction

PHIM = mean wind direction

The model was later modified in the light of experience. It was reasoned that if a two-dimensional wind gust had rectangular co-ordinates aligned with the mean wind speed then the gust magnitude would cause the wind direction to change, in which case there would be a correlation between the statistical properties of magnitude and direction. This was established using a scaling factor which was formed by the ratio of the two standard deviations, that is the set of random numbers generated for the magnitude of the wind was scaled by the ratio of standard deviations to give their directions. A similar scaling was applied to the rate of the tidal stream. Based upon these figures the computer equtions used in subroutines WINCUR became

UCURR(K+1) = 0.606*UCURR(K) + 0.394*WCURR(K) (A8.7)

ALPHS(K+1) = 0.368*ALPHS(K)+0.632*WALPHA(K) (A8.8)

UAIRS(K+1) = 0.606*UAIRS(K) + 0.394*WAIR(K) (A8.9)

PHIS(K+1) = 0.368*PHIS(K) + 0.632*WPHI(K) (A8.10)

```
C
C     *********************************************
C
C      SUBROUTINE WINCUR(WUS, N, M)
C
C THIS SUBROUTINE CALLS A NAG ROUTINE & GENERATES DISTURBANCE
C VARIATIONS ABOUT A MEAN VALUE.  IT REQUIRES DISTURBANCE
C STANDARD DEVIATIONS AS INPUT
C
C * WIND AND  CURRENT GENERATION
C
      REAL*8 UCURR(300), WCURR(300), UCURS(300)
      REAL*8 ALPHA(300), WALPHA(300), ALPHS(300)
      REAL*8 UAIR(300), WAIR(300), UAIRS(300)
      REAL*8 PHI(300), WPHI(300), PHIS(300)
      REAL*8 UCURM, ALPHM, UAIRM, PHIM
      REAL*8 G05DDF
      REAL*4 WUS(N, M)

      CALL G05CBF(0)
      UCURM=0.0D0
      ALPHM=0.0D0
      UAIRM=0.0D0
      PHIM=0.0D0
      UCURR(1)=UCURM
      ALPHA(1)=ALPHM
      UAIR(1)=UAIRM
      PHI(1)=PHIM

      DO 20 K=1,N
      WCURR(K)=G05DDF(0.0D0,0.9457D0)
      WALPHA(K)=WCURR(K)*(0.4915D0/0.9457D0)
      WAIR(K)=G05DDF(0.0D0,5.6742D0)
      WPHI(K)=WAIR(K)*(0.4915D0/5.6742D0)

      UCURS(K+1)=0.606D0*UCURS(K)+0.394D0*WCURR(K)
      UCURR(K+1)=UCURS(K+1)+UCURM
      ALPHS(K+1)=0.368D0*ALPHS(K)+0.632D0*WALPHA(K)
      ALPHA(K+1)=ALPHS(K+1)+ALPHM
      UAIRS(K+1)=0.606D0*UAIRS(K)+0.394D0*WAIR(K)
      UAIR(K+1)=UAIRS(K+1)+UAIRM
      PHIS(K+1)=0.368D0*PHIS(K)+0.632D0*WPHI(K)
      PHI(K+1)=PHIS(K+1)+PHIM

      WRITE(6,101)UCURR(K),ALPHA(K),UAIR(K),PHI(K)
      WUS(K,1)=UCURR(K)
      WUS(K,2)=ALPHA(K)
      WUS(K,3)=UAIR(K)
      WUS(K,4)=PHI(K)
   20 CONTINUE
  101 FORMAT(4F10.5)

      RETURN
      END
```

8.2 Measurement Noise

In modelling the measurement noise the standard deviations used were based upon those of actual sensors in use on board a typical ship. A random number generator was used to produce a set of noise values, based upon the standard deviations. These were in turn superimposed upon the true values of the state vector in accordance with the measurement equation

$$z(k+1) = Hx(k+1) + v(k+1) \tag{A8.11}$$

Whilst the vessel was seen to navigate successfully through this noise the actual values would not, in practice, vary so rapidly. To improve the realism of the digital simulation it was then decided to introduce a first order filter, similar to that used for disturbance noise, so that the measurement noise vector at a discrete point (k+1) was related to the value at k in the following way

$$v((k+1) = Av(k) + (1-A)\, N'(k) \tag{A8.12}$$

Where $N'(k)$ is the random number generated at the kth instant. The filter did however reduce the standard deviations of the noise, as with the disturbance noise. Continuing the comparison with disturbances the value of A in equationa 8.12 can be given by

$$A = e^{-T/T_c} \tag{A8.13}$$

where T is the sample time and T_c is a time constant given by

$$T_c = 1/2\pi f$$

as no information regarding the peaks of the deviations from the means was available, other than that they would be low frequency, it was decided to use a value for A of 0.6. For a low frequency giving a time constant of 10 seconds and with the usual sample time of 5 seconds then

$$A = e^{-0.5} = 0.606$$

```
C       SUBROUTINE NOISE(V,N,M)
C
C  INSTRUMENT NOISE RANDOM NOISE GENERATOR
C
C  THIS SUBROUTINE CALLS A NAG ROUTINE ROUTINE & GENERATES
C  MEASUREMENT NOISE.  IT REQUIRES MEASUREMENT NOISE
C  STANDARD DEVIATIONS AS INPUT
C
      REAL*8 DEL(300),REV(300),XO(300),USHIP(300)
      REAL*8 YO(300),VSHIP(300),PSI(300),R(300)
      REAL*8 G05DDF
      REAL*4 V(N,M)

  * * * * * * * * *

      CALL G05CBF(0)
      DO 20 K=1,N
      DEL(K)=G05DDF(0.0D0,0.002D0)
      REV(K)=G05DDF(0.0D0,0.002D0)
      XO(K)=G05DDF(0.0D0,200.000D0)
      USHIP(K)=G05DDF(0.0D0,0.02500D0)
      YO(K)=G05DDF(0.0D0,200.000D0)
      VSHIP(K)=G05DDF(0.0D0,0.02500D0)
      PSI(K)=G05DDF(0.0D0,0.01700D0)
      R(K)=G05DDF(0.0D0,0.01700D0)

      V(K+1,1)=0.6D0*V(K,1)+0.4D0*DEL(K)
      V(K+1,2)=0.6D0*V(K,2)+0.4D0*REV(K)
      V(K+1,3)=0.6D0*V(K,3)+0.4D0*XO(K)
      V(K+1,4)=0.6D0*V(K,4)+0.4D0*USHIP(K)
      V(K+1,5)=0.6D0*V(K,5)+0.4D0*YO(K)
      V(K+1,6)=0.6D0*V(K,6)+0.4D0*VSHIP(K)
      V(K+1,7)=0.6D0*V(K,7)+0.4D0*PSI(K)
      V(K+1,8)=0.6D0*V(K,8)+0.4D0*R(K)

      WRITE(6,101) V(K+1,1),V(K+1,2),V(K+1,3),
     * V(K+1,4),V(K+1,5),V(K+1,6),V(K+1,7),V(K+1,8)
 20   CONTINUE
 101  FORMAT(8F10.5)
      RETURN
      END
```

APPENDIX 9

CONTROLLER DESIGN

A9.1 Proportional plus Derivative Control

In the early simulations of Chapter 6 a simple autopilot was used. This consisted of a proportional term, the actual heading of the ship, together with the velocity of the vessel.

The demanded heading RIN(7,K) was differenced with the best estimate of heading XHAT(7) to give the course error, CERROR, to which was applied the velocity feedback term. Gains used were 1 for the proportional term and 30 for the velocity feedback term, giving the following terms in the computer program:-

```
CERROR = RIN(7,K) - XHAT(7)
U(1) = -(CERROR) -30.0*XHAT(8)
```

The minus sign on the right hand side of the control equation is to comply with the sign convention used, i.e., a negative rudder angle u(1) gives a positive yaw rate.

A9.2 The Optimal Controller

The tracking or servomechanism problem is one of applying a control u to drive a ship so that its states follow a desired trajectory in some optimal sense. The regulator is a special case of the tracking problem, the desired trajectory being a zero state. In its continuous form the quadratic criterion to be minimised is

$$J = \int_{t_0}^{t_1} \left\{ (x-R_1)^T Q(X-R_1) + u^T R u \right\} dt \tag{A9.1}$$

where R_1 is the desired value of the state vector. Kirk (1970) has shown that constrained functional minimisation yields the matrix Riccati equations

$$\dot{W} = -WF - F^T W - Q + WGR^{-1}G^T W \tag{A9.2}$$

together with the reverse-time differential equations set

$$\dot{\underline{M}} = (\underline{F}-\underline{G}\underline{R}^{-1}\underline{G}^T\underline{W})^T\underline{M}_1 - \underline{Q}\underline{R}_1 \tag{A9.3}$$

The boundary condition is

$\underline{M}_1(t_1) = 0$

and the optimal control

$$\underline{u}_{opt} = -\underline{R}^{-1}\underline{G}^T(\underline{W}\underline{X} + \underline{M}_1) \tag{A9.4}$$

Discrete minimisation produces the recursive Riccati equations together with the difference equation

$$\underline{M}(N-K)T) = \underline{D}(T,KT)\underline{M}(N-(K+1)T) + \underline{E}(T,KT)\underline{R}((N-(K+1)T) \tag{A9.5}$$

having the boundary condition

$\underline{M}(N-1) = 0$

and the optimal control at the kth instant

$$\underline{U}(KT)_{OPT} = -\underline{S}\{[N-(K+1)]T\}\,\underline{X}(KT) - \underline{R}^{-1}\underline{G}^T\underline{M}_1\{[N-(K+1)]T\} \tag{A9.6}$$

The deterministic optimal controller for a ship tracking system is shown in Figure A9.1

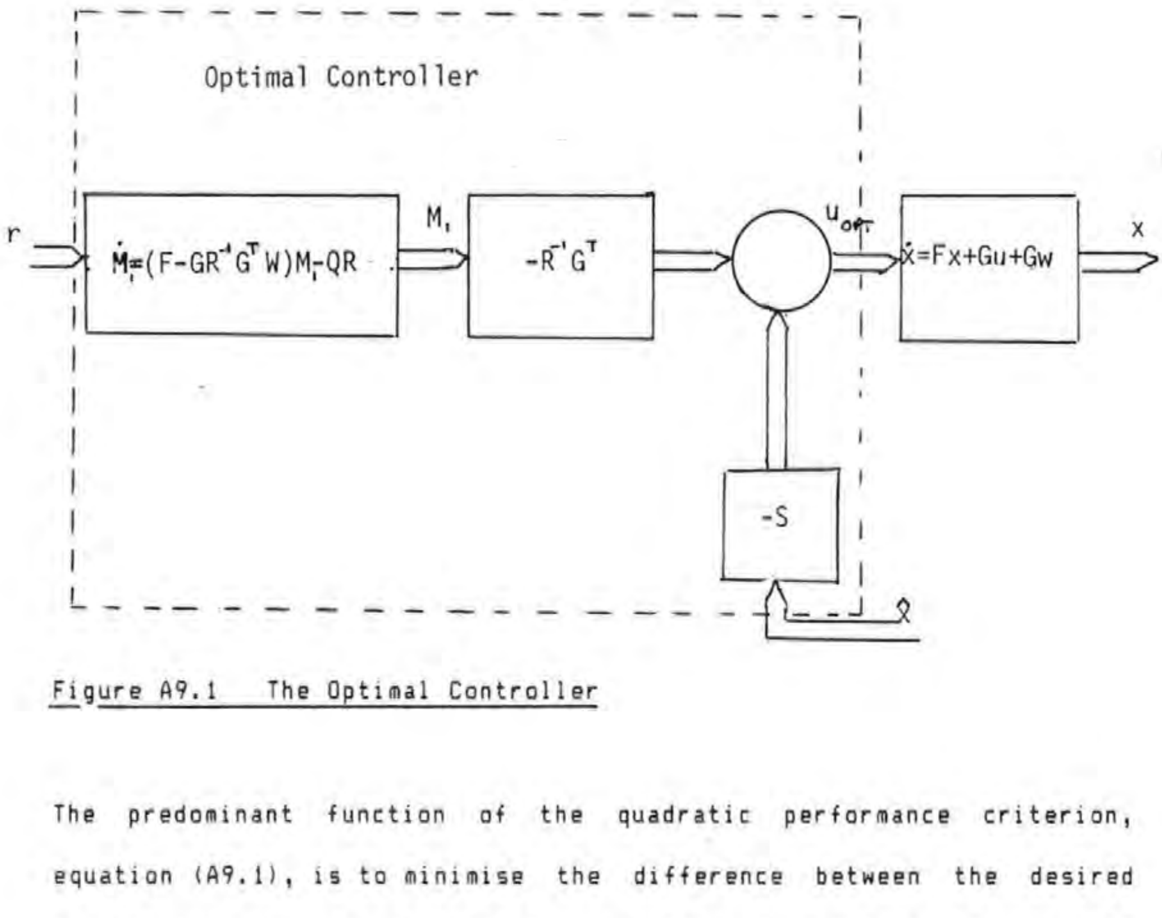

Figure A9.1 The Optimal Controller

The predominant function of the quadratic performance criterion, equation (A9.1), is to minimise the difference between the desired states and the actual states. A second cost term in the criterion limits the magnitude of the control. Without this term, the criterion would be impractical, giving rise to infinitely large controls.

The relative weighting of the elements in the diagonal Q matrix determines which of the states track to the greatest accuracy. The matrix R, is chosen so that the control u stays within the bounds of an admissable set of control values. The relative values of Q and R are changed during alterations of course, when the course control dominates. During the remainder of each passage the track control dominates. For a tracking system of this type, an optimal control can only be found if the desired state trajectory is known beforehand.

A9.3 Controller Subroutines

The function of the optimal controller is undertaken by subroutine OPTCON. Prior to harbour passage however subroutine RICAL calculates the Riccatti Feedback matrix and the command matrix, whilst subroutine RICATI is used to obtain a discrete solution of the matrix Riccatti Equation. RICAL also calls subroutine TRACK to generate the reverse time discrete tracking matrices. During the passage the optimal controller then continually updates the control by differencing VFOR with the product of the feedback gain matrix and the best estimate of state, so producing the optimal control.

Variables used in these subroutines and not previously defined are:-

VFOR(2,500)	Command Matrix
S(2,8)	Feedback Gain Matrix
RIN(8,500)	Desired State Matrix
REVIN(8,500)	Reverse time desired states
X1,Y1	Way points
RIN7	Desired heading along each leg of a passage

```
      SUBROUTINE OPTCON(XOLD,K,S,VFOR,UD1,UD2,U,N,NB,NX,NN,
     &TSAMP,DRUDD,MODE,ABCER,CERROR,XO,YO,RIN7,YI,XI,XHAT5)
C
C * SUBROUTINE TO COMPUTE OPTIMAL CONTROL LAW
C
      REAL*4 XOLD(8),VFOR(2,500),S(2,8),SX(2),U(2),DRUDD(500)
      REAL*4 XO(250),YO(250)
      COMMON RIN(8,500),YOUT(8,250)
C
C
C * RECALULATE XOLD(5) USING CO-ORDINATE TRANSFORMATION
C
      IF(K.GT.46) GO TO 21
      YI=2590.0
      XI=0.0
      RIN7=-0.173076
      GO TO 22
 21   IF(K.GT.79) GO TO 23
      YI=2290.974
      XI=1710.378
      RIN7=0.7135
      GO TO 22
 23   IF(K.GT.129) GO TO 24
      YI=3124.321
      XI=2673.084
      RIN7=1.209397
      GO TO 22
 24   YI=4928.924
      XI=3355.213
      RIN7=0.0
C
 22   XHAT5=XOLD(5)
      XOLD(5)=(YO(K)-YI)*COS(RIN7)-(XO(K)-XI)*SIN(RIN7)
C
C * UOPT=VFOR-S*X
C
C * CHANGE TO COURSE-KEEPING
C * IF COURSE ERROR EXCEEDS 20 DEGREES.
C
      WRITE(1,101)XOLD(5)
  101 FORMAT('TERROR='F10.5)
      CERROR=RIN(7,K)-XOLD(7)
      ABCER=ABS(CERROR)
      IF(ABCER.GT.0.349) GOTO 18
      CALL MATMUL(SX,S,XOLD,NB,N,NX,NN)
      U(1)=VFOR(1,K)-SX(1)+UD1
      GO TO 19
   18 U(1)=-(CERROR-30.0*XOLD(8))+UD1
   19 U(2)=VFOR(2,K)-SX(2)+UD2
      U2UL=1.5*RIN(2,K)
      U2LL=0.5*RIN(2,K)
      IF(U(2).GT.U2UL) U(2)=U2UL
      IF(U(2).LT.U2LL) U(2)=U2LL
C
      XOLD(5)=XHAT5
      IF(MODE)1,1,2
```

```
C
C MAXIMUM RUDDER ANGLE = +OR- 0.6RADIANS
C
    1 IF(U(1).LT.0.610865) GOTO 3
      U(1)=0.610865
    3 CONTINUE
      IF(U(1).GT.-0.610865) GOTO 5
      U(1)=-0.610865
    5 CONTINUE
C
C MAXIMUM RATE OF CHANGE OF RUDDER IS 2.5DEG/SEC.
C
C
C MAXRTE IS MAXIMUM RATE OF CHANGE OF RUDDER ANGLE
C CURRTE IS CURRENT RATE OF CHANGE OF RUDDER ANGLE
C
      MAXRTE=0.0436332313
      IF(K-1)12,12,13
   12 CURRTE=U(1)/TSAMP
      IF(CURRTE.LT.0.0436) GOTO 14
      U(1)=0.0436*TSAMP
   14 CONTINUE
      IF(CURRTE.GT.-0.0436) GOTO 66
      U(1)=-0.0436*TSAMP
      GO TO 66
   13 CURRTE=(U(1)-DRUDD(K-1))/TSAMP
      IF(CURRTE.LT.0.0436) GOTO 44
      U(1)=DRUDD(K-1)+(0.0436*TSAMP)
   44 CONTINUE
      IF(CURRTE.GT.-0.0436) GOTO 66
      U(1)=DRUDD(K-1)-(0.0436*TSAMP)
   66 CONTINUE
C
C
    2 RETURN
      END
```

```
      SUBROUTINE RICAL(F,G,GU,AA,BB,Q,R,S,W,
     &XD,YD,VFOR,TSAMP,N,NB,NM,NN,IFIN)
C
C * SUBROUTINE CALCULATES THE RICCATI FEEDBACK MATRIX
C * AND COMMAND MATRIX
C
      REAL*4 AA(8,8),BB(8,2),Q(8,8),R(2,2),W(8,8),WP1(8,8)
      REAL*4 S(2,8),F(8,8),G(8,6),GU(8,2),D(8,8),E(8,8)
      REAL*4 REVIN(8,500),GT(2,8),RGT(2,8)
      REAL*4 RGTM(2,8),UREV(8),DM(8,1),EU(8,1)
      REAL*4 OLDM(8),VREV(2),VFOR(2,500),C(8,4)
      REAL*4 XD(500),YD(500)
      COMMON RIN(8,500),YOUT(8,250)
C
C * PUT W MATRIX TO TERMINAL(NULL)VALUE
      DO 15 J=1,N
      DO 15 I=1,N
 15   W(I,J)=0.0
C
      DO 10 M=1,IFIN
      CALL RICATI(AA,BB,Q,R,S,W,WP1,TSAMP,N,NB,NN)
C
C * UPDATE W MATRIX
C
      DO 20 J=1,N
      DO 20 I=1,N
   20 W(I,J)=WP1(I,J)
   10 CONTINUE
      S(1,3)=-S(1,3)
      S(1,5)=-S(1,5)
C     CALL MATPRN(S,NB,N,NN,6HS      )
C     CALL MATPRN(W,N,N,NN,6HW      )
      WRITE(1,114)
  114 FORMAT(1H ,'OK')
C
C * DETERMINE GU(8X2) MATRIX FROM G(8X6)
C
      DO 45 I=1,N
      DO 45 J=1,NB
   45 GU(I,J)=G(I,J)
C * CALCULATE REVERSE TIME TRACKING MATRICES D AND E
      CALL TRACK(F,GU,R,Q,W,S,D,E,TSAMP,N,NB,NN)
C     CALL MATPRN(D,N,N,NN,6HD      )
C     CALL MATPRN(E,N,N,NN,6HE      )
C
C * GENERATE DESIRED STATES
C * INITIALISE
C
      CALL MATZER(RIN,N,IFIN,NN)
C
C * RIN IS THE DESIRED STATE MATRIX:
C   RIN(1)= DELTD    RIN(2)=ND
C   RIN(3)= XOD      RIN(4)=UD
C   RIN(5)= YOD      RIN(6)=VD
C   RIN(7)=PSID      RIN(8)=RD
C
```

```
      RIN(2,1)=6.439
      RIN(3,1)=0.0
      RIN(4,1)=7.717
      RIN(5,1)=0.0
      RIN(7,1)=-0.173076
      XD(1)=0.0
      YD(1)=2590.0
C
C * STAGE ONE
      DO 30 I=2,46
      RIN(2,I)=6.439
      RIN(4,I)=7.717
      RIN(3,I)=RIN(3,I-1)+RIN(4,I)*TSAMP
 30   RIN(7,I)=-0.173076
C
C * STAGE TWO
      DO 32 I=47,79
      RIN(2,I)=6.439
      RIN(4,I)=7.717
      RIN(3,I)=RIN(3,I-1)+RIN(4,I)*TSAMP
 32   RIN(7,I)=0.7135
C
C * STAGE THREE
      DO 34 I=80,129
      RIN(2,I)=6.439
      RIN(4,I)=7.717
      RIN(3,I)=RIN(3,I-1)+RIN(4,I)*TSAMP
 34   RIN(7,I)=1.209397
C
C * STAGE FOUR
      DO 36 I=130,IFIN
      RIN(2,I)=6.439
      RIN(4,I)=7.717
      RIN(3,I)=RIN(3,I-1)+RIN(4,I)*TSAMP
 36   RIN(7,I)=0.0
      DO 39 I=2,IFIN
      XD(I)=XD(I-1)+RIN(4,I)*TSAMP*COS(RIN(7,I))
   39 YD(I)=YD(I-1)+RIN(4,I)*TSAMP*SIN(RIN(7,I))
      DO 41 J=38,46
      RIN(7,J)=0.7135
   41 CONTINUE
      DO 42 J=70,79
      RIN(7,J)=1.209397
   42 CONTINUE
      DO 43 J=116,129
      RIN(7,J)=0.0
   43 CONTINUE
C     WRITE(6,107)
C 107 FORMAT(1H ,'DESIRED STATE MATRIX RIN')
C     DO 37 J=1,IFIN
C     WRITE(6,108)J,(RIN(I,J),I=1,N)
C  37 CONTINUE
C 108 FORMAT(I5,1X,8E14.7)
C
C * REVERSE TIME DESIRED STATES
      DO 40 J=1,IFIN
```

```
      NBACK=IFIN-(J-1)
      DO 40 I=1,N
   40 REVIN(I,J)=RIN(I,NBACK)
C     WRITE(6,109)
C 109 FORMAT(1H ,'REVERSE TIME DESIRED STATES REVIN')
C     DO 38 J=1,IFIN
C     WRITE(6,108)J,(REVIN(I,J),I=1,N)
C  38 CONTINUE
C
C * REVERSE-TIME TRACKING USING THE DISCRETE EQUATION:
C     M(K+1)=D(T)*M(K)+E(T)*UREV(K)
C * INITIALISE AT TERMINAL TIME
      CALL MATRED(OLDM,N,NM,NN)
C     CALL MATPRN(OLDM,N,NM,NN,6HMOLD   )
C
C * CALCULATE  -R**-1*G'
      ONEM=-1.0
      CALL MATINV(R,NB,NB)
C
      CALL MATRNS(GT,GU,N,NB,NN)
      CALL MATMUL(RGT,R,GT,NB,NB,N,NN)
      CALL MATSCL(RGTM,ONEM,RGT,NB,N,NN)
C
      DO 60 K=1,IFIN
      DO 70 I=1,N
   70 UREV(I)=REVIN(I,K)
      CALL MATMUL(DM,D,OLDM,N,N,NM,NN)
      CALL MATMUL(EU,E,UREV,N,N,NM,NN)
      CALL MATADD(OLDM,DM,EU,N,NM,NN)
      CALL MATMUL(VREV,RGTM,OLDM,NB,N,NM,NN)
      NFOR=IFIN-(K-1)
      DO 80 I=1,NB
   80 VFOR(I,NFOR)=VREV(I)
   60 CONTINUE
C
C * RECALCULATE VFOR
C
      DO 65 K=1,IFIN
      VFOR(1,K)=0.0
      VFOR(2,K)=0.0
      DO 64 I=1,N
      VFOR(1,K)=VFOR(1,K)+S(1,I)*RIN(I,K)
 64   VFOR(2,K)=VFOR(2,K)+S(2,I)*RIN(I,K)
 65   VFOR(2,K)=VFOR(2,K)+6.439
C
      T=0.0
C     WRITE(6,103)
C     DO 95 I=1,IFIN
C     WRITE(6,104)T,VFOR(1,I),VFOR(2,I)
C  95 T=T+TSAMP
C 103 FORMAT(1H ,3X'TIME(S)',6X,'RUDDER COMMAND',6X,'ENGINE C
OMMAND')
C 104 FORMAT(1H ,3(6X,E14.7))
C
      RETURN
      END
```

```
      SUBROUTINE RICATI(A,B,Q,R,S,W,WP1,TSAMP,N,NB,NN)
C
C *****DISCRETE SOLUTION OF THE MATRIX RICCATI EQUATION*****
C
      REAL*4 PA(8,8),BS(8,8),BSM(8,8),V(8,8),VT(8,8),VTW(8,8)
      REAL*4 VTWV(8,8),B(8,2),BT(2,8),BTW(2,8),W(8,8),WP1(8,8)
      REAL*4 BTWB(2,2),R(2,2),TR(2,2),TRBTWB(2,2)
      REAL*4 A(8,8),BTWA(2,8),S(2,8),ST(8,2)
      REAL*4 STT(8,2),STTR(8,2),STTRS(8,8),Q(8,8),QT(8,8)
C
C     S=(T*R+B'*W*B)**-1*B'*W*A
C     WHERE T IS A SCALAR,R A 2X2 DIAGONAL MATRIX
C                         B A 8X2 MATRIX
C                         W A 8X8 SQUARE MATRIX
C                         A A 8X8 SQUARE MATRIX
C                         S A 2X8 MATRIX
C
C * TRANSPOSE OF B MATRIX
      CALL MATRNS(BT,B,N,NB,NN)
C
C * PRODUCT OF B' AND W
      CALL MATMUL(BTW,BT,W,NB,N,N,NN)
C
C * PRODUCT OF BTW AND B
      CALL MATMUL(BTWB,BTW,B,NB,N,NB,NN)
C
C * PRODUCT OF SCALAR TSAMP AND MATRIX R
      CALL MATSCL(TR,TSAMP,R,NB,NB,NN)
C
C * ADD MATRICES TR AND BTWB
      CALL MATADD(TRBTWB,TR,BTWB,NB,NB,NN)
C
C * INVERT MATRIX TRBTWB
      CALL MATINV(TRBTWB,NB,NB)
C
C * PRODUCT OF BTW AND A
      CALL MATMUL(BTWA,BTW,A,NB,N,N,NN)
C
C * COMPUTE S MATRIX
      CALL MATMUL(S,TRBTWB,BTWA,NB,NB,N,NN)
C
C     WP1=(T*Q+S'*T*R*S)+(A-B*S)'*W*(A-B*S)
C     WHERE Q IS A 8X8 DIAGONAL MATRIX
C     W,S,T,R,A AND B DEFINED EARLIER
C
C * TRANSPOSE OF S MATRIX
      CALL MATRNS(ST,S,NB,N,NN)
C
C * PRODUCT OF S' AND SCALAR TSAMP
      CALL MATSCL(STT,TSAMP,ST,N,NB,NN)
C
C * PRODUCT OF STT AND R
      CALL MATMUL(STTR,STT,R,N,NB,NB,NN)
C * PRODUCT OF STTR AND S
      CALL MATMUL(STTRS,STTR,S,N,NB,N,NN)
C
```

```
C * PRODUCT OF Q AND SCALAR TSAMP
      CALL MATSCL(QT, TSAMP, Q, N, N, NN)
C
C * ADD QT AND STTRS
      CALL MATADD(PA, QT, STTRS, N, N, NN)
C
      ONEM=-1.0
C
C * PRODUCT OF B AND S
      CALL MATMUL(BS, B, S, N, NB, N, NN)
      CALL MATSCL(BSM, ONEM, BS, N, N, NN)
      CALL MATADD(V, A, BSM, N, N, NN)
C
C * TRANSPOSE OF V
      CALL MATRNS(VT, V, N, N, NN)
C
C * PRODUCT OF VT AND W AND V
      CALL MATMUL(VTW, VT, W, N, N, N, NN)
      CALL MATMUL(VTWV, VTW, V, N, N, N, NN)
C
C * NEW VALUE FOR W MATRIX=WP1
      CALL MATADD(WP1, PA, VTWV, N, N, NN)
C
      RETURN
      END
```

```
      SUBROUTINE TRACK(F,GU,R,Q,W,S,D,E,TSAMP,N,NB,NN)
C
C * THE SUBROUTINE GENERATES THE REVERSE TIME DISCRETE
C * TRACKING MATRICES D AND E BY SOLVING THE EQUATION:
C   MDOT=FF*M+GG*RIN
C   WHERE,  FF=(F-G*R**-1*G'*W)'
C           GG=-Q
C           R**-1*G'*W=S
C
      REAL*4 F(8,8),GU(8,2),R(2,2),Q(8,8),W(8,8),S(2,8)
      REAL*4 D(8,8),E(8,8),GM(8,2),GMS(8,8),FGMS(8,8)
      REAL*4 FF(8,8),GG(8,8)
C
      ONEM=-1.0
      CALL MATSCL(GM,ONEM,GU,N,NB,NN)
C
C * PRODUCT OF -G AND S
      CALL MATMUL(GMS,GM,S,N,NB,N,NN)
C
C * ADD F AND GMS
      CALL MATADD(FGMS,F,GMS,N,N,NN)
C
C * FF IS TRANSPOSE OF FGMS
      CALL MATRNS(FF,FGMS,N,N,NN)
C
C * GG IS -Q
      CALL MATSCL(GG,ONEM,Q,N,N,NN)
C
C * USE REVMAT(REVERSE TRNMAT) TO FIND DISCRETE MATRICES D AND
 E
      CALL REVMAT(FF,GG,D,E,N,N,TSAMP,NN)
C
      RETURN
      END
```

```
      SUBROUTINE REVMAT(F,G,A,B,N,NG,TSAMP,NN)
C
C EVALUATES DISCRETE STATE TRANSITION MATRIX A(T)
C AND DISCRETE FORCING MATRIX B(T)
C
      REAL*4 ST(8,8),F(8,8),A(8,8),INTEGA(8,8),B(8,8),G(8,8)
      REAL INTEGA
      INTEGER POWER
      NORMFT=0.0
      DO 1 I=1,N
      DO 1 J=1,N
      ST(I,J)=F(I,J)*TSAMP
    1 A(I,J)=ST(I,J)
      POWER=50
      DO 7 I=2,POWER
      FPOWR=POWER-I+2
      DO 5 J=1,N
      DO 3 K=1,N
    3 INTEGA(J,K)=A(J,K)/FPOWR
    5 INTEGA(J,J)=INTEGA(J,J)+1.0
      CALL MATMUL(A,ST,INTEGA,N,N,N,NN)
    7 CONTINUE
      DO 9 J=1,N
      A(J,J)=A(J,J)+1.0
      DO 9 K=1,N
    9 INTEGA(J,K)=TSAMP*INTEGA(J,K)
      CALL MATMUL(B,INTEGA,G,N,N,NG,NN)
C
      RETURN
      END
```

APPENDIX 10

COMPUTER DETAILS

A10.1 Prime Mainframe Computer

Plymouth Polytechnic runs a dual-processor Prime computer system (Prime 9950/850) with a total of 16 million bytes of memory, five 300 million-byte disc drives and two 600 million-byte disc drives. Both processors have a line printer and magnetic tape facilities. The processors communicate with each other via a PRIMENET network, allowing resources to be shared between the processors, which run under control of the Prime operating system, PRIMOS. Access to the system is currently by means of up to 164 terminal lines, and batch queues which allow jobs to be run independently of terminals. Networked connections to other computer systems will provide access to an increasing range of other computing services.

The main components of the system are:-

Processor A	Prime 9950 with 10 MB memory 1x600, 3x300 MB disc
Processor B	Prime 850 with 6 MB memory 1x600, 2x300 MB disc file storage
Line Printers	1 at 480 lines/minute, 2 at 300 lines minute
Graph Plotter	CalComp 1039 plotter Paper Tape Reader - 300 characters/second

	Punch - 120 characters/second
Floppy disc	Two 8" industry-compatible units
Magnetic disc	Four dual-density nine-track units
Digitiser	CalComp digitiser with A0 size digitising area.

A10.2 Microcomputer

The Texas Instruments 16 bit microcomputer used in the physical model consisted of the following components:-

TM 990/101M	MICROPROCESSOR	4K RAM	8K EPROM
TM 990/302	SOFTWARE DEVELOPMENT	16K RAM	8K EPROM
TM 990/201-43	MEMORY EXPANSION	64K RAM	16K EPROM
TM 990/1241	A-D/D-A CONVERTER		

Photocopy of a paper presented at an International Symposium on Multivariable Control Systems held under the auspices of The Institute of Measurement and Control at the Royal Naval Engineering College, Manadon, Plymouth in October 1982.

AUTOMATIC PILOTAGE OF LARGE SHIPS IN CONFINED WATERS - A MULTIVARIABLE APPROACH

R.S. Burns, M.J. Dove, T.H. Bouncer.
Plymouth Polytechnic.

The feasability of a guidance system for automatically controlling a large ship in the pilotage phase of a voyage is investigated. Identification, Optimal Control and Estimation Techniques are applied to a mathematical model of a vessel in the approaches to Plymouth.

INTRODUCTION

It is beyond question that the overall standard of navigation at sea is very high indeed, and the probability of completing a voyage successfully must be very close to unity. However, (1), a brief summary of marine traffic accidents shows that the majority occur within congested waters, particularly within port limits. Congestion, coupled with the increased size and complexity of operation, Has focussed attention on the control of pilotage and berthing, for, not only must the safety and cost factors be considered, but also the environmental aspects of, say, the spillage of large quantities of crude oil at, or near, the approaches to a port.

This paper investigates the possibilities of employing multivariable control theory to the problem of automatically piloting a large vessel in the approaches to a port.

A discrete, time-varying non-linear model has been developed based upon eight system states, namely forward and lateral position and velocity, heading, yaw-rate, rudder angle and engine speed. The model has two deterministic inputs - demanded rudder and engine speed plus four stochastic disturbance inputs in the form of wind and current vectors. The measurements of the state vector, contaminated with random noise, are passed through an optimal, time-varying filter.

The best estimate of the state variables are used by an adaptive optimal controller to compute those inputs (demanded rudder and engine speed) which minimise a given performance criterion. The dynamics of both the filter and controller are updated frequently by a system identification algorithm that can be either based upon apriori knowledge of the hydrodynamic coefficients of the vessel, or by on-line measurements of the state variables.

An outline of the proposed system is given in Figure 1.

MATHEMATICAL MODEL

Equations of Motion

The ship is considered to be a rigid body with three degrees of freedom, in surge, sway and yaw. Ship motions in the other three degrees of freedom, roll, pitch and heave are considered small enough to be neglected. It is convenient to describe the motion in terms of a moving system of axes coincident with the mass centre of the hull as illustrated in Figure 2. This gives rise to an Eulerian set of equations of motion which may be written in the form

$$
\begin{aligned}
m\dot{u} - mr\nu &= X \\
m\dot{\nu} + mur &= Y \\
I_z\dot{r} &= N
\end{aligned}
\qquad \text{(1)}
$$

Techniques employed in obtaining expressions for hydrodynamic forces and moments are well covered in the literature (2) and the usual method is to apply a Taylor series expansion. For applications such as course-keeping, where changes in rudder and heading angles do not usually exceed five degrees, a linear approximation, using only the first order terms in the expansion, is normally quite adequate. In a track-keeping situation where large changes in heading can be expected, it becomes necessary to include second and third order expansion terms.

Surge Equation. The complete surge equation in dimensionalised form is

$$
\begin{aligned}
m\dot{u} - mr\nu = {} & X_{\dot{u}}\dot{u} + X_u(u + u_c) + \overline{X}_{uu}u^2 + \overline{X}_{uuu}u^3 + \overline{X}_{\nu\nu}\nu^2 + \overline{X}_{rr}r^2 + \overline{X}_{\delta\delta}\delta_A{}^2 + \overline{X}_{uu}un_A + \overline{X}_{nn}n_A{}^2 \\
& + X_{u_a}u_a \qquad \text{(2)}
\end{aligned}
$$

In the above equation a shorthand subscript and bar notation has been adopted, for instance

$$
X_u = \frac{\partial X}{\partial u}, \quad \overline{X}_{uu} = \tfrac{1}{2}X_{uu} = \tfrac{1}{2}\left(\frac{\partial^2 X}{\partial u^2}\right)
$$

The dimensionalised hydrodynamic coefficients are obtained from the non-dimensional values in the usual manner

$$
X_u = (\tfrac{1}{2}\rho L^2 U)X_u{}'
$$

Sway and Yaw Equations. The dimensionalised sway and yaw equations are

$$
\begin{aligned}
m\dot{\nu} + mur = {} & Y_{\dot{\nu}}\dot{\nu} + Y_\nu(\nu + \nu_c) + Y_{\dot{r}}\dot{r} + Y_r r + \overline{Y}_{nn}n_A{}^2 + \overline{Y}_{\nu\nu\nu}\nu^3 + \overline{Y}_{r\nu\nu}r\nu^2 + \overline{Y}_{nn\delta}n_A{}^2\delta_A + \overline{Y}_{nn\delta\delta\delta}n_A{}^2\delta_A{}^3 \\
& + \overline{Y}_{\delta\nu\nu}\delta_A\nu^2 + Y_{\nu_a}\nu_a \qquad \text{(3)}
\end{aligned}
$$

$$I_z\dot{r} = N_{\dot{v}}\dot{v} + N_v(v + v_c) + N_{\dot{r}}\dot{r} + N_r r + \overline{Y}_{nn}n_A{}^2 + \overline{N}_{vvv}v^3 + \overline{N}_{rvv}rv^2 + \overline{N}_{nn\delta}n_A{}^2\delta_A + \overline{N}_{nn\delta\delta\delta}n_A{}^2\delta_A{}^3$$

$$+ \overline{Y}_{\delta vv}\delta_A v^2 + Y_{v_a}v_a \quad \ldots\ldots \quad (4)$$

<u>Steering Gear and Main Engine</u>. These are both modelled by first order linear differential equations

$$\dot{\delta}_A = \frac{1}{T_R}\delta_D - \frac{1}{T_R}\delta_A \quad \ldots\ldots \quad (5)$$

$$\dot{n}_A = \frac{1}{T_N}n_D - \frac{1}{T_N}n_A \quad \ldots\ldots \quad (6)$$

Where δ_D and n_D are the demanded rudder angle and demanded engine speed respectively.

<u>State Space Formulation</u>

Much attention was devoted to the choice of state variables in relationship to the tracking problem and the state vector was finally based on the ship body axes

$$\chi^T = (\delta_A \; n_A \; x \; u \; y \; v \; \psi \; r) \quad \ldots\ldots \quad (7)$$

This state is affected by the forcing vector

$$U^T = (\delta_D \; n_D \; u_c \; v_c \; u_a \; v_a) \quad \ldots\ldots \quad (8)$$

Equations (5), (6), (2), (3) and (4) can be arranged in the following set

$$\begin{aligned}
\dot{\delta}_A &= -\frac{1}{T_R}\delta_A + \frac{1}{T_R}\delta_D \\
\dot{n}_A &= -\frac{1}{T_N}n_A + \frac{1}{T_N}n_D \\
\dot{x} &= u \\
\dot{u} &= A_1\delta_A + A_2 n_A + A_4 u + A_6 v + A_8 r + A_{u3}u_c + A_{u5}u_a \\
\dot{y} &= v \\
\dot{v} &= B_1\delta_A + B_2 n_A + B_4 u + B_6 v + B_8 r + B_{u4}v_c + B_{u6}v_a \\
\dot{\psi} &= r \\
\dot{r} &= C_1\delta_A + C_2 n_A + C_4 u + C_6 v + C_8 r + C_{u4}v_c + C_{u6}v_a
\end{aligned} \quad \ldots\ldots \quad (9)$$

The coefficients A, B, and C are all time-varying and so, for example

$$A_1 = \frac{\overline{X}_{\delta\delta}.\delta_A}{m - X_{\dot{u}}} = \frac{(\frac{1}{2}\rho L^2 U).\overline{X}'_{\delta\delta}\delta_A}{m - X_{\dot{u}}}$$

A_1, therefore, is a function of the instantaneous total velocity U and rudder angle δ_A.

Equation set (9) represent the time-varying state equations for the ship and are expressed by the state matrix vector differential equation

$$\dot{\mathbb{X}}(t) = \mathbb{F}(t)\mathbb{X}(t) + \mathbb{G}(t)\mathbb{U}(t) \quad \text{..........} \quad (10)$$

It is convenient to partition the $\mathbb{G}$ matrix in terms of the control forcing function δ_A and n_A and the disturbance forcing functions u_c, ν_c, u_a and ν_a so that

$$\dot{\mathbb{X}}(t) = \mathbb{F}(t)\mathbb{X}(t) + \mathbb{G}_C(t)\mathbb{U}(t) + \mathbb{G}_D(t)W(t) \quad \text{..........} \quad (11)$$

The corresponding discrete solution is

$$\mathbb{X}((K + 1)T) = \mathbb{A}(T, KT)\mathbb{X}(KT) + \mathbb{B}(T, KT)\mathbb{U}(KT) + \mathbb{C}(T,KT)W(KT) \quad \text{..........} \quad (12)$$

MEASUREMENT AND FILTERING

Separation Principle

This is an important feature of stochastic optimal control theory that allows a given optimisation problem to be reduced into two problems whose solutions are known, namely an optimal filter in cascade with a deterministic optimal controller.

The Measurement Process. The measured state $\mathbb{Z}(K + 1)$ is considered to contain noise $V(K + 1)$, where $V(K + 1)$ is a stationary gaussian process with convariance $\mathbb{M}$. The measurement process is then represented by

$$\mathbb{Z}((K + 1)T) = \mathbb{H}((K + 1)T)\mathbb{X}((K + 1)T) + V((K + 1)T) \quad \text{..........} \quad (13)$$

Estimation of the State Vector

The Kalman filter used here is a recursive computational algorithm which remembers past data, receives future positions, and bases the estimate of the state upon a combination of past and present information. It should be noted however that this technique assumes the system is linear and the errors gaussian. As a ship constitutes a non-linear system, when parameters such as large alterations of course and speed, shallow water effects, and trim are considered there must be some limitations to the technique.

The filter is characterised by containing a model of the ship and the equations are

$$\hat{X}((K+1)T) = A(T,KT)\hat{X}(KT) + K((K+1)T)\left[Z((K+1)T) - H((K+1)T)A(T,KT)\hat{X}(KT)\right] \quad \ldots\ldots\ldots\ldots \quad (14)$$

The filter gain matrix $K(K+1)$ and the two covariance matrices $P(K+1/K)$, $P(K+1/K+1)$ are governed by

$$P(K+1/K) = A(T,KT)P(K/K)A^T(T,KT) + B(T,KT)N(K/K)B^T(T,KT)$$

$$K((K+1)T) = P(K+1/K)H^T((K+1)T)\left[H((K+1)T)P(K+1/K)H^T((K+1)T) + M((K+1)T)\right]^{-1} \quad \ldots \quad (15)$$

$$P(K+1/K+1) = \left[I - K((K+1)T)H((K+1)T)\right]P(K+1/K)$$

In determining the value of the filter gain matrix consideration has to be given to the control vector $U(KT)$ and its associated control matrix $B(T,KT)$. A model of $B(T,KT)$ is required in the filter and the complete filter model is shown in Figure 3, leading to the overall filter equations as

$$\hat{X}((K+1)T) = A(T,KT)\hat{X}(K/K) + B(T,KT)U(KT) + K((K+1)T)\Big[Z((K+1)T) - H((K+1)T)\Big\{A(T,KT)\hat{X}(KT) + B((T,KT)U(KT)\Big\}\Big] \quad \ldots\ldots\ldots \quad (16)$$

CONTROLLER DESIGN

Stochastic Optimal Control

The stochastic optimal control problem is to find a control U which causes the system

$$\dot{X} = g(X(t),\ U(t),\ W(t),t)$$

to follow an optimal trajectory $X(t)$ that minimises a performance criterion

$$J = \int_{t_0}^{t_1} h(X(t),\ U(t),t)dt$$

whilst being subjected to a measurement process

$$Z = f(X(t),\ V(t),t)$$

Deterministic Optimal Control

Tracking Problem with Quadratic Performance Criterion. The tracking or servomechanism problem is one of applying a control U to drive a ship so that its states follow a desired trajectory in some optimal sense. The regulator problem is a special case of the tracking problem, the desired trajectory being a zero state.

Continuous Form. The quadratic criterion to be minimised is

$$J = \int_{t_0}^{t_1} \left\{ (X - R)^T Q(X - R) + U^T R U \right\} dt \qquad (17)$$

where R is the desired value of the state vector it can be shown (3) that constrained functional minimisation yields the matrix Riccati equations

$$\dot{W} = -WF - F^T W - Q + WGR^{-1} G^T W \qquad (18)$$

together with the reverse-time differential equation set

$$\dot{M} = (F - GR^{-1} G^T W)^T M - QR \qquad (19)$$

The boundary condition is

$$M(t_1) = 0$$

and the optimal control

$$U_{opt} = -R^{-1} G^T (WX + M) \qquad (20)$$

Discrete Form. Discrete minimisation produces the recursive Riccati equations together with the difference equation

$$M_{((N-K)T)} = D(T,KT) M_{((N-(K+1)T)} + E(T,KT) R_{((N-(K+1)T)} \qquad (21)$$

having the boundary condition

$$M_{(N-1)} = 0$$

and the optimal control at the K^{th} instant

$$U(KT)_{opt} = -S_{((N-(K+1))T)} X(KT) - R^{-1} G^T M_{((N-(K+1))T)} \qquad (22)$$

The deterministic optimal controller for a ship tracking system is shown in Figure 4.

IDENTIFICATION

Method of Linear Least Squares

Put $\quad J = \Sigma(N_i^2),\ i = 0,1,2,3,\ldots,K$

$$= N_i^T N_i$$

$$= (Z_i - Y\beta)^T (Z_i - Y\beta)$$

If we differentiate with respect to $\hat{\beta}$ and set $\frac{\partial}{\partial \hat{\beta}}(J(\hat{\beta})) = 0$, we obtain the L.L.S. estimate given by

$$\hat{\beta} = P_K Y^T Z \qquad (23)$$

where

$$P_K^{-1} = Y^T Y$$

A recursive form of equation (23) is available, which has the form

$$P_{K+1} = P_K - P_K Y(1 + Y^T P_K Y)^{-1} Y^T P_K \qquad (24)$$

$$\hat{\beta}_{K+1} = \hat{\beta}_K + P_{K+1} Y(Z - Y^T \hat{\beta}_K) \qquad (25)$$

The pair of equations 24 and 25 enable revised estimates of the parameter matrix $\hat{\beta}_{K+1}$ to be calculated from the prior estimate $\hat{\beta}_K$, based on a knowledge of Y^T and Z obtained by measurements made at the (K+1)th sampling instant.

COMPUTER SIMULATION

The vessel chosen for the simulation was of the Mariner Class. Good agreement between full-scale test results and data obtained from the mathematical model was found with all standard manoeuvres and Figure 5 shows a typical turning circle for 20 degree starboard rudder. The recommended track for deep draught vessels into Plymouth Sound was selected as a suitable design specification for the automatic guidance system. This requires simultaneous control of the ship's position, heading and forward velocity and implementation of the matrix control equation (22) produces the optimal trajectory illustrated in Figure 6 when the desired forward speed is 7.717 m/s (15 knots).

CONCLUSIONS

Much work is still to be done before automatic guidance systems of the type described here are actually fitted to surface ships. Manufacturers are, however, already moving towards the replacement of conventional analogue auto-pilots with adaptive micrprocessor based minimum energy course-keeping systems and the possibility exists that in the none to distant future a new generation of auto-pilots with both course and track-keeping facilities will emerge.

REFERENCES

1. Dove, M.J., 1974, "Automatic Control of Large Ships in Pilotage and Berthing", J.Inst. Nav. (U.K.) 27, 4.

2. Abkowitz, M., 1964, "Lectures on Ship Hydrodynamics, Steering and manoeuvrability", Hy-A Report, Hy. 5., Denmark.

3. Kirk, D.E., 1970, "Optimal Control Theory - An Introduction", Prentice-Hall Inc., New Jersey.

NOTATION

Matrices and Vectors

A	Discrete State Transition Matrix.
B	Discrete Control Matrix.
C	Discrete Disturbance Matrix.
D	Discrete Reverse Transition Matrix.
E	Discrete Reverse Control Matrix.
F	Continuous Time System Matrix.
G	Continuous Time Forcing Matrix.
H	Measurement Matrix.
K	Kalman Gain Matrix.
M	Covariance of Noise Vector.
M	Reverse Time State Vector.
N	Covariance of Control Vector.
N	Residual Vector.
P	Covariance of State Vector.
Q	State Error Weighting Matrix.
R	Control Weighting Matrix.
R	Desired State Vector.
S	Feedback Gain Matrix.
U	Control Vector.
V	Command Matrix.
V	Noise Vector.
W	Riccati Coefficient Matrix.
W	Disturbance Vector.
X	State Vector.
$\hat{X}$	Best Estimate of State Vector.
Y	Combined State and Control Vector.
Z	Measured State Vector.

Scalar Symbols

A,B,C	State Equation Coefficients.
I_z	Moment of Inertia about z axis (kg m^2).
L	Length of ship between perpendiculars (m).
m	Mass of ship (kg).
n_A, n_D	Actual and Demanded engine speeds (rad/s).
N	Total moment applied to ship (Nm).
N_u, N_δ etc.	Yaw hydrodynamic coefficients.
r	Angular velocity of ship about z axis.
T	Sampling time interval (s).
t	Time (s).
T_N	Time constant of main engines (s).
T_R	Time constant of rudder servo (s).
K, i	Interger counters.
J	Performance Index.
U	Track velocity (m/s).
u	Forward velocity of ship (m/s).
u_a, u_c	Forward components of wind and current velocities (m/s).
ν	Lateral velocity of ship (m/s).
ν_a, ν_c	Lateral components of wind and current velocities (m/s).
x, y, z	Ship related orthogonal co-ordinates (m).
X	Total force on ship in forward direction (N).
X_u, X_δ etc.	Surge hydrodynamic coefficients.
X_o, Y_o, Z_o	Earth related orthogonal co-ordinates.
Y	Total lateral force on ship (N).
Y_u, Y_δ etc.	Sway hydrodynamic coefficients.

GREEK SYMBOLS

$\beta, \hat{\beta}$	Transpose of Augmented State Transition Matrix and best estimate.
δ_A, δ_D	Actual and Demanded rudder angles (rad).
ρ	Density of water (kg/m^3).
ψ	Actual heading of ship (rad).

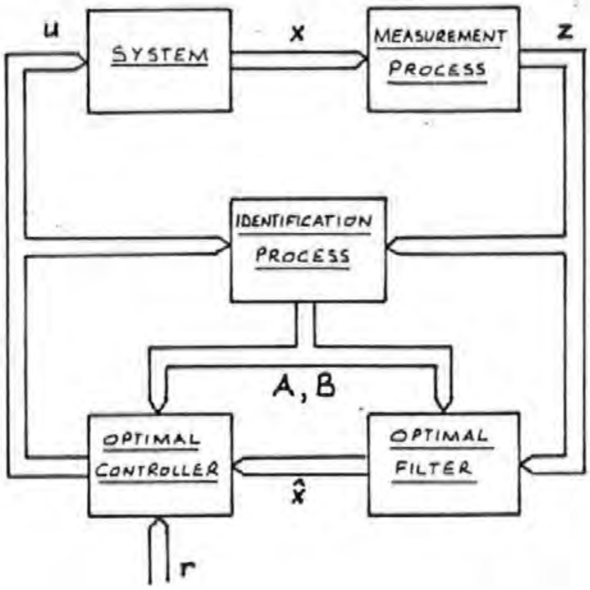

Figure 1 Proposed Automatic Guidance System

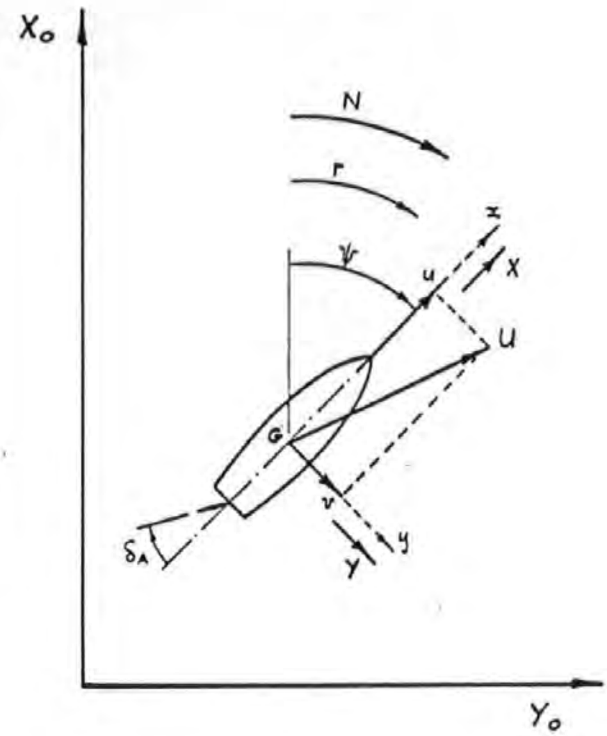

Figure 2 Co-ordinate Systems

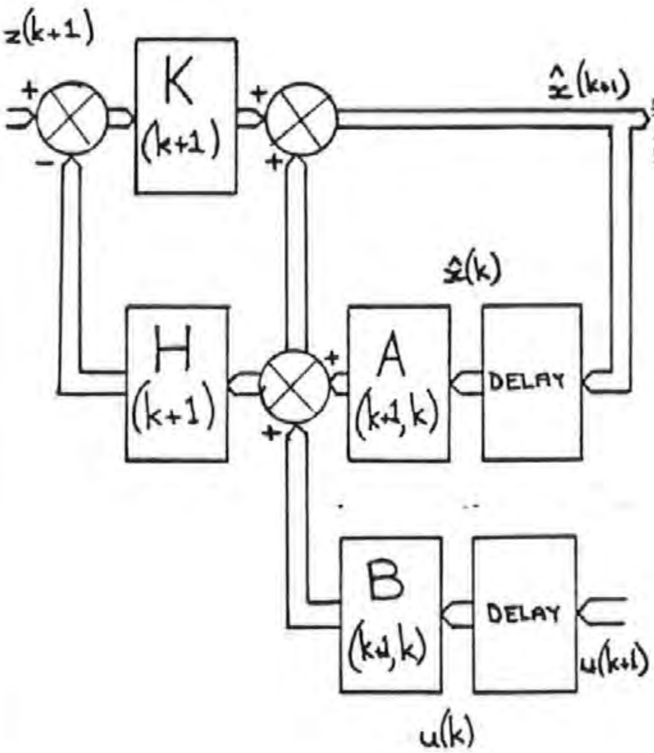

Figure 3 Optimal Filter

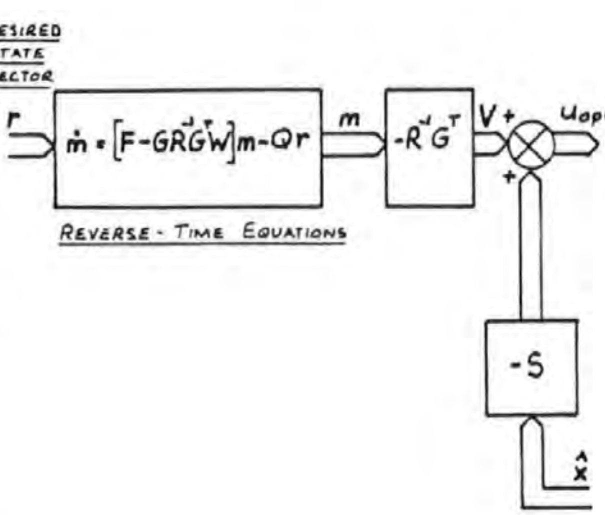

Figure 4 Optimal Controller

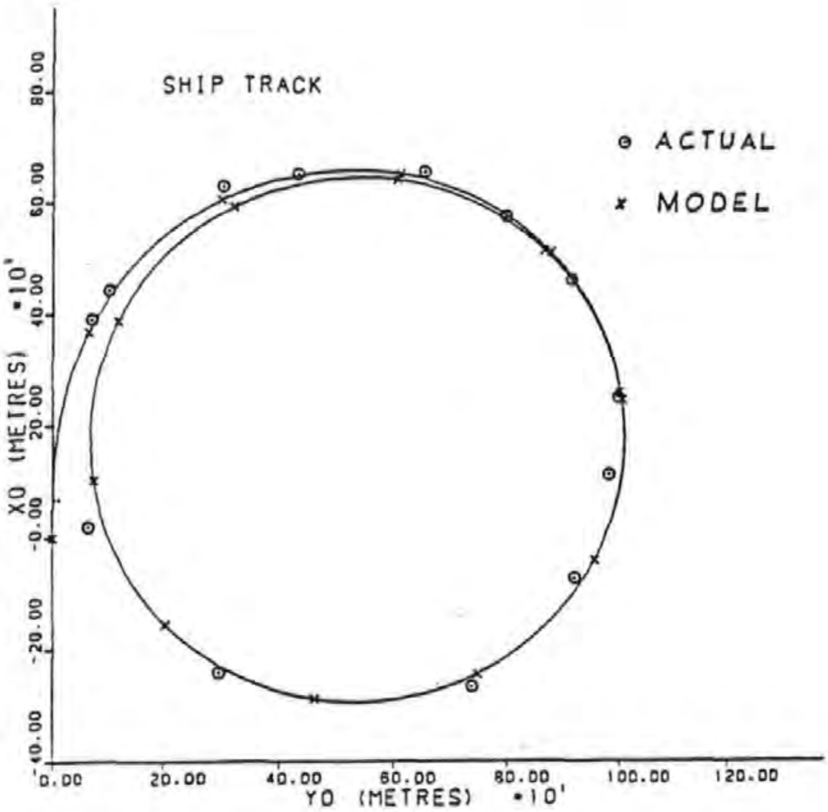

Figure 5 Turning Circle, 20° Starboard Rudder, 7.717 m/s.

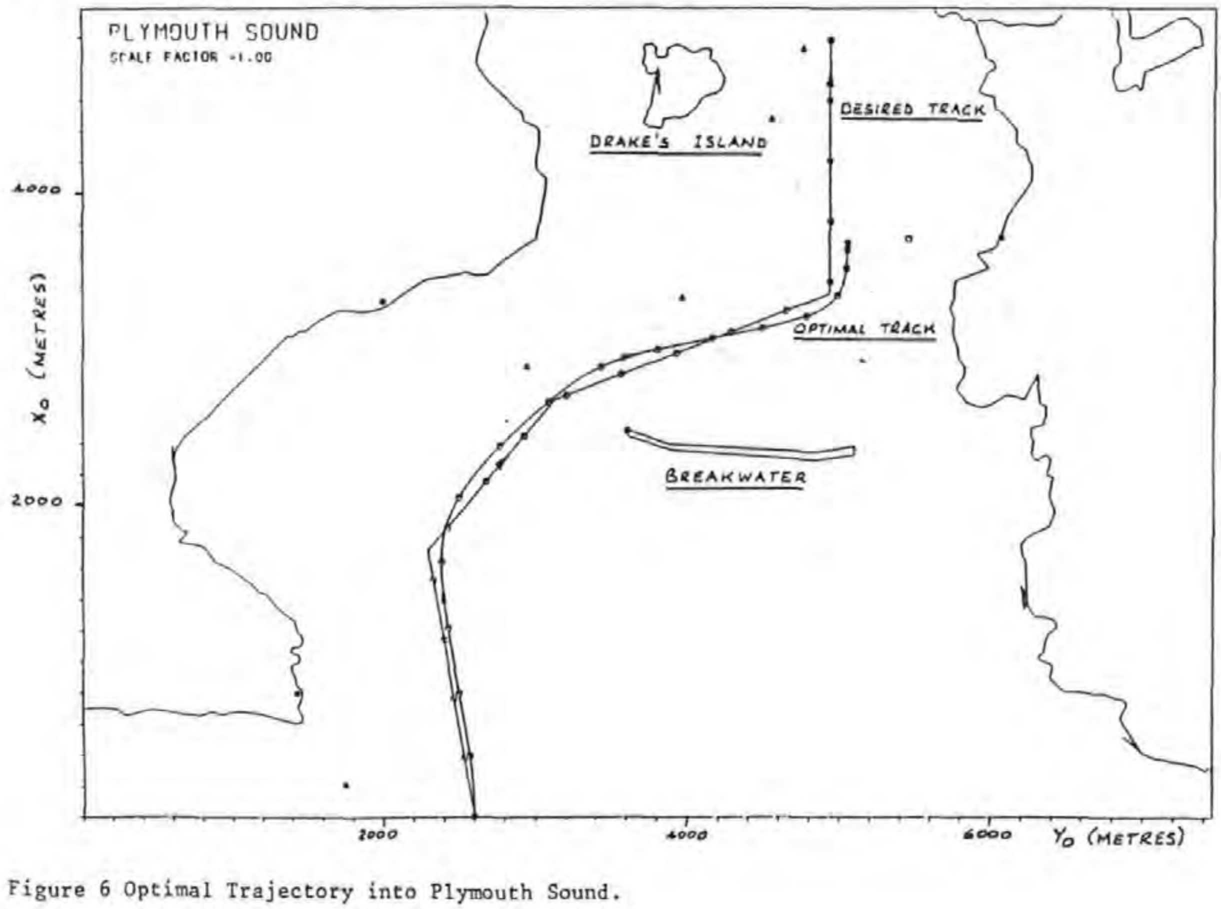

Figure 6 Optimal Trajectory into Plymouth Sound.